

THEORY OF THE POSITIVE COLUMN  
OF A GAS DISCHARGE

Thesis by  
Robert Gary Lindgren

In Partial Fulfillment of the Requirements  
For the Degree of  
Doctor of Philosophy

California Institute of Technology  
Pasadena, California  
1970  
(Submitted May 8, 1970)

#### ACKNOWLEDGMENTS

I wish to express my sincere appreciation to my research advisor, Professor G. R. Gavalas, for his invaluable guidance and assistance throughout the course of this investigation. I also wish to acknowledge the many helpful conversations with Professor F. H. Shair.

I am deeply indebted to the Fannie and John Hertz Foundation, whose fellowship provided my financial support during most of my graduate study.

ABSTRACT

An attempt is made to provide a theoretical explanation of the effect of the positive column on the voltage-current characteristic of a glow or an arc discharge. Such theories have been developed before, and all are based on balancing the production and loss of charged particles and accounting for the energy supplied to the plasma by the applied electric field. Differences among the theories arise from the approximations and omissions made in selecting processes that affect the particle and energy balances. This work is primarily concerned with the deviation from the ambipolar description of the positive column caused by space charge, electron-ion volume recombination, and temperature inhomogeneities.

The presentation is divided into three parts, the first of which involves the derivation of the final macroscopic equations from kinetic theory. The final equations are obtained by taking the first three moments of the Boltzmann equation for each of the three species in the plasma. Although the method used and the equations obtained are not novel, the derivation is carried out in detail in order to appraise the validity of numerous approximations and to justify the use of data from other sources. The equations are applied to a molecular hydrogen discharge contained between parallel walls. The applied electric field is parallel to the walls, and the dependent variables--electron and ion flux to the walls, electron and ion densities, transverse electric field, and gas temperature--vary only in the direction perpendicular to the walls. The mathematical description is given by a sixth-order

nonlinear two-point boundary value problem which contains the applied field as a parameter. The amount of neutral gas and its temperature at the walls are held fixed, and the relation between the applied field and the electron density at the center of the discharge is obtained in the process of solving the problem. This relation corresponds to that between current and voltage and is used to interpret the effect of space charge, recombination, and temperature inhomogeneities on the voltage-current characteristic of the discharge.

The complete solution of the equations is impractical both numerically and analytically, and in Part II the gas temperature is assumed uniform so as to focus on the combined effects of space charge and recombination. The terms representing these effects are treated as perturbations to equations that would otherwise describe the ambipolar situation. However, the term representing space charge is not negligible in a thin boundary layer or sheath near the walls, and consequently the perturbation problem is singular. Separate solutions must be obtained in the sheath and in the main region of the discharge, and the relation between the electron density and the applied field is not determined until these solutions are matched.

In Part III the electron and ion densities are assumed equal, and the complicated space-charge calculation is thereby replaced by the ambipolar description. Recombination and temperature inhomogeneities are both important at high values of the electron density. However, the formulation of the problem permits a comparison of the relative effects, and temperature inhomogeneities are shown to be

important at lower values of the electron density than recombination. The equations are solved by a direct numerical integration and by treating the term representing temperature inhomogeneities as a perturbation.

The conclusions reached in the study are primarily concerned with the association of the relation between electron density and axial field with the voltage-current characteristic. It is known that the effect of space charge can account for the subnormal glow discharge and that the normal glow corresponds to a close approach to an ambipolar situation. The effect of temperature inhomogeneities helps explain the decreasing characteristic of the arc, and the effect of recombination is not expected to appear except at very high electron densities.

TABLE OF CONTENTS

Acknowledgments . . . . .	ii
Abstract . . . . .	iii
Table of Contents . . . . .	vi
PART I. DERIVATION OF EQUATIONS . . . . .	1
Introduction . . . . .	2
Plasma Properties and Processes . . . . .	4
Abstract Representation of the Problem . . . . .	5
Description of Objectives . . . . .	7
Correspondence between Theoretical and Experimental Characteristics . . . . .	8
Basis for the Equations . . . . .	9
1. Basis of Equations in Kinetic Theory . . . . .	10
Preliminary Error Analysis . . . . .	10
Boltzmann Equations . . . . .	11
2. Macroscopic Equations . . . . .	13
Equation of Change for $\langle \phi_\alpha \rangle$ . . . . .	13
Continuity Equations . . . . .	15
Momentum Equations . . . . .	18
Energy Equations . . . . .	25
Closure of Moment Equations . . . . .	28
Final Moment Equations . . . . .	35
3. Application of Equations to the Positive Column . . . . .	37
Equations of Change . . . . .	37
Boundary Conditions . . . . .	40

4. Sources of Data . . . . .	42
Data for Electrons . . . . .	42
Data for Ions . . . . .	47
Recombination Coefficient . . . . .	49
Thermal Conductivity . . . . .	50
Domain of Data . . . . .	51
5. Dimensionless Problem . . . . .	53
Dimensionless Coefficients and Variables . . . . .	53
Dimensionless Equations and Boundary Conditions . . . . .	56
Solution at $N_{e0} = 0$ . . . . .	58
Discussion of Problem . . . . .	61
Appendix A. Expressions for Collision Rates . . . . .	63
Definition of Cross Section . . . . .	63
Application to Velocity Distributions . . . . .	65
Appendix B. Expressions for Elastic Momentum and Energy Transfer Rates . . . . .	68
Basic Collision Kinematics . . . . .	68
Momentum Transfer . . . . .	72
Energy Transfer . . . . .	73
Appendix C. Calculation of Plasma Properties from Kinetic Theory . . . . .	76
Behavior of Ions . . . . .	77
Behavior of Electrons . . . . .	79
Response of $f_e$ to Changes in $N_n$ . . . . .	81
Ambipolar Diffusion Time . . . . .	84
Nomenclature . . . . .	86
List of Figures . . . . .	91
Bibliography . . . . .	101

PART II. EFFECT OF RECOMBINATION AND SPACE CHARGE . . . . .	104
Introduction . . . . .	105
Uniform-Temperature Approximation . . . . .	106
Production and Loss of Electrons . . . . .	107
$N_{eo} - \hat{E}_z$ Relation . . . . .	109
Interpretation of the Experimental Characteristic . . . . .	112
Stability in the Positive Column . . . . .	113
Analytical Procedure . . . . .	115
Relation to Previous Work . . . . .	116
1. Working Equations . . . . .	118
Equations for Dependent Variables . . . . .	118
Constant Coefficients . . . . .	120
Final Equations . . . . .	123
Relations among the Variables . . . . .	124
2. Separation of the Plasma Column into Main Region and Sheath . . . . .	126
Asymptotic Expansions . . . . .	126
Zero-Order Problem in the Main Region . . . . .	128
Breakdown of Main-Region Solution . . . . .	133
Validity of Boundary Condition on $n_{eo}$ at the Wall. . . . .	136
Equations in the Sheath . . . . .	138
3. Zero-Order Solution in the Main Region . . . . .	141
Relation to the Ambipolar Diffusion Equation . . . . .	141
Statement of Problem . . . . .	142
Approximate Solution . . . . .	143
Final Form of the Approximate Solution . . . . .	148
Exact Solution . . . . .	150
$\epsilon^* - \gamma^*$ Expansion Derived from the Exact Results . . . . .	158
Comparison of Exact and Approximate Solutions . . . . .	162

4.	First-Order Solution in the Main Region . . . . .	164
	First-Order Problem in the Main Region . . . . .	164
	Approximate Solution for $n_{e1}$ . . . . .	170
	Lowest-Order Contribution to $s$ . . . . .	174
5.	Approximate Asymptotic Sheath Solution . . . . .	177
	Validity of the Equations in the Sheath . . . . .	178
	Zero-Order Equations . . . . .	179
	Approximation for Large $\tau_0$ . . . . .	181
	Asymptotic Solution to the Approximate Zero-Order Equations . . . . .	185
	Comparison of the Approximate Sheath Solution with the Main-Region Solution . . . . .	187
	Numerical Calculation of $\tilde{E}_0(0)$ . . . . .	190
6.	Exact Asymptotic Sheath Solution . . . . .	197
	Working Equations . . . . .	197
	Asymptotic Solution . . . . .	199
	Numerical Calculation of $\tilde{E}(0)$ . . . . .	204
7.	Matching Main - Region and Sheath Solutions . . . . .	211
	Matching $J$ and $\tilde{J}$ . . . . .	211
	Matching $n_e$ and $\tilde{n}_e$ : Determination of $\mu_1$ and $\gamma_1$ . . . . .	214
	Matching $E$ and $\tilde{E}$ . . . . .	218
	Matching $s$ and $\tilde{s}$ . . . . .	220
	Numerical Calculation of $\gamma_1$ . . . . .	221
8.	Summary . . . . .	224
	Objectives and Techniques . . . . .	224
	Results . . . . .	225
	Interpretation of Results . . . . .	226

Appendix A. Proofs of Relations among the Variables	
$J, n_e, n_i, E$ . . . . .	227
Lemma 1 . . . . .	228
Theorem 1 . . . . .	230
Lemma 2 . . . . .	232
Theorem 2 . . . . .	233
Corollary . . . . .	234
Lemma 3 . . . . .	234
Theorem 3 . . . . .	235
Theorem 4 . . . . .	242
Appendix B. Orthogonality Requirement . . . . .	245
Appendix C. The Zero-Order Solution in Cylindrical Geometry . . . . .	247
Appendix D. Expansions of Trigonometric Functions . . . . .	256
Appendix E. Determination of $\gamma_0^*$ and $\gamma_1^*$ by Matching . . . . .	259
Nomenclature . . . . .	264
List of Tables . . . . .	267
List of Figures . . . . .	276
Bibliography . . . . .	287
PART III. EFFECT OF TEMPERATURE INHOMOGENEITIES . . . . .	288
Introduction . . . . .	289
1. Working Equations . . . . .	292
Equations for Dependent Variables . . . . .	293
Equation for Pressure . . . . .	296
Discussion of Problem . . . . .	296

2.	Solution when $\zeta = 0$ . . . . .	301
	Reference Values for $\hat{E}_z$ and $p$ . . . . .	301
	Solution for $T_0$ and $p_0$ . . . . .	302
	Solution for $J_0, n_0,$ and $\hat{E}_{z0}$ . . . . .	304
3.	Perturbation Solution . . . . .	307
	Expansions of Variables and Coefficients . . . . .	307
	First-Order Problem . . . . .	310
	Solution for $T_1$ and $p_1$ . . . . .	311
	Solution for $\hat{E}_{z1}$ and $n_1$ . . . . .	312
	Numerical Results . . . . .	315
4.	Numerical Solution . . . . .	317
	Outline of Procedure . . . . .	317
	Step 1 . . . . .	318
	Step 2 . . . . .	318
	Step 3 . . . . .	318
	Step 4 . . . . .	319
	Step 5 . . . . .	322
	Step 6 . . . . .	323
	Results . . . . .	324
5.	Summary . . . . .	326
	Combined Effects . . . . .	326
	Interpretation of Results . . . . .	327
	Appendix A. Numerical Differentiation of Coefficients . . . . .	331
	Differentiation Formula . . . . .	331
	Error Analysis . . . . .	332
	Appendix B. Calculation of $\psi$ . . . . .	333
	Nomenclature . . . . .	336

List of Tables . . . . .	338
List of Figures . . . . .	346
Bibliography . . . . .	355
PROPOSITIONS . . . . .	356
Proposition 1. Relaxation of the Electron Distribution Function to the Maxwellian State . . . . .	357
The Boltzmann Equation . . . . .	358
Expansion of the Left-Hand Side . . . . .	361
Expansion of the Collision Integral . . . . .	363
Equations for $f_0$ and $f_1$ . . . . .	366
Formulation of the Problem . . . . .	367
Statement of the Problem . . . . .	368
Solution for $f_1$ . . . . .	371
Estimate of Relaxation Time . . . . .	372
Dimensionless Equations . . . . .	374
Numerical Solution . . . . .	376
Appendix A. Preliminary Calculations . . . . .	378
Appendix B. The Finite-Difference Calculation . . . . .	385
Nomenclature . . . . .	387
Figures . . . . .	390
Bibliography . . . . .	393
Proposition 2. Jump Discontinuities in Concentration Profiles for Fixed-Column Adsorption . . . . .	395
Material Balance . . . . .	395
The Continuous Solution . . . . .	397
Introduction of the Discontinuity . . . . .	398
Location of the Discontinuity . . . . .	400
Literature Treatment of the Discontinuity . . . . .	403
The Equilibrium Assumption . . . . .	405
Figures . . . . .	407
Bibliography . . . . .	410

Proposition 3. The Equations of Surface Flow in a Rotating Frame of Reference . . . . .	411
Surface Coordinates and the Velocity . . . . .	412
The Continuity Equation . . . . .	415
The Momentum Equation . . . . .	416
The Momentum Equation in Surface Coordinates . . .	419
Conclusion . . . . .	421
Appendix A. Formulas from Differential Geometry .	423
Appendix B. Time Differentiation Formulas . . . .	425
Appendix C. Time Differentiation of an Integral .	429
Appendix D. Relation between Derivatives in the Rotating and the Inertial Frames of Reference . . . . .	431
Nomenclature . . . . .	432
Bibliography . . . . .	435

PART I

DERIVATION OF EQUATIONS

## INTRODUCTION

When a potential difference is applied between two electrodes in a cylindrical discharge tube, a current flows if charged particles are present in the gas. If the electric field is sufficiently strong, the electrons acquire enough energy to undergo ionizing collisions with the neutral molecules, and enough new charged particles may be formed to balance those lost to the discharge by diffusion to the walls and by other means. In this case a steady state may be maintained, and a glow or an arc discharge is established.

The interaction between the electric field and the charged particles in such a discharge is a complex phenomenon, and a unified theoretical treatment of the entire discharge is not available. Near the electrodes there are strong axial variations in the electric field and in the plasma properties, and the behavior depends strongly on the properties of the electrodes themselves. However, a distance away from the electrodes the discharge is essentially uniform in the axial direction, and this region is called the positive column. Actually, axial nonuniformities such as striations can often be observed, but in general the properties of the positive column are accountable by theories neglecting axial dependencies<sup>\*</sup>. Because of its uniformity the positive column is quite amenable to theoretical analysis.

The fundamental principles basic to the various theoretical approaches to the positive column simply state that under steady-state

---

<sup>\*</sup>See, for instance, von Engel [26] or Cobine [6]

conditions the production and the loss of charged particles must balance and the energy supplied to the system through the applied electric field must be dissipated. The differences among the theories arise from the approximations and omissions made in selecting processes that effect changes in particle densities and energies. Most past investigations have not considered electron-ion volume recombination and neutral temperature inhomogeneities. In this work, however, these phenomena and their effects are studied in detail. This work also differs from previous efforts by using experimental data for the plasma properties of a particular gas, and the resulting calculations are more complex than those occurring in theories using model plasmas.

In the process of determining the effect of the various physical phenomena on the overall operation of the discharge, the analysis entails consideration of molecular processes and the mean properties of the various species--electrons, ions, and neutral molecules. The molecular behavior is coupled with such macroscopic quantities as the electric field, so the analysis gives information on various levels. Detailed knowledge of properties such as mean electron energy can be very important. For instance, in using discharges for purposes of illumination or for the study of chemical reactions, the excitation of energy levels is most efficient at particular electron energies. Furthermore, in the study of temperature gradients, the molecular properties vary across the discharge, and these variations may be of considerable importance in operating the discharge for particular purposes.

In the analysis which follows, an attempt is made to determine the importance and effect of individual physical phenomena by comparing the results with the known experimental behavior. From this comparison comes a better understanding of the fundamental physical processes occurring in the positive column. Experimental results pertaining only to the positive column and subject to the conditions assumed in the analysis are not available, but such measurements could be made. In lieu of the data needed to make a quantitative comparison with the calculated results, we use information that provides a qualitative description of the entire discharge and shows its response to changes in various parameters.

#### Plasma Properties and Processes

Before describing the various theoretical approaches more explicitly, it is convenient to discuss briefly the physical nature of the positive column. In the situation of interest the pressure in the discharge is of the order of mm Hg, and the gas is slightly ionized with fraction of gas ionized less than  $10^{-5}$ . The electron and ion densities may vary over several orders of magnitude and are typically between  $10^8$  and  $10^{12}$   $\text{cm}^{-3}$  in a glow discharge. The electrons are rapidly accelerated by the axial field and on the average gain a considerable amount of energy in the course of a mean free path. This energy is transferred to the neutrals through elastic and inelastic collisions. Because of the small mass of the electrons, the much more numerous elastic collisions are inefficient in transferring energy. As a result the mean energy of the electrons is greater than that of the

neutrals by a factor the order of 100. The neutrals in turn transfer the energy out of the system, and temperature, and hence density, gradients are associated with this process. Since the electron mean free path is directly related to the neutral density, the energy gained between collisions, and thus also the mean energy of the electrons, is affected by the neutral temperature. The positive ions gain less energy from the axial field and lose it more readily in collisions; consequently the mean ion energy is not much higher than that of the neutrals. The charged-particle populations are maintained through ionization of neutrals by electron impact. This production is balanced by various loss processes, the most significant of which is diffusion to the wall of the column. Since the electrons tend to diffuse more rapidly than the ions, a charge separation is produced that results in a radial electric field retarding the flux of electrons and augmenting the flux of ions. Other loss processes which may affect the particle balance are electron-ion recombination and negative-ion formation.

#### Abstract Representation of the Problem

Among the physical quantities whose radial variations are of interest are the electron and ion number densities, the radial electric field, and the temperature of the neutral gas. The axial field, which is essentially constant across the column, is of fundamental importance in determining the values of these variables. It affects the mean electron energy, which in turn alters such quantities as the ionization and diffusion coefficients. In fact the equations for the variables have solutions only for certain values of the axial field.

The problem can be written as a nonlinear operator equation  $F(u, \lambda) = 0$ , where the vector  $u$  represents the physical variables and the parameter  $\lambda$  represents the axial field. Although it is not strictly a norm, it is convenient to adopt as a measure of the magnitude of  $u$ ,  $\|u\|$ , the electron density at the center of the discharge. The plot of  $\|u\|$  versus  $\lambda$  for the solutions  $u(\lambda)$  is called the response diagram in the jargon of bifurcation theory<sup>\*</sup>. The equation  $F(u, \lambda) = 0$  happens to have a trivial solution for all  $\lambda$ , which with the proper choice of variables can be written  $u = 0$ . This solution, for which  $\|u\| = 0$ , corresponds physically to the absence of a discharge; although an axial field is present, the charged particle densities and the radial field are zero, and the temperature is constant. The bifurcation point  $\lambda_b$  at which a nontrivial solution of infinitesimal magnitude  $\|u\|$  first appears is called the free diffusion limit by Allis and Rose [1] and Cohen and Kruskal [7]. It is characterized by the diffusion of electrons and ions to the wall in the absence of a significant radial electric field. Cohen and Kruskal give a complete analysis of the continuation of this curve to large  $\|u\|$  (electron density) for a situation in which the neutral temperature is constant and the only electron and ion losses are by diffusion to the wall. The response curve for their analysis is sketched in Fig. 1. As  $\|u\| \rightarrow \infty$ ,  $\lambda$  approaches a particular value  $\lambda_a$ . The limiting solution  $u(\lambda_a)$  corresponds to the classical ambipolar approximation

---

<sup>\*</sup>See Keller and Antman [17] pp. xi-xiv.

in which electron and ion number densities are assumed equal and the flux to the wall is characterized solely by the ambipolar diffusion coefficient\* .

### Description of Objectives

The present work seeks to obtain a modification to this response curve by considering the effects of volume recombination and spatial temperature variations. Since both of these effects are of little importance at low electron density (small  $||u||$ ), the primary interest is centered about the deviation from the ambipolar limit. In order to ease the mathematical difficulties and separate the two effects, two distinct cases are treated. In Part II temperature variations are neglected, and a solution is obtained that is valid over a large range of  $||u||$ . The qualitative modification of the response curve is readily anticipated by physical intuition and is given by the dashed curve of Fig. 1. Part III is primarily concerned with the effect of temperature inhomogeneities. However, recombination is also considered and the relative importance of the two effects is investigated. The difference between electron and ion densities is neglected, so the results are restricted to large  $||u||$ , where the approximation is good. In this case even the qualitative nature of the response curve is difficult to predict and depends strongly on the nature of the gas in the discharge.

Because of the availability of data, all calculations are performed for an  $H_2$  discharge. Experimental evidence indicates that  $H_2^-$

---

\* See, for instance, von Engel [26] or Cobine [6].

is not formed in the discharge<sup>\*</sup>, so direct negative-ion formation need not be considered as an electron loss process. Although  $H^-$  is formed by dissociative attachment, the cross section for the reaction is very small<sup>\*</sup>, and the process can be neglected. Furthermore, experimental data show that very little atomic hydrogen is present at the plasma conditions considered<sup>\*\*</sup>. Consequently all aspects of dissociation can be neglected, and only one neutral species need be considered.

#### Correspondence between Theoretical and Experimental Characteristics

Ideally the theoretical analysis would be examined by comparing the theoretical results with the experimental relation between the electron density and the axial electric field in the positive column. However, such information is not available, and in its place we use a qualitative description of the entire discharge. The experimental behavior of the discharge can be described by a plot of the potential difference between electrodes versus the current passing through the discharge. This curve is called the voltage-current characteristic of the discharge and is related to the response diagram described above; indeed, the response diagram shall frequently be called the characteristic of the positive column. To demonstrate this relationship, the current through the discharge can be obtained from quantities known in the positive column by integrating the product of electron density and

---

\* See McDaniel [19], pp. 413-414.

\*\* See von Engel [26], pp.270-271; Cobine [6], pp. 337-338.

axial drift velocity over a cross section of the column. Its value is roughly proportional to the electron density at the center of the discharge. The axial field in the positive column contributes directly to the total potential difference, but other sectors of the discharge, such as the cathode region, also contribute. In fact von Engel [26] and Cobine [6] attribute the shape of the subnormal and abnormal portions of the discharge characteristic to cathode effects (See Fig. 2). However, Cohen and Kruskal [7] have used positive column arguments to explain the subnormal discharge, and volume recombination and temperature effects, which are studied in Part II and Part III, may have a significant influence on the shape of the voltage-current characteristic at electron densities typical of an abnormal glow or an arc discharge.

#### Basis for the Equations

The development of the working equations that eventually yield the axial field-electron density relationship begins in kinetic theory. The macroscopic equations that are eventually obtained from them are not novel. However, the use of the data for an  $H_2$  discharge depends heavily on the microscopic formulation, and for that reason the entire development of the equations is carried out in detail. The equations that are solved are actually written not for the cylindrical discharge, but for the corresponding slab geometry. The purpose, of course, is to make the equations more tractable while retaining their basic features. The results in the different geometries may reasonably be expected to be qualitatively equivalent.

## 1. BASIS OF EQUATIONS IN KINETIC THEORY

The development of the problem begins with a Boltzmann equation for the velocity distribution function that is written for each of the species in the plasma. The transition from kinetic theory to equations which describe macroscopically observable phenomena is accomplished by multiplying the Boltzmann equations by suitable functions of velocity and then integrating them over all values of the velocity. The equations which result describe, after certain manipulations, the time and space variation of average quantities which are equivalents of the density, momentum, and energy of the various species. However, not all of these moment equations are destined to evolve into the final working equations. Some provide no noteworthy information in the situation of interest, and others are replaced by results from different experimental or theoretical work. The introduction of this extraneous information involves approximations that must be justified. However, many other approximations must also be justified before the final equations are obtained.

### Preliminary Error Analysis

The first approximation is concerned with the applicability of the Boltzmann equation to the situation of interest. The collision integral of the Boltzmann equation is capable of handling only binary collisions and is thus restricted to particle interactions characterized by short-range forces. Consequently the charged-particle Coulomb interactions cannot be treated and are in fact neglected. This procedure is valid provided the electron and ion densities are

sufficiently small in comparison with the neutral density. The criteria for neglecting Coulomb interactions are discussed by Holt and Haskell [14] and are satisfied in our problem except at very large electron densities.

Various approximations are also involved in obtaining the final moment equations. In fact one is intrinsic to the use of moment equations in general and arises from the need to modify certain terms in order to obtain a well-posed problem. Errors are also introduced in evaluating coefficients that appear in the final equations. They are generally obtained as complicated expressions involving integrals of velocity distribution functions. However, they are usually evaluated with the use of theoretical and experimental data from other sources. Further approximations are made in neglecting various terms that are expected to be small.

### Boltzmann Equations

The Boltzmann equation as applied to the species of a glow discharge can be written

$$\frac{\partial f_{\alpha}}{\partial t} + \underline{v}_{\alpha} \cdot \frac{\partial f_{\alpha}}{\partial \underline{r}} + \frac{q_{\alpha}}{m_{\alpha}} \hat{E}_t \cdot \frac{\partial f_{\alpha}}{\partial \underline{v}_{\alpha}} = \left( \frac{\partial f_{\alpha}}{\partial t} \right)_c \quad (1.1)$$

$$= \left( \frac{\partial f_{\alpha}}{\partial t} \right)_{e.c.} + \left( \frac{\partial f_{\alpha}}{\partial t} \right)_{i.c.} \quad (1.2)$$

where  $\alpha$  is a subscript representing the species and equals e, i, or n for electrons, ions, or neutrals, respectively. The neutral particles, of course, are  $H_2$  molecules, and the ions are assumed to be

$H_3^+$  \*. No other species is considered.

$f_\alpha(\underline{r}, \underline{v}_\alpha, t)$  is the velocity distribution function defined so that  $f_\alpha \underline{dr} \underline{dv}_\alpha$  represents the number of particles of type  $\alpha$  that are expected to lie in the element of phase space  $\underline{dr} \underline{dv}_\alpha$ . Thus the number density as a function of time and position is obtained by integrating  $f_\alpha$  over all values of the velocity:

$$N_\alpha(\underline{r}, t) = \int f_\alpha(\underline{r}, \underline{v}_\alpha, t) \underline{dv}_\alpha \quad . \quad (1.3)$$

Since the only force field considered in our analysis of the glow discharge is the total electric field  $\hat{\underline{E}}_t$ , the expression for the force per unit mass in Eq. (1.1) is written  $q_\alpha \hat{\underline{E}}_t / m_\alpha$ , where  $q_\alpha$  is the electric charge and  $m_\alpha$  is the mass of a particle of type  $\alpha$ .

The right-hand side of (1.1) represents the net rate at which  $f_\alpha$  increases as a result of all processes other than the normal motion of particles in the force field. Actually this rate is accountable by interparticle collisions, and  $(\partial f_\alpha / \partial t)_c$  is in fact called the collision integral. Since Coulomb interactions are neglected, only electron-neutral, ion-neutral, and neutral-neutral collisions are considered. The effect of these collisions on the rate is divided into two parts,  $(\partial f_\alpha / \partial t)_{e.c.}$  and  $(\partial f_\alpha / \partial t)_{i.c.}$ , representing elastic and inelastic collisions, respectively. The elastic collisions are much more numerous than the inelastic. However, the inelastic collisions cause phenomena such as ionization to which elastic collisions do not contribute, so they must be considered.

---

\* See McDaniel [19], pp. 472-473; Hirshfelder, Curtiss, and Bird [13], p. 1095.

## 2. MACROSCOPIC EQUATIONS

The equations of change for such quantities as number density, average momentum, and average energy of the three species are obtained by multiplying the Boltzmann equation by different powers of the velocity and integrating over velocity space. Various manipulations are necessary to produce the final equations with terms involving densities, fluxes, temperatures, and other macroscopic variables. Since the resulting equations are fewer in number than the unknowns, approximations must be introduced in order to obtain a well-posed problem. This entire procedure including the closure of the set of equations is quite standard but is repeated here in order to present clearly the approximations involved in its application to the glow discharge.

### Equation of Change for $\langle \phi_\alpha \rangle$

Instead of multiplying the Boltzmann equation by specific functions of velocity, it is economical to execute the procedure once with a function  $\phi_\alpha(\underline{v}_\alpha)$  that may represent momentum, kinetic energy, etc.  $\phi_\alpha(\underline{v}_\alpha)$  is to be understood as an extensive property whose total value for the species  $\alpha$  is the sum of that belonging to each particle.

Multiplication of the Boltzmann equation of (1.1) by  $\phi_\alpha(\underline{v}_\alpha)$  and subsequent integration over  $\underline{v}_\alpha$  results in derivatives on the left-hand side that can be simplified by integration by parts. For the time derivative we have

$$\int \phi_{\alpha} \frac{\partial f_{\alpha}}{\partial t} d\underline{v}_{\alpha} = \int \frac{\partial}{\partial t} (\phi_{\alpha} f_{\alpha}) d\underline{v}_{\alpha} - \int \frac{\partial \phi_{\alpha}}{\partial t} f_{\alpha} d\underline{v}_{\alpha} \quad (2.1)$$

$$= \frac{\partial}{\partial t} (N_{\alpha} \langle \phi_{\alpha} \rangle) \quad , \quad (2.2)$$

since  $\phi_{\alpha}$  is a function of velocity only and the average of a quantity depending on  $\underline{v}_{\alpha}$  is defined by

$$\langle \phi_{\alpha} \rangle = \frac{\int \phi_{\alpha} f_{\alpha} d\underline{v}_{\alpha}}{\int f_{\alpha} d\underline{v}_{\alpha}} \quad (2.3)$$

$$= \frac{1}{N_{\alpha}} \int \phi_{\alpha} f_{\alpha} d\underline{v}_{\alpha} \quad . \quad (2.4)$$

Similarly the spatial derivative is given by

$$\int \phi_{\alpha} \underline{v}_{\alpha} \cdot \frac{\partial f_{\alpha}}{\partial \underline{r}} = \frac{\partial}{\partial \underline{r}} \cdot (N_{\alpha} \langle \underline{v}_{\alpha} \phi_{\alpha} \rangle) \quad (2.5)$$

and the velocity derivative by

$$\int \frac{q_{\alpha}}{m_{\alpha}} \phi_{\alpha} \hat{\underline{E}}_t \cdot \frac{\partial f_{\alpha}}{\partial \underline{v}_{\alpha}} d\underline{v}_{\alpha} = \frac{q_{\alpha}}{m_{\alpha}} \hat{\underline{E}}_t \cdot \int \frac{\partial}{\partial \underline{v}_{\alpha}} (\phi_{\alpha} f_{\alpha}) d\underline{v}_{\alpha} - \frac{q_{\alpha}}{m_{\alpha}} \hat{\underline{E}}_t \cdot \int \frac{\partial \phi_{\alpha}}{\partial \underline{v}_{\alpha}} f_{\alpha} d\underline{v}_{\alpha} \quad (2.6)$$

$$= - \frac{q_{\alpha}}{m_{\alpha}} N_{\alpha} \hat{\underline{E}}_t \cdot \langle \frac{\partial \phi_{\alpha}}{\partial \underline{v}_{\alpha}} \rangle \quad (2.7)$$

The first integral on the right-hand side of (2.6) vanishes, since  $f_{\alpha}$  is assumed to approach zero strongly as  $|\underline{v}_{\alpha}| \rightarrow \infty$ . Using (2.2), (2.5) and (2.7), Eq. (1.1) becomes, after multiplication by  $\phi_{\alpha}$  and integration over  $\underline{v}_{\alpha}$ ,

$$\frac{\partial}{\partial t} (N_{\alpha} \langle \phi_{\alpha} \rangle) + \frac{\partial}{\partial \underline{r}} \cdot (N_{\alpha} \langle \underline{v}_{\alpha} \phi_{\alpha} \rangle) - \frac{q_{\alpha}}{m_{\alpha}} N_{\alpha} \hat{E}_{\underline{r}} \cdot \langle \frac{\partial \phi_{\alpha}}{\partial \underline{v}_{\alpha}} \rangle = \int \phi_{\alpha} \left( \frac{\partial f_{\alpha}}{\partial t} \right)_c d\underline{v}_{\alpha} \quad (2.8)$$

$N_{\alpha}$  and the various average quantities depend in general on  $t$  and  $\underline{r}$ .

From the interpretation of  $(\partial f_{\alpha} / \partial t)_c$  given in Section 1, it is apparent that the integral on the right-hand side of (2.8) is the rate per unit volume at which  $\phi_{\alpha}$  is increasing in species  $\alpha$  as a result of interparticle collisions. A detailed expression for the effect of a specific type of collision between two species is given in Eq. (A.11) of Appendix A. The integral in (2.8) consists of a sum of such expressions, and the summation must in general be taken over the various combinations of species and over the different collision processes. The omissions and approximations that can accurately be made are discussed when particular forms of  $\phi_{\alpha}(\underline{v}_{\alpha})$  are considered.

### Continuity Equations

The continuity equations for the individual species are obtained by taking

$$\phi_{\alpha}(\underline{v}_{\alpha}) = 1 \quad . \quad (2.9)$$

Equation (2.8) becomes

$$\frac{\partial N_{\alpha}}{\partial t} + \frac{\partial}{\partial \underline{r}} \cdot \hat{\underline{J}}_{\alpha} = \int \left( \frac{\partial f_{\alpha}}{\partial t} \right)_{i.c.} \quad (2.10)$$

where the number flux  $\hat{\underline{J}}_{\alpha}$  is defined by

$$\hat{\underline{J}}_{\alpha} \equiv N_{\alpha} \langle \underline{v}_{\alpha} \rangle \quad . \quad (2.11)$$

The right-hand side of (2.10) represents the net rate per unit volume at which particles of type  $\alpha$  are produced by collisions. The

description of an  $H_2$  glow discharge presented in the Introduction leaves only two collision processes that can cause a significant change in the total number of particles of a species. These are ionization of neutrals by electron impact and recombination by electron-ion interaction. Ion-neutral and neutral-neutral collisions involve insufficient energy to cause ionization. Ionization occurs as a result of a simple electron-neutral collision, but various recombination mechanisms have been proposed<sup>\*</sup>, which are characterized by different collision processes. We assume that recombination occurs by means of the dissociative process



although the amount of H present in the discharge is considered negligible.

The rate at which ionization and recombination occur can now be obtained from Eq. (A.10) of Appendix A. Defining  $R_I$  and  $R_R$  as the rates per unit volume of ionization and recombination collisions, we have

$$R_I = \iiint f_e(\underline{v}_e) f_n(\underline{v}_n) g Q_I(g) d\underline{v}_e d\underline{v}_n \quad (2.13)$$

$$R_R = \iiint f_e(\underline{v}_e) f_i(\underline{v}_i) g Q_R(g) d\underline{v}_e d\underline{v}_i \quad (2.14)$$

where  $Q_I$  is the total cross section for ionization and  $Q_R$  is the

---

<sup>\*</sup> See McDaniel [19], pp. 588 ff., for a discussion and appraisal of mechanisms.

total cross section for dissociative recombination. Equations (C.6) and (C.17) show that the ion and neutral velocities are small compared to the electron velocity at those values for which the distribution functions have significant magnitude. Hence  $g$  can be accurately replaced by  $v_e$  and integrations over  $\underline{v}_m$  and  $\underline{v}_i$  can be performed to yield

$$R_I = N_n \int f_e(\underline{v}_e) v_e Q_I(v_e) d\underline{v}_e \quad (2.15)$$

$$= N_e N_n \langle v_e Q_I(v_e) \rangle \quad (2.16)$$

and

$$R_R = N_i \int f_e(\underline{v}_e) v_e Q_R(v_e) d\underline{v}_e \quad (2.17)$$

$$= N_e N_i \langle v_e Q_R(v_e) \rangle . \quad (2.18)$$

The ionization and recombination coefficients,  $\hat{v}_I$  and  $\hat{\alpha}$ , are defined by

$$\hat{v}_I \equiv N_n \langle v_e Q_I(v_e) \rangle \quad (2.19)$$

$$\hat{\alpha} \equiv \langle v_e Q_R(v_e) \rangle , \quad (2.20)$$

so  $R_I$  and  $R_R$  become

$$R_I = \hat{v}_I N_e \quad (2.21)$$

$$R_R = \hat{\alpha} N_e N_i . \quad (2.22)$$

$\hat{v}_I$  and  $\hat{\alpha}$  depend in general on  $t, \underline{r}$  and other parameters which affect  $f_e$ . Although Eqs. (2.19) and (2.20) show the origins and functional dependencies of  $\hat{v}_I$  and  $\hat{\alpha}$ , they are not used to obtain

numerical values. Data from other sources are available and their applicability and use are discussed later.

Ionization and recombination affect the rates of production of electrons and ions identically, and this rate in particles per unit volume per unit time is given by  $R_I - R_R$ . Equation (2.10) written for the two species is

$$\frac{\partial N_e}{\partial t} + \frac{\partial}{\partial \underline{r}} \cdot \hat{\underline{J}}_e = \hat{v}_I N_e - \hat{\alpha} N_e N_i \quad (2.23)$$

$$\frac{\partial N_i}{\partial t} + \frac{\partial}{\partial \underline{r}} \cdot \hat{\underline{J}}_i = \hat{v}_I N_e - \hat{\alpha} N_e N_i \quad (2.24)$$

The production rate of neutrals is the negative of that for electrons and ions. Since the production rates have equal magnitudes, the fluxes of charged particles and of neutrals whose spatial derivatives appear in (2.10) are of the same order of magnitude. However, because of their much greater density, the flux of neutrals is of negligible importance and the transport of neutrals can be ignored. Since the equations obtained here are eventually applied to steady-state conditions,  $\partial N_n / \partial t$  is of no importance and Eq. (2.10) applied to the neutrals serves no purpose. In its place we make the approximation that the average velocity of neutral molecules is zero:

$$\langle \underline{v}_n \rangle = 0 \quad (2.25)$$

### Momentum Equations

The momentum equations are obtained from Eq. (2.8) by taking

$$\phi_\alpha = m_\alpha \underline{v}_\alpha \quad (2.26)$$

The immediate result is

$$m_{\alpha} \frac{\partial}{\partial t} (N_{\alpha} \langle \underline{v}_{\alpha} \rangle) + m_{\alpha} \frac{\partial}{\partial \underline{r}} \cdot (N_{\alpha} \langle \underline{v}_{\alpha} \underline{v}_{\alpha} \rangle) - q_{\alpha} N_{\alpha} \hat{E}_{\underline{t}} = m_{\alpha} \int \underline{v}_{\alpha} \left( \frac{\partial f_{\alpha}}{\partial t} \right)_{\underline{c}} d\underline{v}_{\alpha} . \quad (2.27)$$

In order to interpret the averages occurring in (2.27) as macroscopic state variables, it is necessary to introduce the peculiar velocity, which measures the deviation of the velocity from its mean value:

$$\underline{V}_{\alpha} = \underline{v}_{\alpha} - \langle \underline{v}_{\alpha} \rangle . \quad (2.28)$$

Using this expression  $\langle \underline{v}_{\alpha} \underline{v}_{\alpha} \rangle$  is calculated as

$$\langle \underline{v}_{\alpha} \underline{v}_{\alpha} \rangle = \langle \underline{V}_{\alpha} \underline{V}_{\alpha} \rangle + \langle \underline{v}_{\alpha} \rangle \langle \underline{v}_{\alpha} \rangle . \quad (2.29)$$

The pressure tensor of a component of a perfect gas is defined by

$$\underline{\Psi}_{\alpha} = N_{\alpha} m_{\alpha} \langle \underline{V}_{\alpha} \underline{V}_{\alpha} \rangle , \quad (2.30)$$

and its physical interpretation as the actual pressure is discussed by Chapman and Cowling [5], pp. 31-35. The right-hand side of (2.27) represents the net rate of increase per unit volume of the total momentum of species  $\alpha$  as a result of collisions with other types of particles. Elastic collisions are as effective as inelastic collisions in transferring momentum between particles. Since they occur much more frequently, the inelastic collisions are neglected. Replacing  $(\partial f / \partial t)_{\underline{c}}$  by  $(\partial f / \partial t)_{\underline{e.c.}}$  and using (2.11), (2.29), and (2.30), Eq. (2.27) becomes

$$\begin{aligned}
 m_{\alpha} \frac{\partial \hat{J}_{\alpha}}{\partial t} + \frac{\partial}{\partial \underline{r}} \cdot \underline{\Psi}_{\alpha} + m_{\alpha} \frac{\partial}{\partial \underline{r}} \cdot (N_{\alpha} \langle \underline{v}_{\alpha} \rangle \langle \underline{v}_{\alpha} \rangle) - q_{\alpha} N_{\alpha} \hat{\underline{E}}_t \\
 = m_{\alpha} \int \underline{v}_{\alpha} \left( \frac{\partial f_{\alpha}}{\partial t} \right)_{e.c.} d\underline{v}_{\alpha} \quad . \quad (2.31)
 \end{aligned}$$

In applying Eq. (2.31) to electrons, it is possible to neglect the term containing  $\langle \underline{v}_{\alpha} \rangle \langle \underline{v}_{\alpha} \rangle$ . Equations (C.17) and (C.21) of Appendix C show that the magnitude of  $\langle \underline{v}_e \rangle$  is much smaller than that of  $\sqrt{\langle v_e^2 \rangle}$ , so the velocity of the electrons consists of a slow drift superimposed on a large random motion. Equation (2.30) then shows that the third term of (2.31) is negligible in comparison with the second, and the momentum equation for electrons becomes

$$m_e \frac{\partial \hat{J}_e}{\partial t} + \frac{\partial}{\partial \underline{r}} \cdot \underline{\Psi}_e + N_e e \hat{\underline{E}}_t = m_e \int \underline{v}_e \left( \frac{\partial f_e}{\partial t} \right)_{e.c.} d\underline{v}_e \quad , \quad (2.32)$$

where  $e$  is the magnitude of the electronic charge.

Only elastic electron-neutral interactions are considered in calculating momentum transfer to the electrons by collisions. An expression for the rate per unit volume at which electrons acquire momentum from neutrals is available in Eq. (B.31) of Appendix B. In the nomenclature of this section we have

$$m_e \int \underline{v}_e \left( \frac{\partial f_e}{\partial t} \right)_{e.c.} d\underline{v}_e = - m_e \int \underline{v}_e f_e(\underline{v}_e) \nu_m(\underline{v}_e) d\underline{v}_e \quad (2.33)$$

$$= - m_e N_e \langle \nu_m(\underline{v}_e) \underline{v}_e \rangle \quad . \quad (2.34)$$

A substantial simplification would occur if  $\nu_m$  were independent of  $\underline{v}_e$  so that

$$\langle \nu_m \underline{v}_e \rangle = \nu_m \langle \underline{v}_e \rangle \quad . \quad (2.35)$$

Although  $\nu_m(v_e)$  does in fact depend on  $v_e$ , we seek to define an effective  $\nu_m$  by the relation above. Such a definition is not in general possible, since  $\langle \underline{v}_m \underline{v}_e \rangle$  and  $\langle \underline{v}_e \rangle$  need not have the same direction. However, only the radial components of the momentum equations are used in applying them to the glow discharge, and if only a particular component of (2.35) is considered, an effective  $\nu_m$  can certainly be defined. Also,  $f_e(\underline{v}_e)$  is almost isotropic and  $\nu_m(v_e)$  is not a very strong function of  $v_e$ , so the particular component used in the definition of an effective  $\nu_m$  has little effect on the numerical value. In fact we adopt (2.35) as the defining equation and regard its deviation from the truth as being of no practical importance. Using (2.35) and (2.11) in (2.34), the final form of the momentum equation given previously in (2.32) becomes

$$m_e \frac{\partial \hat{J}_e}{\partial t} + \frac{\partial}{\partial \underline{r}} \cdot \underline{\Psi}_e + N_e e \hat{E}_t = - m_e \nu_m \hat{J}_e \quad (2.36)$$

$\nu_m$  as defined by (2.35) and used in (2.36) depends in general not on  $v_e$  but on  $t$ ,  $\underline{r}$ , and other parameters that influence  $f_e$ . Blank [4], in his analysis of the positive column, studies the effect of a non-constant  $\nu_m(v_e)$  on a transport equation equivalent to (2.36). He concludes that except in special cases an equation using an effective  $\nu_m$  is of no use unless  $\nu_m$  is known a priori. In our case, data for the effective  $\nu_m$  are provided by the work of Frost and Phelps [11] and Engelhardt and Phelps [10]. The applicability of their data to our situation is discussed later.

In applying Eq. (2.31) to the ions, the term containing

$\langle \underline{v}_\alpha \rangle \langle \underline{v}_\alpha \rangle$  is also neglected. In this case, however, the omission cannot be justified quite as casually as it was with electrons. Equations (C.6) and (C.11) of Appendix C show that the drift velocity of ions is not small in comparison with the random thermal motion. Self and Ewald [24] study the effect of the term containing  $\langle \underline{v}_i \rangle \langle \underline{v}_i \rangle$  on the theoretical behavior of a glow discharge and conclude that it is not always negligible. In our application there is no axial spatial variation, and the momentum equations are used only in the radial direction, so in comparing the magnitudes of the second and third terms of (2.31), only the average radial velocity need be compared to the random velocity. An estimate of the radial velocity is provided by Eq. (C.40), and it is seen to be considerably smaller. Thus Eq. (2.31) becomes

$$m_i \frac{\partial \hat{J}_i}{\partial t} + \frac{\partial}{\partial r} \cdot \underline{\Psi}_i - N_i e \hat{E}_t = m_i \int \underline{v}_i \left( \frac{\partial f_i}{\partial t} \right)_{e.c.} d\underline{v}_i \quad (2.37)$$

Only elastic ion-neutral collisions contribute significantly to the transfer of momentum to ions from other species. An expression for the rate per unit volume at which ion momentum increases is available in Eq. (B.28) of Appendix B, and in the nomenclature of this section is

$$m_i \int \underline{v}_i \left( \frac{\partial f_i}{\partial t} \right)_{e.c.} d\underline{v}_i = \frac{-m_i m_n}{m_i + m_n} \frac{1}{N_n} \iint (\underline{v}_i - \underline{v}_n) f_i(\underline{v}_i) f_n(\underline{v}_n) \times v_{mi}(g) d\underline{v}_i d\underline{v}_n \quad (2.38)$$

where  $v_m(g)$  is replaced by  $v_{mi}(g)$  to avoid confusion with the electron frequency. The presence of  $g$  in the integrand introduces

a strong coupling between  $\underline{v}_i$  and  $\underline{v}_n$  and renders further simplification difficult. Instead of making assumptions about the distribution functions and continuing with tedious manipulations, it is convenient to make an appeal to intuition. Such an approach is particularly appropriate because the data that are eventually used in the ion momentum equation are not directly related to the distribution functions. It is only necessary that the integral when simplified exhibit the proper form. If  $\nu_{mi}$  were independent of  $g$ , the integral in (2.38) would become

$$\begin{aligned} & \frac{m_i m_n}{m_i + m_n} \frac{1}{N_n} \iint (\underline{v}_i - \underline{v}_n) f_i(\underline{v}_i) f_n(\underline{v}_n) \nu_{mi}(g) d\underline{v}_i d\underline{v}_n \\ &= \frac{m_i m_n}{m_i + m_n} \nu_{mi} N_i (\langle \underline{v}_i \rangle - \langle \underline{v}_n \rangle) \end{aligned} \quad (2.39)$$

$$= \frac{m_i m_n}{m_i + m_n} \nu_{mi} N_i \langle \underline{v}_i \rangle \quad . \quad (2.40)$$

In fact  $\nu_{mi}$  depends only weakly on  $g$ , and the expression in (2.40) is regarded as a definition of an effective collision frequency  $\nu_{mi}$ . The critical assumption in this procedure is that the term in the integrand that includes  $\underline{v}_n$  as a factor vanishes when integrated over  $\underline{v}_i$  and  $\underline{v}_n$ . For a  $\nu_{mi}$  which depends on  $g$ , this assumption is not valid in general, particularly when the mean ion velocity is significant in comparison with the random neutral velocity. In our application the momentum equations are applied only in the radial direction, so it is the mean radial ion velocity that should be used in the comparison. Equation (C.40) of Appendix C shows that it is considerably less than

the random neutral velocity, which is slightly greater than the value for ions given in (C.6). On this basis Eq. (2.40) is adopted as a good approximation and is used in (2.38) to yield

$$m_i \int \underline{v}_i \left( \frac{\partial f_i}{\partial t} \right)_{e.c.} d\underline{v}_i = -m_i v_i N_i \langle \underline{v}_i \rangle \quad , \quad (2.41)$$

where  $v_i$  replaces  $m_n v_{ni} / (m_i + m_n)$ . Equation (2.41) can be used to interpret  $v_i$  as the effective ion collision frequency for momentum transfer. Like  $v_m$  it depends in general on  $t$ ,  $\underline{r}$ , and other factors which influence the distribution functions.  $v_i$  is eventually combined with other factors to yield diffusion and mobility coefficients. These coefficients are evaluated with data from other sources, and hence these data determine  $v_i$  indirectly. The applicability of the data is discussed later.

The final ion momentum equation is obtained by substituting (2.41) into (2.37) and introducing the ion flux:

$$m_i \frac{\partial \hat{J}_i}{\partial t} + \frac{\partial}{\partial \underline{r}} \cdot \underline{\Psi}_i - N_i e \hat{E}_t = -m_i v_i \hat{J}_i \quad . \quad (2.42)$$

The approximations involved in the derivation should be kept in mind, since the apparent generality of the vector notation tends to belie the geometrical restrictions on the applicability of the equation.

The momentum equation for the neutral species reduces to the simple statement that the pressure is constant.  $\langle \underline{v}_n \rangle = 0$ ,  $q_n = 0$ , and at steady state  $\partial \hat{J}_n / \partial t$  vanishes, so Eq. (2.31) applied to the neutrals involves only two terms representing the spatial variation of the pressure tensor and the rate of momentum transfer from other

species. The rate of momentum transfer can be obtained directly from the rates calculated for the electrons and ions, and in the electron and ion momentum equations the rates are significant terms. However, the pressure tensor  $\underline{\Psi}_\alpha$  defined in (2.30) is proportional to the density  $N_\alpha$ , and  $N_n$  is so much larger than  $N_e$  or  $N_i$  that the fractional spatial change in  $\underline{\Psi}_n$  given by (2.31) is negligible. If the neutral hydrostatic pressure  $p_n$  is associated with  $\underline{\Psi}_n$ ,  $p_n$  must be constant. Because of the preponderance of neutrals the pressure  $p$  in the discharge is essentially equal to  $p_n$ . Mechanical equilibrium in the system requires that  $p$  be uniform, so in place of the neutral momentum equation, we adopt the equation

$$p_n = p \quad (2.43)$$

where  $p$  is independent of  $\underline{r}$ .

### Energy Equations

The energy equations are obtained from (2.8) by taking

$$\phi_\alpha = \frac{1}{2} m_\alpha v_\alpha^2 \quad (2.44)$$

Actually only the neutral equation is used, and after various manipulations and approximations it becomes an equation for the neutral temperature. However, important quantities are defined in the process, so it is carried out in general. Substituting (2.44) into (2.8)

$$\begin{aligned} \frac{1}{2} m_\alpha \frac{\partial}{\partial t} (N_\alpha \langle v_\alpha^2 \rangle) + \frac{1}{2} m_\alpha \frac{\partial}{\partial \underline{r}} \cdot (N_\alpha \langle \underline{v}_\alpha v_\alpha^2 \rangle) - q_\alpha N_\alpha \hat{E}_t \cdot \langle \underline{v}_\alpha \rangle \\ = \frac{1}{2} m_\alpha \int v_\alpha^2 \left( \frac{\partial f_\alpha}{\partial t} \right)_c d\underline{v}_\alpha \end{aligned} \quad (2.45)$$

since

$$\frac{\partial}{\partial v_{-\alpha}} (v_{\alpha}^2) = 2v_{-\alpha} \quad (2.46)$$

Introducing the peculiar velocity from Eq. (2.28) and using the fact that

$$\langle \underline{v}_{-\alpha} \rangle = 0 \quad , \quad (2.47)$$

we obtain the relations

$$\langle v_{\alpha}^2 \rangle = \langle \underline{v}_{-\alpha} \cdot \underline{v}_{-\alpha} \rangle = \langle \underline{V}_{-\alpha} \cdot \underline{V}_{-\alpha} \rangle + \langle \underline{v}_{-\alpha} \rangle \cdot \langle \underline{v}_{-\alpha} \rangle \quad (2.48)$$

and

$$\begin{aligned} \langle \underline{v}_{-\alpha} v_{\alpha}^2 \rangle &= \langle \underline{V}_{-\alpha} \underline{V}_{-\alpha} \cdot \underline{V}_{-\alpha} \rangle + 2 \langle \underline{V}_{-\alpha} \underline{V}_{-\alpha} \rangle \cdot \langle \underline{v}_{-\alpha} \rangle + \langle \underline{v}_{-\alpha} \rangle \langle \underline{V}_{-\alpha} \cdot \underline{V}_{-\alpha} \rangle \\ &\quad + \langle \underline{v}_{-\alpha} \rangle \langle \underline{v}_{-\alpha} \rangle \cdot \langle \underline{v}_{-\alpha} \rangle \end{aligned} \quad (2.49)$$

The kinetic-theory temperature\* of a species is defined by the relation

$$\frac{3}{2} k \hat{T}_{\alpha} = \frac{1}{2} m_{\alpha} \langle v_{\alpha}^2 \rangle \quad , \quad (2.50)$$

where  $k$  is Boltzmann's constant. We also define the heat-flux vector  $\underline{Q}_{\alpha}$  by

$$\underline{Q}_{\alpha} = \frac{1}{2} N_{\alpha} m_{\alpha} \langle \underline{V}_{-\alpha} \underline{V}_{-\alpha} \cdot \underline{V}_{-\alpha} \rangle \quad . \quad (2.51)$$

Its meaning in the context of our problem is discussed in detail later.

The physical quantities  $\underline{\Psi}_{\alpha}$ ,  $T_{\alpha}$ , and  $\underline{Q}_{\alpha}$  now enter the energy equation through the expressions for  $\langle v_{\alpha}^2 \rangle$  and  $\langle \underline{v}_{-\alpha} v_{\alpha}^2 \rangle$ . From (2.48)

---

\* Its definition and relation to the thermodynamic temperature is discussed by Chapman and Cowling [5], pp. 37, 40-41.

and (2.50)

$$\frac{1}{2} m_{\alpha} \langle v_{\alpha}^2 \rangle = \frac{3}{2} k \hat{T}_{\alpha} + \frac{1}{2} m_{\alpha} \langle \underline{v}_{\alpha} \rangle \cdot \langle \underline{v}_{\alpha} \rangle . \quad (2.52)$$

Using (2.30), (2.50), and (2.51) in (2.49)

$$\begin{aligned} \frac{1}{2} N_{\alpha} m_{\alpha} \langle v_{\alpha}^2 \rangle &= Q_{\alpha} + \underline{\Psi}_{\alpha} \cdot \langle \underline{v}_{\alpha} \rangle + \frac{3}{2} N_{\alpha} k \hat{T}_{\alpha} \langle v_{\alpha} \rangle \\ &+ \frac{1}{2} N_{\alpha} m_{\alpha} \langle \underline{v}_{\alpha} \rangle \langle \underline{v}_{\alpha} \rangle \cdot \langle \underline{v}_{\alpha} \rangle . \end{aligned} \quad (2.53)$$

Substituting (2.52) and (2.53) into (2.45), the energy equation becomes

$$\begin{aligned} \frac{3}{2} \frac{\partial}{\partial t} (N_{\alpha} k \hat{T}_{\alpha}) + \frac{1}{2} m_{\alpha} \frac{\partial}{\partial t} (N_{\alpha} \langle \underline{v}_{\alpha} \rangle \cdot \langle \underline{v}_{\alpha} \rangle) + \frac{\partial}{\partial \underline{r}} \cdot Q_{\alpha} \\ + \frac{\partial}{\partial \underline{r}} \cdot (\underline{\Psi}_{\alpha} \cdot \langle \underline{v}_{\alpha} \rangle) + \frac{3}{2} \frac{\partial}{\partial \underline{r}} \cdot (N_{\alpha} k \hat{T}_{\alpha} \langle \underline{v}_{\alpha} \rangle) \\ + \frac{1}{2} m_{\alpha} \frac{\partial}{\partial \underline{r}} \cdot (N_{\alpha} \langle \underline{v}_{\alpha} \rangle \langle \underline{v}_{\alpha} \rangle \cdot \langle \underline{v}_{\alpha} \rangle) - q_{\alpha} N_{\alpha} \hat{E}_t \cdot \langle \underline{v}_{\alpha} \rangle \\ = \frac{1}{2} m_{\alpha} \int v_{\alpha}^2 \left( \frac{\partial f_{\alpha}}{\partial t} \right)_c dv_{\alpha} . \end{aligned} \quad (2.54)$$

In applying Eq. (2.54) to the neutrals, a vast simplification occurs because  $\langle \underline{v}_n \rangle$  and  $q_n$  are zero. The equation becomes

$$\frac{3}{2} \frac{\partial}{\partial t} (N_n k \hat{T}_n) + \frac{\partial}{\partial \underline{r}} \cdot Q_n = \frac{1}{2} m_n \int v_n^2 \left( \frac{\partial f_n}{\partial t} \right)_c dv_n . \quad (2.55)$$

Eventually (2.55) becomes an equation for  $\hat{T}_n$ , but further approximations are necessary and are considered later.

Equation (2.54) is not applied to the electrons and ions. The electron temperature is determined directly from the solution to the Boltzmann equation for  $f_e$ , which is available in the work of Frost

and Phelps [11]. The applicability of their results to our problem is discussed later. The ion temperature is assumed equal to the neutral temperature, so in place of the ion energy equation we have

$$\hat{T}_i = \hat{T}_n . \quad (2.56)$$

This assumption has been used in previous treatments of the positive column by Ecker and Zoller [9], Blank [4], and others, and its justification is usually given verbally: because of their large mass the ions gain energy from the applied field relatively slowly and readily transfer it to the neutrals through elastic collisions. A simplified model is set up in Appendix C to test this hypothesis, and the results of Eq. (C.13) show  $\hat{T}_i$  to be considerably greater than  $\hat{T}_n$  for conditions typical of our glow discharge. Nevertheless (2.56) is adopted as an approximation in the work that follows. A study of the variables and parameters used in Part II shows that this approximation has very little effect on the solution for the dimensionless quantities. The same is probably true of the work in Part III, although the analysis is more difficult.

#### Closure of Moment Equations

The equations obtained above can be regarded as equations for the densities, fluxes, and temperatures of the three species. However, in the derivations other quantities were introduced, which are indeterminate. In particular, the question of what to do with  $\underline{\Psi}_\alpha$  and  $\underline{Q}_n$  must be confronted. The answer chosen is a standard method of closing the system of equations.

Before applying approximations to the form of the pressure tensor, it is convenient to define the scalar pressure  $p_\alpha$  as one-third of its trace. Using (2.30),

$$p_\alpha = \frac{1}{3} \underline{\underline{I}} : \underline{\underline{\Psi}}_\alpha = \frac{1}{3} N_\alpha m_\alpha \langle v_\alpha^2 \rangle \quad (2.57)$$

where  $\underline{\underline{I}}$  is the unit tensor. The interpretation of  $p_\alpha$  as the hydrostatic pressure is discussed in books on kinetic theory\*. The definition of  $p_\alpha$  by (2.57) ignores intermolecular forces and considers only momentum transfer. Hence  $p_\alpha$  represents the pressure of a perfect gas, and in fact (2.57) and (2.50) show that

$$p_\alpha = N_\alpha k \hat{T}_\alpha \quad (2.58)$$

The assumption made to permit determination of  $\underline{\underline{\Psi}}_\alpha$  is that the pressure is isotropic, i.e.,

$$\underline{\underline{\Psi}}_\alpha = p_\alpha \underline{\underline{I}} \quad (2.59)$$

Equation (2.30) shows that this relation is certainly true when the distribution function  $f_\alpha$  is isotropic in velocity space about the mean velocity. In the case of the neutral molecules the mean velocity is almost zero, and compared to the large number of neutral-neutral collisions, there is little to cause anisotropy; the approximation of (2.59) is surely valid. Equations (C.17) and (C.21) of Appendix C

---

\* See Chapman and Cowling [5], pp. 31-35.

show that the random thermal velocity of the electrons is much larger than the drift velocity. On this basis the deviation of the electron distribution function from an isotropic state is regarded as a small perturbation, and Eq. (2.59) is a correspondingly good approximation. On the other hand, (C.6) and (C.11) show that the same argument is not applicable to the ions. Nevertheless, the momentum interchange as a result of ion-neutral collisions is considerable, and the distribution of ion velocities about the mean is expected to be primarily random. In any case, the approximation of (2.56) assumes such a thorough interaction between ions and neutrals that consistency requires  $\underline{\Psi}_i$  to be considered isotropic.

The two terms on the left-hand side of Eq. (2.55) refer to random translational energy and its transfer. However, in a diatomic gas such as  $H_2$  where rotational and vibrational energy is also involved, the interchange of internal and translational energy complicates the separation of the two types of energy transfer. The difficulty emerges in the calculation of the integral on the right-hand side, since it must account for all the mechanisms producing translational energy. On the other hand, if Eq. (2.55) had been derived by setting  $\phi_\alpha$  in Eq. (2.44) equal to the total energy of a particle, the integral would represent the total rate of energy transfer per unit volume to the neutrals and could be easily determined.  $\frac{3}{2} k\hat{T}_n$  would then be replaced by the average total energy per neutral molecule and  $\underline{Q}_n$  by the total energy flux. At steady state the difficulty in separating internal and translational energy would occur in  $\underline{Q}_n$

rather than in the integral. When the gas molecules possess only translational energy, a Chapman-Enskog analysis of the Boltzmann equation leads to an expression for  $\underline{Q}_n$  given by

$$\underline{Q}_n = - \hat{\lambda} \frac{\partial \hat{T}_n}{\partial \underline{r}} \quad * \quad (2.60)$$

The analysis of "rough spherical molecules" suggests that the effect of rotational energy transfer can be included in (2.60) by modifying the value of  $\hat{\lambda}$  \*\*. However, the work of Engelhardt and Phelps [10] shows that a large portion of the energy transferred to  $H_2$  molecules by electron impact appears as vibrational energy. Nevertheless calculations and physical intuition \*\*\* show that conduction of internal energy is less efficient than conduction of translational energy, and we assume as an approximation that the total heat flux can be represented by Eq. (2.60). The assumption is particularly appropriate, since the experimental data used in evaluating  $\hat{\lambda}$  do not distinguish between the different means of energy transfer.

Since we assume  $\underline{Q}_n$  to be the total heat flux, the right-hand side of (2.55) represents the net rate per unit volume at which the neutral energy increases as a result of particle interactions. Radiation need not be considered as an energy loss, since it has been found

---

\* See Chapman and Cowling [5], pp. 121-122.

\*\* Chapman and Cowling [5], pp. 210-212.

\*\*\* Chapman and Cowling [5], pp. 236-237; Jeans [16], pp. 296-298; Hirschfelder, Curtiss and Bird [13], pp. 498-506.

to be negligible<sup>\*</sup>. We also neglect any energy lost by direct interaction of the charged particles with the walls of the discharge. With these considerations the rate at which the neutrals acquire energy in a steady state is the same as the rate at which the charged particles acquire it from the applied electric field. For a charged particle of type  $\alpha$  the rate per unit volume is given by

$$R_{\alpha} = \int q_{\alpha} \hat{E}_z \cdot \underline{v}_{\alpha} f(\underline{v}_{\alpha}) d\underline{v}_{\alpha} \quad (2.61)$$

$$= N_{\alpha} q_{\alpha} \hat{E}_z \cdot \langle \underline{v}_{\alpha} \rangle \quad (2.62)$$

$$= N_{\alpha} |q_{\alpha}| \hat{E}_z w_{\alpha} \quad (2.63)$$

where  $\hat{E}_z$  is the axial electric field and  $w_{\alpha}$  is the drift velocity. This expression shows that the relative rates at which electrons and ions transfer energy are in the proportion of their drift velocities, since their densities are approximately equal. The ratio of drift velocities is given in Eq. (C.22) of Appendix C and shows the contribution of the ions to the energy transfer can be neglected as an approximation. This approximation is consistent with the previous assumption that  $\hat{T}_i = \hat{T}_n$ . We now write

$$\frac{1}{2} m_n \int v_n^2 \left( \frac{\partial f_n}{\partial t} \right)_c d\underline{v}_n = \hat{h} N_e \quad (2.64)$$

where

$$\hat{h} = e \hat{E}_z w_e \quad (2.65)$$

---

<sup>\*</sup>Cobine [6], p. 235.

represents the average energy transferred per electron per unit time. The use of data for the evaluation of  $w_e$  is discussed later.

It is of interest to calculate the rate at which neutrals gain translational energy directly from electron impact. In view of the ambiguity involved in relating  $Q_n$  to  $\hat{\lambda}$  and  $\hat{T}_n$ , this rate and the one calculated in (2.63) provide bounds on the appropriate value of the right-hand side of (2.55). However, the interchange between internal and translational energy is sufficiently rapid\* that the translational energy-transfer rate is not a close approximation to  $\hat{h}$  unless it is the predominant mechanism for electron energy loss. Its calculation below permits a comparison between its value and that of  $\hat{h}$ . An expression for the translational energy-transfer rate from neutrals to electrons is available in Eq. (B.34) of Appendix B. The transfer rate from electrons to neutrals is just the negative of this expression and in the nomenclature of this section becomes

$$R = 2 \frac{m_e}{m_n} \int \left( \frac{1}{2} m_e v_e^2 - \left\langle \frac{1}{2} m_n v_n^2 \right\rangle \right) f_e(\underline{v}_e) v_m(\underline{v}_e) d\underline{v}_e \quad (2.66)$$

We define an average or effective  $v_m$  by rewriting (2.66) as

$$R = 2 \frac{m_e}{m_n} v_m N_e \left( \left\langle \frac{1}{2} m_e v_e^2 \right\rangle - \left\langle \frac{1}{2} m_n v_n^2 \right\rangle \right) \quad (2.67)$$

A comparison of this definition of the effective  $v_m$  with that described in the discussion following Eq. (2.35) shows that the averages involved

---

\* See Vincenti and Kruger [25], pp. 198-206, for a discussion of internal energy relaxation.

are somewhat different. However,  $v_m(v_e)$  does not vary greatly as  $v_e$  changes, so the numerical values of the two effective  $v_m$ 's differ only slightly, and the same data are used for both. The average energies in (2.67) can be expressed in terms of the temperatures with the use of Eq. (2.52). Since the mean velocity is much less than the random velocity for both electrons and neutrals (compare (C.17) and (C.21) of Appendix C), Eq. (2.67) can be written as

$$R = 2 \frac{m_e}{m_n} v_m N_e \left( \frac{3}{2} kT_e - \frac{3}{2} kT_n \right) \quad (2.68)$$

$$= \hat{h}_o N_e \quad (2.69)$$

where

$$\hat{h}_o = 2 \frac{m_e}{m_n} v_m \left( \frac{3}{2} kT_e - \frac{3}{2} kT_n \right) \quad (2.70)$$

represents the average translational energy transferred per electron per unit time. The comparison of  $\hat{h}$  and  $\hat{h}_o$  in Fig. 4 shows that roughly 10% of the electron-neutral energy transfer involves translational energy.

In using the rate expressions of (2.64) or (2.68) in (2.55), it is implicitly assumed that the electron energy is transferred to the neutrals at the same location where it is acquired from the axial field. The accuracy of this assumption can be checked by comparing the time required for an electron to lose its energy with the time during which it changes its position by a representative amount. Since quantities do not vary in the axial direction in the positive column, it is the time required for movement in the radial direction that must be

determined. An estimate of this time is provided by  $\tau_a$  in Eq. (C.41) of Appendix C. The electron energy relaxation time for elastic collisions provides a measure of the time during which an electron loses most of its energy; it can be found by dividing the mean energy of an electron  $\frac{3}{2} k\hat{T}_e$  by  $\hat{h}_o$ . Since  $\hat{T}_e \gg \hat{T}_n$ , Eq. (2.70) shows that

$$\tau_e = \frac{1}{2 \frac{m_e}{m_n} v_m} \quad . \quad (2.71)$$

Using the value for  $v_m$  in (C.20), we obtain

$$\tau_e = 2.90 \times 10^{-7} \text{ sec.} \quad (2.72)$$

and find that  $\tau_e \ll \tau_a$ . Since  $\hat{h} > \hat{h}_o$ , the actual energy relaxation time is less than  $\tau_e$ . Hence we conclude that the expression in (2.65) can accurately be used in Eq. (2.55) in an inhomogeneous situation.

### Final Moment Equations

Using the approximations considered above, the continuity, momentum, and energy equations can be written in their final form. It should be remembered that although the vector notation appears general, approximations have been made that depend on the geometry of the application. The continuity equations can be rewritten directly from Eqs. (2.23) and (2.24) :

$$\frac{\partial N_e}{\partial t} + \frac{\partial}{\partial \underline{r}} \cdot \underline{\hat{J}}_e = \hat{\nu}_I N_e - \hat{\alpha} N_e N_i \quad (2.73)$$

$$\frac{\partial N_i}{\partial t} + \frac{\partial}{\partial \underline{r}} \cdot \underline{\hat{J}}_i = \hat{\nu}_I N_e - \hat{\alpha} N_e N_i \quad . \quad (2.74)$$

Equations (2.36) and (2.42) are rewritten using (2.59) and (2.58):

$$m_e \frac{\partial \underline{\hat{J}}_e}{\partial t} + \frac{\partial}{\partial \underline{r}} (N_e k \hat{T}_e) + N_e e \underline{\hat{E}}_t = -m_e \nu_m \underline{\hat{J}}_e \quad (2.75)$$

$$m_i \frac{\partial \underline{\hat{J}}_i}{\partial t} + \frac{\partial}{\partial \underline{r}} (N_i k \hat{T}_i) - N_i e \underline{\hat{E}}_t = -m_i \nu_i \underline{\hat{J}}_i \quad . \quad (2.76)$$

The neutral energy equation is obtained from (2.55) using (2.43), (2.58), (2.60) and (2.64):

$$\frac{3}{2} \frac{\partial p}{\partial t} - \frac{\partial}{\partial \underline{r}} \cdot (\hat{\lambda} \frac{\partial \hat{T}_n}{\partial \underline{r}}) = \hat{h} N_e \quad . \quad (2.77)$$

The use of (2.58) assumes the neutral species behaves as a perfect gas. Since (2.43) associates  $p_n$  with the mechanical pressure  $p$ , which is uniform throughout the system, the equation

$$p = N_n k \hat{T}_n \quad (2.78)$$

relates  $N_n$  to  $\hat{T}_n$  in a simple manner. Although  $N_n$  does not appear directly in the equations of change above, it is needed for the determination of many of the coefficients.

Equations (2.73) - (2.77) form a system of five equations for the unknowns  $N_e$ ,  $N_i$ ,  $\underline{\hat{J}}_e$ ,  $\underline{\hat{J}}_i$ , and  $\hat{T}_n$ . Before they can be solved, boundary conditions appropriate to the application must be applied, and the variation of  $\underline{\hat{E}}_t$  and the coefficients  $\nu_m$ ,  $\nu_i$ ,  $\hat{\lambda}$ , and  $\hat{h}$  must be determined.

### 3. APPLICATION OF EQUATIONS TO THE POSITIVE COLUMN

In applying the equations of change to the positive column several simplifications occur. In the first place, only the steady state problem is considered, so all the time derivatives disappear. Also, it has been mentioned that there is no variation along the column in the axial direction. The discussion in the Introduction stated that in the interest of mathematical simplicity the actual cylindrical geometry would be replaced by the corresponding slab geometry. In this case the discharge is contained between two parallel walls, and the axial field is applied parallel to them. The discharge is symmetric about a plane dividing it, and the only spatial variation is in the direction perpendicular to the walls.

#### Equations of Change

At steady state Eqs. (2.73) and (2.74) show that  $\hat{J}_e$  and  $\hat{J}_i$  have equal radial components. This conclusion is easily reached by considering the integration of both equations from a particular value of  $x$ , the coordinate perpendicular to the wall. Only the "radial" or  $x$ -derivatives of the "radial" components of the fluxes appear in the equations, and these derivatives are equal. From symmetry considerations there can be no flux toward the walls at the center of the discharge, and hence integration from the center shows the electron and ion "radial" fluxes to be equal everywhere. Equations (2.73) and (2.74) now become

$$\frac{d\hat{J}}{dx} = \hat{v}_i N_e - \hat{\alpha} N_e N_i \quad (3.1)$$

where  $\hat{J}$  is the common value of the "radial" or transverse components of  $\hat{J}_e$  and  $\hat{J}_i$ .

The momentum equations (2.75) and (2.76) are used in the transverse direction only. After a slight rearrangement, they become

$$\hat{J} = -\hat{D}_e \frac{dN_e}{dx} - \frac{k}{m_e v_m} N_e \frac{dT_e}{dx} - \hat{\mu}_e N_e \hat{E} \quad (3.2)$$

and

$$\hat{J} = -\hat{D}_i \frac{dN_i}{dx} - \frac{k}{m_i v_i} N_i \frac{dT_i}{dx} + \hat{\mu}_i N_i \hat{E} \quad (3.3)$$

where

$$\hat{D}_e = \frac{kT_e}{m_e v_m} \quad (3.4)$$

$$\hat{\mu}_e = \frac{e}{m_e v_m} \quad (3.5)$$

$$\hat{D}_i = \frac{kT_i}{m_i v_i} \quad (3.6)$$

$$\mu_i = \frac{e}{m_i v_i} \quad (3.7)$$

and  $\hat{E}$  is the transverse component of the electric field.  $\hat{D}_e$ ,  $\hat{\mu}_e$ ,  $\hat{D}_i$ ,  $\hat{\mu}_i$  are the diffusion and mobility coefficients of electrons and ions, and the Einstein relations follow immediately from their definitions:

$$\frac{\hat{D}_e}{\hat{\mu}_e} = \frac{kT_e}{e} \quad (3.8)$$

$$\frac{\hat{D}_i}{\hat{\mu}_i} = \frac{kT_i}{e} \quad (3.9)$$

Equations (3.2) and (3.3) are written so as to show the contribution

of various terms to the flux toward the walls. The first term represents diffusion as a result of a density gradient; the second involves the effect of electron and ion temperature gradients; and the third gives the contribution from the transverse field. In preparation for the eventual mathematical analysis, it is convenient to rewrite the momentum equations so that the density gradients appear alone. Using (3.4) - (3.9), Eqs. (3.2) and (3.3) become

$$\frac{dN_e}{dx} + \frac{1}{\hat{T}_e} N_e \frac{d\hat{T}_e}{dx} = - \frac{e}{k\hat{T}_e} N_e \hat{E} - \frac{1}{\hat{D}_e} \hat{J} \quad (3.10)$$

$$\frac{dN_i}{dx} + \frac{1}{\hat{T}_i} N_i \frac{d\hat{T}_i}{dx} = \frac{e}{k\hat{T}_i} N_i \hat{E} - \frac{1}{\hat{D}_i} \hat{J} \quad (3.11)$$

The energy equation (2.77) is most conveniently written in the form

$$\frac{d^2 \hat{T}}{dx^2} + \frac{1}{\hat{\lambda}} \frac{d\hat{\lambda}}{dx} \frac{d\hat{T}}{dx} = - \frac{\hat{h}}{\hat{\lambda}} N_e \quad (3.12)$$

where  $\hat{T}$  has replaced  $\hat{T}_n$  in a notational change.

The transverse electric field  $\hat{E}$  enters rather intimately in Eqs. (3.10) and (3.11), and an equation for it is obtained from Poisson's equation for the electric field\*

$$\frac{\partial}{\partial \underline{r}} \cdot \hat{\underline{E}}_t = \frac{\rho}{\epsilon_0} \quad (3.13)$$

where  $\rho$  is the charge density and  $\epsilon_0$  is the permittivity of free

---

\* See, for instance, Panofsky and Phillips [20], p. 11.

space. The equation is written in rationalized mks units. Since the charge density is the result of electron and ion concentrations, Poisson's equation applied to the positive column becomes

$$\frac{d\hat{E}}{dx} = \frac{e}{\epsilon_0} (N_i - N_e) \quad . \quad (3.14)$$

### Boundary Conditions

(3.1), (3.10)-(3.12), and (3.14) constitute a set of five equations for the five unknowns  $\hat{J}$ ,  $N_e$ ,  $N_i$ ,  $\hat{T}$ ,  $\hat{E}$ . The other quantities appearing in the equations can be expressed as functions of  $\hat{T}$ ,  $N_n$ , and  $\hat{E}_t$  with the use of data from other sources.

Before the equations can be solved, boundary conditions must be imposed upon the variables. Several are easily determined from the symmetry about the center of the discharge. Designating the center plane by  $x = 0$  we have

$$x = 0 : \quad \hat{J} = 0 \quad (3.15)$$

$$\hat{E} = 0 \quad (3.16)$$

$$\frac{d\hat{T}}{dx} = 0 \quad . \quad (3.17)$$

The boundary conditions at the wall are not as easily determined. We assume as an approximation that the electron and ion densities are zero there<sup>\*</sup>. This condition is not exact, of course, since the equation  $\frac{\hat{J}}{-\alpha} = N_\alpha \langle \underline{v}_\alpha \rangle$  would then predict a zero flux of charged particles to the

---

<sup>\*</sup>A detailed discussion of the boundary conditions is given in McDaniel [19], pp. 496-497.

wall. However, the wall absorbs essentially all of the electrons and ions that strike it, and the densities are very small near it. The transfer of heat to the wall by conduction by the neutral gas is influenced by conditions outside the plasma. As a boundary condition we choose to specify the temperature of the neutrals at the wall. The conditions at the wall now become

$$x = L : \quad N_e = 0 \quad (3.18)$$

$$N_i = 0 \quad (3.19)$$

$$\hat{T} = \hat{T}_w \quad (3.20)$$

where  $L$  is the distance from the center of the discharge to the wall. The equations are solved for  $0 \leq x \leq L$ , and the solution in the other half of the discharge can be obtained by symmetry.

#### 4. SOURCES OF DATA

The equations for  $\hat{J}$ ,  $N_e$ ,  $N_i$ ,  $\hat{T}$ , and  $\hat{E}$  involve coefficients that have to be determined from experimental data. The derivation of the equations shows that these coefficients are or involve integrals over cross sections and distribution functions, both of which are unknown. However, data are available from various sources, and their use and applicability are discussed below.

##### Data for Electrons

Data for the coefficients depending on the electron distribution function are obtained from the work of Frost and Phelps [11] and Engelhardt and Phelps [10]. They solve the Boltzmann equation directly for  $f_e(\underline{v}_e)$  in a steady-state, spatially uniform situation. There is an applied electric field and the collision integral includes, in addition to elastic electron-neutral collisions, such inelastic effects as ionization and rotational, vibrational and electronic excitation. The cross sections for these processes appear in the equation and are initially unknown. Using assumed values for them, the Boltzmann equation is solved, and  $f_e(\underline{v}_e)$  is used to evaluate such macroscopic quantities as drift velocity and electron temperature. These quantities are compared to experimentally determined values, and the assumed cross sections are varied and  $f_e$  recalculated until agreement is reached. The final result is a set of cross sections that can be used to calculate drift velocities, electron temperatures, diffusion coefficients, etc. over a wide range of the parameters appearing in the Boltzmann equation. These parameters are the electric field and variables determining the

state of the neutral gas— $p$ ,  $\hat{T}$ , and  $N_n$  (related to  $p$  and  $\hat{T}$  by Eq. (2.78)). It is found that at constant  $N_n$  the distribution function varies very little with  $\hat{T}$ . Also,  $N_n$  and the electric field  $\hat{E}_t$  always appear together in the Boltzmann equation in the form  $\hat{E}_t/N_n$ . Consequently, the calculated quantities such as drift velocities and mobilities can be expressed as functions of  $\hat{E}_t/N_n$  multiplied perhaps by simple multiples of  $\hat{E}_t$  or  $N_n$ . Graphical results for these quantities are presented in the publications cited above, and the details involved in their use in our equations are discussed below. First, however, it is necessary to consider the general applicability of the data.

In our situation the total electric field  $\hat{E}_t$  and the neutral number density  $N_n$  vary with position in the transverse direction. The variation of  $\hat{E}_t$  constitutes no problem and is easily disposed of. Equations (C.2) - (C.4) of Appendix C show that the effect of a representative value of the transverse field on  $\hat{E}_t$  is very small. In fact, in applying the data to our problem,  $\hat{E}_t$  is replaced by our  $\hat{E}_z$ . The variation of  $N_n$ , however, requires a more detailed analysis. In evaluating the coefficients at a particular position we wish to use the local value of  $N_n$ . The justification of such a procedure requires that the electron distribution function  $f_e$  adjust very rapidly to a change in  $N_n$ . A criterion to establish whether the adjustment is sufficiently rapid is discussed in Appendix C. It consists of a comparison of the time required for  $f_e$  to respond significantly to a change in  $N_n$  with the time required for a typical group of electrons to travel between locations of significantly different  $N_n$ . An

estimate of the latter time is given by the ambipolar diffusion time in Eq. (C.41). A comparison of the ambipolar diffusion time with the response time of Eq. (C.36) shows the adjustment of  $f_e$  to be faster by several orders of magnitude. Thus we conclude that we are justified in using the local value of  $N_n$  to evaluate the coefficients in our equations from the data.

Data for electron temperature, ionization coefficient, and drift velocity in  $H_2$  are presented by Frost and Phelps [11] and Engelhardt and Phelps [10] in the form

$$kT_e/e = f_E(\hat{E}_z/N_n) \quad (4.1)$$

$$\hat{\alpha}_I/N_n = f_I(\hat{E}_z/N_n) \quad (4.2)$$

$$w_e = w_e(\hat{E}_z/N_n) \quad (4.3)$$

$\hat{\alpha}_I$  is Townsend's first ionization coefficient and represents the expected number of ionizing collisions an electron experiences in travelling a net distance of one centimeter in the field direction. It is related to the ionization coefficient  $\hat{v}_I$  by

$$\hat{v}_I = \hat{\alpha}_I w_e \quad (4.4)$$

Graphs displaying the data for  $f_E$ ,  $f_I$ , and  $w_e$  are presented in Figs. 5, 6, and 7. The data are adapted to computer calculations through the use of least-squares polynomial fits which determine  $f_E$ ,  $f_I$ , and  $w_e$  as functions of  $\hat{E}_z/N_n$ .

A number of the coefficients appearing in the equations of change can now be expressed in terms of  $f_E$ ,  $f_I$ , and  $w_e$ . In writing the expressions it is convenient to use Eq. (2.78) to eliminate  $N_n$  as a variable in preference to  $p$  and  $\hat{T}$ . The dependence of the variables on  $\hat{E}_z$ ,  $p$ , and  $\hat{T}$  is written explicitly. Although  $\hat{E}_z$  and  $p$  are constant throughout the discharge,  $\hat{T}$  is a dependent variable in the equations, so the coefficients vary with  $x$ . The electron temperature in Eq. (4.1) is now written as

$$\hat{T}_e(\hat{T}; \hat{E}_z, p) = \frac{e}{k} f_E \left( \frac{\hat{E}_z}{p} k\hat{T} \right) \quad (4.5)$$

Using (4.2) - (4.4), the ionization coefficient is evaluated by the equation

$$\hat{v}_I(\hat{T}; \hat{E}_z, p) = \frac{p}{k\hat{T}} w_e \left( \frac{\hat{E}_z}{p} k\hat{T} \right) f_I \left( \frac{\hat{E}_z}{p} k\hat{T} \right) \quad (4.6)$$

The electron mobility as defined by Eq. (3.5) can be determined from knowledge of  $v_m$ , and data for  $v_m$  are available in Frost and Phelps [11]. Furthermore, our definition of an effective  $v_m$ , as discussed following Eq. (2.35), coincides with theirs. However,  $v_m$  can be related to  $w_e$  by applying the electron momentum equation in the axial direction. Although  $w_e$  is usually defined as the magnitude of the mean velocity in the direction of the field, the differences between the axial field and axial velocity and the total field and total velocity are negligible (see Appendix C, Eqs. (C.2), (C.4), (C.21), (C.40)). Equation (2.75) in the axial direction now becomes

$$N_e e \hat{E}_z = m_e v_m N_e w_e \quad (4.7)$$

or

$$v_m = \frac{e \hat{E}_z}{m_e w_e} \quad (4.8)$$

In evaluating the coefficients in the equations, the data for  $w_e$  are used rather than that for  $v_m$ . From (3.5) and (4.8),  $\mu_e$  is found by

$$\hat{\mu}_e(\hat{T}; \hat{E}_z, p) = w_e \left( \frac{\hat{E}_z}{p} k\hat{T} \right) / \hat{E}_z \quad (4.9)$$

$\hat{D}_e$  is now obtained from (3.8) using (4.5) and (4.9):

$$\hat{D}_e(\hat{T}; \hat{E}_z, p) = w_e \left( \frac{\hat{E}_z}{p} k\hat{T} \right) f_E \left( \frac{\hat{E}_z}{p} k\hat{T} \right) / \hat{E}_z \quad (4.10)$$

The expressions for  $\hat{h}$  and  $\hat{h}_o$  in Eqs. (2.65) and (2.70) become

$$\hat{h}(\hat{T}; \hat{E}_z, p) = e \hat{E}_z w_e \left( \frac{\hat{E}_z}{p} k\hat{T} \right) \quad (4.11)$$

$$\hat{h}_o(\hat{T}; \hat{E}_z, p) = \frac{3k e \hat{E}_z}{m_n w_e \left( \frac{\hat{E}_z}{p} k\hat{T} \right)} \left[ \frac{e}{k} f_E \left( \frac{\hat{E}_z}{p} k\hat{T} \right) - \hat{T} \right] \quad (4.12)$$

The derivative of  $\hat{T}_e$  appearing in Eq. (3.10) is converted to a derivative of  $\hat{T}$  with the use of Eq. (4.5):

$$\frac{d\hat{T}_e}{dx} = \frac{\partial \hat{T}_e}{\partial \hat{T}} \frac{d\hat{T}}{dx} \quad (4.13)$$

$$= \frac{e \hat{E}_z}{p} f'_E \left( \frac{\hat{E}_z}{p} k\hat{T} \right) \frac{d\hat{T}}{dx} \quad (4.14)$$

The numerical evaluation of  $f'_E$  by the computer is accomplished by

differentiation of the least-squares polynomial for  $f_E$ . Figure 8 compares this computation with an attempted direct numerical differentiation of the data.

### Data for Ions

Data that are sufficient to determine the ion mobility and diffusion coefficient for our application are given in McDaniel [19], p. 472. Experimental and theoretical results show that, as in the case of electrons,  $\hat{E}_z/N_n$  is a basic parameter in determining the property of the ions. It is found that at constant  $\hat{E}_z$  and  $N_n$  the ion mobility is very insensitive to changes in temperature\*. Also, at constant  $\hat{E}_z/N_n$  it varies inversely with  $N_n^*$ . Through deference to tradition the neutral density is seldom mentioned in the presentation of mobility data, and in its place appears a "reduced" pressure  $p_o$  given by

$$p_o = \frac{\hat{T}^o}{\hat{T}} p \quad (4.15)$$

$$= N_n k \hat{T}^o \quad , \quad (4.16)$$

where

$$\hat{T}^o = 273^oK \quad . \quad (4.17)$$

The reduced mobility  $\hat{\mu}_i^o$  (mobility at a gas temperature of  $\hat{T}^o = 273^oK$  and a pressure of  $p^o = 760$  mm Hg) is presented by McDaniel [19], p.472, as a function of  $\hat{E}_z/p_o$ . It is related to the mobility under other

---

\*McDaniel [19], pp. 427-428.

conditions by the equation

$$\hat{\mu}_i = \frac{N_n^0}{N_n} \hat{\mu}_i^0 \quad (4.18)$$

where

$$N_n^0 = \frac{p^0}{kT^0} \quad (4.19)$$

$$= 2.69 \times 10^{19} \text{ cm}^{-3} \quad (4.20)$$

Again we eliminate  $N_n$  as a variable by means of the perfect gas law and write  $\hat{\mu}_i$  as a function of  $\hat{E}_z$ ,  $p$ , and  $\hat{T}$  in the form

$$\hat{\mu}_i(\hat{T}; \hat{E}_z, p) = \frac{p^0}{p} \frac{\hat{T}}{\hat{T}^0} \hat{\mu}_i^0 \left( \frac{\hat{E}_z \hat{T}}{p \hat{T}^0} \right) \quad (4.21)$$

The data are adapted to computer calculations by means of a least-squares polynomial expressing  $\hat{\mu}_i^0$  as a function of  $\hat{E}_z \hat{T} / (p \hat{T}^0)$  or  $\hat{E}_z / p_0$ . A graph of the data is given in Fig. 9. The ion diffusion coefficient can now be obtained from Eq. (3.9).  $\hat{T}_i$  has already been assumed equal to  $\hat{T}$  (Eq. (2.56)), so  $\hat{D}_i$  becomes

$$\hat{D}_i(\hat{T}; \hat{E}_z, p) = \frac{k}{e} \frac{p^0}{p} \frac{\hat{T}^2}{\hat{T}^0} \hat{\mu}_i^0 \left( \frac{\hat{E}_z \hat{T}}{p \hat{T}^0} \right) \quad (4.22)$$

It is now necessary to perform an analysis similar to that done for the electrons to show that the data are applicable in a nonuniform situation.  $\mu_i$  is related to the ion distribution function through Eq. (3.7), which involves  $v_i$ , and Eqs. (2.40) and (2.41), which give  $v_i$  as an average quantity obtained from integrations over  $f_i(v_i)$ . This relation shows that the time for  $\hat{\mu}_i$  and  $\hat{D}_i$  to respond to

changes in  $N_n$  is the same as the response time for  $f_i$ . Because of the efficient energy interchange between ions and neutral molecules, the response time for  $f_i$  is essentially the same as the energy relaxation time given in Eq. (C.10) of Appendix C. In order to justify use of the local  $N_n$  in evaluating  $\hat{\mu}_i$  and  $\hat{D}_i$ , the response time must be much less than the time during which the ions experience a significant change in  $N_n$ . This latter time is of the same order of magnitude as the ambipolar diffusion time found in Eq. (C.41). A comparison of the two times shows that it is indeed appropriate to express the transverse variation of  $\hat{\mu}_i$  and  $\hat{D}_i$  in the positive column through use of the local neutral density.

#### Recombination Coefficient

The data available for the electron-ion recombination coefficient in  $H_2$  are scarce and unreliable. It was once thought that the dissociative recombination reaction of Eq. (2.12) was characterized by a large recombination coefficient\*. In fact microwave measurements by Biondi and Brown [3] in the afterglow of an  $H_2$  plasma yielded a value for  $\hat{\alpha}$  of  $2 \times 10^{-6}$  cm<sup>3</sup>/sec. However, a later paper by Persson and Brown [22] attributes such a high value to other factors and concludes that in  $H_2$  the recombination coefficient is negligible within experimental error and is thus less than  $3 \times 10^{-8}$  cm<sup>3</sup>/sec. The same conclusion is also reached by Popov and Afanaseva [23]. Furthermore,

---

\* See McDaniel [19], pp. 590-591, 607-609; Hasted [12], pp. 267-268; Bates [2], p. 267.

in the afterglow the electron and neutral temperatures are equal. In the positive column, where the electron temperature is much higher, the recombination coefficient is expected to be less because of the increased difficulty in dissipating the kinetic energy of electrons. Nevertheless, in the absence of better data  $\hat{\alpha}$  is given the value

$$\hat{\alpha} = 3.00 \times 10^{-8} \text{ cm}^3/\text{sec} \quad (4.23)$$

in studying the effect of recombination in the positive column. The numerical calculations which depend critically on the value of  $\hat{\alpha}$  in the solution of the equations in Part II must be regarded with considerable skepticism, but the qualitative nature of the solutions is the same as for a smaller  $\hat{\alpha}$ . A larger value of  $\hat{\alpha}$  results in the effect of recombination becoming significant at lower values of the electron density. Although the recombination coefficient in an  $\text{H}_2$  plasma is small, it is considerably larger for certain other gases and may be an important factor in the abnormal-glow or arc regimes of the discharge characteristic.

#### Thermal Conductivity

The data used for the numerical evaluation of the thermal conductivity in  $\text{H}_2$  are found in the International Critical Tables [15] Vol. 5, pp. 213-214. At the conditions of interest  $\hat{\lambda}$  is essentially independent of pressure at constant temperature, and an empirical formula is presented there for  $\hat{\lambda}$  as a function of  $\hat{T}$ . A slight modification results in the following formula, valid in the range  $20.8^\circ\text{K} < \hat{T} < 373^\circ\text{K}$  :

$$\hat{\lambda}(\hat{T}) = \hat{\lambda}(300^{\circ}\text{K}) \frac{394^{\circ}\text{K}}{\hat{T} + 94^{\circ}\text{K}} \left(\frac{\hat{T}}{300^{\circ}\text{K}}\right)^{3/2} \quad (4.24)$$

where

$$\hat{\lambda}(300^{\circ}\text{K}) = 1.706 \times 10^4 \text{ gm cm sec}^{-3} \text{ }^{\circ}\text{K}^{-1} . \quad (4.25)$$

A moderate extrapolation by this formula is used to evaluate  $\hat{\lambda}$  for  $\hat{T} > 373^{\circ}\text{K}$ . Thermal conductivity data for gases in general are of rather low accuracy, and the extrapolation is not likely to cause significant error. In fact, the value of  $\hat{\lambda}(273^{\circ}\text{K})$  differs from that listed in Perry's Handbook [21], p.3-206 by roughly 10%. Data for  $\hat{\lambda}$  are available there at higher temperatures, and the deviation of that data from the extrapolated values indicates that the extrapolation is a reasonable approximation.

The derivative of  $\hat{\lambda}$  appearing in Eq. (3.12) is now converted into a derivative of  $\hat{T}$ :

$$\frac{d\hat{\lambda}}{dx} = \frac{d\hat{\lambda}}{d\hat{T}} \frac{d\hat{T}}{dx} . \quad (4.26)$$

$(1/\hat{\lambda})d\hat{\lambda}/d\hat{T}$  is evaluated using the empirical formula for  $\hat{\lambda}$ :

$$\frac{1}{\hat{\lambda}} \frac{d\hat{\lambda}}{d\hat{T}} = \frac{d}{d\hat{T}} \ln \hat{\lambda} \quad (4.27)$$

$$= \frac{\hat{T} + 282^{\circ}\text{K}}{2\hat{T}(\hat{T} + 94^{\circ}\text{K})} . \quad (4.28)$$

#### Domain of Data

Most coefficients in the equations of change are determined from experimental data for  $f_E$ ,  $f_I$ ,  $w_e$ , and  $\hat{\mu}_i^{\circ}$ , which are obtained as

functions of  $\hat{E}_z/N_n$ . However, the range of  $\hat{E}_z/N_n$  for which the various quantities are known differs, and the data can be used only in the range

$$0.43 \times 10^{-15} \text{ volt-cm}^2 < \hat{E}_z/N_n < 1.00 < 10^{-15} \text{ volt-cm}^2 \quad (4.29)$$

in which all coefficients can be evaluated. Although this range seems quite restricted, the variation of  $\hat{E}_z/N_n$  within its bounds causes  $\hat{v}_I$  to change over several orders of magnitude. The development of the problem in Part II shows that because of the large change in  $\hat{v}_I$  there are no practical limits on  $\hat{E}_z$  in the interpretation of  $\hat{E}_z$  as the parameter  $\lambda$  discussed in the Introduction. However, the bounds on  $\hat{E}_z/N_n$  do impose a limitation on the behavior of  $\hat{T}$  in the temperature-dependent studies of Part III.

5. DIMENSIONLESS PROBLEM

The final working equations are obtained by writing the equations for  $\hat{J}$ ,  $N_e$ ,  $N_i$ ,  $\hat{T}$  and  $\hat{E}$  in dimensionless form. They are then ready for the particular applications in Part II and Part III.

Dimensionless Coefficients and Variables

Reference values  $\hat{E}_{zr}$  and  $p_r$  for the axial electric field and the pressure are introduced in making the coefficients appearing in the equations dimensionless. The dimensionless coefficients are then defined as follows:

$$v_I(T; \hat{E}_z, p) = \frac{\hat{v}_I(\hat{T}; \hat{E}_z, p)}{\hat{v}_I(\hat{T}_w; \hat{E}_{zr}, p_r)} \quad (5.1)$$

$$T_e(T; \hat{E}_z, p) = \frac{\hat{T}_e(\hat{T}; \hat{E}_z, p)}{\hat{T}_e(\hat{T}_w; \hat{E}_{zr}, p_r)} \quad (5.2)$$

$$\mu_e(T; \hat{E}_z, p) = \frac{\hat{\mu}_e(\hat{T}; \hat{E}_z, p)}{\hat{\mu}_e(\hat{T}_w; \hat{E}_{zr}, p_r)} \quad (5.3)$$

$$D_e(T; \hat{E}_z, p) = \frac{\hat{D}_e(\hat{T}; \hat{E}_z, p)}{\hat{D}_e(\hat{T}_w; \hat{E}_{zr}, p_r)} \quad (5.4)$$

$$\mu_i(T; \hat{E}_z, p) = \frac{\hat{\mu}_i(\hat{T}; \hat{E}_z, p)}{\hat{\mu}_i(\hat{T}_w; \hat{E}_{zr}, p_r)} \quad (5.5)$$

$$D_i(T; \hat{E}_z, p) = \frac{\hat{D}_i(\hat{T}; \hat{E}_z, p)}{\hat{D}_i(\hat{T}_w; \hat{E}_{zr}, p_r)} \quad (5.6)$$

$$h(T; \hat{E}_z, p) = \frac{\hat{h}(\hat{T}; \hat{E}_z, p)}{\hat{h}(\hat{T}_w; \hat{E}_{zr}, p_r)} \quad (5.7)$$

$$h_o(T; \hat{E}_z, p) = \frac{\hat{h}_o(\hat{T}; \hat{E}_z, p)}{\hat{h}_o(\hat{T}_w; \hat{E}_{zr}, p_r)} \quad (5.8)$$

$$\lambda(T) = \frac{\hat{\lambda}(\hat{T})}{\hat{\lambda}(\hat{T}_w)} \quad (5.9)$$

where

$$T = \frac{\hat{T}}{\hat{T}_w} \quad (5.10)$$

The choice of  $\hat{E}_{zr}$  and  $p_r$  differs in the applications of Parts II and III, but in either case they are chosen so that the magnitude of the coefficients are of order unity throughout the discharge.

The dependent variables of the problem are also made dimensionless in such a way that their magnitudes are near unity in most of the discharge. The proper definition of some of the dimensionless variables is not obvious a priori and depends on hindsight gained in solving the problem. For notational simplicity in the definitions, it is convenient to give a special symbol  $N_{eo}$  to the electron density at the center of the discharge:

$$N_{eo} = N_e(0) \quad (5.11)$$

The dimensionless electron and ion densities are now defined by

$$n_e = N_e / N_{eo} \quad (5.12)$$

$$n_i = N_i / N_{eo} \quad (5.13)$$

The definition (5.12) artificially introduces another boundary condition into the problem, because  $n_e$  must be unity at the center of the discharge. However, the definition also introduces the unknown  $N_{eo}$  into the problem and gives the problem a desirable measure of versatility. The dimensioned formulation of the problem in Section 3 suggests that the equations are to be solved directly for  $\hat{J}$ ,  $N_e$ ,  $N_i$ ,  $\hat{T}$ ,  $\hat{E}$  after specifying values of the parameters  $\hat{E}_z$  and  $p$ . Now, however, the explicit presence of  $N_{eo}$  in the problem permits more flexibility. In fact, the solutions in Parts II and III are obtained by specifying  $N_{eo}$  in advance and determining  $\hat{E}_z$  as an eigenvalue. As mentioned in the Introduction, one of the primary objectives of the study of the positive column is the relationship between the electron density and the applied electric field. This relationship can now be expressed quantitatively as the relation between  $N_{eo}$  and  $\hat{E}_z$ . The remaining variables  $\hat{J}$  and  $\hat{E}$  are expressed in dimensionless form as

$$J = \frac{L}{\hat{D}_i(\hat{T}_w; \hat{E}_{zr}, p_r) N_{eo}} \cdot \frac{\hat{T}_w}{\hat{T}_e(\hat{T}_w; \hat{E}_{zr}, p_r)} \hat{J} \quad (5.14)$$

$$E = \frac{L e}{k \hat{T}_e(\hat{T}_w; \hat{E}_{zr}, p_r)} \hat{E} \quad (5.15)$$

The dimensionless temperature is the  $T$  defined by Eq. (5.10), and the new independent variable  $y$  is defined by

$$y = x/L \quad . \quad (5.16)$$

Dimensionless Equations and Boundary Conditions

The equations of Section 3 are made dimensionless by substituting into them the expressions above for the variables and coefficients. As a result of this process various constant coefficients appear in the equations which depend on  $N_{e0}$ ,  $\hat{T}_w$ ,  $\hat{E}_{zr}$ ,  $p_r$ . The procedures used to solve the problem for the  $N_{e0} - \hat{E}_z$  relationship require that the electron density  $N_{e0}$  retain its identity in the equations. For this purpose and to avoid the appearance of dimensioned quantities in the equations, a spurious parameter  $N$  is introduced.  $N$  is a reference density whose value is of no essential significance and is specified for convenience in Parts II and III. A dimensionless electron density  $\zeta$  is defined by

$$\zeta = N_{e0}/N \tag{5.17}$$

and this equation is used to replace  $N_{e0}$  wherever it appears in the dimensionless equations.

With the use of (2.56), (4.13), and (4.26), Eqs. (3.1), (3.10)-(3.12), and (3.14) become

$$\frac{dJ}{dy} = \gamma v_I(T; \hat{E}_z, p) n_e - \epsilon \zeta n_e n_i \tag{5.18}$$

$$\begin{aligned} \frac{dn_e}{dy} + \frac{1}{T_e(T; \hat{E}_z, p)} \frac{\partial T_e}{\partial T} n_e \frac{dT}{dy} &= \frac{-1}{T_e(T; \hat{E}_z, p)} n_e E \\ &- \delta \tau \frac{1}{D_e(T; \hat{E}_z, p)} J \end{aligned} \tag{5.19}$$

$$\frac{dn_i}{dy} + \frac{1}{T} n_i \frac{dT}{dy} = \tau \frac{1}{T} n_i E - \tau \frac{1}{D_i(T; \hat{E}_z, p)} J \quad (5.20)$$

$$\frac{d^2 T}{dy^2} + \frac{1}{\lambda(T)} \frac{d\lambda}{dT} \left(\frac{dT}{dy}\right)^2 = -\beta \zeta \frac{h(T; \hat{E}_z, p)}{\lambda(T)} n_e \quad (5.21)$$

$$\frac{dE}{dy} = \chi \zeta (n_i - n_e) \quad (5.22)$$

where

$$\gamma = \frac{L^2 \hat{v}_I(\hat{T}_w; \hat{E}_{zr}, p_r)}{\hat{D}_i(\hat{T}_w; \hat{E}_{zr}, p_r)} \cdot \frac{\hat{T}_w}{\hat{T}_e(\hat{T}_w; \hat{E}_{zr}, p_r)} \quad (5.23)$$

$$\epsilon = \frac{L^2 \hat{\alpha} N}{\hat{D}_i(\hat{T}_w; \hat{E}_{zr}, p_r)} \cdot \frac{\hat{T}_w}{\hat{T}_e(\hat{T}_w; \hat{E}_{zr}, p_r)} \quad (5.24)$$

$$\tau = \frac{\hat{T}_e(\hat{T}_w; \hat{E}_{zr}, p_r)}{\hat{T}_w} \quad (5.25)$$

$$\delta = \frac{\hat{D}_i(\hat{T}_w; \hat{E}_{zr}, p_r)}{\hat{D}_e(\hat{T}_w; \hat{E}_{zr}, p_r)} \quad (5.26)$$

$$\beta = \frac{\hat{h}(\hat{T}_w; \hat{E}_{zr}, p_r) NL^2}{\hat{\lambda}(\hat{T}_w) \hat{T}_w} \quad (5.27)$$

$$\chi = \frac{L^2 N_e^2}{\epsilon_o k \hat{T}_e(\hat{T}_w; \hat{E}_{zr}, p_r)} \quad (5.28)$$

Of the constant coefficients in the equations, only  $\zeta$  depends on  $N_{e0}$ ;  $\gamma$ ,  $\epsilon$ ,  $\tau$ ,  $\delta$ ,  $\beta$ , and  $\chi$  all depend on  $\hat{T}_w$ ,  $\hat{E}_{zr}$ , and  $p_r$ . These dependencies play a prominent role in the methods used to solve the equations.

The boundary conditions on  $J$ ,  $n_e$ ,  $n_i$ ,  $T$ , and  $E$  now become

$$y = 0 : \quad n_e = 1 \quad (5.29)$$

$$J = 0 \quad (5.30)$$

$$\frac{dT}{dy} = 0 \quad (5.31)$$

$$E = 0 \quad (5.32)$$

$$y = 1 : \quad n_e = 0 \quad (5.33)$$

$$n_i = 0 \quad (5.34)$$

$$T = 1 \quad (5.35)$$

The equations are to be solved for  $J$ ,  $n_e$ ,  $n_i$ ,  $T$ , and  $E$  on  $0 \leq y \leq 1$ , and a relation between  $N_{eo}$  (or  $\zeta$ ) and  $\hat{E}_z$  is to be obtained.

Solution at  $N_{eo} = 0$

The discussion in the Introduction describes in a general manner the  $N_{eo} - \hat{E}_z$  relationship. In particular it asserts the existence of a trivial solution to the equations. An examination of Eqs. (3.1), (3.10) - (3.12), (3.14) - (3.20) shows that the trivial solution is

$$\hat{J} = N_e = N_i = \hat{E} = 0 \quad (5.36)$$

$$\hat{T} = \hat{T}_w \quad (5.37)$$

$$N_{eo} = N_e(0) = 0 \quad (5.38)$$

and that  $\hat{E}_z$  is arbitrary.

However, the corresponding solution in dimensionless variables is not trivial and  $\hat{E}_z$  is not arbitrary. This behavior is explained

by the transformations (5.12) - (5.14) and the corresponding boundary condition (5.29). The use of the dimensionless equations when  $N_{eo} = 0$  requires special consideration, because their derivation in that case entails division by zero. A conceptual justification for their use involves the consideration of a process in which  $N_{eo}$  approaches zero. A schematic representation of this process is observed by following the curve in Fig. 1 to  $N_{eo} = 0$ , and the conclusion so determined is that  $\hat{E}_z$  is not arbitrary but instead corresponds to the bifurcation point  $\lambda_b$ .

This value of  $\hat{E}_z$  is obtained in the course of solving the equations. For  $N_{eo} = 0$  (hence  $\zeta = 0$ ), Eqs. (5.21), (5.22), (5.31), (5.32), (5.35) show that

$$T = 1 \quad (5.39)$$

and

$$E = 0 \quad (5.40)$$

The equations and boundary conditions for  $J$ ,  $n_e$ , and  $n_i$  then become

$$\frac{dJ}{dy} = \gamma v_I(1; \hat{E}_z, p) n_e \quad (5.41)$$

$$\frac{dn_e}{dy} = -\delta\tau \frac{1}{D_e(1; \hat{E}_z, p)} J \quad (5.42)$$

$$\frac{dn_i}{dy} = -\tau \frac{1}{D_i(1; \hat{E}_z, p)} J \quad (5.43)$$

$$y = 0 : \quad n_e = 1 \quad (5.44)$$

$$J = 0 \quad (5.45)$$

$$y = 1 : \quad n_e = 0 \quad (5.46)$$

$$n_i = 0 \quad (5.47)$$

Eliminating  $J$  between (5.41) and (5.42), the problem for  $n_e$  becomes

$$\frac{d^2 n_e}{dy^2} + \gamma \delta \tau \frac{v_I(1; \hat{E}_z, p)}{D_e(1; \hat{E}_z, p)} n_e = 0 \quad (5.48)$$

$$y = 0 : \quad n_e = 1 \quad (5.49)$$

$$\frac{dn_e}{dy} = 0 \quad (5.50)$$

$$y = 1 : \quad n_e = 0 \quad (5.51)$$

The solution to this eigenvalue problem is

$$n_e = \cos \frac{\pi}{2} y \quad (5.52)$$

$$\gamma \delta \tau \frac{v_I(1; \hat{E}_z, p)}{D_e(1; \hat{E}_z, p)} = \frac{\pi^2}{4} \quad (5.53)$$

Using (5.1), (5.4), (5.10), (5.23), (5.25), and (5.26), Eq. (5.53)

becomes

$$\frac{L^2 \hat{v}_I(\hat{T}_w; \hat{E}_z, p)}{\hat{D}_e(\hat{T}_w; \hat{E}_z, p)} = \frac{\pi^2}{4} \quad (5.54)$$

For specified values of  $L$ ,  $\hat{T}_w$ , and  $p$ , this equation can be solved to find the value of  $\hat{E}_z$  corresponding to  $\lambda_b$  in Fig. 1. By eliminating  $J$  between Eqs. (5.42) and (5.43) and integrating the resulting equation using the boundary conditions at the wall, it is easily seen

that  $n_i$  is a constant multiple of  $n_e$  and is larger by several orders of magnitude.

### Discussion of Problem

The solution for small  $N_{eo}$  can be found by expanding  $\hat{E}_z$  and the dependent variables in asymptotic series consisting of powers of  $\zeta$ , and this procedure is carried out by Cohen and Kruskal [7] for the case in which  $T$  is constant ( $\beta = 0$ ) and recombination is absent ( $\varepsilon = 0$ ). Our interest, however, is in situations in which  $N_{eo}$  is large. In fact, the work in Parts II and III involves the expansions of  $\hat{E}_z$  and the dependent variables in asymptotic series whose lowest-order terms correspond to the ambipolar situation, in which  $\hat{E}_z$  is represented by  $\lambda_a$  in Fig. 1. In each case the problem is approached by specifying  $N_{eo}$  in advance and determining  $\hat{E}_z$  in the course of solving the differential equations. Of course, the reasoning can be inverted after the solution is obtained so that  $J$ ,  $n_e$ ,  $n_i$ ,  $T$ , and  $E$  are regarded as functions of  $\hat{E}_z$  and  $y$ , and  $N_{eo}$  as a function of  $\hat{E}_z$ .

In solving the problem no study is made of the response of the solution to changes in such parameters as  $L$ ,  $T_w$ , and the amount of neutral gas (or the pressure  $p$ ) in the discharge. These parameters and the nature of the particular gas in the discharge play a critical role in determining even the crudest approximation to the solution, and hence their effects can be evaluated from a study of the ambipolar situation\*. The work here analyzes the deviation of the actual solution from the ambipolar approximation.

---

\*The effects are discussed in Cobine [6] and von Engel [26].

Until now the behavior of the pressure  $p$  has not been discussed except to say that it is constant throughout the discharge. Indeed, the pressure enters the equations as an unrestricted parameter, and it must be determined by the particular physical application considered. In our case we wish to study the behavior of a discharge containing a fixed amount of neutral gas as the applied electric field  $\hat{E}_z$  varies. Although the pressure is constant across the discharge, its value depends upon the temperature distribution and can be calculated by use of the perfect gas law. Since the temperature is a variable of the equations only in Part III, its calculation is deferred until then.

The correspondence between the  $N_{eo} - \hat{E}_z$  relation and the voltage-current characteristic of the discharge is described in the Introduction. The relationship of the electron density to the current can now be given more explicitly as

$$I = \int (e N_e w_e + e N_i w_i) dA \quad , \quad (5.55)$$

where the integration extends over the cross sectional area of the discharge. Equation (C.22) of Appendix C shows that  $w_i \ll w_e$ , so the contribution of the ions to the current is negligible. Using (4.3) and (5.12), Eq. (5.55) then becomes

$$I = e N_{eo} \int n_e w_e \left( \frac{\hat{E}_z}{p} k\hat{T} \right) dA \quad . \quad (5.56)$$

The results of Parts II and III show that  $N_{eo}$  varies much more rapidly than  $\hat{E}_z$ , so the current is essentially proportional to  $N_{eo}$ .

## Appendix A

### EXPRESSIONS FOR COLLISION RATES

A quantitative assessment of the collective effects of interparticle collisions requires a detailed consideration of particle interactions. The calculation of interest may seek the rate at which momentum or energy is transferred from one species in the plasma to another by elastic collisions, or it may seek the number of collisions causing ionization by electron impact. Although the net result of such calculations is statistical in nature, the statistics are provided by the velocity distribution function, and it is still necessary to know the overall kinematics of any hypothetical binary collision. This information is provided in very convenient form through the concept of a collision cross section.

#### Definition of Cross Section

The use of the cross section provides a compact expression for the rate at which particles engage in a specific class of collisions. The rudimental physical situation through which the concept is introduced consists of the scattering by a fixed center of a uniform flux of particles of velocity  $\underline{v}$  (see Fig. 3). The differential cross section for the process  $k$ , which may be elastic scattering, ionization, etc., is defined by the equation

$$R = \Phi(\underline{v}) q_k(v, \chi) d\Omega^* \quad , \quad (\text{A.1})$$

---

\* See Delecroix [8], pp. 97 ff.

where  $d\Omega = \sin \chi d\chi d\epsilon$  (A.2)

is an element of solid angle in the direction  $(\chi, \epsilon)$ .  $\chi$  and  $\epsilon$  are the polar and azimuthal angles, respectively;  $\Phi(\underline{v})$  is the magnitude of the flux of particles with velocity  $\underline{v}$  and is uniform throughout space;  $R$  with dimensions of collisions per unit time is the rate at which particles engaging in collisions of type  $k$  are scattered into the solid angle  $d\Omega$ ;  $q_k(\underline{v}, \chi)$  is the differential cross section for process  $k$ . The symmetry suggested by Fig. 3 indicates that  $q_k$  is independent of  $\epsilon$ .

For the situation in which the scatterer is a moving particle, the coordinate system of Fig. 3 is taken relative to the scatterer, and the velocities are relative velocities. Although the velocity of the scatterer, and hence the flux of particles relative to it, changes as a result of a collision, the use of cross sections in physical situations involves a distribution of scatterers with various velocities, and the concept introduced above actually pertains to the interaction of sets of particles characterized by their velocities. As shown by the more concrete calculations of Appendix B, the angle  $\chi$  in this case is the deflection angle for the collision of two particles in their center-of-mass coordinate system. Furthermore, these calculations show that the knowledge of  $\chi, \epsilon$ , and the pre-collision velocities together with the laws of conservation of momentum and energy suffice to determine the velocities after collision.

For some collision processes the velocities after the collision are not of interest. For instance, in the calculation of the rate of

ionization, the only object of interest regarding the outcome of a collision is whether ionization occurs. In such cases Eq. (A.1) may be integrated over  $\Omega$  to yield

$$R = \Phi(\underline{v}) Q_k(\underline{v}) \quad (\text{A.3})$$

where

$$Q_k(\underline{v}) = \int q_k(\underline{v}, \chi) d\Omega \quad (\text{A.4})$$

is the total cross section for the process  $k$ .

#### Application to Velocity Distributions

As preparation for the use of cross sections in rate expressions for processes occurring in a plasma, we consider the interaction of two types of particles characterized by the velocity distribution functions  $f(\underline{v})$  and  $F(\underline{V})$ . Collisions between the particles are, of course, sufficiently localized so that the spatial variation of  $f$  and  $F$  is not pertinent to the calculations. In order to correlate the physical situation with that represented by Eq. (A.1), it is necessary to consider collisions between particles whose velocities differ only infinitesimally from two particular velocities  $\underline{v}$  and  $\underline{V}$ . In this case the magnitude of the flux of scattered particles is  $g f(\underline{v}) d\underline{v}$ , where

$$g = |\underline{v} - \underline{V}| \quad (\text{A.5})$$

is the relative speed of the particles in  $d\underline{v}$  with respect to the scatterer with velocity  $\underline{V}$ . Using (A.1), the rate at which these collisions are occurring is given by

$$R = f(\underline{v})g q_k(g, \chi) d\Omega d\underline{v} , \quad (\text{A.6})$$

and the total rate of deflection into  $d\Omega$  would be found by integrating over  $\underline{v}$ . In order to include collisions with other scatterers, Eq. (A.6) is multiplied by  $F(\underline{V}) d\underline{V}$ , the number density of all scatterers with velocities in  $d\underline{V}$  about  $\underline{V}$ .  $R$  now has dimensions of collisions per unit time per unit volume and is given by

$$R = f(\underline{v}) F(\underline{V}) g q_k(g, \chi) d\Omega d\underline{v} d\underline{V} \quad . \quad (A.7)$$

Equation (A.7) is very versatile and can be used to obtain rates for a wide variety of processes. If the objective is the rate at which momentum is transferred from one species to another, for instance, it is only necessary to multiply (A.7) by the momentum lost in a collision by a particle with velocity  $\underline{v}$ . For generality we introduce the extensive property  $\phi(\underline{v})$  whose total value for the scattered species is the sum of that belonging to each particle. Designating the velocity after collision by  $\underline{\tilde{v}}$ , we have

$$R = [\phi(\underline{\tilde{v}}) - \phi(\underline{v})] f(\underline{v}) F(\underline{V}) g q_k(g, \chi) d\Omega d\underline{v} d\underline{V} \quad (A.8)$$

where  $R$  represents the rate per unit volume at which  $\phi$  is increasing in the scattered species as a result of collisions between particles with velocities  $\underline{v}$  and  $\underline{V}$  such that  $\underline{v}$  is deflected into  $d\Omega$ . It has been noted that  $\underline{\tilde{v}}$  is determined uniquely as a function of  $\underline{v}$ ,  $\underline{V}$ ,  $\chi$ ,  $\epsilon$ .

Values of the rates as a result of all collisions between the two species are found by integrating over  $\underline{v}$ ,  $\underline{V}$ , and  $\Omega$ . From (A.7) the total number of collisions of type  $k$  per unit volume per unit

time is

$$R = \iiint f(\underline{v}) F(\underline{V})_g q_k(g, \chi) d\Omega d\underline{v} d\underline{V} \quad (\text{A.9})$$

$$= \iint f(\underline{v}) F(\underline{V})_g Q_k(g) d\underline{v} d\underline{V} \quad . \quad (\text{A.10})$$

From (A.8) the rate per unit volume at which  $\phi$  is increasing in the scattered particles is

$$R = \iiint [\phi(\underline{\tilde{v}}) - \phi(\underline{v})] f(\underline{v}) F(\underline{V})_g q_k(g, \chi) d\Omega d\underline{v} d\underline{V} \quad . \quad (\text{A.11})$$

Here immediate integration over  $\Omega$  is not permissible, since  $\underline{\tilde{v}}$  in general depends upon  $\chi$  and  $\varepsilon$  .

Appendix B

EXPRESSIONS FOR ELASTIC MOMENTUM AND

ENERGY TRANSFER RATES

In order to obtain useful expressions for the elastic collision integrals for momentum and energy transport between species, it is necessary to consider the kinematics of binary collisions in some detail. The general rate expressions of Appendix A are used, but it is necessary to substitute into them explicit forms for the velocity after collision  $\tilde{\underline{v}}$ . The resulting expressions are simplified by performing some integrations and making approximations where appropriate.

Basic Collision Kinematics

Equation (A.11) of Appendix A contains velocities  $\underline{v}$ ,  $\underline{V}$ ,  $\tilde{\underline{v}}$  in the laboratory frame of reference and other variables  $g, \chi$  associated with the center-of-mass frame of reference. In order to transform the right-hand side, it is necessary, of course, to relate the two systems. The velocity of the center of mass  $\underline{W}$  and the relative velocity  $\underline{g}$  associated with two interacting particles are given by

$$(m + M)\underline{W} = m\underline{v} + M\underline{V} \quad (\text{B.1})$$

and

$$\underline{g} = \underline{v} - \underline{V} \quad (\text{B.2})$$

where  $\underline{v}$  and  $\underline{V}$  are the velocities of particles with mass  $m$  and  $M$  respectively, in the laboratory frame. The post-collision velocities are distinguished from their pre-collision values by a tilde. The

detailed dynamical behavior during the collision need not be considered. It is often convenient to measure the velocities from the center of mass. These expressions are easily obtained from (B.1) and (B.2) and are listed below:

$$\underline{v} - \underline{W} = \frac{M}{m + M} \underline{g} \quad (\text{B.3})$$

$$\underline{V} - \underline{W} = -\frac{m}{m + M} \underline{g} \quad (\text{B.4})$$

$$\underline{\tilde{v}} - \underline{\tilde{W}} = \frac{M}{m + M} \underline{\tilde{g}} \quad (\text{B.5})$$

$$\underline{\tilde{V}} - \underline{\tilde{W}} = -\frac{m}{m + M} \underline{\tilde{g}} \quad (\text{B.6})$$

The collision is so rapid an event that other forces have no significant effect on the post-collision velocities. The physical law for conservation of momentum then becomes

$$m\underline{\tilde{v}} + M\underline{\tilde{V}} = m\underline{v} + M\underline{V} \quad (\text{B.7})$$

or in the center-of-mass frame,

$$\underline{\tilde{W}} = \underline{W} \quad . \quad (\text{B.8})$$

Since only elastic collisions are considered, conservation of energy involves only kinetic energy, and the law is written as

$$\frac{1}{2} m \tilde{v}^2 + \frac{1}{2} M \tilde{V}^2 = \frac{1}{2} m v^2 + \frac{1}{2} M V^2 \quad . \quad (\text{B.9})$$

Using (B.1) and (B.2), the total energy of the two particles becomes, in the center-of-mass variables,

$$\frac{1}{2} m v^2 + \frac{1}{2} M V^2 = \frac{1}{2} (m+M) W^2 + \frac{1}{2} \frac{mM}{m+M} g^2 \quad . \quad ^* \quad (B.10)$$

(B.8), (B.9), and (B.10) now show that the conservation of energy can be expressed very conveniently by

$$\tilde{g} = g \quad . \quad (B.11)$$

Expressions for  $\tilde{\underline{v}} - \underline{v}$  and  $\tilde{v}^2 - v^2$  in center-of-mass-variables are needed in order to simplify the collision integrals that occur when the transport of momentum and energy between species is studied. The expressions are obtained quite mechanically from the relations presented above. The form of  $\tilde{\underline{v}} - \underline{v}$  is derived with particular ease from (B.3), (B.5), and (B.8):

$$\tilde{\underline{v}} - \underline{v} = \frac{M}{m+M} (\tilde{\underline{g}} - \underline{g}) \quad . \quad (B.12)$$

The angle of deflection  $\chi$  enters (B.12) by expressing its right-hand side in spherical coordinates. The direction of  $\underline{g}$  is taken as the polar axis, so  $\chi$  is the polar angle when  $\tilde{\underline{g}}$  is written in these coordinates. The azimuthal angle  $\epsilon$  is measured from a unit vector  $\underline{\ell}$  representing a coordinate perpendicular to  $\underline{g}$ . The direction of increasing  $\epsilon$  is such that when  $\epsilon = \chi = \pi/2$ ,  $\tilde{\underline{g}}$  is in the direction of  $\underline{m} = \underline{g} \times \underline{\ell}/g$ . Using Eq. (B.11),  $\tilde{\underline{g}}$  is then given by

$$\tilde{\underline{g}} = \underline{g} \cos \chi + \underline{\ell} g \sin \chi \cos \epsilon + \underline{m} g \sin \chi \sin \epsilon \quad , \quad (B.13)$$

---

\* This transformation and others of this section are given in detail by Holt and Haskell [14].

and (B.12) becomes

$$\underline{\tilde{v}} - \underline{v} = -\frac{M}{m+M} [\underline{g}(1 - \cos \chi) - \underline{\ell} g \sin \chi \cos \varepsilon - \underline{m} g \sin \chi \sin \varepsilon] \quad . \quad (\text{B.14})$$

The desired form of  $\underline{\tilde{v}}^2 - \underline{v}^2$  is somewhat more tedious to derive. We begin by using (B.4) and (B.5) to write  $\underline{\tilde{v}} - \underline{v}$  in a more complex form:

$$\underline{\tilde{v}} - \underline{v} = (\underline{\tilde{v}} - \underline{W}) - (\underline{v} - \underline{W}) \quad (\text{B.15})$$

$$= \frac{M}{m+M} \underline{\tilde{g}} + \frac{m}{m+M} \underline{g} \quad . \quad (\text{B.16})$$

Squaring both sides, using (B.11) and (B.13), and rearranging,

$$\underline{\tilde{v}}^2 - 2\underline{\tilde{v}} \cdot \underline{v} + \underline{v}^2 = \frac{m^2 + M^2}{(m+M)^2} g^2 + 2 \frac{mM}{(m+M)^2} g^2 \cos \chi \quad (\text{B.17})$$

$$= g^2 - 2 \frac{mM}{(m+M)^2} g^2 (1 - \cos \chi) \quad (\text{B.18})$$

$$= \underline{v}^2 - 2\underline{v} \cdot \underline{v} + \underline{v}^2 - 2 \frac{mM}{(m+M)^2} g^2 (1 - \cos \chi) \quad . \quad (\text{B.19})$$

Simplifying and using (B.14) with  $\underline{g}$  replaced by  $\underline{v} - \underline{v}$ , we obtain the final form:

$$\underline{\tilde{v}}^2 - \underline{v}^2 = 2(\underline{\tilde{v}} - \underline{v}) \cdot \underline{v} - 2 \frac{mM}{(m+M)^2} g^2 (1 - \cos \chi) \quad (\text{B.20})$$

$$= -\frac{2M}{m+M} \underline{v} \cdot \underline{v} (1 - \cos \chi) + \frac{2M}{m+M} \underline{v}^2 (1 - \cos \chi)$$

$$- 2 \frac{mM}{(m+M)^2} (\underline{v}^2 - 2\underline{v} \cdot \underline{v} + \underline{v}^2) (1 - \cos \chi)$$

$$+ \frac{2M}{m+M} g \sin \chi (\underline{\ell} \cdot \underline{v} \cos \varepsilon + \underline{m} \cdot \underline{v} \sin \varepsilon) \quad (\text{B.21})$$

$$\begin{aligned}
 &= - \frac{2M}{(m+M)^2} (mv^2 - MV^2) (1 - \cos \chi) \\
 &\quad - \frac{2M(M-m)}{(m+M)^2} \underline{v} \cdot \underline{V} (1 - \cos \chi) \\
 &\quad + \frac{2M}{m+M} g \sin \chi (\underline{l} \cdot \underline{V} \cos \epsilon + \underline{m} \cdot \underline{V} \sin \epsilon) \quad . \quad (B.22)
 \end{aligned}$$

### Momentum Transfer

The net rate per unit volume at which the momentum of one species is increasing as a result of elastic collisions with another is now obtained from Eq. (A.11) of Appendix A. In the equation  $q(g, \chi)$  is used to denote the elastic scattering cross section, and  $\phi(\underline{v})$  is set equal to  $m\underline{v}$ , so the rate becomes

$$R = m \iiint (\underline{\hat{v}} - \underline{v}) f(\underline{v}) F(\underline{V}) g q(g, \chi) d\Omega d\underline{v} d\underline{V} \quad . \quad (B.23)$$

Before substituting the expression for  $\underline{\hat{v}} - \underline{v}$  from (B.14) into (B.23), it is expedient to note that the only dependence of the integrand on  $\epsilon$  is contained in the terms of (B.14) with  $\cos \epsilon$  and  $\sin \epsilon$ . From (A.2) it is apparent that these terms contribute nothing when integrated over  $\Omega$ , and hence the rate becomes

$$R = - \frac{mM}{m+M} \iiint (\underline{v} - \underline{V}) f(\underline{v}) F(\underline{V}) g q(g, \chi) (1 - \cos \chi) d\Omega d\underline{v} d\underline{V} \quad . \quad (B.24)$$

The cross section and the collision frequency for momentum transfer are defined by

$$Q_m(g) = \int q(g, \chi) (1 - \cos \chi) d\Omega \quad (B.25)$$

and

$$v_m(g) = N g Q_m(g) \quad (B.26)$$

where

$$N = \int F(\underline{V}) d\underline{V} \quad (B.27)$$

is the number density of the other species. Using these, (B.24) becomes

$$R = - \frac{mM}{m+M} \frac{1}{N} \iint (\underline{v} - \underline{V}) f(\underline{v}) F(\underline{V}) v_m(g) d\underline{v} d\underline{V} \quad (B.28)$$

The dependence of  $g$  on both  $\underline{v}$  and  $\underline{V}$  makes further simplification difficult, but for the case in which  $f(\underline{v})$  represents electrons and  $F(\underline{V})$  neutrals, good approximations are available. In this case  $mM/(m+M) \approx m$ , and at those values of  $\underline{v}$  and  $\underline{V}$  for which the factor  $f(\underline{v}) F(\underline{V})$  contributes significantly to the integral,  $V \ll v$  and  $g \approx v$ . With these approximations  $R$  becomes

$$R = - \frac{m}{N} \iint (\underline{v} - \underline{V}) f(\underline{v}) F(\underline{V}) v_m(v) d\underline{v} d\underline{V} \quad (B.29)$$

$$= - m \int (\underline{v} - \langle \underline{V} \rangle) f(\underline{v}) v_m(v) d\underline{v} \quad (B.30)$$

In the glow discharge of interest,  $\langle \underline{V} \rangle$  is essentially zero, so

$$R = - m \int \underline{v} f(\underline{v}) v_m(v) d\underline{v} \quad (B.31)$$

### Energy Transfer

The rate per unit volume at which the energy of the electrons is increasing as a result of elastic collisions with the neutrals is found by setting  $\phi(\underline{v})$  equal to the energy of an electron,  $\frac{1}{2} m v^2$ . With  $f(\underline{v})$  representing the electrons and  $F(\underline{V})$  the neutrals, Eq. (A.11)

becomes

$$R = \frac{1}{2} m \iiint (\underline{v}^2 - v^2) f(\underline{v}) F(\underline{V}) v q(v, \chi) d\Omega d\underline{v} d\underline{V} \quad (\text{B.32})$$

after making the approximation  $g \approx v$ . Again it is expedient to examine carefully the expression for  $\underline{v}^2 - v^2$  in Eq. (B.22) before substituting it into (B.32), and again the terms that depend on  $\epsilon$  vanish when integrated over  $\Omega$ . The second term of (B.22), when substituted into (B.32) and integrated over  $\underline{V}$ , yields the average velocity  $\langle \underline{V} \rangle$  multiplied by an integral over the other variables. Since  $\langle \underline{V} \rangle$  is essentially zero in the glow discharge of interest, the rate of energy transfer becomes

$$R = - \frac{2mM}{(m+M)^2} \iiint \left( \frac{1}{2} m v^2 - \frac{1}{2} M V^2 \right) f(\underline{v}) F(\underline{V}) v q(v, \chi) (1 - \cos \chi) d\Omega d\underline{v} d\underline{V}. \quad (\text{B.33})$$

$Q_m(v)$  and  $v_m(v)$  as defined by (B.25) and (B.26) appear after integrating over  $\Omega$ . We continue by making the approximations  $mM/(m+M)^2 \approx m/M$  and integrating over  $\underline{V}$  to obtain

$$R = - 2 \frac{m}{M} \int \left( \frac{1}{2} m v^2 - \langle \frac{1}{2} M V^2 \rangle \right) f(\underline{v}) v_m(v) d\underline{v}. \quad (\text{B.34})$$

It is interesting to consider the form  $R$  would assume if  $v_m$  were independent of  $v$ . The integration over  $\underline{v}$  in (B.34) could then be performed to yield

$$R = - 2 \frac{m}{M} \left( \langle \frac{1}{2} m v^2 \rangle - \langle \frac{1}{2} M V^2 \rangle \right) n v_m, \quad (\text{B.35})$$

where  $n$  is the electron density. Since  $R$  is the rate at which the

total electron energy increases per unit volume and  $n$  is the number of electrons per unit volume, treating  $\nu_m$  as the collision frequency allows  $2 \frac{m}{M} (\langle \frac{1}{2} mv^2 \rangle - \langle \frac{1}{2} MV^2 \rangle)$  to be interpreted as the average energy lost by an electron in an elastic collision with a neutral molecule.

Although the dependence of  $\nu_m$  on  $v$  complicates the situation, the same interpretation can be applied to  $\nu_m$  and  $2 \frac{m}{M} (\langle \frac{1}{2} mv^2 \rangle - \langle \frac{1}{2} MV^2 \rangle)$  by considering only those electrons with velocity  $\underline{v}$  and density  $f(\underline{v}) d\underline{v}$ .

Appendix C  
CALCULATION OF PLASMA PROPERTIES  
FROM KINETIC THEORY

In order to fully appreciate the kinetic-theory description of a plasma, it is necessary to have an understanding of the orders of magnitude of the variables involved. Not only is such an understanding essential for an intuitive physical concept of the situation, but it is also needed to evaluate the accuracy of approximations that are made. In this appendix calculations are performed to obtain such quantities as mean energies, mean free paths, and relaxation times for electrons and ions. Such calculations require some knowledge of the state of the neutral gas, the size of the discharge, and the magnitude of the electric field. Although some of these parameters depend on the solution to the entire problem, the estimates made here result in order of magnitude values for electron and ion properties. The neutral gas temperature and the pressure in the discharge are chosen to be 300<sup>o</sup>K and 1 mm Hg, and the distance from the center to the wall of the discharge in slab geometry is

$$L = 1 \text{ cm} . \tag{C.1}$$

Representative values for the axial and transverse electric fields are selected from the results of Part II. Values chosen for the calculations of this appendix are

$$\hat{E}_z = 20 \text{ volts/cm} \tag{C.2}$$

for the axial field and

$$\hat{E} = 2.88 \text{ volts/cm} \quad (\text{C.3})$$

for the transverse field. However, the value of the transverse field is considerably higher in a thin sheath by the wall of the discharge. The values of  $\hat{E}_z$  and  $\hat{E}$  predict a total electric field with magnitude

$$\hat{E}_t = 20.2 \text{ volts/cm} \quad (\text{C.4})$$

Because of the small difference between  $\hat{E}_z$  and  $\hat{E}_t$ ,  $\hat{E}_z$  is used in the following calculations.

#### Behavior of Ions

The discussion on pp. 472-473 of McDaniel [19] indicates that the ion present in an  $\text{H}_2$  glow discharge is  $\text{H}_3^+$ . In Section 2 the approximation is made that the ion temperature equals the neutral temperature, i.e.,  $\hat{T}_i = 300^\circ\text{K}$ . The root-mean-square velocity or random thermal velocity of the ions is calculated on the basis of this approximation from the formula

$$\frac{1}{2} m_i \langle v_i^2 \rangle = \frac{3}{2} k \hat{T}_i \quad (\text{C.5})$$

The numerical result is

$$\sqrt{\langle v_i^2 \rangle} = 1.57 \times 10^5 \text{ cm/sec} \quad (\text{C.6})$$

The mean free path of the ions is difficult to obtain directly because of its critical dependence on the electrostatic dipole force between ions and neutral molecules. However, kinetic theory provides a formula for the ion mobility that involves the mean free path  $\lambda_i$ . It was derived by P. Langevin and is given in Loeb [18] as

$$\hat{\mu}_i = 0.815 \frac{e\lambda_i}{m_n \sqrt{\langle v_n^2 \rangle}} \sqrt{1 + \frac{m_n}{m_i}} . \quad (C.7)$$

By using experimental data for  $\hat{\mu}_i$ , we obtain the value

$$\lambda_i = 0.00393 \text{ cm} . \quad (C.8)$$

The concept of a mean free path in the context of (C.7) refers to collisions between smooth rigid elastic spheres. The collision frequency is obtained by dividing  $\lambda_i$  into the average speed  $\langle v_i \rangle$ . Since the value of  $\langle v_i \rangle$  is very close to that of  $\sqrt{\langle v_i^2 \rangle}$ , we use the value in (C.6) and obtain

$$v_i = 4.00 \times 10^7 \text{ sec}^{-1} . \quad (C.9)$$

The ion energy relaxation time pertains to a situation in which the mean ion energy differs from that of the neutrals. It is a measure of the time required for the ion energy to change significantly as a result of elastic collisions with the neutrals. Because of the efficient interchange of energy during collisions, the relaxation time is comparable in magnitude to the time between collisions\*, and we calculate its value from (C.9):

$$\tau_r = 1/v_i = 2.50 \times 10^{-8} \text{ sec} . \quad (C.10)$$

The ion drift velocity in the axial direction is obtained from mobility data through the use of the equation  $w_i = \hat{\mu}_i \hat{E}_z$ . For

---

\* See Jeans [16], p. 244.

$\hat{E}_z = 20$  volts/cm, we have

$$w_i = 2.05 \times 10^5 \text{ cm/sec} . \quad (\text{C.11})$$

The fact that  $w_i > \sqrt{\langle v_i^2 \rangle}$  casts considerable doubt upon the assumption that  $\hat{T}_i = \hat{T}_n$ . We now seek an estimate for  $\hat{T}_i$  by making an energy balance on an average ion. The ion gains energy from the axial field at the rate  $e \hat{E}_z w = 1.26 \times 10^{-13}$  ergs/sec and loses this energy through elastic collisions with the neutrals. If it is assumed that the ion loses with each collision an amount of energy equal to the difference between ion and neutral energies, the energy balance becomes

$$\left( \frac{3}{2} k\hat{T}_i - \frac{3}{2} k\hat{T}_n \right) v_i = e \hat{E}_z w . \quad (\text{C.12})$$

Using (C.9) and solving for  $\hat{T}_i$ ,

$$\hat{T}_i - \hat{T}_n = 796^\circ\text{K} \quad (\text{C.13})$$

$$\hat{T}_i = 1096^\circ\text{K} \quad (\text{C.14})$$

Although the value of  $\hat{T}_i$  is correct only in order of magnitude, it is apparent that the assumption  $\hat{T}_i = \hat{T}_n$  is quite poor.

### Behavior of Electrons

The data for electrons are obtained from the papers of Frost and Phelps [11] and Engelhardt and Phelps [10], in which they obtain the electron distribution function by solving the Boltzmann equation. The mean electron energy depends strongly on the electric field, and for  $\hat{E}_z = 20$  volts/cm ,

$$\hat{T}_e = 33400^\circ\text{K} \quad . \quad (\text{C.15})$$

From

$$\frac{1}{2} m_e \langle v_e^2 \rangle = \frac{3}{2} k \hat{T}_e \quad (\text{C.16})$$

we obtain

$$\sqrt{\langle v_e^2 \rangle} = 1.23 \times 10^8 \text{ cm/sec} \quad . \quad (\text{C.17})$$

An electron mean free path is defined by dividing the momentum transfer collision frequency  $\nu_m(g)$  of Eq. (B.26) of Appendix B into the relative velocity  $g \approx v$  to obtain

$$\lambda_e(v) = \frac{1}{N_n Q_m(v)} \quad (\text{C.18})$$

where  $v$  is the electron velocity and  $N_n$  is the neutral number density. Evaluating  $Q_m(v)$  for  $v = \sqrt{\langle v_e^2 \rangle}$  from the data of Frost and Phelps [11], we obtain

$$\lambda_e = 0.0194 \text{ cm} \quad . \quad (\text{C.19})$$

Using the same value for  $v$ , the momentum-transfer collision frequency is

$$\nu_m = 6.34 \times 10^9 \text{ sec}^{-1} \quad . \quad (\text{C.20})$$

The electron drift velocity in the axial direction is obtained from Frost and Phelps' [11] data and is

$$w_e = 6.60 \times 10^6 \text{ cm/sec} \quad . \quad (\text{C.21})$$

Since the electron and ion densities in the discharge are approximately

equal, the contribution of each to the total current is proportional to its drift velocity. The rate at which the particles gain energy from the axial field equals  $e \hat{E}_z w$ , and the ratio of these rates for the two types of particles is

$$\frac{e \hat{E}_z w_e}{e \hat{E}_z w_i} = \frac{w_e}{w_i} = 32.2 \quad . \quad (C.22)$$

Response of  $f_e$  to Changes in  $N_n$

The data used in the calculations above pertain to a situation in which  $N_n$  is constant. However, the temperature gradients present in the glow discharge cause corresponding variations in the neutral density. In that case the data at a particular location may be determined from the local value of  $N_n$  provided the electron and ion distribution functions respond sufficiently rapidly to a change in  $N_n$ . The response time for the ions is expected to be approximately the value of  $\tau_r$  in (C.10). The response time for the electrons is calculated below by determining the rate at which the electron distribution function changes as a result of a sudden change in neutral density.

An equation for the electron distribution function  $f_e$  as a function of time and velocity can be obtained by expanding it in spherical harmonics in velocity space and substituting the expansion into the Boltzmann equation. The approach is standard, and if the higher-order harmonics are neglected, equations are obtained for the isotropic term  $f_0$  and the coefficient of the first-order harmonic  $f_1$ . The further approximations of neglecting inelastic collisions and assuming the mean free path to be constant lead to Eqs. (32) and (33)

of Proposition 1. The discussion in the Proposition shows that the term involving the neutral temperature is small if the electric field is so strong that the mean electron energy is much greater than that of the neutrals. We neglect this term and rewrite the equations in the notation used here:

$$\frac{\partial f_o}{\partial t} = \frac{e\hat{E}_z}{3m_e} \frac{1}{v^2} \frac{\partial}{\partial v} (v^2 f_1) + \frac{m_e}{m_n} \frac{1}{\lambda_e} \frac{1}{v^2} \frac{\partial}{\partial v} (v^4 f_o) \quad (C.23)$$

$$\frac{\partial f_1}{\partial t} = \frac{e\hat{E}_z}{m_e} \frac{\partial f_o}{\partial v} - \frac{1}{\lambda_e} v f_1 \quad . \quad (C.24)$$

The steady-state solution for  $f_o$  is the well-known Druyvesteyn distribution

$$f_o = C \exp \left( \frac{-3m_e^3 v^4}{4m_n e^2 \hat{E}_z^2 \lambda_e^2} \right) \quad . \quad (C.25)$$

The problem of interest is one in which a sudden change in the neutral density upsets a steady-state situation. We must calculate the rate at which  $f_o$  then approaches the new steady state. Actually we need calculate only the initial rate to obtain an estimate of the response time. The neutral density enters Eqs. (C.23) and (C.24) solely through the mean free path  $\lambda_e$ , and hence we consider an abrupt change in  $\lambda_e$  from  $\lambda_e$  to  $\lambda_e + \delta\lambda_e$ . For  $|\delta\lambda_e| < \lambda_e$ , Eq. (C.23) can be written

$$\frac{\partial f_o}{\partial t} = \frac{e\hat{E}_z}{3m_e} \frac{1}{v^2} \frac{\partial}{\partial v} (v^2 f_1) + \frac{m_e}{m_n} \frac{1}{\lambda_e (1 + \delta\lambda_e/\lambda_e)} \frac{1}{v^2} \frac{\partial}{\partial v} (v^4 f_o) \quad (C.26)$$

$$\begin{aligned}
 &= \frac{\hat{E}_z}{3m_e} \frac{1}{v} \frac{\partial}{\partial v} (v^2 f_1) + \frac{m_e}{m_n} \frac{1}{\lambda_e} \frac{1}{v} \frac{\partial}{\partial v} (v^4 f_0) \\
 &\quad - \frac{\delta \lambda_e}{\lambda_e} \frac{m_e}{m_n} \frac{1}{\lambda_e} \frac{1}{v} \frac{\partial}{\partial v} (v^4 f_0)
 \end{aligned} \tag{C.27}$$

where higher powers of  $\delta \lambda_e / \lambda_e$  have been neglected. Immediately after the change in  $\lambda_e$ ,  $f_0$  and  $f_1$  still possess their former steady-state values, and the first two terms on the right-hand side of (C.27) cancel. Thus initially

$$\frac{\partial f_0}{\partial t} = - \frac{\delta \lambda_e}{\lambda_e} \frac{m_e}{m_n} \frac{1}{\lambda_e} \frac{1}{v} \frac{\partial}{\partial v} (v^4 f_0) \tag{C.28}$$

$\frac{\partial f_0}{\partial t}$  is a function of  $v$ , and the rate of interest is one for which  $v$  is near the mean random velocity. Since the mean velocity is of the same order of magnitude as those for which  $f_0$  varies most rapidly, a representative velocity is chosen as one for which the exponent in (C.25) is unity. Thus we seek to evaluate  $\partial f_0 / \partial t$  at

$$v = v_0 \equiv \left[ \frac{4m_e^2 \hat{E}_z^2 \lambda_e^2}{3m_e^3} \right]^{1/4} \tag{C.29}$$

From (C.25)

$$v \frac{\partial f_0}{\partial v} = - \frac{3m_e^3 v^4}{m_n e^2 \hat{E}_z^2 \lambda_e^2} f_0 = - 4f_0 \tag{C.30}$$

at  $v = v_0$ . Hence for  $v$  near  $v_0$  the order of magnitude of the  $v$ -dependence of (C.28) is

$$\frac{1}{v} \frac{\partial}{\partial v} (v^4 f_0) = 0(v_0 f_0) \tag{C.31}$$

and considering  $\delta\lambda_e/\lambda_e$  to be of order unity, we obtain

$$\frac{\partial f_o}{\partial t} = \pm \frac{1}{\tau} f_o, \quad (C.32)$$

where

$$\tau = \frac{m_n \lambda_e}{m_e v_o} \quad (C.33)$$

$$= \frac{m_n}{m_e} \lambda_e \left[ \frac{3m_e^3}{4m_n e^2 \hat{E}_z^2 \lambda_e^2} \right]^{1/4} \quad (C.34)$$

Using the value of  $\lambda_e$  from (C.19), we find

$$v_o = 2.19 \times 10^8 \text{ cm/sec} \quad (C.35)$$

$$\tau = 3.26 \times 10^{-7} \text{ sec} \quad (C.36)$$

The value of  $\tau$  is an estimate of the time required for the electron distribution function to adjust to the neutral density.

#### Ambipolar Diffusion Time

In order to determine whether the local value of  $N_n$  suffices to determine the electron and ion distribution functions, it is necessary to compare the response times of the particles to the time during which an average particle experiences a significant change in  $N_n$ . The neutral density varies only in the radial direction, and the time we seek is the approximate length of time for a particle to diffuse from the center of the discharge to the wall. The results of Parts II and III show that the transport of charged particles to the wall can be approximated by ambipolar diffusion at the electron densities of interest. In such a situation the densities and mean radial

velocities of electrons and ions are approximately equal, and the flux to the wall is given by

$$Nu = - \hat{D}_a \nabla N \quad (C.37)$$

where  $u$  is the mean radial velocity,  $N$  the number density, and  $\hat{D}_a$  the ambipolar diffusion coefficient. Since  $N$  is zero at the walls, an order-of-magnitude estimate of the density gradient is  $\nabla N = N/L$ . A representative value for  $u$  is then given by

$$u = \hat{D}_a / L \quad (C.38)$$

and the ambipolar diffusion time is defined by

$$\tau_a = \frac{L}{u} = \frac{L^2}{\hat{D}_a} \quad (C.39)$$

The numerical values are

$$u = 2.24 \times 10^4 \text{ cm/sec} \quad (C.40)$$

$$\tau_a = 4.47 \times 10^{-5} \text{ sec} \quad (C.41)$$

Since the ambipolar diffusion time is so much larger than the response times for ions and electrons given in (C.10) and (C.36), we conclude that the determination of ion and electron properties through the use of the local neutral density is valid.

## NOMENCLATURE

The number following the descriptions gives the page on which the symbol first appears. Some symbols are used in different contexts in different parts of the report and have a corresponding number of definitions. Others, whose use is very temporary, do not appear here.

### Derivatives:

$d\mathbf{r}$	volume element (12)
$d\mathbf{v}_{-\alpha}$	element of velocity space (12)
$d\Omega$	element of solid angle (63)
$\partial/\partial\mathbf{r}$	spatial gradient operator (11)
$\partial/\partial\mathbf{v}_{-\alpha}$	gradient operator in velocity space (11)
$(\partial f_{\alpha}/\partial t)_{\text{c}}$	total collision integral (11)
$(\partial f_{\alpha}/\partial t)_{\text{e.c.}}$	elastic collision integral (11)
$(\partial f_{\alpha}/\partial t)_{\text{i.c.}}$	inelastic collision integral (11)

### Roman:

$D_{\text{e}}$	dimensionless electron diffusion coefficient (53)
$D_{\text{i}}$	dimensionless ion diffusion coefficient (53)
$\hat{D}_{\text{a}}$	ambipolar diffusion coefficient (85)
$\hat{D}_{\text{e}}$	electron diffusion coefficient (38)
$\hat{D}_{\text{i}}$	ion diffusion coefficient (38)
$e$	magnitude of the electronic charge (20)
$E$	dimensionless electric field (55)
$\hat{E}$	transverse electric field (38)
$\hat{E}_{\text{t}}$	total electric field (11)

$\hat{E}_z$	axial electric field (32)
$\hat{E}_{zr}$	reference value for $\hat{E}_z$ (53)
$f(\underline{v})$	velocity distribution function (65)
$f_E$	data for electron temperature (44)
$f_I$	data for ionization coefficient (44)
$f_\alpha(\underline{r}, \underline{v}_\alpha, t)$	distribution function for species $\alpha$ (11)
$F(\underline{V})$	velocity distribution function (65)
$g$	magnitude of relative velocity (16)
$\underline{g}$	relative velocity (68)
$\tilde{\underline{g}}$	relative velocity after collision (69)
$h$	dimensionless energy transfer coefficient (54)
$h_o$	dimensionless elastic energy transfer coefficient (54)
$\hat{h}$	energy transfer coefficient (32)
$\hat{h}_o$	elastic energy transfer coefficient (34)
$I$	current (62)
$\underline{\underline{I}}$	unit tensor (29)
$J$	dimensionless flux (55)
$\hat{J}$	transverse particle flux (37)
$\hat{J}_\alpha$	total particle flux for species $\alpha$ (15)
$k$	Boltzmann's constant (26)
$L$	distance from wall to center of discharge (41)
$m$	mass (68)
$M$	mass (68)
$m_\alpha$	mass of species $\alpha$ (11)
$n$	number density (74)
$n_c$	dimensionless electron density (54)

$n_i$	dimensionless ion density (54)
$N$	number density (73)
$N_{eo}$	electron number density at center of discharge (54)
$N_\alpha$	number density of species $\alpha$ (12)
$p$	mechanical pressure (25)
$p_r$	reference value for $p$ (53)
$p_\alpha$	scalar pressure of species $\alpha$ (29)
$p_o$	reduced pressure (47)
$q_k(v, \chi)$	differential cross section for process $k$ (63)
$q_\alpha$	electrostatic charge on species $\alpha$ (11)
$Q_k(v)$	total cross section for process $k$ (65)
$Q_m(g)$	cross section for momentum transfer (72)
$Q_I$	total cross section for ionization (16)
$Q_R$	total cross section for dissociative recombination (16)
$\underline{Q}_\alpha$	heat-flux vector for species $\alpha$ (26)
$\underline{r}$	position vector (12)
$R_I$	rate of ionization collisions (16)
$R_R$	rate of recombination collisions (16)
$t$	time (12)
$T$	dimensionless temperature (53)
$T_e$	dimensionless electron temperature (53)
$\hat{T}$	temperature of neutral molecules (39)
$\hat{T}_w$	temperature of neutrals at wall (41)
$\hat{T}_\alpha$	temperature of species $\alpha$ (26)
$u$	abstract representation of dimensionless variables (6) mean radial velocity (85)

$\ u\ $	magnitude of u (6)
$\underline{v}$	velocity (63)
$\underline{v}_\alpha$	velocity of a particle of species $\alpha$ (11)
$\underline{v}^{\sim}$	velocity after collision (66)
$\underline{v}$	velocity (65)
$\underline{v}_\alpha$	peculiar velocity of a particle of species $\alpha$ (19)
$\underline{v}^{\sim}$	velocity after collision (69)
$\underline{w}_\alpha$	drift velocity of species $\alpha$ (32)
$\underline{W}$	velocity of center of mass (68)
$\underline{W}^{\sim}$	velocity of center of mass after collision (69)
x	distance coordinate perpendicular to wall of discharge(37)
y	dimensionless independent variable (55)

Greek:

$\hat{\alpha}$	recombination coefficient (17)
$\hat{\alpha}_I$	Townsend's first ionization coefficient (44)
$\beta$	dimensionless constant coefficient (57)
$\gamma$	dimensionless constant coefficient (56)
$\delta$	dimensionless constant coefficient (56)
$\epsilon$	dimensionless constant coefficient (56)
	azimuthal angle (64)
$\epsilon_0$	permittivity of free space (39)
$\zeta$	dimensionless constant coefficient (56)
$\nu_i$	effective ion collision frequency for momentum transfer ion collision frequency (78) (24)
$\nu_m$	effective electron collision frequency for momentum transfer (20)

$\nu_m(v_e)$	electron collision frequency for momentum transfer(20)
$\nu_m(g)$	collision frequency for momentum transfer (73)
$\nu_{mi}(g)$	ion collision frequency for momentum transfer (22)
$\nu_I$	dimensionless ionization coefficient (53)
$\hat{\nu}_I$	ionization coefficient (17)
$\lambda$	nonlinear eigenvalue (6)
	dimensionless thermal conductivity (54)
$\lambda_a$	eigenvalue $\lambda$ at ambipolar diffusion limit (6)
$\lambda_b$	eigenvalue $\lambda$ at free diffusion limit (6)
$\lambda_e$	electron mean free path (80)
$\lambda_i$	ion mean free path (77)
$\hat{\lambda}$	thermal conductivity (31)
$\mu_e$	dimensionless electron mobility (53)
$\mu_i$	dimensionless ion mobility (53)
$\hat{\mu}_e$	electron mobility (38)
$\hat{\mu}_i$	ion mobility (38)
$\hat{\mu}_i^o$	reduced ion mobility (47)
$\tau$	dimensionless constant coefficient (56)
	electron distribution function response time (84)
$\tau_a$	ambipolar diffusion time (35)
$\tau_e$	electron energy relaxation time (35)
$\tau_r$	ion energy relaxation time (78)
$\phi_\alpha(\underline{v}_\alpha)$	extensive property of particles of species $\alpha$ (13)
$\Phi(\underline{v})$	flux of particles (63)
$\chi$	dimensionless constant coefficient (57)
	polar angle (63)
$\underline{\Psi}_\alpha$	pressure tensor for species $\alpha$ in a perfect gas (19)

LIST OF FIGURES

1. Response Curve
2. Voltage-Current Characteristic
3. Scattering of a Monoenergetic Flux by a Fixed Center
4. Comparison of  $\hat{h}$  and  $\hat{h}_0$
5.  $f_E$  as a Function of  $\hat{E}_z/N_n$
6.  $f_I$  as a Function of  $\hat{E}_z/N_n$
7.  $w_e$  as a Function of  $\hat{E}_z/N_n$
8.  $f'_E$  as a Function of  $\hat{E}_z/N_n$
9.  $\hat{\mu}_i^0$  as a Function of  $\hat{E}_z/p_0$

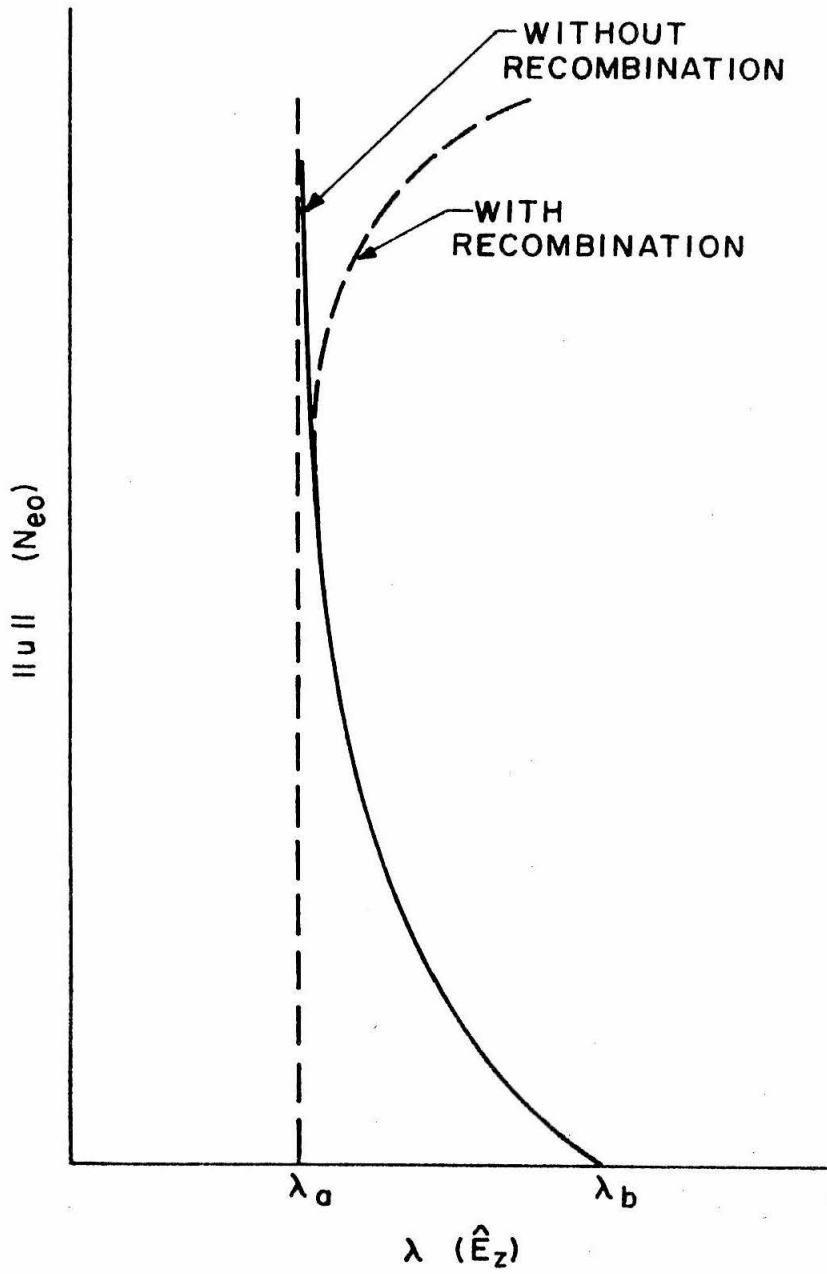


Figure 1: Response Curve

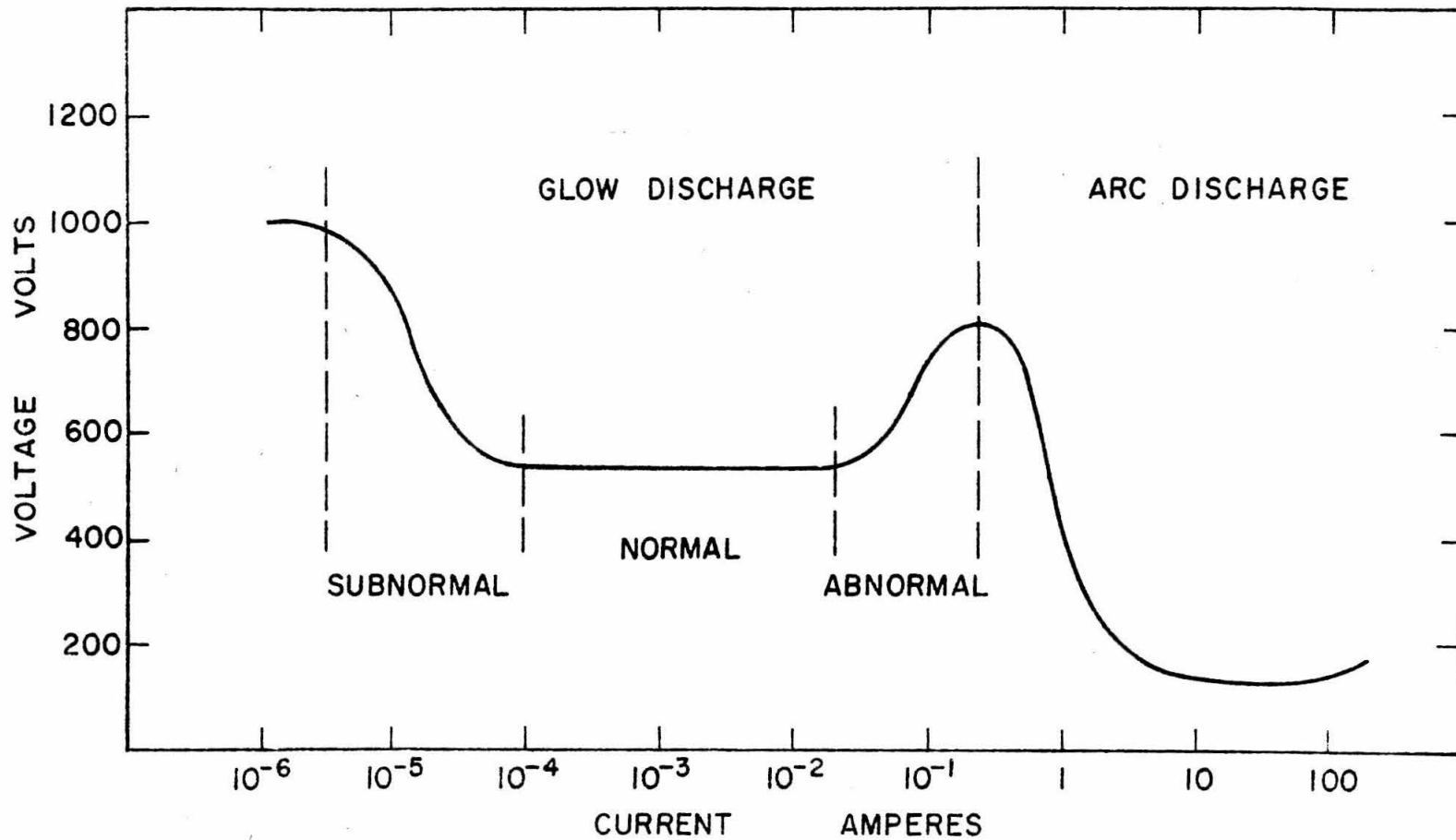


Figure 2: Voltage-Current Characteristic

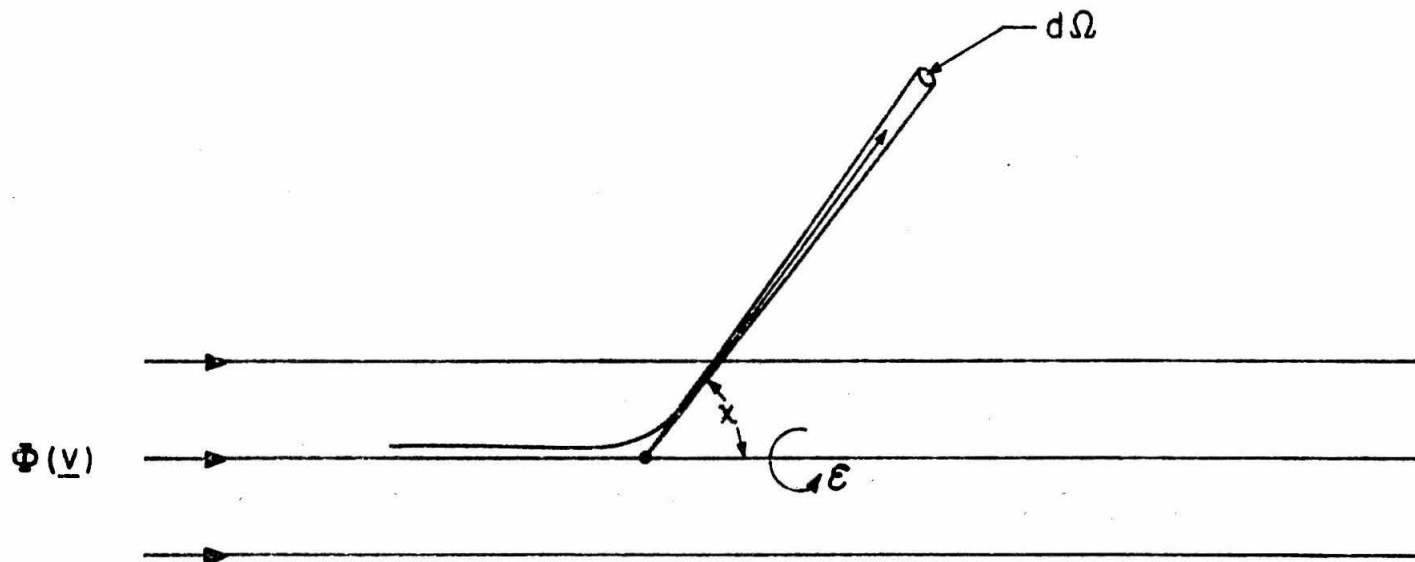


Figure 3: Scattering of a Monoenergetic Flux by a Fixed Center

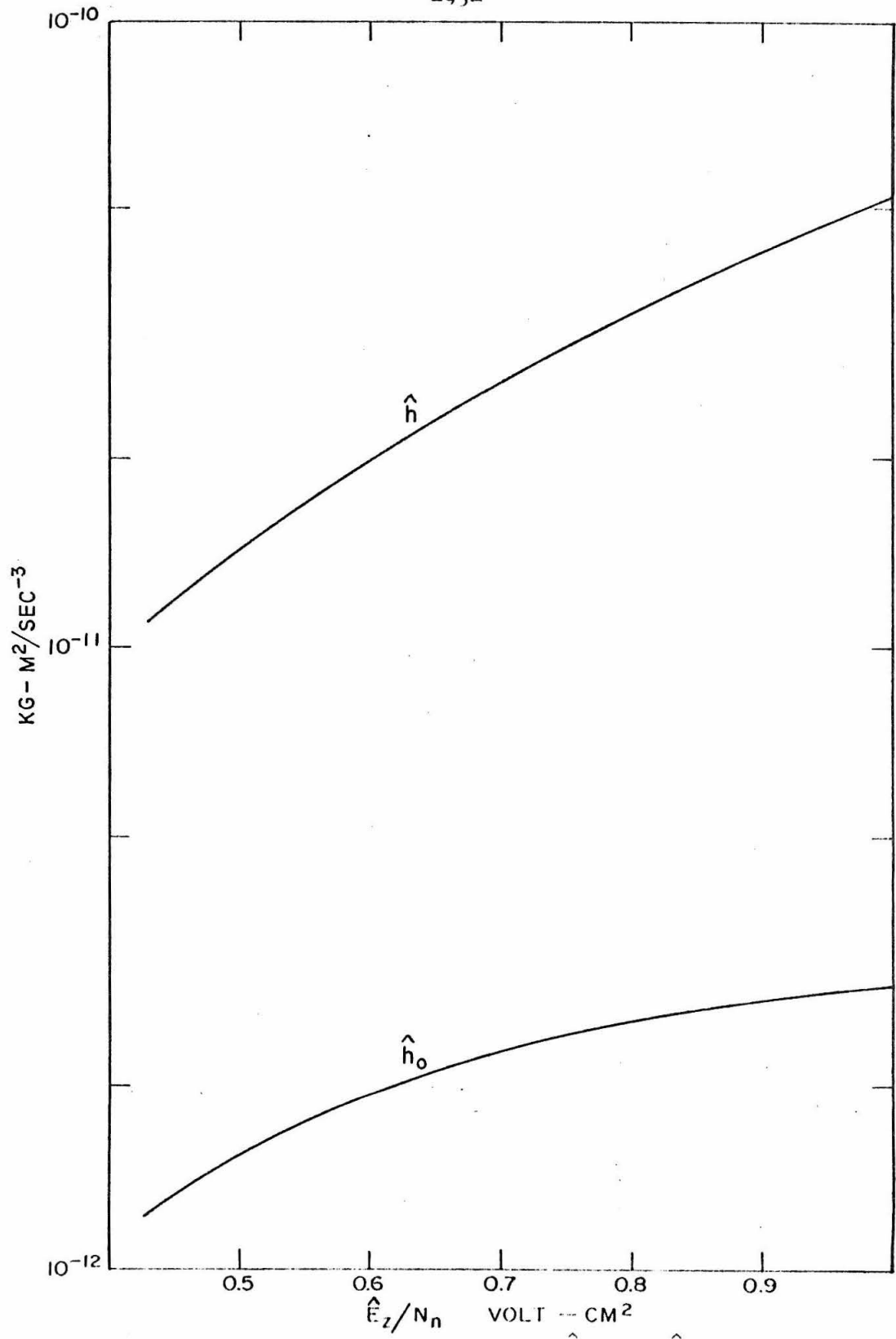


Figure 4: Comparison of  $\hat{h}$  and  $\hat{h}_0$

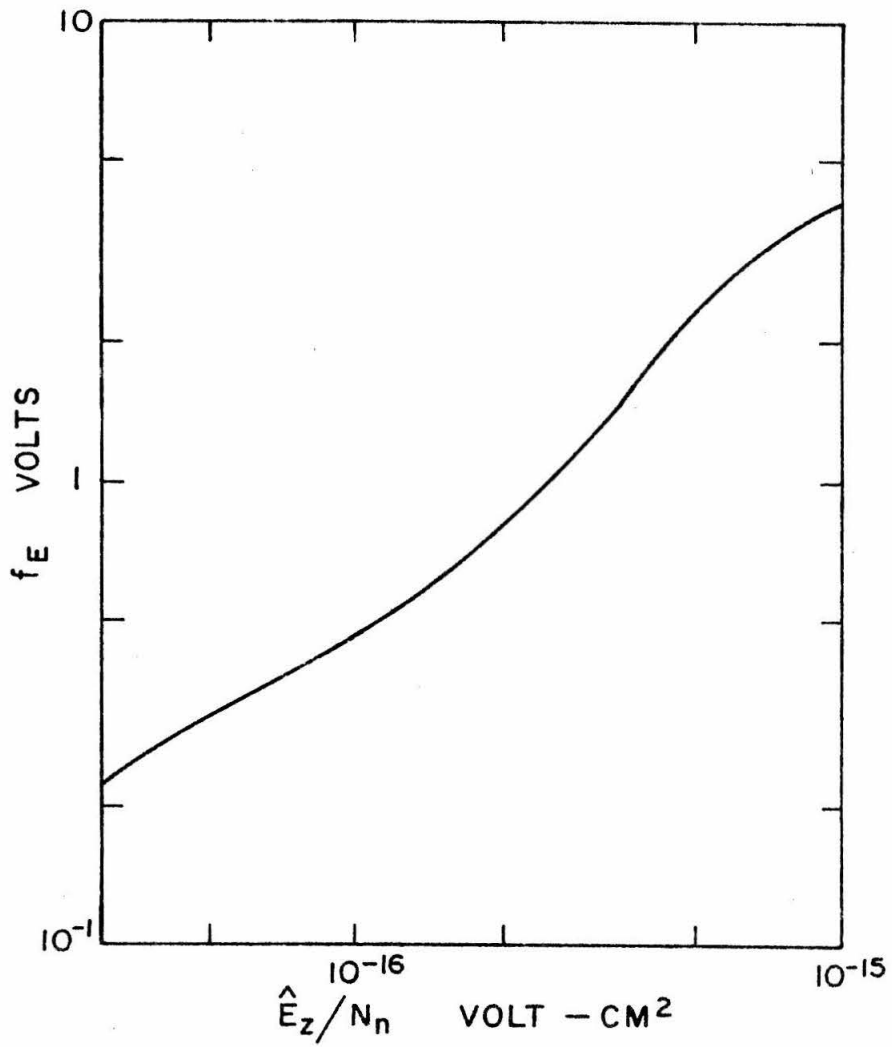


Figure 5:  $f_E$  as a Function of  $\hat{E}_z / N_n$

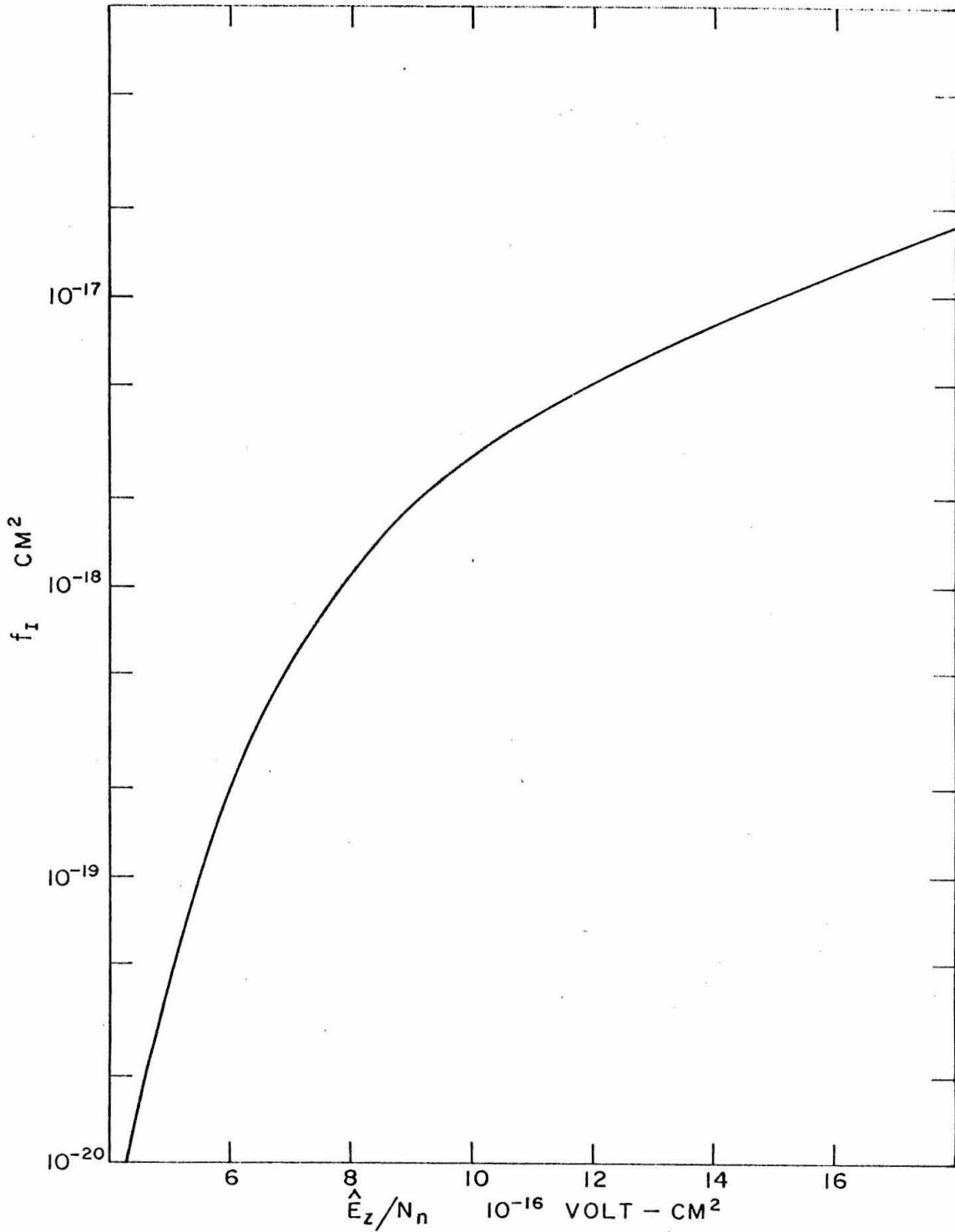


Figure 6:  $f_I$  as a Function of  $\hat{E}_z / N_n$

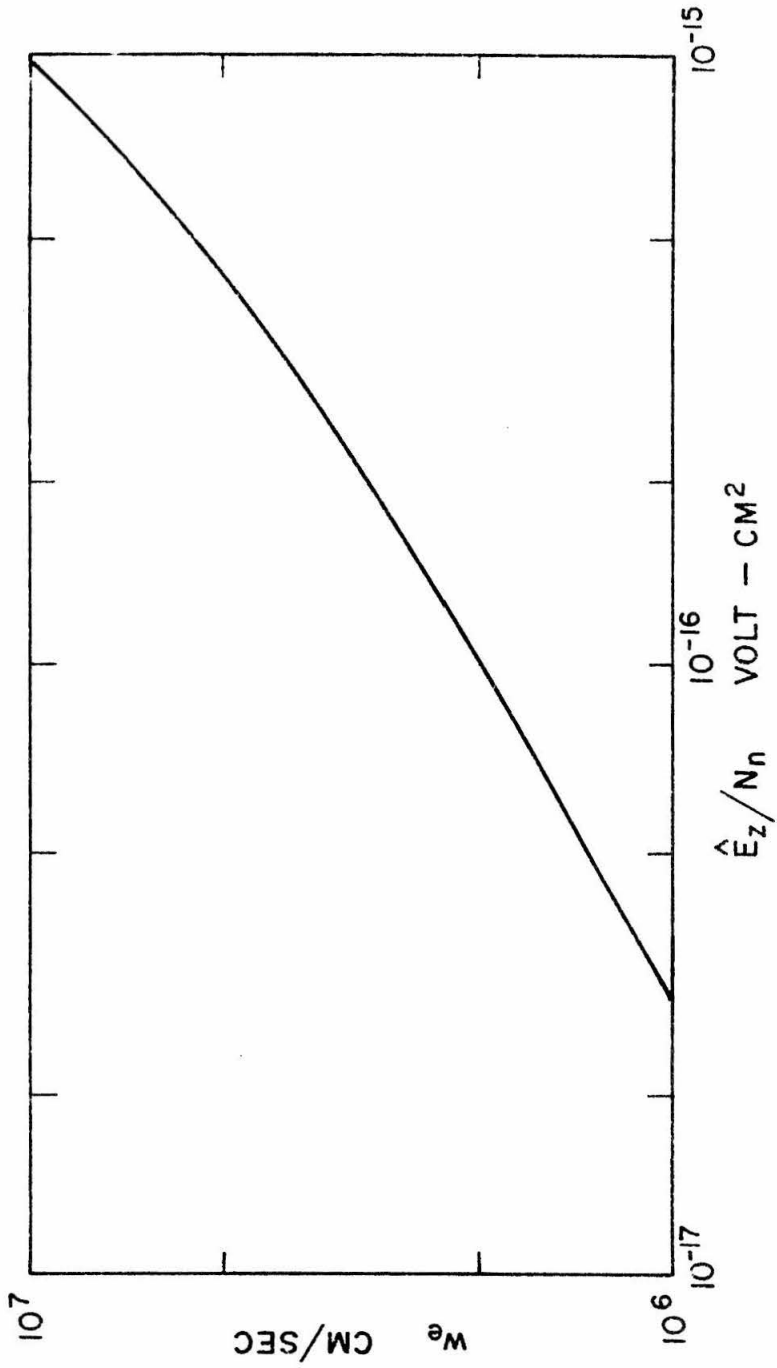


Figure 7:  $w_e$  as a Function of  $\hat{E}_z/N_n$

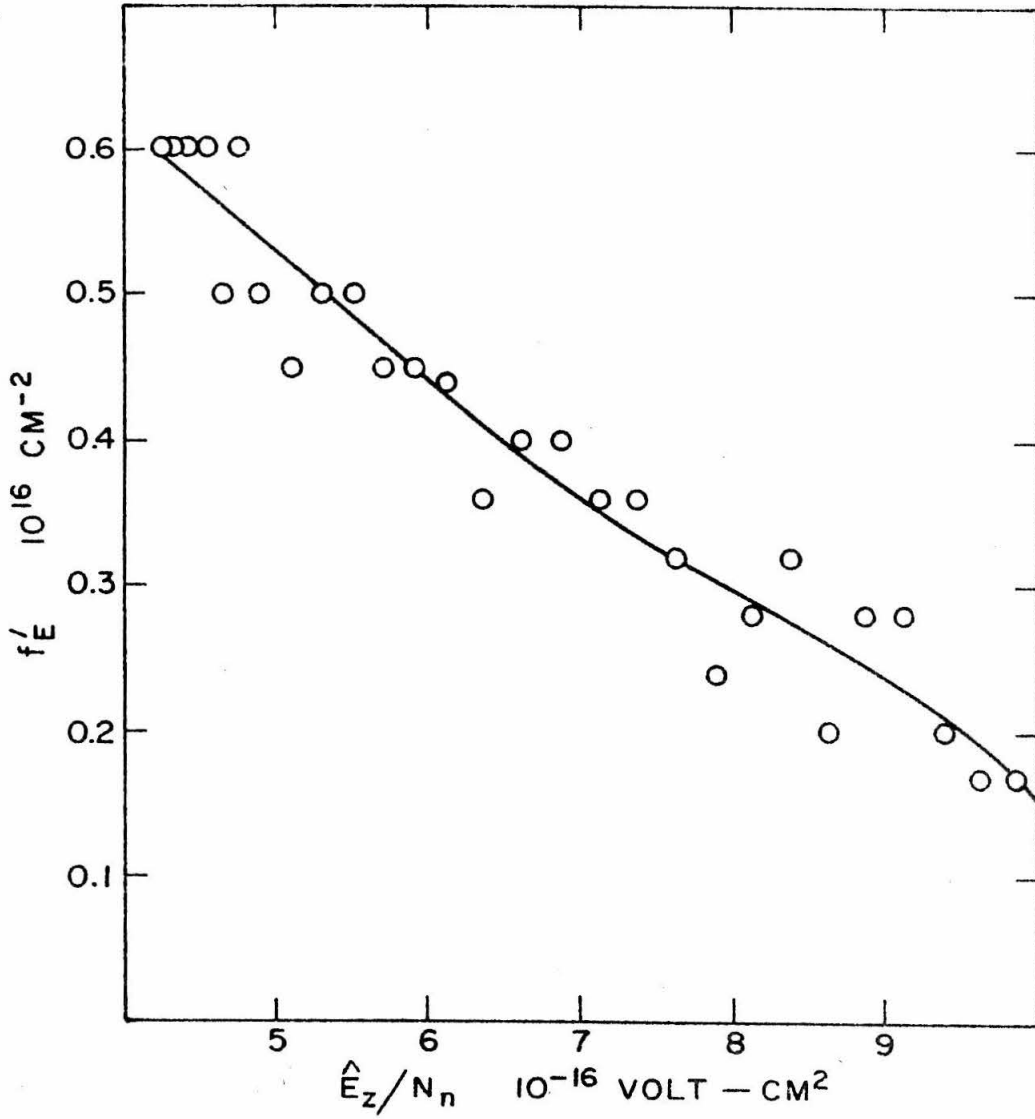


Figure 8:  $f'_E$  as a Function of  $\hat{E}_z / N_n$

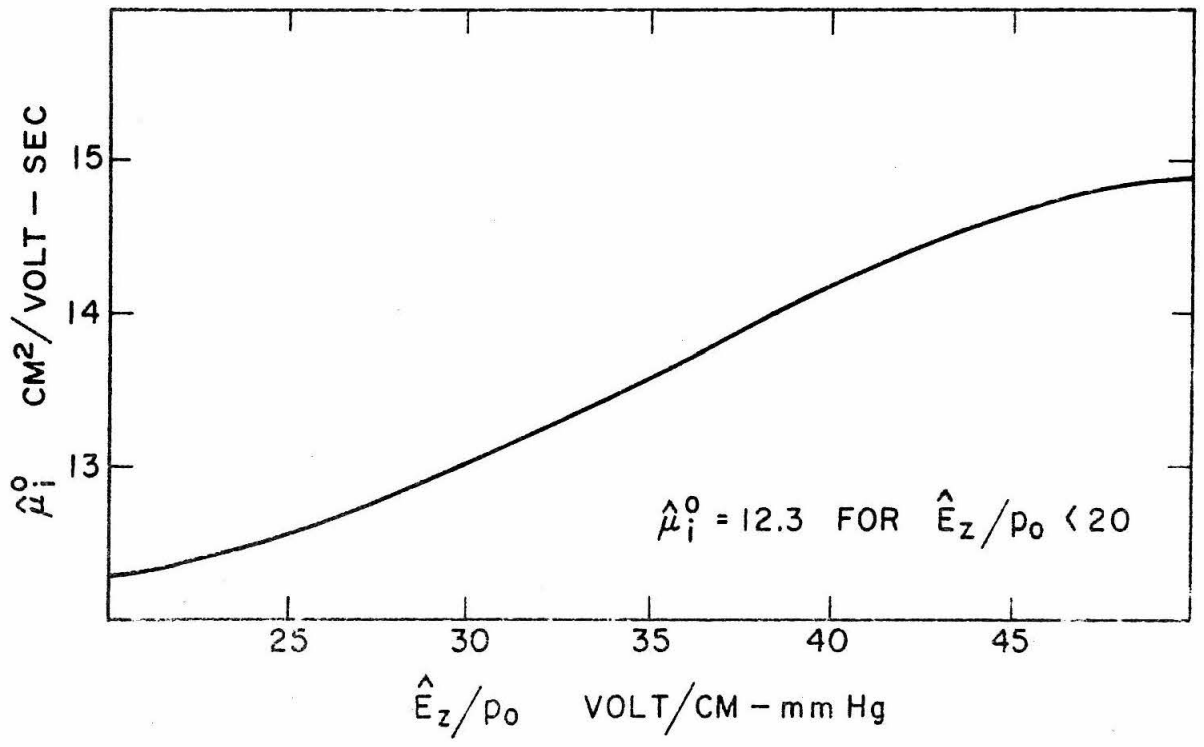


Figure 9:  $\hat{\mu}_i^0$  as a Function of  $\hat{E}_z/p_0$

Bibliography

1. Allis, W. P. and D. J. Rose, "The Transition from Free to Ambipolar Diffusion," Physical Review 93, 84-93 (1954).
2. Bates, D. R. Atomic and Molecular Processes, Academic Press, 1962.
3. Biondi, Manfred A. and Sanborn C. Brown, "Measurement of Electron-Ion Recombination," Physical Review 76, 1697-1700 (1949).
4. Blank, J. L., "Collision-Dominated Positive Column of a Weakly Ionized Gas," Physics of Fluids 11, 1686-1698 (1968).
5. Chapman, Sydney and T. G. Cowling The Mathematical Theory of Non-Uniform Gases, Cambridge University Press, 1952.
6. Cobine, James Dillon Gaseous Conductors, Dover, 1958.
7. Cohen, Ira M. and Martin D. Kruskal, "Asymptotic Theory of the Positive Column of a Gas Discharge," Physics of Fluids 8, 920-934 (1965).
8. Delcroix, J. L. Plasma Physics, Wiley & Sons, Ltd., 1965.
9. Ecker, G. and O. Zöllner, "Thermally Inhomogeneous Plasma Column," Physics of Fluids 7, 1996-2000 (1964).
10. Engelhardt, A. G. and A. V. Phelps, "Elastic and Inelastic Collision Cross Sections in Hydrogen and Deuterium from Transport Coefficients," Physical Review 131, 2115-2128 (1963).
11. Frost, L. S. and A. V. Phelps, "Rotational Excitation and Momentum Transfer Cross Sections for Electrons in H<sub>2</sub> and N<sub>2</sub> from Transport Coefficients," Physical Review 127, 1621-1633 (1962).
12. Hasted, J. B. Physics of Atomic Collisions, Butterworth & Co., Ltd. London, 1964.
13. Hirschfelder, Joseph O., Charles F. Curtiss, and R. Byron Bird Molecular Theory of Gases and Liquids, Wiley & Sons, Inc., 1954.
14. Holt, E. H. and R. E. Haskell Foundations of Plasma Dynamics, The Macmillan Company, 1965.

15. International Critical Tables, Vol. V, McGraw-Hill Co., New York, 1929.
16. Jeans, J. H. The Dynamical Theory of Gases, Dover, 1954.
17. Keller, Joseph B. and Stuart Antman Bifurcation Theory and Nonlinear Eigenvalue Problems, W. A. Benjamin, Inc., 1969.
18. Loeb, L. B. Basic Processes of Gaseous Electronics, University of California Press, Berkeley, 1960.
19. McDaniel, Earl W. Collision Phenomena in Ionized Gases, Wiley & Sons, Inc., 1964.
20. Panofsky, Wolfgang K. H. and Melba Phillips Classical Electricity and Magnetism, Addison-Wesley, 1962.
21. Perry's Chemical Engineers' Handbook, McGraw-Hill, New York, 1963.
22. Persson, Karl B. and Sanborn C. Brown, "Electron Loss Process in the Hydrogen Afterglow," Physical Review 100, 729-733 (1955).
23. Popov, N. A. and E. A. Afanas'eva, "Investigation of Deionization with Probes and by a Photoelectric Method," Soviet Physics-- Technical Physics 4, 764-769 (1960).
24. Self, S. A. and H. N. Ewald, "Static Theory of a Discharge Column at Intermediate Pressures," Physics of Fluids 9, 2486-2492 (1966).
25. Vincenti, Walter G. and Charles H. Kruger, Jr. Introduction to Physical Gas Dynamics, Wiley & Sons, Inc., 1965.
26. Von Engel, A. Ionized Gases, Oxford University Press, 1965.

103 / -104-

PART II

EFFECT OF RECOMBINATION AND SPACE CHARGE

## INTRODUCTION

The complete equations derived in Part I are too difficult to solve directly and require further simplification. The simplifications made here and in Part III correspond to the neglect of certain physical processes and thereby serve to isolate the effect of the remaining phenomena. Although the separate treatments of the various phenomena cannot be combined to yield the same quantitative results as the solution of the complete equations, the qualitative and, to a good approximation, the quantitative effects of the individual physical processes are clearly discernible.

The basic simplification of this part is to neglect temperature inhomogeneities and to assume the neutral temperature uniform at a specified value. The primary purpose now becomes the study of the effect of recombination and space charge on the  $N_{eo} - \hat{E}_z$  relation. The space charge, which results from the difference between electron and ion densities, is always important except at very small values of the electron density (see Part I, pp. 58 ff. for the solution at  $N_{eo} = 0$ ). However, as the electron density becomes large, the effect of space charge on the  $N_{eo} - \hat{E}_z$  relation and on the spatial behavior of the dependent variables approaches a limit. Near this limit,  $\hat{E}_z$  and the variables are insensitive to changes in  $N_{eo}$ , and we speak of space charge as being "negligible"; we consider the effect of space charge to be "important" for those smaller values of  $N_{eo}$  at which  $\hat{E}_z$  and the dependent variables vary significantly with changes in  $N_{eo}$ . Since space charge is important for small  $N_{eo}$  whereas recombination in

hydrogen is only significant at those larger values of  $N_{eo}$  where space charge has little influence, the effects of space charge and recombination are quite distinct and could be considered separately. However, if the calculations were performed for a gas with a larger recombination coefficient, the range of  $N_{eo}$  in which the effects overlap to a noticeable extent would be greater. Since the conjunction of the separate treatments is not equivalent to the treatment of the combined effects, the analysis which follows considers space charge and recombination simultaneously and serves as a useful model for gases with larger recombination coefficients. Furthermore, the analysis is an interesting example of the application of singular perturbation techniques to a complex problem.

#### Uniform-Temperature Approximation

The assumption of uniform temperature engenders a considerable simplification in the equations. First, of course, the equation for the temperature is eliminated from the problem. Also, the pressure depends only on the neutral temperature and the amount of gas in the discharge, so it is independent of  $N_{eo}$  and  $\hat{E}_z$ . Since the variable coefficients in the equations depend only on  $T$ ,  $\hat{E}_z$ , and  $p$ , they become constants and vary only with  $\hat{E}_z$  (or with  $N_{eo}$  through the  $N_{eo} - \hat{E}_z$  relation).

The correspondence of the resulting equations to the actual physical situation may be rendered unreasonable by the neglect of temperature inhomogeneities. The studies in Part III show that temperature effects become important at a smaller electron density than does

recombination and hence the behavior of the  $N_{eo} - \hat{E}_z$  relation at large values of  $N_{eo}$  may be so dominated by temperature inhomogeneities that recombination is relatively unimportant. Furthermore, the recombination coefficient in hydrogen is expected to be less than the value actually used (see p. 50, Part I). However, other gases have larger recombination coefficients, and recombination in such cases may become important at a smaller value of  $N_{eo}$  than temperature inhomogeneities. For such gases the calculations of this part serve as a useful model.

#### Production and Loss of Electrons

A considerable amount of qualitative information can be obtained by studying the rates of production and loss of electrons. Electrons are produced by ionization and are lost by diffusion to the walls and by recombination. These processes depend upon the axial electric field and the electron density, and the requirement that production and loss balance at steady-state operation determines the  $N_{eo} - \hat{E}_z$  relation. The ionization coefficient is a strongly increasing function of  $\hat{E}_z$ , so if the electron density is held fixed, the production rate increases rapidly with  $\hat{E}_z$ . The loss by diffusion is also affected by changes in  $\hat{E}_z$ , but its dependence on  $\hat{E}_z$  is weak relative to that of ionization. For lack of better data, the recombination coefficient is assumed constant and is independent of  $\hat{E}_z$  (see pp. 49 ff., Part I). In general, however, the recombination loss rate would depend on  $\hat{E}_z$ . If  $\hat{E}_z$  is held fixed as the electron density is varied, it is observed that the ionization rate is essentially proportional to the electron density  $N_{eo}$ . The rate of loss by diffusion increases as  $N_{eo}$  increases, but the detailed behavior is complicated by space-charge

effects, and a more elaborate qualitative description is postponed for a short interval. The recombination coefficient is very small, so the recombination loss rate is significant only for very large values of the electron density. When it does become important, the rate increases very rapidly, because it depends quadratically on the electron density.

It is instructive to plot the production and the loss rates as functions of electron density for specified values of the axial electric field, and this process is carried out in Fig. 1. The production rates are represented by the straight lines emanating from the origin, since the rates are proportional to the electron density. The slopes of the lines increase rapidly with  $\hat{E}_z$  and thus reflect the dependence of the ionization coefficient on the applied field. The loss rate depends weakly on  $\hat{E}_z$  in comparison with the production rate, and hence for qualitative purposes it is permissible to represent the loss rate by a single curve independent of  $\hat{E}_z$ . The reasons for the shape of the curve are explained in the subsequent discussion of the  $N_{eo} - \hat{E}_z$  relation.

Since the electron production and loss rates must be equal for steady operation, the steady states are represented by the intersections of the production and loss curves. The intersection at the origin of the loss curve with production lines of arbitrary slope corresponds, of course, to the trivial solution in which the electron density is zero and  $\hat{E}_z$  is arbitrary. The sketch also clarifies the manner in which the restriction to steady state determines the  $N_{eo} - \hat{E}_z$  relation: from a given intersection on the loss curve, the electron density can be found immediately, and the axial field can be determined from the slope

of the line connecting the point to the origin. It is apparent from the sketch that the determination of the  $N_{eo} - \hat{E}_z$  relation by specifying  $\hat{E}_z$  and finding  $N_{eo}$  is not a simple procedure. Depending on the value of  $\hat{E}_z$ , there may be zero, one, or two nontrivial steady states. On the other hand,  $\hat{E}_z$  is determined uniquely from a given  $N_{eo}$ , since the slopes of the production lines vary monotonically with  $\hat{E}_z$ . In fact, the analytical solution for the  $N_{eo} - \hat{E}_z$  relation is obtained by specifying  $N_{eo}$  and calculating  $\hat{E}_z$ . However, the analytical proceedings are considerably more complicated than this diagrammatic presentation, because  $\hat{E}_z$  is only determined through the process of solving the differential equations and the dependence of all the coefficients on  $\hat{E}_z$  must be taken into account.

#### $N_{eo} - \hat{E}_z$ Relation

The qualitative form of the  $N_{eo} - \hat{E}_z$  relation can be inferred from Fig. 1 by observing the behavior of  $\hat{E}_z$  at steady state as  $N_{eo}$  increases from zero. This description is complemented here by the corresponding discussion of the physical processes which determine the form of the production and loss curves.

For  $N_{eo}$  near zero the transverse electric field, produced by the difference between electron and ion densities, is insignificant in affecting the diffusion of electrons and ions to the walls of the discharge. Recombination, of course, is negligible except at very large values of  $N_{eo}$ , so the electron loss rate is characterized solely by the electron diffusion coefficient and the density gradient. The loss rate is essentially proportional to  $N_{eo}$  in a neighborhood of

$N_{eo} = 0$  , and this behavior is depicted in Fig. 1 by the emergence of the loss curve from the origin with a finite slope. In order to obtain a nontrivial steady-state solution in this neighborhood, the production curve must assume the same slope, and hence the axial electric field must assume a particular value. This value,  $\hat{E}_{z1}$  on Fig. 1, is the axial field at the free diffusion limit and is referred to in Part I, p. 6 and Fig. 1. The analytical nature of the eigenvalue problem which determines  $\hat{E}_{z1}$  is displayed in the discussion of the trivial solution in Part I (pp. 58 ff.).

Since electrons and ions are produced at equal rates, they must also diffuse to the walls at equal rates. The electron diffusion coefficient is much larger than the ion diffusion coefficient, so in order that the diffusional fluxes be equal, the ion density must exceed that of the electrons by the corresponding factor. The positive charge in the plasma is balanced by a negative charge on the walls, established during transient operation, and a transverse electric field is produced. As  $N_{eo}$  increases, the space charge also increases, and the transverse field so produced exerts a significant influence on the motion of electrons and ions: it inhibits the diffusion of electrons and augments the diffusion of ions. This regime of space-charge importance is represented in Fig. 1 by the portion of the loss curve that is concave downward. The decrease in electron loss relative to production by ionization requires that the ionization coefficient decrease in order to maintain a steady state. The resulting situation is typified by the steady-state operation at Point A in Fig. 1, where the axial electric field assumes the value  $\hat{E}_{z2}$  .

When the electron density is large, a small deviation of the number ratio of electrons to ions from unity produces a very large transverse field. This force affects the motion of electrons and ions so strongly that both diffuse at essentially the same speed and have almost equal densities. The limiting situation is the classical ambipolar diffusion, in which the electron and ion loss processes can be characterized by a single quantity, the ambipolar diffusion coefficient. The loss rate is given by the product of the ambipolar diffusion coefficient and the electron density gradient and is essentially proportional to  $N_{eo}$ . Consequently, if recombination is ignored, the extension of the loss curve in Fig. 1 to very large  $N_{eo}$  would take the form of the dashed line. The axial field in the ambipolar limit is determined by equating the production rate to the loss rate. Since this limit is approached only as  $N_{eo} \rightarrow \infty$ , the intersection of the production and loss curves requires that the production line have the same slope as the ambipolar extension to the loss curve. The analytical determination of the axial field  $\hat{E}_{za}$ , as in the free diffusion limit, is a linear eigenvalue problem. This value of  $\hat{E}_z$  is never actually attained in the model considered here; in fact, Fig. 1 shows that the smallest value the axial field can assume in steady-state operation is  $\hat{E}_{z3}$ , corresponding to operation at Point B.

The loss curve corresponding to the physical phenomena considered here differs from the ambipolar extension, because when recombination becomes important, the loss rate increases strongly with electron density. Accordingly, the loss curve for very large  $N_{eo}$  is concave upward, and the slope of the production line (and hence  $\hat{E}_z$ ) must

increase with  $N_{eo}$ . Point C in Fig. 1 represents a steady state in the regime where recombination is important. It should be noted that the axial field at C is the same as that at A.

The form of the  $N_{eo} - \hat{E}_z$  relation discussed in detail above is shown in Fig. 2. The lettered points and the values of  $\hat{E}_z$  correspond to those of the sketch in Fig. 1, and the dashed line again represents the extension toward the ambipolar limit that would arise if the consideration of recombination were omitted.  $\hat{E}_{za}$ , of course, is the value of the axial field at the ambipolar limit.

Before associating the form of the  $N_{eo} - \hat{E}_z$  relation with the experimental voltage-current characteristic, it is convenient to comment briefly on the effect of recombination on the shape of the electron density profile. Whether or not recombination is included in the model as a physical phenomenon, the electron density is at a maximum at the center of the discharge and decreases to zero at the walls. Since the loss by recombination is of most significance where the density is largest, the greatest relative effect of recombination occurs at the center. If the electron density at the center were constrained to a particular value, the density profile would be flatter in the center and would hence drop more steeply near the walls than if recombination were omitted from consideration.

#### Interpretation of the Experimental Characteristic

The correlation between the electron density and axial electric field in the positive column and the current through the discharge and total voltage drop across it is discussed in Part I, pp. 8-9, 62.

The experimental curve is sketched in Fig. 2 of Part I, and if the change in axes is noted, the  $N_{eo} - \hat{E}_z$  relation in Fig. 2, Part II is seen to possess a shape similar to that of the experimental voltage-current characteristic in the subnormal-normal-abnormal regime. This similarity raises the possibility that recombination may be a factor affecting the voltage-current behavior in the abnormal regime.

However, considerable caution must be exercised in seeking conclusions from this comparison. As mentioned previously, the effect of temperature inhomogeneities on the discharge characteristic is likely to appear before (at smaller currents) the effect of recombination. Furthermore, the uncertainty in the recombination coefficient does not permit a rigid association of the rising portion of the calculated positive-column characteristic with a particular portion of the experimental characteristic. Also, the effect of electrode phenomena is included in the experimental characteristic and has no counterpart in the calculated curve.

#### Stability in the Positive Column

The stability of the steady states represented by the  $N_{eo} - \hat{E}_z$  relation can be inferred in a loose qualitative manner by reference to Fig. 1. If, for instance, the discharge were in a transient state with  $\hat{E}_z = \hat{E}_{z2}$  at an electron density slightly larger than that corresponding to Point C, the electron loss rate would exceed the production rate, and the electron density would tend to decrease. On the other hand, if the electron density were less than that at C, production would exceed loss, and the density would tend to increase. However, a

perturbation from Point A would result in the opposite behavior. If the discharge were in transient operation with an electron density slightly greater than that at A, production would exceed loss and the density would tend to increase still further; if it were less than that at A, it would tend to decrease. On this basis, we would call steady state C stable and A unstable. Furthermore, all steady states above B on the loss curve would be stable, and all those below B except the origin would be unstable as would be all steady states along the ambipolar extension.

These conclusions, however, must be regarded with considerable caution. A perturbation of the electron density from its steady-state value does not suffice to determine stability, and the transient equations must be used to predict the response to more general perturbations of all the variables. Also, the overall bookkeeping of Fig. 1 cannot replace the local considerations required as a result of the spatial dependence of the variables. Furthermore, the stability of the positive column and of the discharge can be modified by the exterior circuit. For example, the energy transferred to the electrons by the applied field is limited by the exterior energy source, and hence this energy source serves as a control to restrain the electron density (current) from excessive values\*. It is obvious from the considerations above that the conclusions concerning the stability of the positive column should be regarded as suggestive only.

---

\*The stability of a circuit containing an electromotive force, a resistor, and a discharge is treated in Cobine [3], pp. 207 ff.

### Analytical Procedure

The problem to be solved is obtained by setting the temperature equal to a constant in the equations of Part I. The resulting equations are still too difficult to solve even numerically, and approximate methods must be employed. The approximations derive from the observation that certain of the terms in the equations are small and can be treated as perturbations under appropriate conditions. The propriety of the conditions depends primarily on the magnitude of the electron density, and hence it is necessary to choose the range of  $N_{eo}$  in which we wish to operate. Our purpose is to investigate the effects of space charge and recombination on the  $N_{eo} - \hat{E}_z$  relation, and consequently we must consider values of  $N_{eo}$  on either side of Point B in Fig. 2.

Point B marks the closest approach of the discharge to the ambipolar limit, and here the terms responsible for the effects of space charge and recombination are both small and can be treated as perturbations. In the crudest approximation these terms are neglected and the equations become the mathematical description of the ambipolar limit. By expanding the variables in asymptotic series which, to lowest order, represent the ambipolar solution, approximate solutions are obtained which incorporate the effect of space charge and recombination in higher-order terms. Since the effect of space charge is greater at small values of  $N_{eo}$  whereas that of recombination is greater for large  $N_{eo}$ , some of the terms in the expansions decrease as  $N_{eo}$  increases, while others increase. In fact, each expansion is

actually a composite of two asymptotic series, one which includes the effect of space charge and another which accounts for recombination.

The analytical proceedings are greatly complicated by the fact that the neglect of the space-charge term is not uniformly valid as an approximation. Near the walls of the discharge column the space-charge term is not small in comparison with other terms of the equations, and its omission leads to unreasonable behavior in the solution. The problem is actually a singular perturbation problem, and the equations must be treated differently in two individual spatial regions. Throughout the central region of the discharge the space-charge term can be neglected, but near the wall in a narrow region or boundary layer called the sheath the term must be retained in the equations. The solutions in the two regions must be made to agree or "match" in some sense in an intermediate region before a solution acceptable throughout the entire positive column is obtained.

#### Relation to Previous Work

Cohen and Kruskal [5] ignore recombination but otherwise treat essentially the same problem by similar means. They also assume uniform temperature (constant coefficients) and treat the effect of space charge by singular perturbation techniques. However, their attitude toward the coefficients makes their work a model illustrating the basic effect of space charge rather than an example calculation for an actual gas. Their coefficients are all arbitrary constant parameters except one, which is proportional to the ionization coefficient and is an eigenvalue corresponding to our  $\hat{E}_z$ . In essence, they assume that only the

ionization coefficient depends on  $\hat{E}_z$ .

The inclusion of recombination in the problem complicates the solution in the main region but to a good approximation does not affect the form of the equations in the sheath. However, the effect of recombination is felt in the sheath through the dependence of the coefficients on  $\hat{E}_z$  and through the necessity of matching the main-region and sheath solutions in an intermediate region. As a consequence, much more computation is necessary in the sheath than would be if recombination were not considered, but the techniques are essentially the same.

## 1. WORKING EQUATIONS

The equations used to study the effects of space charge and recombination are obtained easily from those derived in Part I by setting the temperature equal to a constant. The only basic alteration necessary to secure the desired form of the working equations is the replacement of one dependent variable, the ion density, with a more convenient quantity.

### Equations for Dependent Variables

The uniform-temperature approximation is equivalent to the neglect of energy transfer from electrons to neutral molecules and corresponds to setting  $\beta$  (or  $\hat{h}$ ) equal to zero in the equations of Part I. Equation (5.21) for the temperature can then be solved subject to the boundary conditions (5.31) and (5.35), and we obtain

$$T = 1 \quad (1.1)$$

or, using (5.10),

$$\hat{T} = \hat{T}_w \quad (1.2)$$

The pressure  $p$  is a constant describing the state of the neutral gas. Since the temperature is constant at a value independent of the processes occurring within the discharge,  $p$  depends only on the amount of gas contained in the discharge and can be treated as an arbitrary parameter.

The variable coefficients can be eliminated from the equations by making a judicious choice for the reference values  $\hat{E}_{zr}$  and  $p_r$ . Since  $T$  is constant, the coefficients, of course, are actually

constant. By choosing

$$\hat{E}_{zr} = \hat{E}_z \quad (1.3)$$

and

$$p_r = p \quad (1.4)$$

the dimensionless coefficients in Eqs. (5.1) - (5.9) of Part I all reduce to unity. The only other variable coefficients in the equations occur in terms containing  $dT/dy$  as a factor and hence do not enter the problem considered here.

Equations (5.18) - (5.20), (5.22) and the boundary conditions (5.29), (5.30), (5.32) - (5.34) can now be written as

$$\frac{dJ}{dy} = \gamma n_e - \varepsilon \zeta n_e n_i \quad (1.5)$$

$$\frac{dn_e}{dy} = -n_e E - \delta \tau J \quad (1.6)$$

$$\frac{dn_i}{dy} = \tau n_i E - \tau J \quad (1.7)$$

$$\frac{1}{\zeta} \frac{dE}{dy} = \chi (n_i - n_e) \quad (1.8)$$

$$y = 0: \quad n_e = 1 \quad (1.9)$$

$$J = 0 \quad (1.10)$$

$$E = 0 \quad (1.11)$$

$$y = 1: \quad n_e = 0 \quad (1.12)$$

$$n_i = 0 \quad (1.13)$$

Constant Coefficients

The constant coefficients  $\gamma$ ,  $\epsilon$ ,  $\tau$ ,  $\delta$ ,  $\chi$  are defined by Eqs. (5.23) - (5.26), (5.28) of Part I, and using the reference values given in (1.3) and (1.4), they become

$$\gamma = \frac{L^2 \hat{\nu}_I(\hat{T}_w; \hat{E}_z, p)}{\hat{D}_i(\hat{T}_w; \hat{E}_z, p)} \cdot \frac{\hat{T}_w}{\hat{T}_e(\hat{T}_w; \hat{E}_z, p)} \quad (1.14)$$

$$\epsilon = \frac{L^2 \hat{\alpha} N}{\hat{D}_i(\hat{T}_w; \hat{E}_z, p)} \cdot \frac{\hat{T}_w}{\hat{T}_e(\hat{T}_w; \hat{E}_z, p)} \quad (1.15)$$

$$\tau = \frac{\hat{T}_e(\hat{T}_w; \hat{E}_z, p)}{\hat{T}_w} \quad (1.16)$$

$$\delta = \frac{\hat{D}_i(\hat{T}_w; \hat{E}_z, p)}{\hat{D}_e(\hat{T}_w; \hat{E}_z, p)} \quad (1.17)$$

$$\chi = \frac{L^2 N e^2}{\epsilon_0 k \hat{T}_e(\hat{T}_w; \hat{E}_z, p)} \quad (1.18)$$

The coefficients depend on the axial field  $\hat{E}_z$  and the parameters  $L$ ,  $\hat{T}_w$ ,  $p$ , and  $N$ .  $L$ ,  $\hat{T}_w$ , and  $p$  represent the adjustable structure and nature of the discharge and must be specified before numerical results can be obtained. The dependence of the problem on these parameters is not studied, and for the calculations we choose the values

$$L = 1 \text{ cm} \quad (1.19)$$

$$\hat{T}_w = 300^\circ \text{K} \quad (1.20)$$

$$p = 1 \text{ mm Hg} . \quad (1.21)$$

$N$ , on the other hand, is not a real parameter, and it cancels in forming the products  $\epsilon\zeta$  and  $\chi\zeta$ . It is introduced into the equations for the purpose of separating the dependence of these two terms on  $N_{eo}$  and  $\hat{E}_z$  and can be assigned a value arbitrarily without affecting the problem.  $\chi\zeta$  is a large quantity in the range of electron densities we consider, and for convenience we choose

$$N = 10^6 \text{ cm}^{-3} \quad (1.22)$$

so that the magnitude of  $\chi$  is near unity.

The approach to the problem consists of specifying  $N_{eo}$  (or  $\zeta$ ) in advance and determining  $\hat{E}_z$  in the course of solving the equations. Since the constant coefficients depend on  $\hat{E}_z$ , they are unknown until  $\hat{E}_z$  is obtained. The values which  $\hat{E}_z$  can assume are limited by the domain of the experimental data according to Eq. (4.29) of Part I.  $N_n$  is easily determined from the values of  $p$  and  $\hat{T}$ , and we find that  $\hat{E}_z$  is restricted to the range

$$13.83 \text{ volt/cm} < \hat{E}_z < 32.16 \text{ volt/cm} \quad (1.23)$$

For  $\hat{E}_z$  in this range the constant coefficients are bounded by the inequalities

$$0.0814 < \gamma < 20.5 \quad (1.24)$$

$$6.69 \times 10^{-7} < \epsilon < 1.532 \times 10^{-6} \quad (1.25)$$

$$2.355 \times 10^{-4} < \delta < 3.918 \times 10^{-4} \quad (1.26)$$

$$73.5 < \tau < 152.8 \quad (1.27)$$

$$0.458 < \chi < 0.953 \quad (1.28)$$

$$2.88 \times 10^{-2} < \delta\tau < 3.60 \times 10^{-2} \quad (1.29)$$

Since  $\hat{E}_z$  is a function of  $N_{eo}$ ,  $N_{eo}$  cannot vary so extensively that  $\hat{E}_z$  exceeds its bounds. However, as  $\hat{E}_z$  varies over its range,  $\gamma$ , which is proportional to the ionization coefficient, changes by several orders of magnitude. Consequently the range of  $\hat{E}_z$  is not as limited as it might appear and actually permits a large variation in the production rate of electrons. Hence it happens that  $N_{eo}$  is limited not by the range of  $\hat{E}_z$  but by the approximate methods employed in solving the problem. The value of  $\zeta$  is roughly bounded by the inequality

$$10^2 < \zeta < 10^7 \quad (1.30)$$

and using the relation  $N_{eo} = N\zeta$ , we find that the electron density is restricted to the range

$$10^8 \text{ cm}^{-3} < N_{eo} < 10^{13} \text{ cm}^{-3} \quad (1.31)$$

The electron density in a glow discharge is typically between  $10^8$  and  $10^{12} \text{ cm}^{-3}$ , so our investigation corresponds to the proper regime of the experimental voltage-current characteristic. Also, the values of the coefficients presented above provide qualitative information about the equations and about the physical processes which the various terms represent. Since the dependent variables are made dimensionless in such a way that their magnitudes are expected to be near unity throughout most of the discharge, the relative importance of the terms in the equations can be roughly estimated by the size of their coefficients.

Since  $\hat{E}_z$  does not enter the equations explicitly, it is not conveniently determined as a function of  $N_{eo}$  in the process of solving the problem. It is more convenient to replace it with one of the coefficients by using the functional relationship connecting them.  $\gamma$  is the most widely varying coefficient and is a monotonically increasing function of  $\hat{E}_z$ , so it is possible to solve for  $\hat{E}_z$  as a function of  $\gamma$ . Now the other coefficients can also be determined as functions of  $\gamma$ . The evaluation of  $\epsilon$ ,  $\delta$ ,  $\tau$ ,  $\chi$ , and  $\hat{E}_z$  as functions of  $\gamma$  is adapted to computer calculations through the use of least-squares polynomial fits; the error introduced in the process is completely negligible. In solving the problem we now find  $\gamma$  as a function of  $\zeta$  and need not consider  $\hat{E}_z$ . Hence the  $N_{eo}-\hat{E}_z$  relation is replaced by the  $\zeta-\gamma$  relation and can be easily obtained from it when the solution is complete.

### Final Equations

At the operating conditions considered, the relative difference between electron and ion densities is small, and it is convenient to replace  $n_i$  in the equations with the space-charge variable  $s$ , defined by the equation

$$s = n_i - n_e . \quad (1.32)$$

When this change of dependent variables is made in Eq. (1.7), it becomes

$$\frac{dn_e}{dy} + \frac{ds}{dy} = \tau n_e E + \tau s E - \tau J . \quad (1.33)$$

Equations (1.6) and (1.33) are now replaced by linear combinations of themselves. One equation is obtained by eliminating the term containing

$n_e E$  between the equations, and the other is obtained by eliminating  $J$ . The final set of working equations consists of these two and Eqs. (1.5) and (1.8) with  $n_i$  replaced by  $s$ :

$$\frac{dJ}{dy} - \gamma n_e + \epsilon \zeta n_e^2 = -\epsilon \zeta n_e s \quad (1.34)$$

$$\frac{dn_e}{dy} + \tau \frac{1 + \delta \tau}{1 + \tau} J = \frac{\tau}{1 + \tau} sE - \frac{1}{1 + \tau} \frac{ds}{dy} \quad (1.35)$$

$$\frac{dn_e}{dy} + \frac{1 + \delta \tau}{1 - \delta} n_e E = \frac{\delta}{1 - \delta} \frac{ds}{dy} - \frac{\delta \tau}{1 - \delta} sE \quad (1.36)$$

$$\chi s = \frac{1}{\zeta} \frac{dE}{dy} \quad (1.37)$$

The boundary condition on  $s$  is obtained, of course, from those on  $n_e$  and  $n_i$  in (1.12) and (1.13) and is

$$y = 1 : \quad s = 0 \quad (1.38)$$

### Relations among the Variables

A certain amount of general information about the dependent variables can be obtained directly from the differential equations and boundary conditions. Some information is provided in the theorems of Appendix A, in which various bounds on the variables are established. For instance, it is proved using very simple but involved techniques that under certain conditions  $s$  and  $E$  are positive on the interval  $0 < y < 1$  and that  $d^2 n_i / dy^2 \leq 0$  at  $y = 0$ . Also, upper and lower bounds are established on  $n_i$  at  $y = 0$  in terms of the coefficients. Some of these results may seem so obvious from physical grounds that

any other behavior would appear to be physically unreasonable. However, the interaction of an electric field with mobile charged particles is a complex phenomenon, particularly in the presence of other processes, and it is gratifying to obtain the results rigorously from the equations as well as from physical intuition and approximate mathematical methods. Furthermore, the proofs provide insight into the equations by showing quite intimately the way in which the variables affect each other. An understanding of the motivation behind the proofs can have such practical ramifications as showing what instabilities might be expected to arise in a direct numerical integration of the equations.

## 2. SEPARATION OF THE PLASMA COLUMN INTO MAIN REGION AND SHEATH

The manner in which space charge and recombination are treated as perturbations from the ambipolar situation is described generally in the Introduction. With the equations available the terms corresponding to these phenomena can be discussed more perceptively. The coefficient  $\epsilon$  is proportional to the recombination coefficient and is solely responsible for the representation of recombination in the equations. The inequality (1.25) shows that  $\epsilon$  is very small, and the term in the equations that contains it is unimportant except for very large values of  $\zeta$ . The space charge is measured by the term  $(1/\zeta)dE/dy$ , and its magnitude is greatest at small  $\zeta$ .  $\zeta$  is restricted to a certain range of values by the validity and accuracy of the approximate procedure in which the terms corresponding to space charge and recombination are treated as perturbations. Recombination, of course, establishes the upper limit, and the lower bound is determined by the response of the variables to space-charge effects. The approximate numerical values for the bounds are only discovered in the process of solving the problem and are presented in Eq. (1.30).

### Asymptotic Expansions

The problem is attacked by expanding the variables in asymptotic series composed of functions of  $\zeta$  and substituting the expansions into the equations. Terms containing the same dependence on  $\zeta$  are associated, and equations for the individual terms of the series are obtained. To lowest order  $(1/\zeta)dE/dy$  and the terms containing  $\epsilon$  are

omitted, and their effects are included only in higher-order terms. The expansions actually consist of two asymptotic series which account for recombination and space charge, respectively. However, some terms contain the effects of both processes, so a clean separation of the expansions into two groups of terms is not possible. In fact, if the separation were possible, this approach to the problem would be equivalent to treating recombination and space charge separately and combining the final results. Nevertheless, a useful conceptual division of the series into effects of recombination and space charge can still be made and is referred to loosely below. The portion of the expansions that comprises the effect of recombination is a series in powers of  $\zeta$  (actually  $\epsilon\zeta$ ), and these terms provide their largest and least accurate contribution to the solution at large values of  $\zeta$ . The effect of space charge, on the other hand, is contained in terms or factors that approach zero as  $\zeta$  becomes infinite. In the range of values to which  $\zeta$  is limited, the first few terms of both series combine to form a meaningful and accurate approximation to the solution of the problem.

The expansion of the variables in terms representing space charge and recombination is actually applied in a particular order. First the variables are expanded in asymptotic series whose higher-order terms approach zero as  $\zeta \rightarrow \infty$ . These series are substituted into the equations, and sets of equations are obtained for those terms whose orders of magnitude are the same for large  $\zeta$ . The effect of space charge is absent in the set of lowest order, but is included in higher-order terms. The variables in each set of equations are now expanded in series of powers of  $\zeta$ , and equations are obtained which relate terms containing

the same powers. In these equations the terms representing recombination are perturbations and do not enter in the lowest-order analysis.

The first expansion is actually singular and is not valid throughout the discharge. Its application results in the neglect of  $(1/\zeta)dE/dy$  to lowest order, but this term is not negligible near the wall. It is small throughout most of the discharge because  $1/\zeta$  is very small, but as  $y \rightarrow 1$ ,  $E$  and  $dE/dy$  increase rapidly, while  $n_e$  and  $n_i$  decrease. Consequently, the term  $(1/\zeta)dE/dy$  in Eq. (1.8) is not small in comparison with  $\chi n_i$  and  $\chi n_e$ , and cannot be neglected. In the sheath near the wall a separate treatment of the equations is necessary in which the term is not considered a perturbation. In this domain other approximations are feasible, and separate solutions are obtained in the two regions. The boundary conditions do not suffice to determine either solution completely, and this indeterminacy is removed by the matching process in which the solutions are forced to agree in some intermediate region.

#### Zero-Order Problem in the Main Region

The first asymptotic expansion of the variables is valid in the main region and is written as follows:

$$J \sim J_0 + \mu_1(\zeta) J_1 + \mu_2(\zeta) J_2 + \dots \quad (2.1)$$

$$n_e \sim n_{e0} + \mu_1(\zeta) n_{e1} + \mu_2(\zeta) n_{e2} + \dots \quad (2.2)$$

$$E \sim E_0 + \mu_1(\zeta) E_1 + \mu_2(\zeta) E_2 + \dots \quad (2.3)$$

$$s \sim s_0 + \mu_1(\zeta) s_1 + \mu_2(\zeta) s_2 + \dots \quad (2.4)$$

where

$$\mu_n(\zeta) \rightarrow 0 \quad (2.5)$$

and

$$\mu_{n+1}(\zeta) / \mu_n(\zeta) \rightarrow 0 \quad (2.6)$$

as  $\zeta \rightarrow \infty$ . The manner in which the solution depends on  $\zeta$  is contained in the functions  $\mu_n(\zeta)$ . The form of the dependence is unknown now, and the  $\mu_n$  are not determined until the solution in the main region is matched to that in the sheath. Since  $\gamma$  is to be determined as a function of  $\zeta$  in the course of solving the equations, it must also be expanded. Therefore, we set

$$\gamma \sim \gamma_0 + \mu_1(\zeta) \gamma_1 + \mu_2(\zeta) \gamma_2 + \dots \quad (2.7)$$

Since  $\varepsilon$ ,  $\delta$ ,  $\tau$ , and  $\chi$  are now regarded as functions of  $\gamma$ , this expansion for  $\gamma$  induces expansions in the other coefficients as follows:

$$\varepsilon \sim \varepsilon_0 + \mu_1(\zeta) \varepsilon_1 + \dots \quad (2.8)$$

$$\delta \sim \delta_0 + \mu_1(\zeta) \delta_1 + \dots \quad (2.9)$$

$$\tau \sim \tau_0 + \mu_1(\zeta) \tau_1 + \dots \quad (2.10)$$

$$\chi \sim \chi_0 + \mu_1(\zeta) \chi_1 + \dots \quad (2.11)$$

where

$$\varepsilon_0 = \varepsilon(\gamma_0) \quad (2.12)$$

$$\varepsilon_0 + \mu_1 \varepsilon_1 = \varepsilon(\gamma_0 + \mu_1 \gamma_1) \quad (2.13)$$

or

$$\epsilon_1 = \frac{1}{\mu_1} [\epsilon(\gamma_0 + \mu_1 \gamma_1) - \epsilon(\gamma_0)] \quad (2.14)$$

etc.

If the expansions of variables and coefficients are substituted into Eqs. (1.34) - (1.37) and if only the terms of zero order in  $\zeta$  as  $\zeta \rightarrow \infty$  are retained, equations for the zero-order problem are acquired. In following this procedure,  $\epsilon_0 \zeta$  (also  $\epsilon_1 \zeta$ , etc.) is to be regarded as of zero order in  $\zeta$ . Now Eq. (1.37) immediately implies

$$s_0 \equiv 0 \quad (2.15)$$

and the use of this result in (1.34) - (1.36) yields

$$\frac{dJ_0}{dy} - \gamma_0 n_{eo} + \epsilon_0 \zeta n_{eo}^2 = 0 \quad (2.16)$$

$$\frac{dn_{eo}}{dy} + \rho_0 J_0 = 0 \quad (2.17)$$

$$\frac{dn_{eo}}{dy} + \frac{1 + \delta_0 \tau_0}{1 - \delta_0} n_{eo} E_0 = 0 \quad (2.18)$$

where  $\rho_0 = \tau_0 \frac{1 + \delta_0 \tau_0}{1 + \tau_0}$ . (2.19)

The combination of coefficients called  $\rho_0$  appears quite often in later developments. The bounds on  $\delta$  and  $\tau$  in (1.26), (1.27), and (1.29) show that it is near unity in magnitude.

It should not be inferred from the expansions of variables and coefficients that the coefficients of the  $\mu_n(\zeta)$  are independent of  $\zeta$ . Indeed,  $\zeta$  enters the zero-order problem through the recombination term in (2.16), and hence  $J_0$ ,  $n_{eo}$ ,  $E_0$ ,  $\gamma_0$ , and the other zero-order

coefficients are all functions of  $\zeta$ . The explicit form of the dependence is obtained when the equations are solved.

The zero-order equations are prepared for solution by writing an equation for  $n_{eo}$  alone. Eliminating  $J_o$  between (2.16) and (2.17) we obtain

$$\frac{d^2 n_{eo}}{dy^2} + \gamma_o \rho_o n_{eo} - \epsilon_o \zeta \rho_o n_{eo}^2 = 0 \quad . \quad (2.20)$$

Once  $n_{eo}$  is found,  $J_o$  and  $E_o$  can be obtained from Eqs. (2.17) and (2.18) as

$$J_o = - \frac{1}{\rho_o} \frac{dn_{eo}}{dy} \quad (2.21)$$

$$E_o = - \frac{1 - \delta_o}{1 + \delta_o \tau_o} \frac{1}{n_{eo}} \frac{dn_{eo}}{dy} \quad . \quad (2.22)$$

The formula for  $E_o$  serves to make manifest the breakdown of the main-region solution as the wall of the discharge is approached. If  $n_{eo}$  goes to zero at  $y = 1$  as  $n_e$  must, Eq. (2.22) predicts that  $E_o$  becomes infinite. However, the boundary conditions (1.12) and (1.13) applied to Eq. (1.8) reveal that  $dE/dy = 0$  at  $y = 1$ , and hence  $E$  must approach a finite value at the wall. The solution to the zero-order problem in the main region, which is obtained in the next section, shows that only the behavior of  $E_o$  is obviously inappropriate near the wall, but the electric field strongly affects the other variables through Eqs. (1.6) and (1.7); hence the entire main-region solution must be rejected near  $y = 1$ .

The boundary conditions (1.9) - (1.11) require the zero-order solution to satisfy

$$y = 0 : \quad n_{eo} = 1 \quad (2.23)$$

$$J_o = 0 \quad (2.24)$$

$$E_o = 0 \quad (2.25)$$

A boundary condition on  $dn_{eo}/dy$  that must be used in solving (2.20) is obtained by applying (2.24) to (2.17):

$$y = 0 : \quad \frac{dn_{eo}}{dy} = 0 \quad (2.26)$$

$E_o$  is obtained algebraically in the zero-order solution, but Eqs. (2.26) and (2.22) show that it satisfies the boundary condition (2.25) at  $y = 0$ .

The boundary condition on  $n_e$  at  $y = 1$  belongs to the sheath and cannot properly be applied to the problem in the main region. The main-region solution should be obtained using only the boundary conditions at  $y = 0$ , and the integration constants should be determined by matching with the sheath solution. In fact, this procedure, which parallels the main development of the problem, is followed in Appendix E. However, there only those quantities are obtained that would otherwise be determined by the boundary condition on  $n_{eo}$  at  $y = 1$ . Such a presentation displays considerable esthetic appeal, but the mathematical details are so burdensome that it is uneconomical to develop the complete solution in this spirit. In fact, results identical to those of Appendix E are obtained by assigning to  $n_{eo}$  the boundary condition

$$y = 1 : \quad n_{eo} = 0 \quad (2.27)$$

The use of this condition is justified by the following discussion, which obtains estimates for the magnitudes the variables assume in the sheath. The application of the condition to the zero-order problem eliminates the need to carry several unknowns in the main-region solution. The expansion of the variables that is necessary in the matching process would be particularly unpleasant with these unknowns present.

#### Breakdown of Main-Region Solution

An analysis of the main-region solution as  $y \rightarrow 1$  is necessary in order to ascertain the approximate boundaries of main region and sheath and to estimate the magnitudes of the variables in the two regions and in the transition zone. From these estimates it is also possible to justify (2.27) as the proper boundary condition on  $n_{e0}$ .

The approximate approach to the problem in the main region is based on the assumption that  $(1/\zeta)dE/dy$  is small in comparison with the other terms of the equations, and the asymptotic expansions in the functions  $\mu_n(\zeta)$  provide the formal means of neglecting  $(1/\zeta)dE/dy$  as a first approximation. However,  $E$  and its derivative increase rapidly with  $y$  near the wall, and the approximation ceases to be valid when the left-hand side of Eq. (1.8) becomes comparable in magnitude to  $n_e$  or  $n_i$ . In fact, by equating the order of magnitude of the left-hand side to that of  $n_e$  or  $n_i$ , we obtain a criterion for distinguishing between main region and sheath. Equation (2.22) provides a convenient means of estimating the magnitude of  $E$  and  $dE/dy$  in terms of  $n$ , because  $E_0$  and  $n_{e0}$  are adequate approximations to  $E$  and  $n_e$  in the main region. Since  $E_0$  and  $dE_0/dy$  cannot become large unless  $n_{e0}$  becomes small, the magnitude of  $n_{e0}$  must be near

zero when the main-region solution breaks down. Differentiating Eq. (2.22), we obtain

$$\frac{dE_o}{dy} = - \frac{1 - \delta_o}{1 + \delta_o \tau_o} \left[ \frac{1}{n_{eo}} \frac{d^2 n_{eo}}{dy^2} - \frac{1}{n_{eo}^2} \left( \frac{dn_{eo}}{dy} \right)^2 \right] \quad (2.28)$$

so the estimates for  $E$  and  $dE/dy$  become

$$E = O\left(\frac{1}{n_e}\right) \quad (2.29)$$

$$\frac{dE}{dy} = O\left(\frac{1}{n_e^2}\right) \quad (2.30)$$

The main-region solution becomes invalid when the orders of magnitude of the terms in Eq. (1.8) become equal:

$$\text{ord}\left(\frac{1}{\zeta} \frac{dE}{dy}\right) = \text{ord}(n_e) \quad (2.31)$$

Using (2.30), we find that (2.31) implies

$$n_{eo} = O\left(\frac{1}{\zeta^{1/3}}\right) \quad (2.32)$$

and then (2.29) and (2.30) yield

$$E = O(\zeta^{1/3}) \quad (2.33)$$

$$\frac{dE}{dy} = O(\zeta^{2/3}) \quad (2.34)$$

Equations (2.32) and (2.33) provide estimates for  $n_e$  and  $E$  in terms of  $\zeta$  at the point where the main-region solution breaks down.

These estimates do not describe sufficiently the distinction between the main region and the sheath; it is necessary to determine

the approximate magnitude of  $y$  at the breakdown point. Such an estimate can be obtained by studying the behavior of  $n_e$  in the sheath and requiring agreement between the main-region and sheath solutions in an intermediate (overlapping) region. It is apparent from Eqs. (1.5) and (2.21) that  $J$  is of order unity in  $\zeta$  throughout the discharge:

$$J = 0(1) \quad . \quad (2.35)$$

Then (1.6) implies

$$\left| \frac{dn_e}{dy} \right| = n_e E + \delta \tau J = 0(1) \quad (2.36)$$

provided  $n_e E = 0(1)$ . It is easily seen from (2.22) that  $n_e E = 0(1)$  where the main-region solution is valid. The boundary conditions at the wall suggest that  $n_e E$  must rise from 0 at  $y = 1$  to match the main-region behavior in the far reaches of the sheath. A rather elaborate and tedious investigation of Eqs. (1.5) - (1.8) as  $y$  decreases from 1 yields a convincing argument that  $n_e E = 0(1)$  throughout the sheath. Such a prolix analysis is not included here. It is merely assumed that  $n_e E = 0(1)$ , and the justification is inferred through the consistency of the results. Using (2.36) and the boundary condition (1.12),

$$n_e = 0(1 - y) \quad (2.37)$$

throughout the sheath. Since this behavior must match with that of  $n_{e0}$  in the main region, Eq. (2.32) implies that

$$1 - y = 0\left(\frac{1}{\zeta^{1/3}}\right) \quad (2.38)$$

where the main-region solution breaks down.

Validity of Boundary Condition on  $n_{eo}$  at the Wall

Since  $n_e$  and  $1 - y$  are both  $O(1/\zeta^{1/3})$  when the main-region solution breaks down, it is reasonable to believe that the boundary condition (2.27) yields an  $n_{eo}$  that closely approximates the correct behavior in the main region. However, Eq. (2.20) for  $n_{eo}$  now has three boundary conditions, (2.23), (2.26), and (2.27), and they determine not only  $n_{eo}$  but also the  $\zeta - \gamma_0$  relation. If  $\epsilon_0$  were zero, these equations and boundary conditions would determine  $\gamma_0$  as an eigenvalue. For small  $\zeta$  this value of  $\gamma_0$  is modified slightly by the effect of recombination represented by the factor  $\epsilon_0 \zeta$ , and  $\gamma_0$  is obtained as a function of  $\zeta$ . However, this dependence of  $\gamma_0$  on  $\zeta$  is irrelevant here; we wish to study the effect on  $n_{eo}$  and  $\gamma_0$  of an inexact boundary condition, and the error in the boundary condition is related to the space-charge expansion. Where the effect of space charge is greatest, that of recombination is least, and the qualitative effect of the boundary condition at  $y = 1$  can be evaluated without considering recombination.

Accordingly, Eq. (2.20) is replaced with the equation

$$\frac{d^2 n_{eo}}{dy^2} + \gamma_0 \rho_0 n_{eo} = 0 \quad . \quad (2.39)$$

The boundary conditions (2.23) and (2.26) now yield

$$n_{eo} = \cos \sqrt{\gamma_0 \rho_0} y \quad . \quad (2.40)$$

Since  $\rho_0$  is a function of  $\gamma_0$ , the remaining boundary condition determines  $\gamma_0$ . The condition (2.27) would yield  $\gamma_0 \rho_0 = \pi^2/4$ ,

but this condition can be replaced by a more proper, but inexact, condition based on the estimates of (2.32) and (2.38). The only requirement we actually know now is that the behavior of  $n_{e0}$  must match with that of  $n_e$  in the sheath where the main-region solution breaks down, and thus we merely require that  $n_{e0}(y) = 0(1/\zeta^{1/3})$  when  $1-y = 0(1/\zeta^{1/3})$ . Writing  $\sqrt{\gamma_0 \rho_0}$  as  $\pi/2 - \eta$  and  $1-y$  as  $0(1/\zeta^{1/3})$ , Eq. (2.40) at breakdown becomes

$$n_{e0} = \cos \left[ \left( \frac{\pi}{2} - \eta \right) \left( 1 - 0\left(\frac{1}{\zeta^{1/3}}\right) \right) \right] \quad (2.41)$$

$$= \sin \left( \eta + 0\left(\frac{1}{\zeta^{1/3}}\right) \right) \quad (2.42)$$

$$= \eta - \frac{1}{6} \eta^3 + \dots + 0\left(\frac{1}{\zeta^{1/3}}\right) \quad (2.43)$$

Since  $n_{e0}$  itself must be of order  $0(1/\zeta^{1/3})$ , it follows that

$$\eta = 0\left(\frac{1}{\zeta^{1/3}}\right) \quad (2.44)$$

and

$$\gamma_0 \rho_0 = \frac{\pi^2}{4} + 0\left(\frac{1}{\zeta^{1/3}}\right) \quad (2.45)$$

$\rho_0$  is a slowly varying function of  $\gamma_0$ , so the error in  $\gamma_0$  incurred by the use of the boundary condition (2.27) is also of order  $0(1/\zeta^{1/3})$ . However, we will see later that the  $\mu_1(\zeta)$  occurring in Eqs. (2.1) - (2.11) equals  $1/\zeta^{1/3}$ , so corrections of this magnitude do not enter the zero-order solution. The validity of the condition  $n_{e0}(1) = 0$  is now established.

### Equations in the Sheath

The variables in the final equations of Part I are made dimensionless in such a way that their magnitudes are near unity in the main region. The estimates made above of magnitudes at breakdown of the main - region analysis show that in the sheath the variables have vastly different magnitudes and that these magnitudes depend strongly on  $\zeta$ . In order to analyze the equations more conveniently in the sheath, it is desirable to rescale the variables there so that their magnitudes are near unity and independent of  $\zeta$ .

The proper scalings can be obtained immediately from Eqs. (2.32) (2.33), (2.35), and (2.38). Equation (2.38) shows that the thickness of the sheath, or boundary layer, is of the order  $O(1/\zeta^{1/3})$ , and we define a new independent variable as

$$\xi = \zeta^{1/3}(1 - y) \quad . \quad (2.46)$$

It is convenient to replace  $y$  with  $\xi$  in studying the sheath, because  $\xi$  remains finite as  $\zeta \rightarrow \infty$  provided  $y$  remains in the sheath. The new dependent variables, appropriate for use in the sheath, are defined by the equations

$$\tilde{n}_e(\xi) = \zeta^{1/3} n_e(y) \quad (2.47)$$

$$\tilde{n}_i(\xi) = \zeta^{1/3} n_i(y) \quad (2.48)$$

$$\tilde{J}(\xi) = J(y) \quad (2.49)$$

$$\tilde{E}(\xi) = \frac{1}{\zeta^{1/3}} E(y) \quad (2.50)$$

The magnitude of  $n_i$  where the main-region analysis breaks down has not been determined, but Eq. (2.15) shows that it is roughly the same as that of  $n_e$ , since they are the same to first approximation in the main region.

The problem in the sheath can now be obtained by rewriting Eqs. (1.5) - (1.8) using the new variables. We find

$$\frac{d\tilde{J}}{d\tilde{\xi}} = -\zeta^{-2/3} \gamma \tilde{n}_e - \zeta^{-1} \epsilon \zeta \tilde{n}_e \tilde{n}_i \quad (2.51)$$

$$\frac{d\tilde{n}_e}{d\tilde{\xi}} = \tilde{n}_e \tilde{E} + \delta \tau \tilde{J} \quad (2.52)$$

$$\frac{d\tilde{n}_i}{d\tilde{\xi}} = -\tau \tilde{n}_i \tilde{E} + \tau \tilde{J} \quad (2.53)$$

$$\frac{d\tilde{E}}{d\tilde{\xi}} = -\chi(\tilde{n}_i - \tilde{n}_e) \quad (2.54)$$

The coefficients appearing in these equations now reflect the size and importance of the various terms. The boundary conditions (1.12) and (1.13) are applicable to the sheath and imply

$$\xi = 0 : \quad \tilde{n}_e = 0 \quad (2.55)$$

$$\tilde{n}_i = 0 \quad (2.56)$$

The other conditions needed to solve the four equations arise from the requirement of matching the sheath solution to the main-region solution at large  $\xi$ .

The magnitude estimates used in rescaling the variables are obtained by studying the breakdown of the main-region solution. Since we seek to apply these estimates throughout the sheath, we should

investigate the problem there to verify that the magnitudes do not change excessively. In particular, we want to show that  $E$  does not continue to grow at an increasing rate as we move from the main region into the sheath. Since  $\zeta$  is very large, it is apparent from Eq. (1.8) that  $E$  and  $dE/dy$  are of order unity in the main region only because the difference between  $n_e$  and  $n_i$  is very small there. However, in order to satisfy the equations and the boundary conditions at the wall,  $n_e$  and  $n_i$  must behave differently near  $y = 1$ . As the wall is approached, the difference between  $n_e$  and  $n_i$  increases and results in a corresponding increase in  $dE/dy$  and  $E$ . However, the individual magnitudes of  $n_e$  and  $n_i$  are decreasing while their difference increases. Once  $dE/dy$  becomes comparable in magnitude to  $\zeta n_e$  or  $\zeta n_i$ , no further significant increase is possible, and hence  $dE/dy$  must retain the same order of magnitude. This rough relation is the same as the criterion used to obtain the magnitude estimates and serves to define the sheath. A crude measure of the increase in  $E$  across the sheath can be obtained by multiplying the order of magnitude of  $dE/dy$  by the thickness of the sheath. From (2.33), (2.34), and (2.38) we find that  $O(dE/dy) \cdot O(1 - y) = O(E)$ , so the order of magnitude of  $E$  remains the same throughout the sheath.

### 3. ZERO-ORDER SOLUTION IN THE MAIN REGION

When the electron density is large, the solution to the zero-order problem in the main region is an excellent approximation to the solution of the entire problem. Then the effect of space charge is small, and the sheath is thin and of little importance. The exact zero-order solution for  $\gamma_0$  and  $n_{e0}$  is obtained here, but in the simultaneous treatment of space charge and recombination it is more convenient to work with an approximate solution. The approximate solution involves trigonometric functions instead of elliptic functions and is easier to manipulate in the matching between main region and sheath. Also, the same procedure used to obtain it can be applied to the first-order equations.

#### Relation to the Ambipolar Diffusion Equation

Except for the recombination term Eq. (2.20) is the same as the standard ambipolar diffusion equation\* as can be seen by expressing its coefficients in terms of the original dimensioned quantities. From Eqs. (1.16) and (1.17)

$$\frac{1 + \delta_o \tau_o}{1 + \tau_o} = \frac{1 + \frac{\hat{D}_i}{\hat{D}_e} \frac{\hat{T}_e}{\hat{T}_w}}{1 + \frac{\hat{T}_e}{\hat{T}_w}} \quad (3.1)$$

Using the Einstein relations given in Eqs. (3.8) and (3.9) of Part I,

---

\* See, for instance, von Engel [11], pp. 240-241.

$$\frac{1 + \delta_o \tau_o}{1 + \tau_o} = \frac{1 + \frac{\hat{\mu}_i}{\hat{\mu}_e}}{1 + \frac{\hat{D}_e}{\hat{\mu}_e} \frac{\hat{\mu}_i}{\hat{D}_i}} \quad (3.2)$$

$$= \frac{\hat{\mu}_e + \hat{\mu}_i}{\hat{\mu}_e \hat{D}_i + \hat{\mu}_i \hat{D}_e} \hat{D}_i \quad (3.3)$$

$$= \frac{\hat{D}_i}{\hat{D}_a} \quad , \quad (3.4)$$

where

$$\hat{D}_a = \frac{\hat{\mu}_e \hat{D}_i + \hat{\mu}_i \hat{D}_e}{\hat{\mu}_e + \hat{\mu}_i} \quad (3.5)$$

is the ambipolar diffusion coefficient\*. Using Eqs. (2.19), (1.14), (1.15), (1.16), and the relation  $\zeta = N_{eo}/N$ , we obtain

$$\gamma_o \rho_o = \gamma_o \tau_o \frac{1 + \delta_o \tau_o}{1 + \tau_o} = \frac{L^2 \hat{V}_I}{\hat{D}_a} \quad (3.6)$$

$$\epsilon_o \zeta \rho_o = \frac{L^2 \hat{\alpha} N_{eo}}{\hat{D}_a} \quad (3.7)$$

### Statement of Problem

In order to simplify the notation, it is convenient to relabel some terms for the duration of this section. We let

$$\gamma^* = \gamma_o \rho_o \quad , \quad (3.8)$$

---

\* See von Engel [11], p. 144.

$$\epsilon^* = \epsilon_0 \zeta \rho_0 \quad (3.9)$$

and

$$n = n_{e0} \quad (3.10)$$

Now the problem of Eqs. (2.20), (2.23), (2.26), and (2.27)

becomes

$$\frac{d^2 n}{dy^2} + \gamma^* n - \epsilon^* n^2 = 0 \quad (3.11)$$

$$y = 0 : \quad n = 1 \quad (3.12)$$

$$\frac{dn}{dy} = 0 \quad (3.13)$$

$$y = 1 : \quad n = 0 \quad (3.14)$$

The equation and three boundary conditions serve to determine  $\gamma^*$  as a function of  $\epsilon^*$  and  $n$  as a function of  $y$  and  $\epsilon^*$ .

### Approximate Solution

The approximate solution to Eq. (3.11) is obtained by expanding  $n$  and  $\gamma^*$  in powers of  $\epsilon^*$  as follows:

$$n \sim n_0 + \epsilon^* n_1 + \epsilon^{*2} n_2 + \dots \quad (3.15)$$

$$\gamma^* \sim \gamma_0^* + \epsilon^* \gamma_1^* + \epsilon^{*2} \gamma_2^* + \dots \quad (3.16)$$

The expansions are substituted into the equation and boundary conditions and terms of the same order in  $\epsilon^*$  are equated.  $\epsilon^*$  is proportional to  $\zeta$ , and the expansions have been referred to previously as those in which recombination is regarded as a perturbation.

After substituting these expansions into Eqs. (3.11) - (3.14) and equating equal powers of  $\epsilon^*$ , we obtain as the first approximation to the problem

$$\frac{d^2 n_o}{dy^2} + \gamma_o^* n_o = 0 \quad (3.17)$$

$$y = 0 : \quad n_o = 1 \quad (3.18)$$

$$\frac{dn_o}{dy} = 0 \quad (3.19)$$

$$y = 1 : \quad n_o = 0 \quad (3.20)$$

We obtain immediately from (3.17) - (3.19) that

$$n_o = \cos \sqrt{\gamma_o^*} y \quad (3.21)$$

Now (3.20) implies

$$\gamma_o^* = (2j - 1)^2 \frac{\pi^2}{4} \quad , \quad (3.22)$$

where  $j = 1, 2, \dots$ . Each of these values must be regarded as a candidate for the correct  $\gamma_o^*$ . However, only for  $j = 1$  does (3.21) provide an electron density that is nowhere negative. Therefore on physical grounds we choose

$$n_o = \cos \frac{\pi}{2} y \quad (3.23)$$

$$\gamma_o^* = \frac{\pi^2}{4} \quad (3.24)$$

These results are the solution to the classical ambipolar diffusion problem and form the basic description of the positive column to which

the effects of space charge and recombination are added as perturbations. The first approximation to  $\gamma_0$  is obtained by solving the equation

$$\gamma_a \rho_0(\gamma_a) = \frac{\pi^2}{4} \quad (3.25)$$

where the subscript "a" represents the ambipolar solution. The numerical solution for  $\gamma_a$  yields

$$\gamma_a = 2.4123 \quad (3.26)$$

and from it  $\hat{E}_{za}$  is found to be

$$\hat{E}_{za} = 20.926 \text{ volt/cm} \quad (3.27)$$

Higher-order terms of the series show the effect of recombination. Equation (3.11) and the accompanying boundary conditions to the first power in  $\epsilon^*$  are

$$\frac{d^2 n_1}{dy^2} + \gamma_0^* n_1 = n_0^2 - \gamma_1^* n_0 \quad (3.28)$$

$$y = 0 : \quad n_1 = 0 \quad (3.29)$$

$$\frac{dn_1}{dy} = 0 \quad (3.30)$$

$$y = 1 : \quad n_1 = 0 \quad (3.31)$$

The homogeneous equation associated with (3.28) has a nontrivial solution satisfying (3.30) and (3.31). The results of Appendix B show that the right-hand side of (3.28) must be orthogonal to this solution if the following associations are made:

$$w(y) \equiv 1 \quad (3.32)$$

$$p(y) \equiv 1 \quad (3.33)$$

$$q(y) \equiv \gamma_o^* = \frac{\pi^2}{4} . \quad (3.34)$$

$\gamma_1^*$  can now be obtained without solving Eq. (3.28) for  $n_1$  . From Appendix B ,

$$\langle \cos \frac{\pi}{2} y , n_o^2 - \gamma_1^* n_o \rangle = 0 \quad (3.35)$$

or

$$\gamma_1^* = \frac{\langle \cos \frac{\pi}{2} y , n_o^2 \rangle}{\langle \cos \frac{\pi}{2} y , n_o \rangle} \quad (3.36)$$

$$= \frac{\int_0^1 \cos^3 \frac{\pi}{2} y \, dy}{\int_0^1 \cos^2 \frac{\pi}{2} y \, dy} \quad (3.37)$$

$$= \frac{8}{3\pi} . \quad (3.38)$$

Now Eq. (3.28) becomes

$$\frac{d^2 n_1}{dy^2} + \frac{\pi^2}{4} n_1 = \cos^2 \frac{\pi}{2} y - \frac{8}{3\pi} \cos \frac{\pi}{2} y \quad (3.39)$$

The solution satisfying (3.29) - (3.31) can be found by standard methods\* and is

$$n_1 = \frac{4}{3\pi} (2 - \cos \frac{\pi}{2} y - \cos^2 \frac{\pi}{2} y - 2y \sin \frac{\pi}{2} y) . \quad (3.40)$$

---

\*The technique is illustrated in Appendix C for the corresponding problem in cylindrical geometry.

With  $n_1$  known,  $\gamma_2^*$  can be determined by the same procedure used to obtain  $\gamma_1^*$ . Equating terms of order  $O(\epsilon^{*2})$  in (3.11) - (3.14) yields the problem

$$\frac{d^2 n_2}{dy^2} + \gamma_0^* n_2 = 2n_0 n_1 - \gamma_1^* n_1 - \gamma_2^* n_0 \quad (3.41)$$

$$y = 0 : \quad n_2 = 0 \quad (3.42)$$

$$\frac{dn_2}{dy} = 0 \quad (3.43)$$

$$y = 1 : \quad n_2 = 0 \quad (3.44)$$

The same orthogonality relationship applied in obtaining  $\gamma_1^*$  now requires as a condition for the existence of a solution  $n_2$  that

$$\langle \cos \frac{\pi}{2} y, 2n_0 n_1 - \gamma_1^* n_1 - \gamma_2^* n_0 \rangle = 0 \quad (3.45)$$

or

$$\gamma_2^* = \frac{2 \langle n_0, n_0 n_1 \rangle - \gamma_1^* \langle n_0, n_1 \rangle}{\langle n_0, n_0 \rangle} \quad (3.46)$$

$$= \left\{ \frac{8}{3\pi^2} \int_0^1 [2 \cos^2 \frac{\pi}{2} y - \cos^3 \frac{\pi}{2} y - \cos^4 \frac{\pi}{2} y - 2y \cos^2 \frac{\pi}{2} y \sin \frac{\pi}{2} y] dy \right. \\ \left. - \frac{32}{9\pi^3} \int_0^1 [2 \cos \frac{\pi}{2} y - \cos^2 \frac{\pi}{2} y - \cos^3 \frac{\pi}{2} y - 2y \cos \frac{\pi}{2} y \sin \frac{\pi}{2} y] dy \right\} \\ \Bigg/ \int_0^1 \cos^2 \frac{\pi}{2} y dy \quad (3.47)$$

After a considerable amount of algebra (3.47) reduces to

$$\gamma_2^* = \frac{10}{3\pi^2} - \frac{32}{9\pi^3} - \frac{64}{3\pi^4} \quad (3.48)$$

Higher-order results can be obtained with a rapidly increasing amount of labor, but the terms already obtained are sufficient for our purposes. The expansions of  $n$  and  $\gamma^*$  are given below to the number of terms that have been calculated:

$$\gamma^* \sim \frac{\pi^2}{4} + \frac{8}{3\pi} \epsilon^* + \left( \frac{10}{3\pi^2} - \frac{32}{9\pi^3} - \frac{64}{3\pi^4} \right) \epsilon^{*2} \quad (3.49)$$

$$n \sim \cos \frac{\pi}{2} y + \frac{4}{3\pi^2} [2 - \cos \frac{\pi}{2} y - \cos^2 \frac{\pi}{2} y - 2y \sin \frac{\pi}{2} y] \epsilon^* \quad (3.50)$$

If the coefficients in (3.49) are evaluated numerically,

$$\gamma^* \sim 2.4674 + 0.84883\epsilon^* + 0.004058\epsilon^{*2} \quad (3.51)$$

#### Final Form of the Approximate Solution

Using (3.8) and (3.9) to express the  $\zeta - \gamma_0$  relation in the original nomenclature, we obtain

$$\gamma_0 = \frac{\pi^2}{4} \frac{1}{\rho_0} + \frac{8}{3\pi} \epsilon_0 \zeta + \left( \frac{10}{3\pi^2} - \frac{32}{9\pi^3} - \frac{64}{3\pi^4} \right) \rho_0 \epsilon_0^2 \zeta^2 \quad (3.52)$$

For a given  $\zeta$ ,  $\gamma_0$  must be evaluated by numerical means, but the calculation can be easily performed by a simple iterative procedure.  $\rho_0$  and  $\epsilon_0$  are slowly varying functions of  $\gamma_0$ , and a crude first approximation to  $\gamma_0$  gives a reasonable estimate of their values.

These values of  $\rho_o$  and  $\epsilon_o$  can be used in (3.52) to predict a new  $\gamma_o$ , and this process can be repeated until  $\gamma_o$  converges to its correct value (within a few iterations). The  $\gamma_o$ 's corresponding to various values of  $\zeta$  are presented in Table 7, and a graph of the  $\zeta - \gamma_o$  curve is given by one of the dashed curves in Fig. 9.

Equation (3.50) expressed in the original nomenclature is

$$n_{eo} = \cos \frac{\pi}{2} y + \frac{4}{3\pi^2} [2 - \cos \frac{\pi}{2} y - \cos^2 \frac{\pi}{2} y - 2y \sin \frac{\pi}{2} y] \rho_o \epsilon_o \zeta . \quad (3.53)$$

Equations (2.21) and (2.22) can now be used to express  $J_o$  and  $E_o$  as functions of  $y$ . From (3.53)

$$\frac{dn_{eo}}{dy} = -\frac{\pi}{2} \sin \frac{\pi}{2} y - \frac{4}{3\pi^2} [(2 - \frac{\pi}{2}) \sin \frac{\pi}{2} y + \pi(y - \sin \frac{\pi}{2} y) \cos \frac{\pi}{2} y] \rho_o \epsilon_o \zeta \quad (3.54)$$

so  $J_o$  and  $E_o$  become

$$J_o = \frac{\pi}{2} \frac{1}{\rho_o} \sin \frac{\pi}{2} y + \frac{4}{3\pi^2} [(2 - \frac{\pi}{2}) \sin \frac{\pi}{2} y + \pi(y - \sin \frac{\pi}{2} y) \cos \frac{\pi}{2} y] \epsilon_o \zeta \quad (3.55)$$

$$E_o = \frac{1 - \delta_o}{1 + \delta_o \tau_o} \cdot \frac{\frac{\pi}{2} \sin \frac{\pi}{2} y + \frac{4}{3\pi^2} [(2 - \frac{\pi}{2}) \sin \frac{\pi}{2} y + \pi(y - \sin \frac{\pi}{2} y) \cos \frac{\pi}{2} y] \rho_o \epsilon_o \zeta}{\cos \frac{\pi}{2} y + \frac{4}{3\pi^2} [2 - \cos \frac{\pi}{2} y - \cos^2 \frac{\pi}{2} y - 2y \sin \frac{\pi}{2} y] \rho_o \epsilon_o \zeta} . \quad (3.56)$$

It should be realized that the zero-order solution for the dependent variables is accurate only to order  $O(\epsilon_o \zeta)$ . The accuracy of the approximate solutions for  $\gamma^*$  and  $n$  is appraised by comparing them with the exact solutions obtained below.

Exact Solution

The problem defined by Eqs. (3.11) - (3.14) can be solved exactly in terms of elliptic functions. In so doing Eq. (3.11) is reduced to quadrature, and the resulting integral is expressed as an elliptic integral of the first kind through a change of variables.

Before proceeding it is convenient to introduce a new independent variable  $x$  given by

$$x = \sqrt{\gamma^*} y \tag{3.57}$$

and rewrite the problem as

$$\frac{d^2 n}{dx^2} + n - \frac{\epsilon^*}{\gamma^*} n^2 = 0 \tag{3.58}$$

$$x = 0 : \quad n = 1 \tag{3.59}$$

$$\frac{dn}{dx} = 0 \tag{3.60}$$

$$x = \sqrt{\gamma^*} : \quad n = 0 \tag{3.61}$$

In order to integrate Eq. (3.58) once, the independent variable is eliminated by introducing  $p$  defined by

$$p = \frac{dn}{dx} \tag{3.62}$$

and writing the second derivative as

$$\frac{d^2 n}{dx^2} = \frac{dp}{dx} = \frac{dn}{dx} \frac{dp}{dn} = p \frac{dp}{dn} \tag{3.63}$$

Now (3.58) becomes

$$p \frac{dp}{dn} + n - \frac{\epsilon^*}{\gamma^*} n^2 = 0 \quad . \quad (3.64)$$

Integrating and using the boundary conditions at  $x = 0$  (or  $n = 1$ )

$$p^2 + n^2 - \frac{2}{3} \frac{\epsilon^*}{\gamma^*} n^3 = 1 - \frac{2}{3} \frac{\epsilon^*}{\gamma^*} \quad (3.65)$$

or

$$p = \pm \left\{ 1 - \frac{2}{3} \frac{\epsilon^*}{\gamma^*} - n^2 \left( 1 - \frac{2}{3} \frac{\epsilon^*}{\gamma^*} n \right) \right\}^{1/2} \quad (3.66)$$

Since  $n$  must decrease to zero at  $x = \sqrt{\gamma^*}$ , the negative sign is obviously the one desired. Also,  $p$  must be real, and (3.66) thus provides a condition on  $\epsilon^*/\gamma^*$  —  $\epsilon^*/\gamma^* \leq 3/2$ . However, a more restrictive condition is obtained by studying the differential equation in the form

$$\frac{d^2 n}{dx^2} = -n + \frac{\epsilon^*}{\gamma^*} n^2 \quad . \quad (3.67)$$

At  $x = 0$ ,

$$\frac{d^2 n}{dx^2} = - \left( 1 - \frac{\epsilon^*}{\gamma^*} \right) \quad . \quad (3.68)$$

Thus if  $\epsilon^*/\gamma^* > 1$ , the graph of  $n$  versus  $x$  is concave upward initially, and  $n$  begins to increase from unity. Equation (3.67) then shows that the concavity is enhanced and the behavior of  $n$  is definitely not what is desired. On the other hand, if  $\epsilon^*/\gamma^* < 1$ ,  $n$  is concave downward initially;  $dn/dx$  becomes negative; the term  $-n$  on the right-hand side of (3.67) becomes ever more dominant; and  $n$  decreases monotonically to zero. Thus we pose the condition

$$0 \leq \frac{\epsilon^*}{\gamma^*} < 1 \quad . \quad (3.69)$$

Using (3.62) an integral relation between  $n$  and  $x$  is obtained. If  $p$  is replaced by  $dn/dx$ , Eq. (3.66) becomes

$$\frac{dn}{dx} = -\left\{ \frac{2}{3} \frac{\epsilon^*}{\gamma^*} n^3 - n^2 + 1 - \frac{2}{3} \frac{\epsilon^*}{\gamma^*} \right\}^{1/2} \quad (3.70)$$

and using (3.59)

$$x = \int_0^1 \frac{dn}{n \sqrt{\frac{2}{3} \frac{\epsilon^*}{\gamma^*} n^3 - n^2 + 1 - \frac{2}{3} \frac{\epsilon^*}{\gamma^*}}} \quad (3.71)$$

The relation between  $\gamma^*$  and  $\epsilon^*$  is obtained by applying condition (3.61) :

$$\sqrt{\gamma^*} = \int_0^1 \frac{dn}{\sqrt{\frac{2}{3} \frac{\epsilon^*}{\gamma^*} n^3 - n^2 + 1 - \frac{2}{3} \frac{\epsilon^*}{\gamma^*}}} \quad (3.72)$$

The solution to the original problem is completed by relating  $y$  and  $n$ . Using (3.57) in (3.71)

$$y = \frac{1}{\sqrt{\gamma^*}} \int_0^1 \frac{dn}{n \sqrt{\frac{2}{3} \frac{\epsilon^*}{\gamma^*} n^3 - n^2 + 1 - \frac{2}{3} \frac{\epsilon^*}{\gamma^*}}} \quad (3.73)$$

Although the solution to the problem is given implicitly by (3.72) and (3.73), the integrals can be expressed as standard elliptic integrals by a suitable change of variables. Before proceeding we define

$$a = \frac{2}{3} \frac{\epsilon^*}{\gamma^*} \quad (3.74)$$

to simplify the notation. Now (3.72) and (3.73) become

$$\sqrt{\gamma^*} = \int_0^1 \frac{d\bar{n}}{\sqrt{a\bar{n}^3 - \bar{n}^2 + (1-a)}} \quad (3.75)$$

$$y = \frac{1}{\sqrt{\gamma^*}} \int_n^1 \frac{d\bar{n}}{\sqrt{a\bar{n}^3 - \bar{n}^2 + (1-a)}} \quad (3.76)$$

The transformation necessary to achieve the standard form for elliptic integrals depends on the roots of the polynomial in the integrands. It is immediately observed that  $\bar{n} = 1$  is a root, so we have

$$a\bar{n}^3 - \bar{n}^2 + (1-a) = (\bar{n} - 1)[a\bar{n}^2 - (1-a)\bar{n} - (1-a)] \quad (3.77)$$

Let the roots of the quadratic be  $n_o^{(1)}$  and  $n_o^{(2)}$  with

$$n_o^{(1)} = \frac{(1-a) + \sqrt{1+2a-3a^2}}{2a} \quad (3.78)$$

$$n_o^{(2)} = \frac{(1-a) - \sqrt{1+2a-3a^2}}{2a} \quad (3.79)$$

It is essential to determine the values these roots assume with respect to  $n$  as  $a$  varies. From (3.69) and (3.74)

$$0 \leq a < \frac{2}{3} \quad (3.80)$$

Differentiating  $n_o^{(1)}$  with respect to  $a$ ,

$$\begin{aligned} \frac{dn_o^{(1)}}{da} &= \frac{2a[-1 + \frac{1-3a}{\sqrt{1+2a-3a^2}}] - [(1-a) + \sqrt{1+2a-3a^2}]2}{4a^2} \\ &= \frac{-1 - \frac{1+a}{\sqrt{1+2a-3a^2}}}{2a^2} < 0 \quad (3.81) \end{aligned}$$

Therefore  $n_o^{(1)}$  increases monotonically from 1 to  $\infty$  as  $a$  decreases from  $2/3$  to 0, so for  $a$  as specified by (3.80)

$$n_o^{(1)} > 1 \quad . \quad (3.82)$$

Since  $1 + 2a - 3a^2 = (1 - a)^2 + 4a(1 - a)$ , it is apparent from (3.79) that  $n_o^{(2)} < 0$  for  $0 < a < 2/3$ . It is also easy to determine that  $n_o^{(2)} \rightarrow -1$  as  $a \rightarrow 0$ . We have now arrived at the following set of inequalities:

$$n_o^{(2)} < 0 \leq n \leq 1 < n_o^{(1)} \quad (3.83)$$

for  $a$  satisfying (3.80). (3.77) can now be written

$$a\bar{n}^3 - \bar{n}^2 + (1 - a) = a(1 - \bar{n})(n_o^{(1)} - \bar{n})(\bar{n} - n_o^{(2)}) \quad (3.84)$$

where each factor is greater than or equal to zero. Substituting (3.84) into (3.75) and (3.76),

$$\sqrt{\gamma^*} = \frac{1}{\sqrt{a}} \int_0^1 \frac{d\bar{n}}{\sqrt{(1 - \bar{n})(n_o^{(1)} - \bar{n})(\bar{n} - n_o^{(2)})}} \quad (3.85)$$

$$y = \frac{1}{\sqrt{\gamma^* a}} \int_n^1 \frac{d\bar{n}}{\sqrt{(1 - \bar{n})(n_o^{(1)} - \bar{n})(\bar{n} - n_o^{(2)})}} \quad (3.86)$$

The integrals are obtained in standard form by changing variables from  $\bar{n}$  to  $z$ , where

$$z^2 = \frac{1}{k^2} \cdot \frac{(1 - \bar{n})}{(n_o^{(1)} - \bar{n})} \quad (3.87)$$

and

$$k = \sqrt{\frac{1 - n_o^{(2)}}{n_o^{(1)} - n_o^{(2)}}} \quad (3.88)$$

Differentiating this expression,

$$\begin{aligned} 2z \, dz &= \frac{1}{k^2} \cdot \frac{(n_o^{(1)} - \bar{n})(-d\bar{n}) - (1 - \bar{n})(-d\bar{n})}{(n_o^{(1)} - \bar{n})^2} \\ &= -\frac{1}{k^2} \cdot \frac{n_o^{(1)} - 1}{(n_o^{(1)} - \bar{n})^2} d\bar{n} \end{aligned} \quad (3.89)$$

so

$$d\bar{n} = -2k \frac{(1 - \bar{n})^{1/2} (n_o^{(1)} - \bar{n})^{3/2}}{n_o^{(1)} - 1} dz \quad (3.90)$$

Rearranging (3.87)

$$z^2 = \frac{1}{k^2} \frac{(n_o^{(1)} - \bar{n}) - (n_o^{(1)} - 1)}{n_o^{(1)} - \bar{n}} \quad (3.91)$$

so

$$n_o^{(1)} - \bar{n} = \frac{n_o^{(1)} - 1}{1 - k^2 z^2} \quad (3.92)$$

Again rearranging (3.87),

$$z^2 = \frac{1}{k^2} \frac{(1 - n_o^{(2)}) - (\bar{n} - n_o^{(2)})}{(n_o^{(1)} - n_o^{(2)}) - (\bar{n} - n_o^{(2)})} \quad (3.93)$$

Solving for  $(\bar{n} - n_o^{(2)})$  and using (3.88),

$$\bar{n} - n_o^{(2)} = \frac{(1 - n_o^{(2)}) - k^2 (n_o^{(1)} - n_o^{(2)}) z^2}{1 - k^2 z^2}$$

$$= (1 - n_o^{(2)}) \frac{1 - z^2}{1 - k^2 z^2} \quad (3.94)$$

Using (3.88), (3.90), (3.92), and (3.94)

$$\frac{d\bar{n}}{\sqrt{(1 - \bar{n})(n_o^{(1)} - \bar{n})(\bar{n} - n_o^{(2)})}} = -2k \frac{n_o^{(1)} - \bar{n}}{(n_o^{(1)} - 1)(\bar{n} - n_o^{(2)})^{1/2}} \quad (3.95)$$

$$= \frac{-2k dz}{(1 - n_o^{(2)})^{1/2} (1 - z^2)^{1/2} (1 - k^2 z^2)^{1/2}} \quad (3.96)$$

$$= \frac{-2}{(n_o^{(1)} - n_o^{(2)})^{1/2}} \frac{dz}{\sqrt{(1 - z^2)(1 - k^2 z^2)}} \quad (3.97)$$

Using (3.87) to determine the proper limits of integration, (3.85) and (3.86) now become

$$\sqrt{\gamma^*} = \frac{2}{\sqrt{a(n_o^{(1)} - n_o^{(2)})}} \int_0^{k\sqrt{n_o^{(1)}}} \frac{dz}{\sqrt{(1 - z^2)(1 - k^2 z^2)}} \quad (3.98)$$

$$y = \frac{2}{\sqrt{a\gamma^*(n_o^{(1)} - n_o^{(2)})}} \int_0^{\frac{1}{k} \left( \frac{1 - \bar{n}}{n_o^{(1)} - \bar{n}} \right)^{1/2}} \frac{dz}{\sqrt{(1 - z^2)(1 - k^2 z^2)}} \quad (3.99)$$

The elliptic integral of the first kind is defined by

$$F(x, k) = \int_0^x \frac{dz}{\sqrt{(1 - z^2)(1 - k^2 z^2)}} \quad (3.100)$$

or equivalently,

$$F(\phi, k) = \int_0^{\phi} \frac{d\theta}{\sqrt{1 - k^2 \sin^2 \theta}} \quad (3.101)$$

for  $k^2 < 1$ . The second equation is derived from the first by the change of variables

$$z = \sin \theta \quad (3.102)$$

$$x = \sin \phi \quad (3.103)$$

It is obvious from (3.88) and (3.83) that  $k^2 < 1$ . In this notation (3.98) and (3.99) become

$$\sqrt{\gamma^*} = \frac{2}{\sqrt{a(n_o^{(1)} - n_o^{(2)})}} F\left(\frac{1}{k \sqrt{n_o^{(1)}}}, k\right) \quad (3.104)$$

$$= \frac{2}{\sqrt{a(n_o^{(1)} - n_o^{(2)})}} F(\phi_o, k) \quad (3.105)$$

where

$$\phi_o = \sin^{-1}\left(\frac{1}{k \sqrt{n_o^{(1)}}}\right) \quad (3.106)$$

and

$$y = \frac{2}{\sqrt{a\gamma^*(n_o^{(1)} - n_o^{(2)})}} F\left(\frac{1}{k} \sqrt{\frac{1-n}{n_o^{(1)}-n}}, k\right) \quad (3.107)$$

$$= \frac{2}{\sqrt{a\gamma^*(n_o^{(1)} - n_o^{(2)})}} F(\phi_n, k) \quad (3.108)$$

where

$$\phi_n = \sin^{-1} \left( \frac{1}{k} \sqrt{\frac{1-n}{n_o^{(1)}-n}} \right) \quad (3.109)$$

If  $u = F(x,k)$  as defined by (3.100), the inverse relationship is conventionally written  $x = \text{sn}(u,k)$ . In this manner Eq. (3.107) can be solved for  $n$  :

$$\text{sn}^2 \left( \sqrt{a\gamma^* (n_o^{(1)} - n_o^{(2)})} \frac{y}{2}, k \right) = \frac{1}{k^2} \frac{1-n}{n_o^{(1)}-n} \quad (3.110)$$

or

$$n = \frac{1 - k^2 n_o^{(1)} \text{sn}^2 \left( \sqrt{a\gamma^* (n_o^{(1)} - n_o^{(2)})} \frac{y}{2}, k \right)}{1 - k^2 \text{sn}^2 \left( \sqrt{a\gamma^* (n_o^{(1)} - n_o^{(2)})} \frac{y}{2}, k \right)} \quad (3.111)$$

### $\epsilon^* - \gamma^*$ Expansion Derived from the Exact Results

The first two terms of the series in Eq. (3.49) relating  $\gamma^*$  and  $\epsilon^*$  are easily confirmed correct by expanding the quantities appearing in Eq. (3.105) for small  $\epsilon^*$ . Equation (3.74) shows that  $a$  is small for small  $\epsilon^*$ , and it happens that  $k$  is small for small  $a$ , so  $F$  can be written as a power series in  $k$ . When the entire right-hand side of (3.105) is expressed in terms of  $a$ , Eq. (3.74) defining  $a$  is used to write the result as an expression in  $\gamma^*$  and  $\epsilon^*$ . The equation that is acquired is solved to give  $\gamma^*$  as a series in  $\epsilon^*$ .

The radical appearing in (3.78) and (3.79) can be approximated by

$$\sqrt{1 + 2a - 3a^2} = 1 + \frac{1}{2}(2a - 3a^2) - \frac{1}{8}(2a - 3a^2)^2 + 0(a^3) \quad (3.112)$$

$$= 1 + a - 2a^2 + 0(a^3) \quad (3.113)$$

for small  $a$ . Then  $n_o^{(1)}$  and  $n_o^{(2)}$  become

$$n_o^{(1)} = \frac{1}{a} - a + 0(a^2) \quad (3.114)$$

$$n_o^{(2)} = -1 + a + 0(a^2) \quad (3.115)$$

Now

$$n_o^{(1)} - n_o^{(2)} = \frac{1}{a} + 1 - 2a + 0(a^2) \quad (3.116)$$

so the coefficient in (3.105) becomes

$$\frac{2}{\sqrt{a(n_o^{(1)} - n_o^{(2)})}} = \frac{2}{\sqrt{1 + a + 0(a^2)}} \quad (3.117)$$

$$= 2 - a + 0(a^2) \quad (3.118)$$

and from (3.88)

$$k = \sqrt{\frac{2 - a + 0(a^2)}{\frac{1}{a} + 1 - 2a + 0(a^2)}} \quad (3.119)$$

$$= \sqrt{a} \sqrt{\frac{2 - a + 0(a^2)}{1 + a + 0(a^2)}} \quad (3.120)$$

$$= \sqrt{a} \sqrt{2 - 3a + 0(a^2)} \quad (3.121)$$

$$= \sqrt{2a} \left(1 - \frac{3}{4}a + 0(a^2)\right) \quad (3.122)$$

Using (3.114) and (3.122)

$$\frac{1}{k \sqrt{n_o^{(1)}}} = \frac{1}{\sqrt{2a} \left(1 - \frac{3}{4}a + 0(a^2)\right) \sqrt{\frac{1}{a} - a + 0(a^2)}} \quad (3.123)$$

$$= \frac{1}{\sqrt{2}} \left(1 + \frac{3}{4}a + 0(a^2)\right) \quad (3.124)$$

so Eq. (3.106) becomes

$$\phi_0 = \sin^{-1}\left(\frac{1}{\sqrt{2}} + \frac{3}{4\sqrt{2}} a + O(a^2)\right) \quad (3.125)$$

We now wish to expand the inverse sine about  $1/\sqrt{2}$ . If

$$f(z) = \sin^{-1} z \quad (3.126)$$

$$f'(z) = \frac{1}{\sqrt{1-z^2}} \quad (3.127)$$

so a Taylor's series expansion gives

$$f\left(\frac{1}{\sqrt{2}} + \delta\right) = \sin^{-1} \frac{1}{\sqrt{2}} + \sqrt{2} \delta + O(\delta^2) \quad (3.128)$$

Now  $\phi_0$  becomes

$$\phi_0 = \frac{\pi}{4} + \frac{3}{4} a + O(a^2) \quad (3.129)$$

Using (3.118), (3.122), and (3.129) in (3.105),

$$\sqrt{Y^*} = (2 - a + O(a^2)) F\left(\frac{\pi}{4} + \frac{3}{4} a + O(a^2), \sqrt{2a}\left(1 - \frac{3}{4} a + O(a^2)\right)\right) \quad (3.130)$$

The following expansion for  $F(\phi, k)$  is found in Davis\*:

$$F(\phi, k) = \frac{2K}{\pi} \phi - \sin \phi \cos \phi \left(\frac{k^2}{4}\right) + O(k^4), \quad (3.131)$$

where  $K$  is the complete elliptic integral of the first kind:

$$K = F\left(\frac{\pi}{2}, k\right) = \int_0^{\pi/2} \frac{d\theta}{\sqrt{1 - k^2 \sin^2 \theta}} \quad (3.132)$$

---

\* See Davis [7], pp. 133-136.

An expansion for  $K$  is also given by Davis [7]:

$$K = \frac{\pi}{2} \left[ 1 + \frac{k^2}{4} + O(k^4) \right] \quad . \quad (3.133)$$

Using (3.122), (3.129), and (3.133)

$$k^2 = 2a \left( 1 - \frac{3}{4}a + O(a^2) \right)^2 \quad (3.134)$$

$$= 2a + O(a^2) \quad (3.135)$$

$$K = \frac{\pi}{2} + \frac{\pi}{4}a + O(a^2) \quad (3.136)$$

$$\sin \phi_0 = \frac{1}{\sqrt{2}} + O(a) \quad (3.137)$$

$$\cos \phi_0 = \frac{1}{\sqrt{2}} + O(a) \quad . \quad (3.138)$$

Expanding (3.130) as illustrated by (3.131) and using (3.135) - (3.138),

$$\begin{aligned} \sqrt{\gamma^*} &= (2 - a + O(a^2)) \left\{ \frac{2}{\pi} \left( \frac{\pi}{2} + \frac{\pi}{4}a + O(a^2) \right) \left( \frac{\pi}{4} + \frac{3}{4}a + O(a^2) \right) \right. \\ &\quad \left. - \left( \frac{1}{\sqrt{2}} + O(a) \right) \left( \frac{1}{\sqrt{2}} + O(a) \right) \left( \frac{a}{2} + O(a^2) \right) \right\} \quad (3.139) \end{aligned}$$

$$= (2 - a + O(a^2)) \left\{ \frac{\pi}{4} + \left( \frac{1}{2} + \frac{\pi}{8} \right) a + O(a^2) \right\} \quad (3.140)$$

$$= \frac{\pi}{2} + a + O(a^2) \quad . \quad (3.141)$$

Squaring the equation

$$\gamma^* = \frac{\pi^2}{4} + \pi a + O(a^2) \quad . \quad (3.142)$$

Using equation (3.74) to eliminate  $a$ , we obtain an expression relating  $\gamma^*$  and  $\epsilon^*$ :

$$\gamma^* = \frac{\pi^2}{4} + \frac{2\pi}{3} \frac{\epsilon^*}{\gamma^*} + O(\epsilon^{*2}) \quad (3.143)$$

or

$$\gamma^{*2} - \frac{\pi^2}{4} \gamma^* - \frac{2\pi}{3} \epsilon^* + O(\epsilon^{*2}) = 0 \quad (3.144)$$

The positive root of this equation is approximated by

$$\gamma^* = \frac{\frac{\pi^2}{4} + \sqrt{\frac{\pi^4}{16} + \frac{8\pi}{3} \epsilon^* + O(\epsilon^{*2})}}{2} \quad (3.145)$$

$$= \frac{1}{2} \left\{ \frac{\pi^2}{4} + \frac{\pi^2}{4} \left( 1 + \frac{64}{3\pi^3} \epsilon^* + O(\epsilon^{*2}) \right) \right\} \quad (3.146)$$

or finally,

$$\gamma^* = \frac{\pi^2}{4} + \frac{8\pi}{3} \epsilon^* + O(\epsilon^{*2}) \quad (3.147)$$

This expression for  $\gamma^*$  possesses the same first two terms as does Eq. (3.49), which is obtained by perturbation methods.

#### Comparison of Exact and Approximate Solutions

Since it is more convenient to work with the approximate solution than with the exact, it is compared numerically with the exact results to determine the range of  $\epsilon^*$  over which reasonable accuracy is obtained. The series expansion for  $\gamma^*$  is found to be very accurate even for large  $\epsilon^*$ . For instance, for  $\epsilon^* = 11$  the perturbation calculation of  $\gamma^*$  is in error by roughly 0.5%. Since the  $\epsilon^*$  appearing in

Eq. (3.11) must be compared with  $\gamma^*$  rather than unity, accurate results for such large values of  $\epsilon^*$  are not completely unexpected. Indeed,  $\epsilon^*/\gamma^*$  is the basic parameter appearing in the formulation of Eq. (3.58). Results of the approximate and the exact calculations of  $\gamma^*$  are listed in Table 1. The approximate solution for  $n$  is quite good for  $\epsilon^* < 5$ . For  $\epsilon^* = 11$  it is in error by about 2.5%. Detailed results are presented in Tables 2, 3, and 4. Figures 3 and 4 show the behavior of  $\gamma^*$  and  $n$ , but it is not possible to distinguish between the perturbation and the exact solutions on the graph.

The numerical results establish the accuracy of the perturbation solution in slab geometry. A perturbation solution in cylindrical geometry is obtained by the same method in Appendix C. In this case the exact solution is not available, but the results are assumed accurate on the basis of analogy with the work of this section.

#### 4. FIRST-ORDER SOLUTION IN THE MAIN REGION

The next approximation to Eqs. (1.34) - (1.37) involves terms of order  $\mu_1(\zeta)$  as  $\zeta \rightarrow \infty$ . Substitution of the asymptotic series for the variables and the coefficients into the equations results in equations for  $J_1$ ,  $n_{e1}$ ,  $E_1$ , and  $s_1$ . Solution of these equations again requires a second asymptotic expansion regarding recombination as a perturbation. This time, however,  $\gamma_1$  cannot be determined in the course of solving the problem, and it remains unknown until the main-region solution is matched to the sheath solution.

##### First-Order Problem in the Main Region

The desired equations are obtained by substituting the asymptotic series of (2.1) - (2.11) into Eqs. (1.34) - (1.37) and neglecting terms of higher order than  $\mu_1(\zeta)$ . From equation (1.34)

$$\begin{aligned} \frac{d}{dy}(J_0 + \mu_1 J_1) - (\gamma_0 + \mu_1 \gamma_1)(n_{e0} + \mu_1 n_{e1}) + (\epsilon_0 + \mu_1 \epsilon_1)\zeta(n_{e0} + \mu_1 n_{e1})^2 \\ = -(\epsilon_0 + \mu_1 \epsilon_1)\zeta(n_{e0} + \mu_1 n_{e1})(s_0 + \mu_1 s_1) \end{aligned} \quad (4.1)$$

Using Eqs. (2.15) and (2.16) for  $s_0$  and  $J_0$  and neglecting terms of order  $\mu_1^2$ ,

$$\frac{dJ_1}{dy} - \gamma_0 n_{e1} + 2\epsilon_0 \zeta n_{e0} n_{e1} = \gamma_1 n_{e0} - \epsilon_1 \zeta n_{e0}^2 - \epsilon_0 \zeta n_{e0} s_1 \quad (4.2)$$

Substituting the expansions into Eq. (1.35)

$$\begin{aligned} \frac{d}{dy}(n_{eo} + \mu_1 n_{e1}) + (\tau_o + \mu_1 \tau_1) \frac{1 + (\delta_o + \mu_1 \delta_1)(\tau_o + \mu_1 \tau_1)}{1 + \tau_o + \mu_1 \tau_1} (J_o + \mu_1 J_1) = \\ \frac{\tau_o + \mu_1 \tau_1}{1 + \tau_o + \mu_1 \tau_1} (s_o + \mu_1 s_1)(E_o + \mu_1 E_1) - \frac{1}{1 + \tau_o + \mu_1 \tau_1} \frac{d}{dy} (s_o + \mu_1 s_1) . \end{aligned} \quad (4.3)$$

The expressions for the coefficients must be simplified.

$$\begin{aligned} \frac{1}{1 + \tau_o + \mu_1 \tau_1} &= \frac{1}{(1 + \tau_o)(1 + \frac{\mu_1 \tau_1}{1 + \tau_o})} \\ &= \frac{1}{1 + \tau_o} \left(1 - \frac{\mu_1 \tau_1}{1 + \tau_o}\right) + O(\mu_1^2) \\ &= \frac{1}{1 + \tau_o} - \mu_1 \frac{\tau_1}{(1 + \tau_o)^2} + O(\mu_1^2) \end{aligned} \quad (4.4)$$

$$\begin{aligned} (\tau_o + \mu_1 \tau_1) \frac{1 + (\delta_o + \mu_1 \delta_1)(\tau_o + \mu_1 \tau_1)}{1 + \tau_o + \mu_1 \tau_1} &= (\tau_o + \mu_1 \tau_1) [1 + \delta_o \tau_o + \mu_1 (\delta_o \tau_1 + \delta_1 \tau_o)] \\ &\quad \times \left[ \frac{1}{1 + \tau_o} - \mu_1 \frac{\tau_1}{(1 + \tau_o)^2} \right] + O(\mu_1^2) \\ &= \tau_o \frac{1 + \delta_o \tau_o}{1 + \tau_o} + \mu_1 \left[ \tau_1 \frac{1 + \delta_o \tau_o}{1 + \tau_o} + \tau_o \frac{\delta_o \tau_1 + \delta_1 \tau_o}{1 + \tau_o} - \tau_o \tau_1 \frac{1 + \delta_o \tau_o}{(1 + \tau_o)^2} \right] \\ &\quad + O(\mu_1^2) \\ &= \rho_o + \mu_1 \left[ \tau_o \frac{\delta_o \tau_1 + \delta_1 \tau_o}{1 + \tau_o} + \tau_1 \frac{1 + \delta_o \tau_o}{(1 + \tau_o)^2} \right] + O(\mu_1^2) \end{aligned} \quad (4.5)$$

$$\begin{aligned}
 \frac{\tau_o + \mu_1 \tau_1}{1 + \tau_o + \mu_1 \tau_1} &= (\tau_o + \mu_1 \tau_1) \left( \frac{1}{1 + \tau_o} - \mu_1 \frac{\tau_1}{(1 + \tau_o)^2} \right) + o(\mu_1^2) \\
 &= \frac{\tau_o}{1 + \tau_o} + \mu_1 \left[ \frac{\tau_1}{1 + \tau_o} - \frac{\tau_o \tau_1}{(1 + \tau_o)^2} \right] + o(\mu_1^2) \\
 &= \frac{\tau_o}{1 + \tau_o} + \mu_1 \frac{\tau_1}{(1 + \tau_o)^2} + o(\mu_1^2) \quad . \quad (4.6)
 \end{aligned}$$

Using (4.4), (4.5), (4.6), (2.15) and (2.17) in (4.3),

$$\begin{aligned}
 \frac{dn_{e1}}{dy} + \rho_o J_1 &= - \left[ \tau_o \frac{\delta_o \tau_1 + \delta_1 \tau_o}{1 + \tau_o} + \tau_1 \frac{1 + \delta_o \tau_o}{(1 + \tau_o)^2} \right] J_o \\
 &\quad + \frac{\tau_o}{1 + \tau_o} E_o s_1 - \frac{1}{1 + \tau_o} \frac{ds_1}{dy} \quad . \quad (4.7)
 \end{aligned}$$

Equation (1.36) becomes

$$\begin{aligned}
 \frac{d}{dy} (n_{eo} + \mu_1 n_{e1}) + \frac{1 + (\delta_o + \mu_1 \delta_1)(\tau_o + \mu_1 \tau_1)}{1 - \delta_o - \mu_1 \delta_1} (n_{eo} + \mu_1 n_{e1})(E_o + \mu_1 E_1) &= \\
 \frac{\delta_o + \mu_1 \delta_1}{1 - \delta_o - \mu_1 \delta_1} \frac{d}{dy} (s_o + \mu_1 s_1) - \frac{(\delta_o + \mu_1 \delta_1)(\tau_o + \mu_1 \tau_1)}{1 - \delta_o - \mu_1 \delta_1} (s_o + \mu_1 s_1)(E_o + \mu_1 E_1) &. \quad (4.8)
 \end{aligned}$$

Simplifying the coefficients

$$\begin{aligned}
 \frac{1}{1 - \delta_o - \mu_1 \delta_1} &= \frac{1}{(1 - \delta_o) \left( 1 - \mu_1 \frac{\delta_1}{1 - \delta_o} \right)} \\
 &= \frac{1}{1 - \delta_o} \left( 1 + \mu_1 \frac{1}{1 - \delta_o} \right) + o(\mu_1^2)
 \end{aligned}$$

$$= \frac{1}{1-\delta_o} + \mu_1 \frac{\delta_1}{(1-\delta_o)^2} + o(\mu_1^2) \quad (4.9)$$

$$\begin{aligned} \frac{1 + (\delta_o + \mu_1 \delta_1)(\tau_o + \mu_1 \tau_1)}{1 - \delta_o - \mu_1 \delta_1} &= [1 + \delta_o \tau_o + \mu_1 (\delta_o \tau_1 + \delta_1 \tau_o)] \left[ \frac{1}{1 - \delta_o} \right. \\ &+ \left. \mu_1 \frac{\delta_1}{(1 - \delta_o)^2} \right] + o(\mu_1^2) = \frac{1 + \delta_o \tau_o}{1 - \delta_o} + \mu_1 \left[ \frac{\delta_o \tau_1 + \delta_1 \tau_o}{1 - \delta_o} + \frac{\delta_1 (1 + \delta_o \tau_o)}{(1 - \delta_o)^2} \right] \\ &= \frac{1 + \delta_o \tau_o}{1 - \delta_o} + \mu_1 \frac{\delta_o \tau_1 + \delta_1 \tau_o - \delta_o^2 \tau_1 + \delta_1}{(1 - \delta_o)^2} + o(\mu_1^2) \end{aligned} \quad (4.10)$$

$$\begin{aligned} \frac{\delta_o + \mu_1 \delta_1}{1 - \delta_o - \mu_1 \delta_1} &= (\delta_o + \mu_1 \delta_1) \left[ \frac{1}{1 - \delta_o} + \mu_1 \frac{\delta_1}{(1 - \delta_o)^2} \right] + o(\mu_1^2) \\ &= \frac{\delta_o}{1 - \delta_o} + \mu_1 \left[ \frac{1}{1 - \delta_o} + \frac{\delta_o \delta_1}{(1 - \delta_o)^2} \right] \\ &= \frac{\delta_o}{1 - \delta_o} + \mu_1 \frac{\delta_1}{(1 - \delta_o)^2} + o(\mu_1^2) \end{aligned} \quad (4.11)$$

$$\begin{aligned} \frac{(\delta_o + \mu_1 \delta_1)(\tau_o + \mu_1 \tau_1)}{1 - \delta_o - \mu_1 \delta_1} &= (\delta_o + \mu_1 \delta_1)(\tau_o + \mu_1 \tau_1) \left[ \frac{1}{1 - \delta_o} + \mu_1 \frac{\delta_1}{(1 - \delta_o)^2} \right] + o(\mu_1^2) \\ &= \frac{\delta_o \tau_o}{1 - \delta_o} + \mu_1 \left[ \frac{\delta_o \tau_1 + \delta_1 \tau_o}{1 - \delta_o} + \frac{\delta_o \delta_1 \tau_o}{(1 - \delta_o)^2} \right] + o(\mu_1^2) \\ &= \frac{\delta_o \tau_o}{1 - \delta_o} + \mu_1 \left[ \frac{\delta_o \tau_1 + \delta_1 \tau_o - \delta_o^2 \tau_1}{(1 - \delta_o)^2} \right] + o(\mu_1^2) . \end{aligned} \quad (4.12)$$

Using (4.10), (4.11), (4.12), (2.15) and (2.18) in (4.8)

$$\begin{aligned} \frac{dn_{e1}}{dy} + \frac{1 + \delta_o \tau_o}{1 - \delta_o} n_{e1} E_o + \frac{1 + \delta_o \tau_o}{1 - \delta_o} n_{eo} E_1 = & - \frac{\delta_o \tau_1 + \delta_1 \tau_o - \delta_o^2 \tau_1 + \delta_1}{(1 - \delta_o)^2} n_{eo} E_o \\ & + \frac{\delta_o}{1 - \delta_o} \frac{ds_1}{dy} - \frac{\delta_o \tau_o}{1 - \delta_o} E_o s_1 \quad . \end{aligned} \quad (4.13)$$

Expanding Eq. (1.37)

$$(\chi_o + \mu_1 \chi_1)(s_o + \mu_1 s_1) = \frac{1}{\zeta} \frac{d}{dy} (E_o + \mu_1 E_1) \quad . \quad (4.14)$$

Using (2.15) and retaining the lowest-order terms on each side

$$\chi_o s_1 = \frac{1}{\zeta \mu_1} \frac{dE_o}{dy} \quad . \quad (4.15)$$

Equation (4.15) depends critically on  $\mu_1(\zeta)$ . If  $\mu_1 = 1/\zeta$ , then  $\chi_o s_1 = dE_o/dy$ . However, if  $\mu_1(\zeta) > 1/\zeta$ , then the association of terms with the same orders of magnitude in  $\zeta$  requires  $s_1 \equiv 0$ .  $\mu_1(\zeta)$  is not determined until the main-region solution is matched with the sheath solution in some intermediate region. An attempt to match using  $\mu_1 = 1/\zeta$  fails, and success requires  $\mu_1 = 1/\zeta^{1/3}$ .  $\mu_1$  is left unspecified here in order to see more clearly how it is determined. However, it is necessary to use the fact  $\text{ord}(\mu_1) > 1/\zeta$  so that

$$s_1 \equiv 0 \quad . \quad (4.16)$$

Now Eqs. (4.2), (4.7), and (4.13) simplify considerably and are rewritten below.

$$\frac{dJ_1}{dy} - \gamma_o n_{e1} + 2\epsilon_o \zeta n_{eo} n_{e1} = \gamma_1 n_{eo} - \epsilon_1 \zeta n_{eo}^2 \quad (4.17)$$

$$\frac{dn_{e1}}{dy} + \rho_o J_1 = - \left[ \tau_o \frac{\delta_o \tau_1 + \delta_1 \tau_o}{1 + \tau_o} + \tau_1 \frac{1 + \delta_o \tau_o}{(1 + \tau_o)^2} \right] J_o \quad (4.18)$$

$$\frac{dn_{e1}}{dy} + \frac{1 + \delta_o \tau_o}{1 - \delta_o} n_{e1} E_o + \frac{1 + \delta_o \tau_o}{1 - \delta_o} n_{eo} E_1 = - \frac{\delta_o \tau_1 + \delta_1 \tau_o - \delta_o^2 \tau_1 + \delta_1}{(1 - \delta_o)^2} n_{eo} E_o \quad (4.19)$$

Substitution of the asymptotic expansions for the variables into the boundary conditions (1.9) - (1.11) yields

$$y = 0 : \quad n_{e1} = 0 \quad (4.20)$$

$$J_1 = 0 \quad (4.21)$$

$$E_1 = 0 \quad (4.22)$$

Actually (4.17) and (4.18) are differential equations for  $n_{e1}$  and  $J_1$ , and  $E_1$  is determined algebraically from (4.19). (4.21) and the boundary conditions on the zero-order solution applied to (4.18) show that  $dn_{e1}/dy = 0$  at  $y = 0$ , and hence from (4.19) it is apparent that (4.22) is automatically satisfied.

$J_1$  can be eliminated between (4.17) and (4.18) to produce a second-order equation for  $n_{e1}$ :

$$\begin{aligned} \frac{d^2 n_{e1}}{dy^2} + \gamma_o \rho_o n_{e1} - 2\epsilon_o \zeta \rho_o n_{eo} n_{e1} = & - \gamma_1 \rho_o n_{eo} \\ & + \epsilon_1 \zeta \rho_o n_{eo}^2 - \left[ \tau_o \frac{\delta_o \tau_1 + \delta_1 \tau_o}{1 + \tau_o} + \tau_1 \frac{1 + \delta_o \tau_o}{(1 + \tau_o)^2} \right] \frac{dJ_o}{dy} \end{aligned} \quad (4.23)$$

with boundary conditions

$$y = 0 : \quad n_{e1} = 0 \quad (4.24)$$

$$\frac{dn_{e1}}{dy} = 0 \quad (4.25)$$

One might expect  $\gamma_1$  to be determined by requiring  $n_{e1}(1) = 0$  as in the case of the zero-order solution. However, the problem (4.23) - (4.25) has no nontrivial solution for which  $n_{e1}(1) = 0$ , for any  $\gamma_1$ . An indication of the reason appears in the approximate solution to the equation. Since the boundary condition at  $y = 1$  cannot be applied,  $\gamma_1$  must be determined in the process of matching the main-region solution to that in the sheath.

#### Approximate Solution for $n_{e1}$

An approximation to  $n_{e1}$  is acquired by the same perturbation method used to determine  $n_{eo}$ . An expansion for  $n_{e1}$  in powers of  $\epsilon_0 \zeta$  is assumed.  $\gamma_0$ ,  $n_{eo}$ , and  $J_0$  already possess such expansions, so equations for the various contributions to  $n_{e1}$  are obtained by equating terms of the same order in  $\epsilon_0 \zeta$ . Introducing notation similar to that of Section 3

$$\epsilon^* = \epsilon_0 \zeta \rho_0 \quad (4.26)$$

$$\bar{n} = n_{e1} \quad (4.27)$$

and expanding  $\bar{n}$ ,

$$\bar{n} \sim \bar{n}_0 + \epsilon^* \bar{n}_1 + \dots \quad (4.28)$$

From (3.52), (3.53) and (3.55),

$$\gamma_o \rho_o \sim \frac{\pi^2}{4} + \frac{8}{3\pi} \epsilon^* \quad (4.29)$$

$$n_{eo} \sim \cos \frac{\pi}{2} y + \frac{4}{3\pi^2} [2 - \cos \frac{\pi}{2} y - \cos^2 \frac{\pi}{2} y - 2y \sin \frac{\pi}{2} y] \epsilon^* \quad (4.30)$$

$$J_o \sim \frac{1}{\rho_o} \left\{ \frac{\pi}{2} \sin \frac{\pi}{2} y + \frac{4}{3\pi^2} \left[ \left(2 - \frac{\pi}{2}\right) \sin \frac{\pi}{2} y + \pi \left(y - \sin \frac{\pi}{2} y\right) \cos \frac{\pi}{2} y \right] \epsilon^* \right\} \quad (4.31)$$

$$\begin{aligned} \frac{dJ_o}{dy} \sim \frac{1}{\rho_o} \left\{ \frac{\pi^2}{4} \cos \frac{\pi}{2} y + \frac{4}{3\pi^2} \left[ \frac{\pi^2}{2} + \left(2\pi - \frac{\pi^2}{4}\right) \cos \frac{\pi}{2} y - \pi^2 \cos^2 \frac{\pi}{2} y \right. \right. \\ \left. \left. - \frac{\pi^2}{2} y \sin \frac{\pi}{2} y \right] \epsilon^* \right\} . \quad (4.32) \end{aligned}$$

Making the appropriate substitutions in Eq. (4.23) and using Eq. (2.19)

for  $\rho_o$ ,

$$\begin{aligned} \frac{d^2}{dy^2} (\bar{n}_o + \epsilon^* \bar{n}_1) + \left( \frac{\pi^2}{4} + \frac{8}{3\pi} \epsilon^* \right) (\bar{n}_o + \epsilon^* \bar{n}_1) \\ - 2\epsilon^* \left( \cos \frac{\pi}{2} y \right) \bar{n}_o = -\gamma_1 \rho_o \left( \cos \frac{\pi}{2} y + \frac{4}{3\pi^2} \left[ 2 - \cos \frac{\pi}{2} y - \cos^2 \frac{\pi}{2} y \right. \right. \\ \left. \left. - 2y \sin \frac{\pi}{2} y \right] \epsilon^* \right) + \frac{\epsilon_1}{\epsilon_o} \epsilon^* \cos^2 \frac{\pi}{2} y - \left[ \frac{\delta_o \tau_1 + \delta_1 \tau_o}{1 + \delta_o \tau_o} + \frac{\tau_1}{\tau_o} \frac{1}{1 + \tau_o} \right] \left( \frac{\pi^2}{4} \cos \frac{\pi}{2} y \right. \\ \left. + \frac{4}{3\pi^2} \left[ \frac{\pi^2}{2} + \left( 2\pi - \frac{\pi^2}{4} \right) \cos \frac{\pi}{2} y - \pi^2 \cos^2 \frac{\pi}{2} y - \frac{\pi^2}{2} y \sin \frac{\pi}{2} y \right] \epsilon^* \right) + 0(\epsilon^{*2}) . \quad (4.33) \end{aligned}$$

The equation for  $\bar{n}_o$  now becomes

$$\frac{d^2 \bar{n}_o}{dy^2} + \frac{\pi^2}{4} \bar{n}_o = -(\gamma_1 \rho_o + q) \cos \frac{\pi}{2} y \quad (4.34)$$

where

$$q = \frac{\pi^2}{4} \left[ \frac{\delta_o \tau_1 + \delta_1 \tau_o}{1 + \delta_o \tau_o} + \frac{\tau_1}{\tau_o} \frac{1}{1 + \tau_o} \right] \quad (4.35)$$

Conditions (4.24) and (4.25) imply

$$y = 0 : \quad \bar{n}_o = 0 \quad (4.36)$$

$$\frac{d\bar{n}_o}{dy} = 0 \quad (4.37)$$

The solution is easily obtained as

$$\bar{n}_o = -\frac{1}{\pi} (\gamma_1 \rho_o + q) y \sin \frac{\pi}{2} y \quad (4.38)$$

It is apparent from this expression that the requirement  $n_{e1}(1) = 0$  is not a legitimate way to determine  $\gamma_1$ . Hence  $\gamma_1$  must remain an unknown until the main-region solution is matched to that in the sheath.

Terms of order  $\epsilon^*$  in (4.33) yield an equation for  $\bar{n}_1$ :

$$\begin{aligned} \frac{d^2 \bar{n}_1}{dy^2} + \frac{\pi^2}{4} \bar{n}_1 &= \frac{8}{3\pi^2} (\gamma_1 \rho_o + q) y \sin \frac{\pi}{2} y - \frac{2}{\pi} (\gamma_1 \rho_o + q) y \cos \frac{\pi}{2} y \sin \frac{\pi}{2} y \\ &- \frac{4}{3\pi^2} \gamma_1 \rho_o [2 - \cos \frac{\pi}{2} y - \cos^2 \frac{\pi}{2} y - 2y \sin \frac{\pi}{2} y] + \frac{\epsilon_1}{\epsilon_o} \cos^2 \frac{\pi}{2} y \\ &- \frac{16}{3\pi^4} q \left[ \frac{\pi^2}{2} + (2\pi - \frac{\pi^2}{4}) \cos \frac{\pi}{2} y - \pi^2 \cos^2 \frac{\pi}{2} y - \frac{\pi^2}{2} y \sin \frac{\pi}{2} y \right] \quad (4.39) \end{aligned}$$

$$\begin{aligned} &= -\frac{8}{3\pi^2} (\gamma_1 \rho_o + q) + \frac{4}{3\pi^2} [\gamma_1 \rho_o - (\frac{8}{\pi} - 1)q] \cos \frac{\pi}{2} y \\ &+ \left( \frac{4}{3\pi^2} \gamma_1 \rho_o + \frac{16}{3\pi^2} q + \frac{\epsilon_1}{\epsilon_o} \right) \cos^2 \frac{\pi}{2} y + \frac{16}{3\pi^2} (\gamma_1 \rho_o + q) y \sin \frac{\pi}{2} y \end{aligned}$$

$$-\frac{2}{\pi} (\gamma_1 \rho_o + q) y \cos \frac{\pi}{2} y \sin \frac{\pi}{2} y \quad . \quad (4.40)$$

Conditions (4.24) and (4.25) again imply

$$y = 0 : \quad \bar{n}_1 = 0 \quad (4.41)$$

$$\frac{d\bar{n}_1}{dy} = 0 \quad . \quad (4.42)$$

The solution is laboriously obtained by standard techniques and is

$$\begin{aligned} \bar{n}_1 = & -\left(\frac{32}{3\pi^4} \gamma_1 \rho_o - \frac{8}{3\pi^2} \frac{\epsilon_1}{\epsilon_o}\right) + \left(\frac{16}{3\pi^4} \gamma_1 \rho_o - \frac{4}{3\pi^2} \frac{\epsilon_1}{\epsilon_o}\right) \cos \frac{\pi}{2} y \\ & + \left[\frac{4}{3\pi^3} \left(\frac{4}{\pi} + 1\right) \gamma_1 \rho_o - \frac{4}{3\pi^3} \left(\frac{4}{\pi} - 1\right) q\right] y \sin \frac{\pi}{2} y \\ & - \left(\frac{8}{3\pi^3} \gamma_1 \rho_o + \frac{8}{3\pi^3} q\right) y^2 \cos \frac{\pi}{2} y + \left(\frac{16}{3\pi^4} \gamma_1 \rho_o - \frac{4}{3\pi^2} \frac{\epsilon_1}{\epsilon_o}\right) \cos^2 \frac{\pi}{2} y \\ & + \left(\frac{8}{3\pi^3} \gamma_1 \rho_o + \frac{8}{3\pi^3} q\right) y \cos \frac{\pi}{2} y \sin \frac{\pi}{2} y \quad . \end{aligned} \quad (4.43)$$

Using (4.27) and (4.28), we obtain

$$n_{e1} = \bar{n}_o + \epsilon^* \bar{n}_1 + 0(\epsilon^{*2}) \quad , \quad (4.44)$$

where  $\bar{n}_o$  and  $\bar{n}_1$  are given by (4.38) and (4.43).  $J_1$  and  $E_1$  can now be obtained algebraically from equations (4.18) and (4.19), respectively.

Lowest-Order Contribution to s

Since  $\mu_1(\zeta)$  is such that  $s_1 \equiv 0$ , Eq. (4.15) should actually be written

$$\chi_0(s_0 + \mu_1 s_1 + \mu_2 s_2 + \dots) = \frac{1}{\zeta} \frac{dE_0}{dy} \quad (4.45)$$

and for some n

$$\mu_n(\zeta) = \frac{1}{\zeta} \quad (4.46)$$

so

$$s_n = \frac{1}{\chi_0} \frac{dE_0}{dy} \quad (4.47)$$

and

$$s_j \equiv 0, \quad j = 0, 1, \dots, n-1 \quad (4.48)$$

Equation (3.56) for  $E_0$  can be changed to a form that is more easily differentiated. Using (4.26),

$$E_0 = \frac{1 - \delta_0}{1 + \delta_0 \tau_0} \frac{\frac{\pi}{2} \sin \frac{\pi}{2} y + \frac{4}{3\pi^2} [(2 - \frac{\pi}{2}) \sin \frac{\pi}{2} y + \pi(y - \sin \frac{\pi}{2} y) \cos \frac{\pi}{2} y] \epsilon^*}{\cos \frac{\pi}{2} y \{ 1 + \frac{4}{3\pi^2} [2 \sec \frac{\pi}{2} y - 1 - \cos \frac{\pi}{2} y - 2y \tan \frac{\pi}{2} y] \epsilon^* \}} \quad (4.49)$$

$$= \frac{1 - \delta_0}{1 + \delta_0 \tau_0} \frac{1}{\cos \frac{\pi}{2} y} \left\{ \frac{\pi}{2} \sin \frac{\pi}{2} y + \frac{4}{3\pi^2} [(2 - \frac{\pi}{2}) \sin \frac{\pi}{2} y + \pi(y - \sin \frac{\pi}{2} y) \cos \frac{\pi}{2} y] \epsilon^* \right\}$$

$$\times \left\{ 1 - \frac{4}{3\pi^2} [2 \sec \frac{\pi}{2} y - 1 - \cos \frac{\pi}{2} y - 2y \tan \frac{\pi}{2} y] \epsilon^* \right\} + O(\epsilon^{*2}) \quad (4.50)$$

$$\begin{aligned}
 &= \frac{1 - \delta_o}{1 + \delta_o \tau_o} \frac{1}{\cos \frac{\pi}{2} y} \left\{ \frac{\pi}{2} \sin \frac{\pi}{2} y + \frac{4}{3\pi^2} \left[ \left( 2 - \frac{\pi}{2} \right) \sin \frac{\pi}{2} y + \pi y \cos \frac{\pi}{2} y \right. \right. \\
 &\quad \left. \left. - \pi \cos \frac{\pi}{2} y \sin \frac{\pi}{2} y - \pi \tan \frac{\pi}{2} y + \frac{\pi}{2} \sin \frac{\pi}{2} y + \frac{\pi}{2} \cos \frac{\pi}{2} y \sin \frac{\pi}{2} y \right. \right. \\
 &\quad \left. \left. + \pi y \sec \frac{\pi}{2} y - \pi y \cos \frac{\pi}{2} y \right] \epsilon^* \right\} \quad (4.51)
 \end{aligned}$$

$$\begin{aligned}
 &= \frac{1 - \delta_o}{1 + \delta_o \tau_o} \left\{ \frac{\pi}{2} \tan \frac{\pi}{2} y + \frac{4}{3\pi^2} \left[ 2 \tan \frac{\pi}{2} y - \frac{\pi}{2} \sin \frac{\pi}{2} y \right. \right. \\
 &\quad \left. \left. - \pi \sec \frac{\pi}{2} y \tan \frac{\pi}{2} y + \pi y \sec^2 \frac{\pi}{2} y \right] \epsilon^* \right\} . \quad (4.52)
 \end{aligned}$$

Then

$$\begin{aligned}
 \frac{dE_o}{dy} &= \frac{1 - \delta_o}{1 + \delta_o \tau_o} \left\{ \frac{\pi^2}{4} \sec^2 \frac{\pi}{2} y + \frac{4}{3\pi^2} \left[ \pi \sec^2 \frac{\pi}{2} y - \frac{\pi^2}{4} \cos \frac{\pi}{2} y \right. \right. \\
 &\quad \left. \left. - \frac{\pi^2}{2} \sec^3 \frac{\pi}{2} y - \frac{\pi^2}{2} \sec \frac{\pi}{2} y \tan^2 \frac{\pi}{2} y + \pi \sec^2 \frac{\pi}{2} y \right. \right. \\
 &\quad \left. \left. + \pi^2 y \sec^2 \frac{\pi}{2} y \tan \frac{\pi}{2} y \right] \epsilon^* \right\} \quad (4.53)
 \end{aligned}$$

so

$$\begin{aligned}
 s_n &= \frac{1}{\chi_o} \frac{1 - \delta_o}{1 + \delta_o \tau_o} \left\{ \frac{\pi^2}{4} \sec^2 \frac{\pi}{2} y + \frac{4}{3\pi^2} \left[ \pi^2 y \sec^2 \frac{\pi}{2} y \tan \frac{\pi}{2} y \right. \right. \\
 &\quad \left. \left. - \pi^2 \sec \frac{\pi}{2} y \tan^2 \frac{\pi}{2} y + 2\pi \sec^2 \frac{\pi}{2} y - \frac{\pi^2}{2} \sec \frac{\pi}{2} y \right. \right. \\
 &\quad \left. \left. - \frac{\pi^2}{4} \cos \frac{\pi}{2} y \right] \epsilon_o \zeta \rho_o \right\} . \quad (4.54)
 \end{aligned}$$

Except for  $\mu_1(\zeta)$  and  $\gamma_1$  and the corresponding corrections to the other coefficients, all the terms of the main-region solution written below are known or can be easily calculated.

$$n_e \sim n_{e0} + \mu_1(\zeta) n_{e1} \quad (4.55)$$

$$J \sim J_0 + \mu_1(\zeta) J_1 \quad (4.56)$$

$$E \sim E_0 + \mu_1(\zeta) E_1 \quad (4.57)$$

$$s \sim \frac{1}{\zeta} s_n \quad (4.58)$$

$$n_i = n_e + s \quad (4.59)$$

In order to complete this approximation to the solution, it is necessary to solve the original equations in the sheath where the representations above break down.  $\mu_1$  and  $\gamma_1$  are then determined by comparing the two solutions in some intermediate region.

## 5. APPROXIMATE ASYMPTOTIC SHEATH SOLUTION

The complete equations for  $J$ ,  $n_e$ ,  $n_i$  and  $E$  are written in (2.51) - (2.54) in a form suitable for use in the sheath. The terms on the right-hand side of the equation for  $\tilde{J}$  are small for large  $\zeta$ , and approximate methods, in which these terms are regarded as perturbations, are available. However, even the lowest-order equations are too difficult to solve analytically. In order to obtain expressions that can be matched to the solution in the main region, the equations are solved asymptotically for large  $\xi$ . Nevertheless the entire boundary layer must ultimately be considered in order to relate the asymptotic form for large  $\xi$  to the boundary conditions at  $\xi = 0$ , and some numerical work is necessary.

In this section only the lowest-order equations are considered, and an approximate solution is obtained by expanding the variables in asymptotic series in the large coefficient  $\tau$ . By this method it is possible to express  $\tilde{n}_e$  and  $\tilde{n}_i$  in terms of  $\tilde{E}$ , and a first-order differential equation in  $\tilde{E}$  alone is obtained. The first terms of the asymptotic forms of  $\tilde{n}_e$ ,  $\tilde{n}_i$ , and  $\tilde{E}$  for large  $\xi$  are obtained, and they show the behavior of the sheath solution in the region where it is to be matched with the main-region solution. Because of the expansion in  $\tau$  the asymptotic forms are not precisely correct, and the matching cannot be accomplished until the exact asymptotic solution is obtained in Section 6. However, the numerical integration of the equation for  $\tilde{E}$  provides estimates of  $\tilde{n}_e$ ,  $\tilde{n}_i$  and  $\tilde{E}$  throughout the sheath that are not obtainable in Section 6. Furthermore, the trial-and-error work

associated with the numerical integrations of Section 6 is reduced by using the estimates obtained here.

### Validity of the Equations in the Sheath

Before solving the equations in the sheath, we wish to examine their validity and accuracy there. Quantities vary more rapidly with position in the sheath than they do elsewhere, and some of the assumptions used in deriving the equations must be reexamined. In fact, the basic process of obtaining the macroscopic equations must be questioned. The use of macroscopic equations requires meaningful averages over the particle distribution functions, and such averages are only meaningful in the context of the equations if the particles experience a large number of collisions while diffusing through the sheath. As a criterion for this situation we require that the mean free paths of ions and electrons be less than the sheath thickness. Values for these mean free paths are available in Appendix C of Part I, and they show that the criterion is not well satisfied. When the particles travel too far between collisions, the coefficients appearing in the equations are no longer determined solely by local conditions. The discussion on pp. 43 ff and 48 ff of Part I establishes a criterion for the dependence of the coefficients on the local values of  $\hat{E}_t$  and  $N_n$ . In the sheath the transverse electric field is so large that  $\hat{E}_t$  is not well approximated by  $\hat{E}_z$ , and hence the coefficients actually are not constants. Furthermore the spatial variations in the sheath are so large that it is doubtful whether the local value of  $\hat{E}_t$  could properly be used.

Despite the fact that kinetic-theory methods may be necessary for an accurate investigation of the physics in the sheath, we use the macroscopic equations, and their use may be regarded as an approximate means by which to extend the description of the plasma to the wall of the discharge. Since the sheath may not be described very accurately, it is comforting to realize that the general behavior of the discharge is relatively insensitive to the detailed features of the sheath. The analysis in the sheath is only necessary in order to account for the higher-order effects of space charge on the  $N_{eo} - \hat{E}_z$  relation and on the dependent variables in the main region. These higher-order effects are represented by the higher-order terms of the asymptotic expansions, and these terms provide reasonably accurate values for the complete expressions if only their orders of magnitude are correct. However, the orders of magnitude can be determined by observing the breakdown of the main-region solution, and the sheath calculations only serve to refine the values. Furthermore, the size of the sheath and the magnitudes of the higher-order terms increase whereas the spatial variations across the sheath decrease as  $N_{eo}$  decreases, and hence the results of the sheath calculations are most important where they are most accurate.

### Zero-Order Equations

The sheath problem of Eqs. (2.51) - (2.56) is rewritten below in approximate form by retaining only the terms of order unity in  $\zeta$  for  $\zeta$  large. Only the zero-order terms of the expansions of the coefficients in the  $\mu_n(\zeta)$  are retained, and the dependent variables for this approximate problem are designated by a subscript zero. We obtain

$$\frac{d\tilde{J}_o}{d\xi} = 0 \quad (5.1)$$

$$\frac{d\tilde{n}_{eo}}{d\xi} = \tilde{n}_{eo}\tilde{E}_o + \delta_o\tau_o\tilde{J}_o \quad (5.2)$$

$$\frac{d\tilde{n}_{io}}{d\xi} = \tau_o(-\tilde{n}_{io}\tilde{E}_o + \tilde{J}_o) \quad (5.3)$$

$$\frac{d\tilde{E}_o}{d\xi} = -\chi_o(\tilde{n}_{io} - \tilde{n}_{eo}) \quad (5.4)$$

$$\xi = 0 : \quad \tilde{n}_{eo} = 0 \quad (5.5)$$

$$\tilde{n}_{io} = 0 \quad (5.6)$$

These equations actually depend on  $\zeta$ , because the coefficients depend on  $\gamma_o$ , which in turn depends on  $\zeta$  as shown by Eq. (3.52). However,  $\delta$ ,  $\tau$ , and  $\chi$  all depend weakly on  $\gamma$ , so the equations are affected only weakly by changes in  $\zeta$ .

The behavior of variables in the sheath is easily observed by making one further approximation. Before formally doing so, an indication of the behavior and the motivation for the approximation are seen by considering Eqs. (5.2) and (5.3) for  $\xi$  increasing from zero. Since  $\tilde{n}_{eo}$  and  $\tilde{n}_{io}$  are zero initially, their relative rates of increase depend on the coefficients multiplying  $\tilde{J}_o$ . (1.29) and (1.27) show that  $\delta_o\tau_o$  is small and  $\tau_o$  is large, so  $\tilde{n}_{io}$  grows rapidly as  $\xi$  increases from zero. However, the terms on the right-hand side of (5.2) add to yield  $d\tilde{n}_{eo}/d\xi$  whereas those in (5.3) subtract. As  $\tilde{n}_{io}$  increases, the difference between  $\tilde{J}_o$  and  $\tilde{n}_{io}\tilde{E}_o$

decreases, and the growth of  $\tilde{n}_{i0}$  is retarded. Since  $\tau_0$  is a large parameter, a moderate value of  $d\tilde{n}_{i0}/d\xi$  requires that  $\tilde{J}_0$  and  $\tilde{n}_{i0}\tilde{E}_0$  differ by only a small amount. Hence  $\tilde{n}_{i0}$  is approximately equal to  $\tilde{J}_0/\tilde{E}_0$ .

Approximation for Large  $\tau_0$

The situation just described is ideally suited for a singular perturbation treatment with  $1/\tau_0$  as the small parameter. The derivative in Eq. (5.3) is negligible except in a small region near  $\xi = 0$ . This boundary layer within the sheath is called the "skin" by Allis and Rose [2]. A solution to (5.1) - (5.4) is sought by expanding the variables in asymptotic series in powers of  $1/\tau_0$ . Since only the lowest-order contribution is of interest, new notation is not introduced, and the equations in the main region of the sheath become

$$\tilde{J}_0 = \tilde{J}_0(0) \tag{5.7}$$

$$\frac{d\tilde{n}_{e0}}{d\xi} = \tilde{n}_{e0}\tilde{E}_0 + \delta_0\tau_0\tilde{J}_0(0) \tag{5.8}$$

$$\tilde{n}_{i0} = \frac{\tilde{J}_0(0)}{\tilde{E}_0} \tag{5.9}$$

$$\frac{d\tilde{E}_0}{d\xi} = -\chi_0(\tilde{n}_{i0} - \tilde{n}_{e0}) \tag{5.10}$$

A separate treatment is necessary near  $\xi = 0$ , where  $\tilde{n}_{i0}$  changes rapidly and its derivative is large. An examination of Eq. (5.3) leads one to expect the large change in  $\tilde{n}_{i0}$  to occur as  $\xi$  increases from zero to a magnitude of order  $1/\tau_0$ . We therefore

introduce a new boundary-layer coordinate

$$\eta = \tau_o \xi \quad (5.11)$$

and rewrite Eqs. (5.1) - (5.4) :

$$\frac{d\tilde{J}_o}{d\eta} = 0 \quad (5.12)$$

$$\frac{d\tilde{n}_{eo}}{d\eta} = \frac{1}{\tau_o} (\tilde{n}_{eo} \tilde{E}_o + \delta_o \tau_o \tilde{J}_o) \quad (5.13)$$

$$\frac{d\tilde{n}_{io}}{d\eta} = -\tilde{n}_{io} \tilde{E}_o + \tilde{J}_o \quad (5.14)$$

$$\frac{d\tilde{E}_o}{d\eta} = -\frac{\chi_o}{\tau_o} (\tilde{n}_{io} - \tilde{n}_{eo}) \quad (5.15)$$

To lowest order in  $1/\tau_o$

$$\tilde{J}_o = \tilde{J}_o(0) \quad (5.16)$$

$$\tilde{n}_{eo} = \tilde{n}_{eo}(0) = 0 \quad (5.17)$$

$$\tilde{E}_o = \tilde{E}_o(0) \quad (5.18)$$

$$\frac{d\tilde{n}_{io}}{d\eta} + \tilde{E}_o(0) \tilde{n}_{io} = \tilde{J}_o(0) \quad (5.19)$$

in the skin. (5.19) is easily solved using the boundary condition (5.6)

to yield

$$\tilde{n}_{io} = \frac{\tilde{J}_o(0)}{\tilde{E}_o(0)} (1 - e^{-\tilde{E}_o(0)\eta}) \quad (5.20)$$

$$= \frac{\tilde{J}_o(0)}{\tilde{E}_o(0)} (1 - e^{-\tau_o \tilde{E}_o(0)\xi}) \quad (5.21)$$

Since

$$\lim_{\xi \rightarrow 0} \tilde{n}_{i0}(\xi) = \lim_{\eta \rightarrow \infty} \tilde{n}_{i0}(\eta) = \frac{\tilde{J}_0(0)}{\tilde{E}_0(0)} \quad (5.22)$$

the solutions in the two regions are said to match in an intermediate zone\*. The essential point is that the exponential term of (5.21) becomes negligible before  $\tilde{E}_0(\xi)$  in (5.9) deviates significantly from  $\tilde{E}_0(0)$ . The formal limiting process above expresses this situation provided such an intermediate region exists. It obviously does for a sufficiently large  $\tau_0$ . An expression for  $\tilde{n}_{i0}$  that is uniformly valid in  $\xi$  is obtained by adding the two solutions and subtracting from the sum this common limit in the intermediate region. We obtain

$$\tilde{n}_{i0} = \frac{\tilde{J}_0(0)}{\tilde{E}_0(\xi)} - \frac{\tilde{J}_0(0)}{\tilde{E}_0(0)} e^{-\tau_0 \tilde{E}_0(0) \xi} \quad (5.23)$$

Since the validity of this expression depends upon the exponential term's decaying while  $\tilde{E}_0(\xi)$  is still approximately equal to  $\tilde{E}_0(0)$ ,  $\tilde{E}_0(0)$  can be replaced by  $\tilde{E}_0(\xi)$  in the coefficient without introducing further error. Then (5.23) becomes

$$\tilde{n}_{i0} = \frac{\tilde{J}_0(0)}{\tilde{E}_0(\xi)} (1 - e^{-\tau_0 \tilde{E}_0(0) \xi}) \quad (5.24)$$

This form is more convenient in the following manipulations.

By making appropriate substitutions,  $\tilde{n}_{e0}$  as well as  $\tilde{n}_{i0}$  can be expressed in terms of  $\tilde{E}_0$ . These expressions can then be used to

---

\* See Cole [6], pp. 11 ff. for a discussion.

obtain a single nonlinear differential equation for  $\tilde{E}_o$ . Solving (5.4) for  $\tilde{n}_{eo}$ , using (5.24), and substituting into (5.2)

$$\frac{d\tilde{n}_{eo}}{d\xi} = \left[ \frac{1}{\chi_o} \frac{d\tilde{E}_o}{d\xi} + \frac{\tilde{J}_o(0)}{\tau_o \tilde{E}_o} (1 - e^{-\tau_o \tilde{E}_o(0)\xi}) \right] \tilde{E}_o + \delta_o \tau_o \tilde{J}_o(0) \quad (5.25)$$

$$= \frac{1}{2\chi_o} \frac{d}{d\xi} (\tilde{E}_o^2) + (1 + \delta_o \tau_o) \tilde{J}_o(0) - \tilde{J}_o(0) e^{-\tau_o \tilde{E}_o(0)\xi} \quad (5.26)$$

Integrating and using the boundary condition (5.5),

$$\begin{aligned} \tilde{n}_{eo} &= \frac{1}{2\chi_o} (\tilde{E}_o^2 - \tilde{E}_o^2(0)) + (1 + \delta_o \tau_o) \tilde{J}_o(0) \xi \\ &\quad - \frac{1}{\tau_o} \frac{\tilde{J}_o(0)}{\tilde{E}_o(0)} (1 - e^{-\tau_o \tilde{E}_o(0)\xi}) \quad (5.27) \end{aligned}$$

Since terms of order  $0(1/\tau_o)$  have already been neglected in obtaining  $\tilde{n}_{io}$ , it may appear consistent to neglect the last term of (5.27).

However, the source of this term is in the rapidly changing behavior of  $\tilde{n}_{io}$  in the skin, and its omission would be equivalent to assuming the outer solution for  $\tilde{n}_{io}$  valid to  $\xi = 0$  in the derivation of (5.27).

Furthermore, without this term the differential equation for  $\tilde{n}_{eo}$  would not be uniformly satisfied to lowest order in  $1/\tau_o$ . Such an omission would clearly be a needless introduction of error. In fact, numerical results show that the term is quite essential, particularly for small  $\xi$  where  $\tilde{n}_{eo}$  is small. An equation for  $\tilde{E}_o$  is obtained by substituting (5.23) and (5.27) into (5.4):

$$\begin{aligned} \frac{d\tilde{E}_0}{d\xi} = & \frac{1}{2}(\tilde{E}_0^2 - \tilde{E}_0^2(0)) + \chi_0(1 + \delta_0\tau_0)\tilde{J}_0(0)\xi - \frac{\chi_0\tilde{J}_0(0)}{\tau_0\tilde{E}_0(0)}(1 - e^{-\tau_0\tilde{E}_0(0)\xi}) \\ & - \frac{\chi_0\tilde{J}_0(0)}{\tilde{E}_0} + \frac{\chi_0\tilde{J}_0(0)}{\tilde{E}_0(0)} e^{-\tau_0\tilde{E}_0(0)\xi} \end{aligned} \quad (5.28)$$

$$\begin{aligned} = & \frac{1}{2}(\tilde{E}_0^2 - \tilde{E}_0^2(0)) + \chi_0(1 + \delta_0\tau_0)\tilde{J}_0(0)\xi - \frac{\chi_0\tilde{J}_0(0)}{\tilde{E}_0} \\ & - \frac{\chi_0\tilde{J}_0(0)}{\tau_0\tilde{E}_0(0)} + \frac{(1 + \tau_0)\chi_0\tilde{J}_0(0)}{\tau_0\tilde{E}_0(0)} e^{-\tau_0\tilde{E}_0(0)\xi} . \end{aligned} \quad (5.29)$$

Again terms of order  $0(1/\tau_0)$  are retained even though the possible error is also  $0(1/\tau_0)$ .

If Eq. (5.29) could be solved,  $\tilde{n}_{i0}$  and  $\tilde{n}_{e0}$  could be found from (5.23) and (5.27). However, Eq. (5.29) requires numerical treatment. The asymptotic forms of the variables for large  $\xi$  are obtained without difficulty, but the unknowns  $\tilde{J}_0(0)$  and  $\tilde{E}_0(0)$  enter rather intimately into the final expressions. Since  $\tilde{J}_0$  is constant,  $\tilde{J}_0(0)$  is determined quite easily by matching with the main-region solution, but Eq. (5.29) must be solved for all  $\xi$  to relate the initial value of  $\tilde{E}_0$  to its asymptotic form. This problem is deferred until the asymptotic solution is obtained.

#### Asymptotic Solution to the Approximate Zero-Order Equations

The behavior which  $\tilde{E}_0$  must exhibit for large  $\xi$  is determined quite easily from Eq. (5.29). The term  $\chi_0(1 + \delta_0\tau_0)\tilde{J}_0(0)\xi$  becomes large as  $\xi$  increases, so there must be at least one other term that

grows with it. Since  $\tilde{E}_0(\xi)$  must approach the outer solution  $E_0(y)$  in some manner as  $\xi$  becomes large, the magnitude of  $\tilde{E}_0$  and  $d\tilde{E}_0/d\xi$  cannot be permitted to increase in an unbounded manner. Hence  $\tilde{E}_0$  and  $d\tilde{E}_0/d\xi$  become negligible in asymptotic considerations, and Eq. (5.29) becomes

$$0 \sim -\frac{1}{2} \tilde{E}_0^2(0) + \chi_0(1 + \delta_0 \tau_0) \tilde{J}_0(0) \xi - \frac{\chi_0 \tilde{J}_0(0)}{\tilde{E}_0} - \frac{\chi_0 \tilde{J}_0(0)}{\tau_0 \tilde{E}_0(0)} \quad (5.30)$$

or

$$\tilde{E}_0 \sim \frac{1}{(1 + \delta_0 \tau_0) \xi - \frac{\tilde{E}_0^2(0)}{2\chi_0 \tilde{J}_0(0)} - \frac{1}{\tau_0 \tilde{E}_0(0)}} \quad (5.31)$$

The dominant contributions to  $\tilde{n}_{eo}$  and  $\tilde{n}_{io}$  are now found from (5.27) and (5.24).

$$\tilde{n}_{eo} \sim (1 + \delta_0 \tau_0) \tilde{J}_0(0) \xi - \frac{1}{2\chi_0} \tilde{E}_0^2(0) - \frac{\tilde{J}_0(0)}{\tau_0 \tilde{E}_0(0)} \quad (5.32)$$

$$\tilde{n}_{io} \sim \frac{\tilde{J}_0(0)}{\tilde{E}_0(\xi)} \quad (5.33)$$

$$\sim (1 + \delta_0 \tau_0) \tilde{J}_0(0) \xi - \frac{1}{2\chi_0} \tilde{E}_0^2(0) - \frac{\tilde{J}_0(0)}{\tau_0 \tilde{E}_0(0)} \quad (5.34)$$

These expressions serve to indicate the manner in which  $\tilde{E}_0(0)$  enters the asymptotic sheath solution. However, it is not involved in the largest contribution to any of the variables, and thus may not be involved in matching the main-region and sheath solutions to lowest order. Since the equations from which these expressions are derived involve various approximations, only the highest-order terms are

retained, and the variables are rewritten as

$$\tilde{J}_o \sim \tilde{J}_o(0) \quad (5.35)$$

$$\tilde{n}_{eo} \sim (1 + \delta_o \tau_o) \tilde{J}_o(0) \xi \quad (5.36)$$

$$\tilde{n}_{io} \sim (1 + \delta_o \tau_o) \tilde{J}_o(0) \xi \quad (5.37)$$

$$\tilde{E}_o \sim \frac{1}{1 + \delta_o \tau_o} \frac{1}{\xi} \quad (5.38)$$

Comparison of the Approximate Sheath Solution with the Main-Region Solution

The realization of obtaining an approximation to  $J$ ,  $n_e$ ,  $n_i$  and  $E$  that is valid for all  $y$  requires a consideration of the intermediate zone in which the main region and the sheath blend together. The validity of the perturbation procedure depends on the existence of such a zone in which the main-region and sheath solutions agree in some sense. Although the sheath equations are solved asymptotically as  $\xi \rightarrow \infty$ , the magnitude of  $\xi$  in the context of matching the two solutions is actually limited. In fact, in this context  $\xi$  can be assigned an approximate order of magnitude in  $\zeta$ , since the location of the sheath, and hence also the transition zone, depends on  $\zeta$ . The situation is clarified by reconsidering the relation between  $y$  and  $\xi$  introduced in Eq. (2.46),

$$\xi = \zeta^{1/3} (1 - y) \quad (5.39)$$

Since  $1 - y$  is of order unity in the main region and  $\xi$  is of order unity in the sheath,  $1 < \text{ord } \xi < \zeta^{1/3}$  in the transition zone. In

order to represent the magnitudes of the variables more clearly, the independent variable is rescaled by

$$x_\eta = \frac{1-y}{\eta(\zeta)} \quad (5.40)$$

where  $x_\eta$  is order unity in  $\zeta$  in the transition zone, and

$$\frac{1}{\zeta^{1/3}} < \text{ord } \eta(\zeta) < 1 \quad . \quad (5.41)$$

Since the solution is assumed to depend analytically on  $\zeta$ , the matching is accomplished by equating terms of the main-region and sheath solutions with the same  $\zeta$  dependence in the transition zone. This dependence is made explicit by converting  $y$  and  $\xi$  in the two solutions to  $x_\eta$  by

$$1-y = \eta(\zeta) x_\eta \quad (5.42)$$

$$\xi = \zeta^{1/3} \eta(\zeta) x_\eta \quad . \quad (5.43)$$

The main-region solution must be expanded for  $y$  near 1 before it is in a form convenient for matching. Since a more refined treatment of the sheath is presented later, only the most primitive approximation to the main-region solution is considered. Neglecting terms of order  $0(\epsilon_o \zeta)$ , Eqs. (3.53), (3.55), (3.56) imply for  $y$  near 1,

$$J_o \sim \frac{\pi}{2} \frac{1}{\rho_o} \quad (5.44)$$

$$n_{eo} \sim \frac{\pi}{2} (1-y) \quad (5.45)$$

$$E_o \sim \frac{1-\delta_o}{1+\delta_o \tau_o} \frac{1}{1-y} \quad . \quad (5.46)$$

Substituting from (5.42)

$$\text{(main region): } J_o \sim \frac{\pi}{2} \frac{1}{\rho_o} \quad (5.47)$$

$$\text{(main region): } n_{eo} \sim \frac{\pi}{2} \eta(\zeta) x_\eta \quad (5.48)$$

$$\text{(main region): } E_o \sim \frac{1 - \delta_o}{1 + \delta_o \tau_o} \frac{1}{\eta(\zeta)} \frac{1}{x_\eta} \quad (5.49)$$

If Eqs. (5.35), (5.36), (5.38) are rewritten in terms of  $x_\eta$  and if the dependent sheath variables are returned to their original forms via (2.47), (2.49), and (2.50), we obtain

$$\tilde{J}_o = J_o \sim \tilde{J}_o(0) \quad (5.50)$$

or

$$\text{(sheath): } J_o \sim \tilde{J}_o(0) \quad (5.51)$$

$$\tilde{n}_{eo} = \zeta^{1/3} n_{eo} \sim (1 + \delta_o \tau_o) \tilde{J}_o(0) \zeta^{1/3} \eta(\zeta) x_\eta \quad (5.52)$$

or

$$\text{(sheath): } n_{eo} \sim (1 + \delta_o \tau_o) \tilde{J}_o(0) \eta(\zeta) x_\eta \quad (5.53)$$

$$\tilde{E}_o = \frac{1}{\zeta^{1/3}} E_o \sim \frac{1}{1 + \delta_o \tau_o} \frac{1}{\zeta^{1/3} \eta(\zeta)} \frac{1}{x_\eta} \quad (5.54)$$

or

$$\text{(sheath): } E_o \sim \frac{1}{1 + \delta_o \tau_o} \frac{1}{\eta(\zeta)} \frac{1}{x_\eta} \quad (5.55)$$

If  $\tilde{J}_o(0)$  is selected so that  $J_o$  (main region) and  $J_o$  (sheath) match,

$$\tilde{J}_o(0) = \frac{\pi}{2} \frac{1}{\rho_o} \quad (5.56)$$

the comparison of main-region and sheath solutions is as written below:

$$\text{(main region):} \quad J_o \sim \frac{\pi}{2} \frac{1}{\rho_o} \quad (5.57)$$

$$\text{(sheath):} \quad J_o \sim \frac{\pi}{2} \frac{1}{\rho_o} \quad (5.58)$$

$$\text{(main region):} \quad n_{eo} \sim \frac{\pi}{2} \eta(\zeta) x_\eta \quad (5.59)$$

$$\text{(sheath):} \quad n_{eo} \sim \frac{\pi}{2} \left(1 + \frac{1}{\tau_o}\right) \eta(\zeta) x_\eta \quad (5.60)$$

$$\text{(main region):} \quad E_o \sim \frac{1 - \delta_o}{1 + \delta_o \tau_o} \frac{1}{\eta(\zeta)} \frac{1}{x_\eta} \quad (5.61)$$

$$\text{(sheath):} \quad E_o \sim \frac{1}{1 + \delta_o \tau_o} \frac{1}{\eta(\zeta)} \frac{1}{x_\eta} \quad (5.62)$$

where Eq. (2.19) for  $\rho_o$  has been used. Except for the choice of  $\tilde{J}_o(0)$ , there is nothing to vary in order to effect matching, and the main-region and sheath variables must agree identically. It is apparent that the two  $n_{eo}$ 's and  $E_o$ 's do not agree exactly but differ by amounts proportional to  $1/\tau_o$  and  $\delta_o$ , respectively. However, it can be shown that these discrepancies are caused by the asymptotic expansion in  $1/\tau_o$  used to obtain the zero-order sheath solution. In any case, the two solutions exhibit similar behavior in the transition zone.

#### Numerical Calculation of $\tilde{E}_o(0)$

Although  $\tilde{E}_o(0)$  is not needed for the matching above, its appearance in (5.31) and (5.32) suggests that it may be needed in higher-order matching. In the more complete treatment of the sheath that follows, it is helpful to know its approximate value.

The behavior of  $\tilde{E}_o$  for various choices of  $\tilde{E}_o(0)$  is illustrated by the sketch in Fig. 5. The dashes represent slopes of the  $\tilde{E}_o$

versus  $\xi$  curves and are calculated from the right-hand side of (5.29). The slopes depend on  $\tilde{E}_0(0)$ , of course, but for  $\xi$  large, one of the three terms,  $\frac{1}{2} \tilde{E}_0^2(\xi)$ ,  $\chi_0(1 + \delta_0 \tau_0) \tilde{J}_0(0) \xi$ ,  $-\chi_0 \tilde{J}_0(0) / \tilde{E}_0(\xi)$ , is dominant. Figure 5 is intended to show only the essential behavior, and so contributions from terms other than these three are neglected. The relation of  $\tilde{E}_0(0)$  to the desired asymptotic behavior is seen by observing Eq. (5.29) as  $\xi$  increases from zero. If too small an  $\tilde{E}_0(0)$  is chosen, the term  $-\chi_0 \tilde{J}_0(0) / \tilde{E}_0$  causes the derivative  $d\tilde{E}_0/d\xi$  to become increasingly negative. The further decrease in  $\tilde{E}_0$  exacerbates the situation, and the integration terminates when the magnitude of the derivative becomes infinite at  $\tilde{E}_0 = 0$ . On the other hand, if  $\tilde{E}_0(0)$  is too large, the term  $-\chi_0 \tilde{J}_0(0) / \tilde{E}_0$  fails to prevail over the term  $\chi_0(1 + \delta_0 \tau_0) \tilde{J}_0(0) \xi$ , and  $\tilde{E}_0(\xi)$  begins to grow. The term  $\frac{1}{2} \tilde{E}_0^2(\xi)$  eventually dominates, and  $\tilde{E}_0(\xi)$  increases rapidly to infinity. The curve which separates these two distinctive classes of solutions is the special solution with the required asymptotic properties. As shown by the derivation of Eq. (5.31), the large terms  $\chi_0(1 + \delta_0 \tau_0) \tilde{J}_0(0) \xi$  and  $-\chi_0 \tilde{J}_0(0) / \tilde{E}_0(\xi)$  essentially balance, and the magnitudes of  $\tilde{E}_0$  and  $d\tilde{E}_0/d\xi$  decrease gradually to zero.

A means of calculating  $\tilde{E}_0(0)$  numerically is made apparent by a study of Fig. 5. Since the behavior of  $\tilde{E}_0$  for large  $\xi$  appears to be quite sensitive to the choice of  $\tilde{E}_0(0)$ , it seems reasonable to evaluate  $\tilde{E}_0(\xi)$  for a large  $\xi$  from the asymptotic formula using an assumed  $\tilde{E}_0(0)$ . Integration to  $\xi = 0$  then provides a new  $\tilde{E}_0(0)$  with which to develop an iterative procedure.

Unfortunately the asymptotic representation of  $\tilde{E}_0$  in Eq. (5.31) is not sufficiently accurate to initiate the integration at large  $\xi$ . The reason is that in the derivation of (5.31) from (5.29) the terms involving  $d\tilde{E}_0/d\xi$  and  $\tilde{E}_0^2$  are neglected. Thus if the asymptotic evaluation of  $\tilde{E}_0$  is used in (5.29) to determine the value of  $d\tilde{E}_0/d\xi$  in the initial step of the numerical integration, the result possesses an error the order of  $d\tilde{E}_0/d\xi$  itself. In order to obtain an asymptotic  $\tilde{E}_0$  that is capable of determining  $d\tilde{E}_0/d\xi$  to sufficient accuracy, we begin again from Eq. (5.29). Neglecting only the term containing the exponential and rearranging,

$$\frac{\chi_0 \tilde{J}_0(0)}{\tilde{E}_0} = \chi_0 (1 + \delta_0 \tau_0) \tilde{J}_0(0) \xi - \frac{1}{2} \tilde{E}_0^2(0) - \frac{\chi_0 \tilde{J}_0(0)}{\tau_0 \tilde{E}_0(0)} + \frac{1}{2} \tilde{E}_0^2 - \frac{d\tilde{E}_0}{d\xi} \quad (5.63)$$

or

$$\tilde{E}_0 = \frac{1}{(1 + \delta_0 \tau_0) \xi - \frac{\tilde{E}_0^2(0)}{2\chi_0 \tilde{J}_0(0)} - \frac{1}{\tau_0 \tilde{E}_0(0)} + \frac{\tilde{E}_0^2}{2\chi_0 \tilde{J}_0(0)} - \frac{1}{\chi_0 \tilde{J}_0(0)} \frac{d\tilde{E}_0}{d\xi}} \quad (5.64)$$

Differentiating (5.64)

$$\frac{d\tilde{E}_0}{d\xi} = - \frac{(1 + \delta_0 \tau_0) + \tilde{E}_0 (d\tilde{E}_0/d\xi) / (\chi_0 \tilde{J}_0(0)) - \frac{1}{\chi_0 \tilde{J}_0(0)} \frac{d^2 \tilde{E}_0}{d\xi^2}}{\left[ (1 + \delta_0 \tau_0) \xi - \frac{\tilde{E}_0^2(0)}{2\chi_0 \tilde{J}_0(0)} - \frac{1}{\tau_0 \tilde{E}_0(0)} + \frac{\tilde{E}_0^2}{2\chi_0 \tilde{J}_0(0)} - \frac{1}{\chi_0 \tilde{J}_0(0)} \frac{d\tilde{E}_0}{d\xi} \right]^2} \quad (5.65)$$

The dominant terms in these equations provide the following order-of-magnitude estimates for large  $\xi$ :

$$\tilde{E}_o = 0\left(\frac{1}{\xi}\right) \quad (5.66)$$

$$\tilde{E}_o^2 = 0\left(\frac{1}{\xi^2}\right) \quad (5.67)$$

$$\frac{d\tilde{E}_o}{d\xi} = 0\left(\frac{1}{\xi^2}\right) \quad (5.68)$$

$$\frac{d^2\tilde{E}_o}{d\xi^2} = 0\left(\frac{1}{\xi^3}\right) \quad (5.69)$$

Using (5.64), Eq. (5.65) can be rewritten retaining only the highest-order term in the numerator.

$$\frac{d\tilde{E}_o}{d\xi} = -\left[(1 + \delta_o \tau_o) + 0\left(\frac{1}{\xi^3}\right)\right] \tilde{E}_o^2 \quad (5.70)$$

$$= - (1 + \delta_o \tau_o) \tilde{E}_o^2 + 0\left(\frac{1}{\xi^5}\right) \quad (5.71)$$

With this result Eq. (5.64) now becomes

$$\tilde{E}_o = \frac{1}{(1 + \delta_o \tau_o) \xi - \frac{\tilde{E}_o^2(0)}{2\chi_o J_o(0)} - \frac{1}{\tau_o \tilde{E}_o(0)} + \left(\frac{3}{2} + \delta_o \tau_o\right) \frac{\tilde{E}_o^2}{\chi_o J_o(0)} + 0\left(\frac{1}{\xi^5}\right)} \quad (5.72)$$

or

$$\tilde{E}_o = \frac{1}{(1 + \delta_o \tau_o) \xi - \frac{\tilde{E}_o^2(0)}{2\chi_o J_o(0)} - \frac{1}{\tau_o \tilde{E}_o(0)} + \left(\frac{3}{2} + \delta_o \tau_o\right) \frac{\tilde{E}_o^2}{\chi_o J_o(0)} + 0\left(\frac{1}{\xi^7}\right)} \quad (5.73)$$

For a specified  $\xi$  and an  $\tilde{E}_o(0)$  not too far from the correct value, an accurate numerical value for  $\tilde{E}_o(\xi)$  is easily obtained using the

iterative scheme described by the equations below:

$$\tilde{E}_0^{(0)} = 0 \tag{5.74}$$

$$\tilde{E}_0^{(n+1)} = \frac{1}{(1 + \delta_o \tau_o) \xi - \frac{\tilde{E}_0^{(n)2}}{2\chi_o \tilde{J}_o(0)} - \frac{1}{\tau_o \tilde{E}_0^{(n)}} + (\frac{3}{2} + \delta_o \tau_o) \frac{\tilde{E}_0^{(n)2}}{\chi_o \tilde{J}_o(0)}} \tag{5.75}$$

$$n = 0, 1, 2, \dots \tag{5.76}$$

The convergence is rapid, and the resulting value, when used in Eq. (5.29), provides an accurate estimate of the derivative  $\frac{d\tilde{E}_0}{d\xi}$ .

The iterative method by which  $\tilde{E}_0^{(0)}$  is determined can now be employed. An assumed value of  $\tilde{E}_0^{(0)}$  is used in (5.75) to obtain  $\tilde{E}_0^{(1)}$  at a particular  $\xi$ . In the numerical work performed,  $\tilde{E}_0^{(1)}$  is evaluated at  $\xi = 10$ , and using that as the initial value, Eq. (5.29) is integrated to  $\xi = 0$ . The value of  $\tilde{E}_0^{(2)}$  there provides a new estimate to  $\tilde{E}_0^{(0)}$ , and the entire process is repeated once. In order to present the method more clearly, we let  $g(x)$  represent the solution to (5.29) evaluated at  $\xi = 0$  with  $x$  as the estimate for  $\tilde{E}_0^{(0)}$  used in the right-hand side. Thus we seek a solution  $z$  of the equation

$$z = g(z) \tag{5.77}$$

and such a  $z$  is the correct value for  $\tilde{E}_0^{(0)}$ . The solution of (5.29) using this value in its right-hand side yields the function  $\tilde{E}_0(\xi)$  for  $0 \leq \xi \leq 10$ . The first two steps toward the solution are described verbally above.  $z^{(0)}$  is chosen arbitrarily, and (5.29) is solved to generate  $z^{(1)}$ :

$$z^{(1)} = g(z^{(0)}) \quad . \quad (5.78)$$

The iterative procedure described by  $z^{(n+1)} = g(z^{(n)})$  converges to the solution  $z$  too slowly to be of practical value, but the two values  $z^{(0)}$  and  $z^{(1)}$  permit the initiation of the method of false position<sup>\*</sup>. We define

$$f(x) \equiv g(x) - x \quad (5.79)$$

and determine the succeeding  $z^{(n)}$  by the recursion formula,

$$z^{(n+1)} = z^{(n)} - \frac{z^{(n)} - z^{(n-1)}}{f(z^{(n)}) - f(z^{(n-1)})} f(z^{(n)}) \quad ; \quad (5.80)$$

$$n = 1, 2, \dots \quad . \quad (5.81)$$

The sequence  $\{z^{(n)}\}$  converges rapidly to a solution  $z$  of Eq. (5.77) yielding

$$\tilde{E}_0(0) = z \quad . \quad (5.82)$$

An example of a typical sequence is given in Table 5.

Since  $\zeta$  enters into Eq. (5.29) through the coefficients  $\tau_0$ ,  $\delta_0$ ,  $\chi_0$ , and  $\tilde{J}_0(0)$ , the  $\tilde{E}_0(0)$  obtained is a function of  $\zeta$ , and a separate calculation must be performed for each numerical value of  $\zeta$  considered. Also,  $\tilde{J}_0(0)$  is given by Eq. (5.56), but this expression is not used in the numerical calculations. One of the main purposes of the approximate sheath solution is to provide a good estimate to the solution of the exact sheath equations. In order to make  $\tilde{E}_0(0)$  the

---

<sup>\*</sup> See Isaacson and Keller [9], pp. 99-102.

best possible estimate of  $\tilde{E}(0)$ , we take as  $\tilde{J}_0(0)$  the expression obtained by matching the exact asymptotic solutions, which are presented later.  $\tilde{J}(0)$  is given by Eq. (7.5), and hence for the numerical integration of (5.29) we use

$$\tilde{J}_0(0) = \frac{\pi}{2} \frac{1}{\rho_0} + \frac{4}{3\pi^2} \left(2 - \frac{\pi}{2}\right) \epsilon_0 \zeta . \quad (5.83)$$

The integration is performed using a fourth-order Runge-Kutta method.

$\tilde{E}_0(0)$  is obtained for a number of values of  $\zeta$ , and the results are tabulated in Table 6 along with the exact values  $\tilde{E}(0)$ , which are obtained later. It is apparent that the approximate solution is quite close to the exact solution with the most common difference  $\tilde{E}_0(0) - \tilde{E}(0)$  being 0.002. This accuracy is quite pleasing because the right-hand side of (5.29) can have an error of order  $O(1/\tau_0)$ . When integrated from  $\xi = 10$  to  $\xi = 0$ , an error can be introduced whose magnitude approaches 0.1. It is possible that a significant portion of the error involved in the derivation of Eq. (5.29) cancels when calculating the difference  $\tilde{n}_{i0} - \tilde{n}_{e0}$  in Eq. (5.4). In any case, it is clear that the omission of the terms of order  $O(1/\tau_0)$  in (5.29) would yield much less accurate results.

During the integration of (5.29) values for  $\tilde{n}_{i0}$  and  $\tilde{n}_{e0}$  are obtained from the expressions in (5.24) and (5.27).  $\tilde{E}_0$ ,  $\tilde{n}_{i0}$ , and  $\tilde{n}_{e0}$  all behave as expected. Graphical results are presented in Figs. 6 and 7. The latter shows the rapid variation in  $\tilde{n}_{i0}$  near  $\xi = 0$ . The values for  $\tilde{E}_0$ ,  $\tilde{n}_{i0}$ , and  $\tilde{n}_{e0}$  are in quite accurate agreement with the numerical solution to the exact zero-order sheath equations, which is obtained in Section 6 over a more limited range of  $\xi$ .

6. EXACT ASYMPTOTIC SHEATH SOLUTION

The determination of the asymptotic forms of the variables in the sheath for large  $\xi$  parallels the development by Cohen and Kruskal [5]. The approach differs from that of Section 5 by including in the equations some higher-order terms in  $\zeta$  and by refraining from approximations based on the magnitude of  $\tau$ .  $\tilde{E}(0)$  again enters the asymptotic expressions and must be calculated numerically.

Working Equations

The sheath problem of Eqs. (2.51) - (2.56) is rewritten below with the desired degree of accuracy by retaining only the largest of the higher-order terms in  $\zeta$ . Using the first two terms of the expansions (2.9) - (2.11), we obtain

$$\frac{d\tilde{J}}{d\xi} = -\frac{1}{\zeta^{2/3}} \gamma_0 \tilde{n}_e \quad (6.1)$$

$$\frac{d\tilde{n}_e}{d\xi} = \tilde{n}_e \tilde{E} + [\delta_0 \tau_0 + \mu_1 (\delta_0 \tau_1 + \delta_1 \tau_0)] \tilde{J} \quad (6.2)$$

$$\frac{d\tilde{n}_i}{d\xi} = (\tau_0 + \mu_1 \tau_1) (-\tilde{n}_i \tilde{E} + \tilde{J}) \quad (6.3)$$

$$\frac{d\tilde{E}}{d\xi} = -(\chi_0 + \mu_1 \chi_1) (\tilde{n}_i - \tilde{n}_e) \quad (6.4)$$

$$\xi = 0 : \quad \tilde{n}_e = 0 \quad (6.5)$$

$$\tilde{n}_i = 0 \quad . \quad (6.6)$$

By appropriate manipulations (6.1) - (6.4) are converted to integral equations which are solved asymptotically by an iterative

procedure. One integration is performed by making suitable eliminations between Eqs. (6.2), (6.3), and (6.4). Dividing both sides of (6.3) by  $(\tau_o + \mu_1 \tau_1)$  and adding to (6.2),

$$\frac{d\tilde{n}_e}{d\tilde{\xi}} + \frac{1}{\tau_o + \mu_1 \tau_1} \frac{d\tilde{n}_1}{d\tilde{\xi}} = -\tilde{E}(\tilde{n}_1 - \tilde{n}_e) + [1 + \delta_o \tau_o + \mu_1 (\delta_o \tau_1 + \delta_1 \tau_o)] \tilde{J} . \quad (6.7)$$

$\tilde{n}_1 - \tilde{n}_e$  is eliminated by using Eq. (6.4):

$$\frac{d\tilde{n}_e}{d\tilde{\xi}} + \frac{1}{\tau_o + \mu_1 \tau_1} \frac{d\tilde{n}_1}{d\tilde{\xi}} = \frac{1}{\chi_o + \mu_1 \chi_1} \tilde{E} \frac{d\tilde{E}}{d\tilde{\xi}} + [1 + \delta_o \tau_o + \mu_1 (\delta_o \tau_1 + \delta_1 \tau_o)] \tilde{J} . \quad (6.8)$$

The coefficients can be expressed in a more appealing form by

$$\frac{1}{\tau_o + \mu_1 \tau_1} = \frac{1}{\tau_o} \frac{1}{1 + \mu_1 \tau_1 / \tau_o} \quad (6.9)$$

$$= \frac{1}{\tau_o} - \mu_1 \frac{\tau_1}{\tau_o^2} + O(\mu_1^2) \quad (6.10)$$

and

$$\frac{1}{\chi_o + \mu_1 \chi_1} = \frac{1}{\chi_o} - \mu_1 \frac{\chi_1}{\chi_o^2} + O(\mu_1^2) . \quad (6.11)$$

Since the equations are only accurate to order  $O(\mu_1)$ , no accuracy is lost by the above substitutions. If Eq. (6.8) is integrated from 0 to  $\tilde{\xi}$  using (6.5) and (6.6),

$$\begin{aligned} \tilde{n}_e + \left(\frac{1}{\tau_o} - \mu_1 \frac{\tau_1}{\tau_o^2}\right) \tilde{n}_1 &= \frac{1}{2} \left(\frac{1}{\chi_o} - \mu_1 \frac{\chi_1}{\chi_o^2}\right) (\tilde{E}^2 - \tilde{E}^2(0)) \\ &+ [1 + \delta_o \tau_o + \mu_1 (\delta_o \tau_1 + \delta_1 \tau_o)] \int_0^{\tilde{\xi}} \tilde{J}(\bar{\xi}) d\bar{\xi} . \end{aligned} \quad (6.12)$$

An integral equation for  $\tilde{J}$  is obtained directly from (6.1):

$$\tilde{J} = \tilde{J}(0) - \frac{1}{\zeta^{2/3}} \gamma_0 \int_0^{\xi} \tilde{n}_e(\bar{\xi}) d\bar{\xi} \quad . \quad (6.13)$$

Asymptotic Solution

The determination of the asymptotic expressions from Eqs. (6.12) and (6.13) requires a careful assessment of the orders of magnitude of the various terms. In particular, powers of  $\xi$  must be compared with functions of  $\zeta$ . Since the asymptotic solution is to be used for matching, the discussion centering around Eq. (5.39) is pertinent, and  $\xi$  is assumed to be of order  $\zeta^{1/3} \eta(\zeta)$  as indicated by Eq. (5.43). Using the estimate for  $\tilde{n}_e$  given by (5.36), the second term on the right-hand side of (6.13) is of order  $\eta^2$ , so the lowest-order contribution to  $\tilde{J}$  is again

$$\tilde{J} \sim \tilde{J}(0) \quad . \quad (6.14)$$

Equation (6.12) is used to determine  $\tilde{n}_e$  to lowest order, but it is first necessary to eliminate  $\tilde{n}_i$ . The approximate results of Eq. (5.38) can be used in (6.4) to conclude that

$$\tilde{n}_i - \tilde{n}_e = 0\left(\frac{1}{\zeta^{2/3} \eta^2}\right) \quad (6.15)$$

so  $\tilde{n}_i = \tilde{n}_e$  to lowest order. Also,

$$\tilde{E}^2 = 0\left(\frac{1}{\zeta^{2/3} \eta^2}\right) \quad (6.16)$$

$$\tilde{E}^2(0) = 0(1) \quad (6.17)$$

and

$$\int_0^{\xi} \tilde{J}(\bar{\xi}) d\bar{\xi} = 0(\zeta^{1/3} \eta) \quad (6.18)$$

so the retention of only the largest terms in Eq. (6.12) yields

$$\tilde{n}_e + \frac{1}{\tau_0} \tilde{n}_e = (1 + \delta_0 \tau_0) \int_0^\xi \tilde{J}(0) d\bar{\xi} \quad (6.19)$$

or, using Eq. (2.19) for  $\rho_0$ ,

$$\tilde{n}_e \sim \rho_0 \tilde{J}(0) \xi \quad (6.20)$$

The substitution of this expression for  $\tilde{n}_e$  into (6.13) yields a better approximation to  $\tilde{J}$ . Since only the asymptotic form of  $\tilde{n}_e$  for large  $\xi$  is known, the integral  $\int_0^\xi \tilde{n}_e(\bar{\xi}) d\bar{\xi}$  cannot be evaluated. However, the asymptotic expression can be integrated to yield the asymptotic form of the integral. The integral of the deviation of  $\tilde{n}_e$  from its asymptotic value can be written as an "integration constant" that depends only weakly on  $\xi$  for  $\xi$  large. Thus,

$$\int_0^\xi \tilde{n}_e(\bar{\xi}) d\bar{\xi} = \frac{1}{2} \rho_0 \tilde{J}(0) \xi^2 + C_1 \quad (6.21)$$

where actually

$$C_1 = \int_0^\xi [\tilde{n}_e(\bar{\xi}) - \rho_0 \tilde{J}(0) \bar{\xi}] d\bar{\xi} \quad (6.22)$$

For large  $\xi$  the variation of  $C_1$  with  $\xi$  is negligible compared to  $\xi^2$ , so

$$C_1 = o(\xi^{2/3} \eta^2) \quad (6.23)$$

and (6.13) becomes

$$\tilde{J} \sim \tilde{J}(0) - \frac{\gamma_o \rho_o}{2\zeta^{2/3}} \tilde{J}(0) \xi^2 . \quad (6.24)$$

This expression for  $\tilde{J}$  can be used in (6.12) to provide a better approximation to  $\tilde{n}_e$  .

$$\int_0^\xi \tilde{J}(\bar{\xi}) d\bar{\xi} = \tilde{J}(0) \xi - \frac{\gamma_o \rho_o}{6\zeta^{2/3}} \tilde{J}(0) \xi^3 + C_2 \quad (6.25)$$

where, by the same reasoning as before,  $C_2$  is of lower order than the other terms and

$$\int_0^\xi \tilde{J}(\bar{\xi}) d\bar{\xi} \sim \tilde{J}(0) \xi - \frac{\gamma_o \rho_o}{6\zeta^{2/3}} \tilde{J}(0) \xi^3 . \quad (6.26)$$

It is now necessary to make an assumption on  $\mu_1(\zeta)$  in order to compare the relative magnitudes of terms in (6.12). The term involving  $\tilde{E}(0)$  is of order unity, and all lesser terms may be neglected. However, the substitution of (6.26) into (6.12) results in the term  $\mu_1(\delta_o \tau_1 + \delta_1 \tau_o) \tilde{J}(0) \xi$  , which has order  $\mu_1 \zeta^{1/3} \eta$  . In order to neglect this term, we assume

$$\text{ord}(\mu_1(\zeta)) < \text{ord}\left(\frac{1}{\zeta^{1/3} \eta(\zeta)}\right) . \quad (6.27)$$

The validity of this inequality is established when  $\mu_1(\zeta)$  is determined. Now all terms involving  $\mu_1$  can be neglected, and from (6.15) and (6.16) it is seen that  $\tilde{n}_i - \tilde{n}_e$  and  $\tilde{E}^2$  are also insignificant in comparison with  $\tilde{E}^2(0)$  . Equation (6.12) now becomes

$$\tilde{n}_e + \frac{1}{\tau_o} \tilde{n}_e = -\frac{1}{2\chi_o} \tilde{E}^2(0) + (1 + \delta_o \tau_o) [\tilde{J}(0)\xi - \frac{\gamma_o \rho_o}{6\zeta^{2/3}} \tilde{J}(0)\xi^3] \quad (6.28)$$

or

$$\tilde{n}_e \sim \rho_o \tilde{J}(0)\xi - \frac{\gamma_o \rho_o^2}{6\zeta^{2/3}} \tilde{J}(0)\xi^3 - \frac{1}{2\chi_o} \frac{\tau_o \tilde{E}^2(0)}{1 + \tau_o} . \quad (6.29)$$

The second term is of order  $\zeta^{1/3} \eta^3(\zeta)$ , but it need not be compared with the third, because both can be matched to terms of the main-region solution. However, if (6.29) is to represent the dominant contributions to  $\tilde{n}_e$ , the second term must be larger than the term of order  $\mu_1 \zeta^{1/3} \eta$  that is neglected. In this case we must have

$$\text{ord}(\zeta^{1/3} \eta^3) > \text{ord}(\mu_1 \zeta^{1/3} \eta) . \quad (6.30)$$

It is seen later that  $\mu_1$  must equal  $1/\zeta^{1/3}$ , so (6.30), together with the previous bounds on  $\eta$  implies that

$$\frac{1}{\zeta^{1/6}} < \text{ord}(\eta) < 1 . \quad (6.31)$$

However, it is not necessary that the terms shown in (6.29) be the dominant contributions to  $\tilde{n}_e$ . The matching of sheath and main-region solutions proceeds by equating terms of the two solutions that have the same functional dependence on  $\zeta$ . In principle each term of the asymptotic sheath solution is to be matched individually, and it is not necessary to determine relative magnitudes except for purposes of numerical estimation; it is only necessary that the dependence of each term on  $\zeta$  be different from that of any other. Since the dependence of  $\eta$  on  $\zeta$  is arbitrary within a certain range, the functional

dependence of two terms on  $\zeta$  is the same only if their explicit dependence on  $\zeta$  and their dependence on  $\eta$  are the same. The relative magnitudes of terms depends on the functional form of  $\eta$ , i.e., on the precise location between main region and sheath.

The asymptotic form of  $\tilde{E}$  is obtained from Eqs. (6.2) and (6.3). Subtracting (6.3) from (6.2) and neglecting terms of order  $\mu_1$ ,

$$\frac{d}{d\xi} (\tilde{n}_e - \tilde{n}_i) = (\tilde{n}_e + \tau_o \tilde{n}_i) \tilde{E} - \tau_o (1 - \delta_o) \tilde{J} \quad (6.32)$$

From (6.15),  $\tilde{n}_i - \tilde{n}_e$  and its derivative are negligible with respect to  $\tilde{J}$ , and (6.32) can be solved for  $\tilde{E}$ :

$$\tilde{E} = \tau_o \frac{1 - \delta_o}{1 + \tau_o} \frac{\tilde{J}}{\tilde{n}_e} \quad (6.33)$$

Using (6.24) and (6.29)

$$\tilde{E} \sim \tau_o \frac{1 - \delta_o}{1 + \tau_o} \frac{\tilde{J}(0) [1 - \frac{\gamma_o \rho_o}{2\zeta^{2/3}} \xi^2]}{\rho_o \tilde{J}(0) \xi - \frac{\gamma_o \rho_o^2}{6\zeta^{2/3}} \tilde{J}(0) \xi^3 - \frac{1}{2\chi_o} \frac{\tau_o \tilde{E}^2(0)}{1 + \tau_o}} \quad (6.34)$$

or, using Eq. (2.19) for  $\rho_o$ ,

$$\tilde{E} \sim \frac{1 - \delta_o}{1 + \delta_o \tau_o} \frac{1}{\xi} \cdot \frac{1 - \frac{\gamma_o \rho_o}{2\zeta^{2/3}} \xi^2}{1 - \frac{\gamma_o \rho_o}{6\zeta^{2/3}} \xi^2 - \frac{1}{2\chi_o (1 + \delta_o \tau_o)} \frac{\tilde{E}^2(0)}{\tilde{J}(0)} \frac{1}{\xi}} \quad (6.35)$$

$$\sim \frac{1 - \delta_o}{1 + \delta_o \tau_o} \frac{1}{\xi} \cdot \left[ 1 - \frac{\gamma_o \rho_o}{2\zeta^{2/3}} \xi^2 \right] \cdot \left[ 1 + \frac{\gamma_o \rho_o}{6\zeta^{2/3}} \xi^2 + \frac{1}{2\chi_o (1 + \delta_o \tau_o)} \frac{\tilde{E}^2(0)}{\tilde{J}(0)} \frac{1}{\xi} \right] \quad (6.36)$$

$$\sim \frac{1 - \delta_o}{1 + \delta_o \tau_o} \frac{1}{\xi} - \frac{\gamma_o \tau_o}{3\zeta^{2/3}} \frac{1 - \delta_o}{1 + \tau_o} \xi + \frac{1 - \delta_o}{2\chi_o (1 + \delta_o \tau_o)^2} \frac{\tilde{E}^2(0)}{\tilde{J}(0)} \frac{1}{\xi^2} \quad (6.37)$$

Various terms have been neglected in obtaining this equation, and if we were to insist that the terms presented be the terms of largest orders in  $\zeta$ , we would have to confine  $\eta$  within narrower limits.

The first nonzero contribution to the space-charge density is calculated using only the first term of (6.37). Defining  $\tilde{s}$  by

$$\tilde{s} \equiv \tilde{n}_i - \tilde{n}_e \quad (6.38)$$

and using (6.4), we obtain

$$\tilde{s} \sim -\frac{1}{\chi_o} \frac{d\tilde{E}}{d\xi} \quad (6.39)$$

$$\sim \frac{1}{\chi_o} \frac{1 - \delta_o}{1 + \delta_o \tau_o} \frac{1}{\xi^2} \quad (6.40)$$

Since  $\text{ord}(\tilde{s}) = 1/(\zeta^{2/3} \eta^2)$ ,  $\tilde{n}_i = \tilde{n}_e$  to the accuracy exhibited by Eq. (6.29) provided  $\eta$  is restricted as shown in (6.31).

#### Numerical Calculation of $\tilde{E}(0)$

As in the approximate case considered in Section 5,  $\tilde{E}(0)$  appears in the asymptotic expression and must be calculated by a numerical integration of the sheath equations. Since  $\tilde{E}(0)$  appears

in a higher-order term, the equations need be considered only to lowest order in  $\zeta$ . The lowest-order equations can be transformed to a problem treated by Cohen [4], but here we proceed using manipulations already carried out.

In their lowest-order form one integration of the sheath equations can be performed, and this integral can be obtained directly by simplifying Eq. (6.12). If the largest contribution to  $\tilde{J}$  in (6.13) is used in (6.12), and if higher-order terms in  $\zeta$  are neglected, we obtain

$$\tilde{n}_e + \frac{1}{\tau_o} \tilde{n}_i = \frac{1}{2\chi_o} (\tilde{E}^2 - \tilde{E}^2(0)) + (1 + \delta_o \tau_o) \tilde{J}(0) \xi . \quad (6.41)$$

It is convenient at this time to make a change of variables from  $\tilde{n}_i$  to  $\tilde{s} = \tilde{n}_i - \tilde{n}_e$ . Then Eq. (6.41), when solved for  $\tilde{E}$ , becomes

$$\tilde{E} = \left\{ \tilde{E}^2(0) + \frac{2\chi_o}{\tau_o} [(1 + \tau_o) \tilde{n}_e + \tilde{s}] - 2\chi_o (1 + \delta_o \tau_o) \tilde{J}(0) \xi \right\}^{1/2} . \quad (6.42)$$

Equations (6.2) and (6.3) become, to lowest order in  $\zeta$ ,

$$\frac{d\tilde{n}_e}{d\xi} = \tilde{n}_e \tilde{E} + \delta_o \tau_o \tilde{J}(0) \quad (6.43)$$

$$\frac{d\tilde{s}}{d\xi} = -[(1 + \tau_o) \tilde{n}_e + \tau_o \tilde{s}] \tilde{E} + \tau_o (1 - \delta_o) \tilde{J}(0) \quad (6.44)$$

with  $\tilde{E}$  given by (6.42). The boundary conditions are

$$\xi = 0 : \quad \tilde{n}_e = 0 \quad (6.45)$$

$$\tilde{s} = 0 . \quad (6.46)$$

The problem is now reduced to a system of two differential equations for  $\tilde{n}_e$  and  $\tilde{s}$  and an algebraic equation for  $\tilde{E}$ .  $\tilde{E}(0)$  enters the equations as an unknown. It is determined by requiring that the solutions to (6.42) - (6.44) behave for large  $\xi$  as the corresponding asymptotic formulas just obtained. It is for this reason that  $\tilde{n}_1$  is replaced by  $\tilde{s}$ . Equation (6.40) shows that  $\tilde{s}$  decreases and becomes quite small as  $\xi$  becomes large. If an incorrect  $\tilde{E}(0)$  is selected,  $\tilde{s}$  as obtained from Eq. (6.44) either becomes negative or begins to grow for large  $\xi$ . The reason for such behavior is readily seen by a study of Eqs. (6.42) - (6.44). If too large an  $\tilde{E}(0)$  is chosen and the equations are integrated from  $\xi = 0$ ,  $\tilde{E}$  as determined by (6.42) is too large. The term involving  $\tilde{E}$  on the right-hand side of (6.44) thus becomes too large in magnitude, and  $\tilde{s}$  becomes negative. If too small an  $\tilde{E}(0)$  is chosen, the magnitude of the first term on the right-hand side of (6.44) is too small, and  $\tilde{s}$  increases at large  $\xi$ . This observation forms the basis for the trial-and-error solution of the equations. An  $\tilde{E}(0)$  is selected arbitrarily, and Eqs. (6.43) and (6.44) are integrated numerically from  $\xi = 0$ . The behavior of  $\tilde{s}$  tells whether the assumed  $\tilde{E}(0)$  is too large or too small, and further values are selected on the basis of the results. The two types of behavior are quite distinctive, and an example of the numerical integration for slightly different values of  $\tilde{E}(0)$  is presented in Fig. 8. The results determine  $\tilde{E}(0)$  correctly to three decimal places. The graph also shows that  $\tilde{s}$  experiences the same rapid increase near  $\xi = 0$  as does  $\tilde{n}_1$ .

The numerical integration of Eqs. (6.43) and (6.44) is complicated somewhat because the right-hand side of (6.44) involves the large constant  $\tau_0$  and results in the system's possessing a large Lipschitz constant. Such systems are commonly called "stiff" and cause stability problems with the use of explicit numerical integration algorithms unless very small step sizes are employed\*. The trapezoidal rule does not suffer from such instability and is chosen as the method of integration. For the system of differential equations

$$\frac{dy}{dx} = \underline{f}(x, \underline{y}) \quad (6.47)$$

the algorithm is

$$\underline{y}^{(n+1)} = \underline{y}^{(n)} + \frac{h}{2} [f(x^{(n+1)}, \underline{y}^{(n+1)}) + f(x^{(n)}, \underline{y}^{(n)})] \quad (6.48)$$

Applying this scheme to Eqs. (6.42) - (6.44),

$$\tilde{n}_e^{(n+1)} = \tilde{n}_e^{(n)} + \frac{h}{2} \{ \tilde{n}_e^{(n+1)} \tilde{E}^{(n+1)} + \tilde{n}_e^{(n)} \tilde{E}^{(n)} + 2\delta_0 \tau_0 \tilde{J}(0) \} \quad (6.49)$$

$$\begin{aligned} \tilde{s}^{(n+1)} = \tilde{s}^{(n)} + \frac{h}{2} \{ & - [(1 + \tau_0) \tilde{n}_e^{(n+1)} + \tau_0 \tilde{s}^{(n+1)}] \tilde{E}^{(n+1)} \\ & - [(1 + \tau_0) \tilde{n}_e^{(n)} + \tau_0 \tilde{s}^{(n)}] \tilde{E}^{(n)} + 2\tau_0 (1 - \delta_0) \tilde{J}(0) \} \end{aligned} \quad (6.50)$$

$$\begin{aligned} \tilde{E}^{(n+1)} = \{ \tilde{E}^2(0) + \frac{2\chi_0}{\tau_0} [ & (1 + \tau_0) \tilde{n}_e^{(n+1)} + \tilde{s}^{(n+1)} ] - 2\chi_0 (1 + \delta_0 \tau_0) \tilde{J}(0) \\ & \times \xi^{(n+1)} \}^{1/2} \end{aligned} \quad (6.51)$$

---

\* For a discussion of the problem see, for instance, Seinfeld, Lapidus, and Hwang [10].



Equation (6.57) is solved by obtaining a sequence  $\{\underline{u}_i\}$  which converges to the solution  $\underline{u}$ .  $\underline{g}(\underline{u}_{i+1})$  can be expressed as the Taylor series

$$\underline{g}(\underline{u}_{i+1}) = \underline{g}(\underline{u}_i) + J(\underline{u}_i)(\underline{u}_{i+1} - \underline{u}_i) + \dots \quad (6.59)$$

where  $J(\underline{u}_i)$  is the Jacobian matrix

$$J(\underline{u}_i) \equiv \frac{\partial \underline{g}}{\partial \underline{u}}(\underline{u}_i) \quad (6.60)$$

Newton's method determines  $\underline{u}_{i+1}$  from  $\underline{u}_i$  by equating the truncated series to zero:

$$\underline{g}(\underline{u}_i) + J(\underline{u}_i)(\underline{u}_{i+1} - \underline{u}_i) = 0 \quad (6.61)$$

or

$$J(\underline{u}_i)(\underline{u}_{i+1} - \underline{u}_i) = -\underline{g}(\underline{u}_i) \quad (6.62)$$

for  $i=0,1,2,\dots$ . (6.62) is solved as a linear equation in  $\underline{u}_{i+1} - \underline{u}_i$ .  $\underline{v}_e^{(n+1)}$ ,  $\underline{v}_s^{(n+1)}$ , and  $\underline{v}_E^{(n+1)}$  are thus determined by solving a sequence of linear algebraic systems. However, the convergence is rapid and only a few iterations are necessary. For our equations the Jacobian matrix is

$$J(\underline{u}) \equiv \begin{pmatrix} -1 + \frac{h}{2} w & 0 & \frac{h}{2} u \\ -\frac{h}{2}(1 + \tau_o)w & -1 - \frac{h}{2} \tau_o w & -\frac{h}{2}(1 + \tau_o)u - \frac{h}{2} \tau_o v \\ \frac{\chi_o(1 + \tau_o)}{\tau_o \varepsilon(\underline{u})} & \frac{\chi_o}{\tau_o \varepsilon(\underline{u})} & -1 \end{pmatrix} \quad (6.63)$$

where

$$\varepsilon(\underline{u}) \equiv \left\{ \tilde{E}^2(0) + \frac{2\chi_0}{\tau_0} [(1+\tau_0)u + v] - 2\chi_0(1+\delta_0\tau_0)\tilde{J}(0)\xi^{(n+1)} \right\}^{1/2} . \quad (6.64)$$

The first approximation  $\underline{u}_0$  used to start the iteration is obtained by applying Euler's method to Eq. (6.47):

$$\underline{u}_0 = \underline{y}^{(n)} + hf(x, \underline{y}^{(n)}) \quad (6.65)$$

or, more explicitly,

$$u_0 = \tilde{n}_e^{(n)} + h\{\tilde{n}_e^{(n)} \tilde{E}^{(n)} + \delta_0\tau_0 \tilde{J}(0)\} \quad (6.66)$$

$$v_0 = \tilde{s}^{(n)} + h\{-(1+\tau_0)\tilde{n}_e^{(n)} + \tau_0\tilde{s}^{(n)}\}\tilde{E}^{(n)} + \tau_0(1-\delta_0)\tilde{J}(0)\} \quad (6.67)$$

$$w_0 = \left\{ \tilde{E}^2(0) + \frac{2\chi_0}{\tau_0} [(1+\tau_0)u_0 + v_0] - 2\chi_0(1+\delta_0\tau_0)\tilde{J}(0)\xi^{(n+1)} \right\}^{1/2} . \quad (6.68)$$

The approximate solution  $\tilde{E}_0(0)$  provides a good estimate to the correct value  $\tilde{E}(0)$ . Accuracy to three decimal places is quickly achieved by trial and error. Although  $\tilde{J}(0)$  is unknown at this stage, it is determined by matching independently of the value of  $\tilde{E}(0)$ . Thus in the numerical work we use the expression for  $\tilde{J}(0)$  given by Eq. (7.5):

$$\tilde{J}(0) = \frac{\pi}{2} \frac{1}{\rho_0} + \frac{4}{3\pi^2} \left(2 - \frac{\pi}{2}\right) \varepsilon_0 \zeta . \quad (6.69)$$

Since  $\zeta$  enters the equations through  $\tilde{J}(0)$  and the coefficients  $\tau_0$ ,  $\delta_0$ ,  $\chi_0$ , and  $\varepsilon_0$ ,  $\tilde{E}(0)$  depends on  $\zeta$ . The numerical integration is performed for a number of values of  $\zeta$ , and the results are tabulated in Table 6.

## 7. MATCHING MAIN-REGION AND SHEATH SOLUTIONS

Several terms of the main-region and sheath solutions are now available. However, certain quantities remain unknown, and they must be determined by matching the two solutions in an intermediate region. The items of primary interest are  $\mu_1(\zeta)$  and  $\gamma_1$ . Until they are known, corrections to the lowest-order results in the main region and to the relation between ionization coefficient and electron density are undetermined.  $\tilde{J}(0)$  and  $\tilde{E}(0)$  are found by matching to lowest order.  $\tilde{J}(0)$  is obtained directly and easily. Although  $\tilde{E}(0)$  has been obtained by a numerical integration of the sheath equations, its evaluation is indirectly due to zero-order matching; it is the initial value of  $\tilde{E}$  necessary to produce the only asymptotic behavior capable of matching with the main-region solution. Many terms do not contain unspecified parameters, and these must match identically. The technique and philosophy of matching is the same as that considered in Section 5 in comparing the approximate sheath solution with the main-region solution.

### Matching $J$ and $\tilde{J}$

Before the solution in the main region can be matched with that in the sheath, it must be expanded for  $y$  near 1. Using the formulas of Appendix D in Eq. (3.55) for  $J_o$ ,

$$J_o = \frac{\pi}{2} \frac{1}{\rho_o} \left(1 - \frac{\pi^2}{8} (1-y)^2\right) + \frac{4}{3\pi^2} \left[ \left(2 - \frac{\pi}{2}\right) \left(1 - \frac{\pi^2}{8} (1-y)^2\right) + \pi \left(-\frac{\pi}{2} (1-y)^2\right) \right] \epsilon_o \zeta + 0(1-y)^3 \quad (7.1)$$

$$\begin{aligned}
 &= \frac{\pi}{2} \frac{1}{\rho_o} + \frac{4}{3\pi^2} \left(2 - \frac{\pi}{2}\right) \epsilon_o \zeta \\
 &- \left[ \frac{\pi^3}{16} \frac{1}{\rho_o} + \left(1 - \frac{\pi}{12}\right) \epsilon_o \zeta \right] (1 - y)^2 + O((1 - y)^3) \quad . \quad (7.2)
 \end{aligned}$$

The order of magnitude of the contribution to  $J$  from  $J_1$  can be determined by observing Eq. (4.18) and the limiting behavior of  $n_{e1}$  as  $y \rightarrow 1$ . We conclude that

$$\text{ord}(J_1) = 1 \quad (7.3)$$

in  $(1 - y)$  as  $y \rightarrow 1$ . Although this term is not calculated, there is no need to show that its contribution to  $J$  is smaller in order of magnitude than that of the term containing  $(1 - y)^2$ . Each term is to be matched individually to a term in the sheath solution, and except for the numerical calculations, in which only the largest term is used, there is no need to insist that the terms presented be those of the greatest orders of magnitude. We can now write the main-region expression for  $J$  in a form suitable for matching in the intermediate region. In the expressions the terms omitted are represented by order-of-magnitude estimates. Since  $1 - y$  is of order  $O(\eta)$  in the intermediate region and since the main-region solution for  $J$  is known only to order  $O(\epsilon_o \zeta)$  in  $\epsilon_o \zeta$ , we write  $J$  as

$$\begin{aligned}
 J = & \frac{\pi}{2} \frac{1}{\rho_o} + \frac{4}{3\pi^2} \left(2 - \frac{\pi}{2}\right) \epsilon_o \zeta - \left[ \frac{\pi^3}{16} \frac{1}{\rho_o} + \left(1 - \frac{\pi}{12}\right) \epsilon_o \zeta \right] (1 - y)^2 \\
 & + O((\epsilon_o \zeta)^2, \mu_1(\zeta), \eta^3(\zeta)) \quad . \quad (7.4)
 \end{aligned}$$

The two dominant terms of  $\tilde{J}$  are given by Eq. (6.24). From Eq. (2.49), which relates  $J$  and  $\tilde{J}$ , it is apparent that  $\tilde{J}(0)$  must be given as follows if the lowest-order terms of  $J$  and  $\tilde{J}$  are to match:

$$\tilde{J}(0) = \frac{\pi}{2} \frac{1}{\rho_o} + \frac{4}{3\pi^2} \left(2 - \frac{\pi}{2}\right) \epsilon_o \zeta \quad . \quad (7.5)$$

If the term from  $J_1$  that is of order  $\mu_1(\zeta)$  were calculated for the main-region solution, it would also appear on the right-hand side of (7.5).  $\gamma_o$ , which appears in the second term on the right-hand side of (6.24), is expanded as in Eq. (3.52):

$$\gamma_o = \frac{\pi^2}{4} \frac{1}{\rho_o} + \frac{8}{3\pi} \epsilon_o \zeta + O((\epsilon_o \zeta)^2) \quad . \quad (7.6)$$

Using (7.5) and (7.6) in (6.24),  $\tilde{J}$  becomes

$$\begin{aligned} \tilde{J} &\sim \frac{\pi}{2} \frac{1}{\rho_o} + \frac{4}{3\pi^2} \left(2 - \frac{\pi}{2}\right) \epsilon_o \zeta \\ &- \frac{\rho_o}{2\zeta^{2/3}} \left(\frac{\pi^2}{4} \frac{1}{\rho_o} + \frac{8}{3\pi} \epsilon_o \zeta\right) \left(\frac{\pi}{2} \frac{1}{\rho_o} + \frac{4}{3\pi^2} \left(2 - \frac{\pi}{2}\right) \epsilon_o \zeta\right) \xi^2 \end{aligned} \quad (7.7)$$

$$\begin{aligned} &\sim \frac{\pi}{2} \frac{1}{\rho_o} + \frac{4}{3\pi^2} \left(2 - \frac{\pi}{2}\right) \epsilon_o \zeta \\ &- \frac{1}{\zeta^{2/3}} \left[\frac{\pi^3}{16} \frac{1}{\rho_o} + \left(1 - \frac{\pi}{12}\right) \epsilon_o \zeta\right] \xi^2, \end{aligned} \quad (7.8)$$

where terms of order  $O((\epsilon_o \zeta)^2)$  are neglected.

The expressions for  $J$  and  $\tilde{J}$  are written as functions of the intermediate variable  $x_\eta$  through the use of (5.42) and (5.43). From

(7.4),

$$\begin{aligned}
 \text{(main region):} \quad J &\sim \frac{\pi}{2} \frac{1}{\rho_o} + \frac{4}{3\pi^2} (2 - \frac{\pi}{2}) \epsilon_o \zeta \\
 &- \left[ \frac{\pi^3}{16} \frac{1}{\rho_o} + (1 - \frac{\pi}{12}) \epsilon_o \zeta \right] \eta^2 x_\eta^2 \quad . \quad (7.9)
 \end{aligned}$$

From (2.49) and (7.8),

$$\begin{aligned}
 \text{(sheath):} \quad J &\sim \frac{\pi}{2} \frac{1}{\rho_o} + \frac{4}{3\pi^2} (2 - \frac{\pi}{2}) \epsilon_o \zeta \\
 &- \left[ \frac{\pi^3}{16} \frac{1}{\rho_o} + (1 - \frac{\pi}{12}) \epsilon_o \zeta \right] \eta^2 x_\eta^2 \quad . \quad (7.10)
 \end{aligned}$$

It is apparent that the main-region and sheath solutions for  $J$  match identically to the orders considered.

Matching  $n_e$  and  $\tilde{n}_e$  : Determination of  $\mu_1$  and  $\gamma_1$

In order to obtain the desired results, it is necessary to consider contributions to  $n_e$  from both  $n_{e0}$  and  $n_{e1}$ .  $n_{e0}$  is given by Eq. (3.53), and it is expanded below for  $y$  near 1 using formulas of Appendix D.

$$\begin{aligned}
 n_{e0} &= \frac{\pi}{2} (1 - y) - \frac{\pi^3}{48} (1 - y)^3 + \frac{4}{3\pi^2} \left[ 2 - \frac{\pi}{2} (1 - y) \right. \\
 &\quad \left. + \frac{\pi^3}{48} (1 - y)^3 - \frac{\pi^2}{4} (1 - y)^2 - 2 + 2(1 - y) + \frac{\pi^2}{4} (1 - y)^2 \right. \\
 &\quad \left. - \frac{\pi^2}{4} (1 - y)^3 \right] \rho_o \epsilon_o \zeta + O((1 - y)^4) \quad (7.11)
 \end{aligned}$$

$$\begin{aligned}
 &= \left[ \frac{\pi}{2} + \frac{4}{3\pi^2} (2 - \frac{\pi}{2}) \rho_o \epsilon_o \zeta \right] (1 - y) \\
 &- \left[ \frac{\pi^3}{48} + (\frac{1}{3} - \frac{\pi}{36}) \rho_o \epsilon_o \zeta \right] (1 - y)^3 + O((1 - y)^4) \quad (7.12)
 \end{aligned}$$

Only the largest contribution to  $n_{e1}$  need be calculated. From (4.44)

$$n_{e1} \sim \bar{n}_0 + \epsilon^* \bar{n}_1 \quad (7.13)$$

where  $\bar{n}_0$  and  $\bar{n}_1$  are given by (4.38) and (4.43), respectively.

Expanding  $\bar{n}_0$  with the use of (D.5),

$$\bar{n}_0 = -\frac{1}{\pi} (\gamma_1 \rho_0 + q) + 0(1 - y) \quad (7.14)$$

The smallest terms in  $\bar{n}_1$  for  $y$  near 1 are

$$\begin{aligned} \bar{n}_1 = & - \left( \frac{32}{3\pi^4} \gamma_1 \rho_0 - \frac{8}{3\pi^2} \frac{\epsilon_1}{\epsilon_0} \right) \\ & + \left[ \frac{4}{3\pi^3} \left( \frac{4}{\pi} + 1 \right) \gamma_1 \rho_0 - \frac{4}{3\pi^3} \left( \frac{4}{\pi} - 1 \right) q \right] + 0(1 - y) \end{aligned} \quad (7.15)$$

$$= -\frac{4}{3\pi^3} \left( \frac{4}{\pi} - 1 \right) (\gamma_1 \rho_0 + q) + \frac{8}{3\pi^2} \frac{\epsilon_1}{\epsilon_0} + 0(1 - y) \quad (7.16)$$

Using (7.14), (7.16), (4.26), and (4.35), (7.13) becomes

$$\begin{aligned} n_{e1} = & -\frac{1}{\pi} \left[ 1 + \frac{4}{3\pi^2} \left( \frac{4}{\pi} - 1 \right) \epsilon_0 \zeta \rho_0 \right] \cdot \left[ \gamma_1 \rho_0 \right. \\ & + \frac{\pi^2}{4} \left( \frac{\delta_0 \tau_1 + \delta_1 \tau_0}{1 + \delta_0 \tau_0} + \frac{\tau_1}{\tau_0} \frac{1}{1 + \tau_0} \right) \left. \right] + \frac{8}{3\pi^2} \epsilon_1 \zeta \rho_0 \\ & + \alpha(1 - y), (\epsilon_0 \zeta)^2 \quad (7.17) \end{aligned}$$

$\text{ord}(1 - y) = \text{ord}(\eta(\zeta))$  in the intermediate zone between the main region and the sheath, so when  $n_{e0}$  and  $n_{e1}$  are added as in (2.2), we obtain

$$n_e = \left[ \frac{\pi}{2} + \frac{4}{3\pi^2} \left( 2 - \frac{\pi}{2} \right) \rho_0 \epsilon_0 \zeta \right] (1 - y)$$

$$\begin{aligned}
 & - \left[ \frac{\pi^3}{48} + \left( \frac{1}{3} - \frac{\pi}{36} \right) \rho_o \epsilon_o \zeta \right] (1 - y)^3 \\
 & - \mu_1(\zeta) \left\{ \frac{1}{\pi} \left[ 1 + \frac{4}{3\pi^2} \left( \frac{4}{\pi} - 1 \right) \rho_o \epsilon_o \zeta \right] \cdot [\gamma_1 \rho_o \right. \\
 & \left. + \frac{\pi^2}{4} \left( \frac{\delta_o \tau_1 + \delta_1 \tau_o}{1 + \delta_o \tau_o} + \frac{\tau_1}{\tau_o} \frac{1}{1 + \tau_o} \right) \right] - \frac{8}{3\pi^2} \rho_o \epsilon_1 \zeta \right\} \\
 & + 0(\eta^4, \mu_1(\zeta)\eta, (\epsilon_o \zeta)^2) \quad . \quad (7.18)
 \end{aligned}$$

The asymptotic form of the sheath solution for  $\tilde{n}_e$  is given by Eq. (6.29). If Eqs. (7.5) and (7.6) for  $\tilde{J}(0)$  and  $\gamma_o$  are used in (6.29), we obtain

$$\begin{aligned}
 \tilde{n}_e & \sim \left[ \frac{\pi}{2} + \frac{4}{3\pi^2} \left( 2 - \frac{\pi}{2} \right) \rho_o \epsilon_o \zeta \right] \xi \\
 & - \frac{\rho_o^2}{6\zeta^{2/3}} \left( \frac{\pi^2}{4} \frac{1}{\rho_o} + \frac{8}{3\pi} \epsilon_o \zeta \right) \left( \frac{\pi}{2} \frac{1}{\rho_o} + \frac{4}{3\pi^2} \left( 2 - \frac{\pi}{2} \right) \epsilon_o \zeta \right) \xi^3 \\
 & - \frac{1}{2\chi_o} \frac{\tau_o E^2(0)}{1 + \tau_o} \quad (7.19)
 \end{aligned}$$

$$\begin{aligned}
 & \sim \left[ \frac{\pi}{2} + \frac{4}{3\pi^2} \left( 2 - \frac{\pi}{2} \right) \rho_o \epsilon_o \zeta \right] \xi \\
 & - \frac{1}{\zeta^{2/3}} \left[ \frac{\pi^3}{48} + \left( \frac{1}{3} - \frac{\pi}{36} \right) \rho_o \epsilon_o \zeta \right] \xi^3 - \frac{1}{2\chi_o} \frac{\tau_o E^2(0)}{1 + \tau_o} \quad (7.20)
 \end{aligned}$$

where terms of order  $0((\epsilon_o \zeta)^2)$  are neglected.

The main-region and sheath solutions for  $n_e$  and  $\tilde{n}_e$  are now written as functions of  $x_\eta$ . (7.18) becomes

$$\begin{aligned}
 \text{(main region):} \quad n_e \sim & \left[ \frac{\pi}{2} + \frac{4}{3\pi^2} \left( 2 - \frac{\pi}{2} \right) \rho_o \epsilon_o \zeta \right] \eta x_\eta \\
 & - \left[ \frac{\pi^3}{48} + \left( \frac{1}{3} - \frac{\pi}{36} \right) \rho_o \epsilon_o \zeta \right] \eta^3 x_\eta^3 \\
 & - \mu_1(\zeta) \left\{ \frac{1}{\pi} \left[ 1 + \frac{4}{3\pi^2} \left( \frac{4}{\pi} - 1 \right) \rho_o \epsilon_o \zeta \right] \cdot [\gamma_1 \rho_o \right. \\
 & \left. + \frac{\pi^2}{4} \left( \frac{\delta_o \tau_1 + \delta_1 \tau_o}{1 + \delta_o \tau_o} + \frac{\tau_1}{\tau_o} \frac{1}{1 + \tau_o} \right) \right] - \frac{8}{3\pi^2} \rho_o \epsilon_1 \zeta \right\} . \quad (7.21)
 \end{aligned}$$

From (2.47), (5.43), and (7.20),

$$\begin{aligned}
 \text{(sheath):} \quad n_e \sim & \left[ \frac{\pi}{2} + \frac{4}{3\pi^2} \left( 2 - \frac{\pi}{2} \right) \rho_o \epsilon_o \zeta \right] \eta x_\eta \\
 & - \left[ \frac{\pi^3}{48} + \left( \frac{1}{3} - \frac{\pi}{36} \right) \rho_o \epsilon_o \zeta \right] \eta^3 x_\eta^3 \\
 & - \frac{1}{\zeta^{1/3}} \frac{1}{2\chi_o} \frac{\tau_o \overset{\sim}{E}^2(0)}{1 + \tau_o} . \quad (7.22)
 \end{aligned}$$

The first two terms of the main-region and sheath solutions are identical in the intermediate zone, and the third terms also match provided we choose

$$\mu_1(\zeta) = \frac{1}{\zeta^{1/3}} \quad (7.23)$$

and

$$\begin{aligned}
 & \left[ 1 + \frac{4}{3\pi^2} \left( \frac{4}{\pi} - 1 \right) \rho_o \epsilon_o \zeta \right] [\gamma_1 \rho_o + \frac{\pi^2}{4} \left( \frac{\delta_o \tau_1 + \delta_1 \tau_o}{1 + \delta_o \tau_o} + \frac{\tau_1}{\tau_o} \frac{1}{1 + \tau_o} \right)] \\
 & - \frac{8}{3\pi} \rho_o \epsilon_1 \zeta = \frac{\pi}{2\chi_o} \frac{\tau_o}{1 + \tau_o} \overset{\sim}{E}^2(0) . \quad (7.24)
 \end{aligned}$$

These two equations are among the most important results of the entire perturbation procedure.  $\mu_1(\zeta)$  is at last known, and the orders of magnitude of terms containing it are now known explicitly as functions of  $\zeta$ . In particular, the inequality (6.27) is established and Eq. (4.16) for  $s_1$  is verified.  $\gamma_1$  is determined by Eq. (7.24) and its solution is considered in detail later. Now that  $\mu_1(\zeta)$  and  $\gamma_1$  are available, the solution to the problem is essentially known to order  $O(1/\zeta^{1/3})$ . The matching is completed by showing that the main-region and sheath solutions for  $E$  and  $s$  agree in the intermediate zone.

Matching  $E$  and  $\tilde{E}$

Only the contribution to  $E$  from  $E_0$  in the main region is considered. It is given by Eq. (4.52), and Eqs. (D.8), (D.2), (D.9), and (D.11) of Appendix D are used in expanding the expression for  $y$  near 1 :

$$E_0 = \frac{1 - \delta_0}{1 + \delta_0 \tau_0} \left\{ \frac{1}{x} - \frac{\pi^2}{12} x + \frac{4}{3\pi^2} \left[ \frac{4}{\pi} \frac{1}{x} - \frac{\pi}{3} x - \frac{\pi}{2} - \frac{4}{\pi} \frac{1}{x^2} + \frac{\pi}{6} + \frac{4}{\pi} \frac{1}{x^2} - \frac{4}{\pi} \frac{1}{x} + \frac{\pi}{3} - \frac{\pi}{3} x \right] \epsilon^* \right\} + O(x^2) \quad (7.25)$$

Substituting for  $\epsilon^*$  from Eq. (4.26), for  $x$  from (D.1), and rearranging,

$$E_0 = \frac{1 - \delta_0}{1 + \delta_0 \tau_0} \frac{1}{1 - y} - \frac{1 - \delta_0}{1 + \delta_0 \tau_0} \left[ \frac{\pi^2}{12} + \frac{8}{9\pi} \rho_0 \epsilon_0 \zeta \right] (1 - y) + O(\eta^2) \quad (7.26)$$

Equation (4.19) for  $E_1$  is considered in order to obtain an estimate of its magnitude. The term involving  $n_{e1} E_0$  becomes dominant as

$y \rightarrow 1$ , so the solution of (4.19) for  $E_1$  would involve a term of order  $O((1-y)^{-2})$ . Thus the term neglected has order  $\text{ord}(\mu_1 E_1) = 1/(\zeta^{1/3} \eta^2)$ , and  $E$  is written as

$$E = E_o + O(\eta^2, \frac{1}{\zeta^{1/3} \eta^2}, (\epsilon_o \zeta)^2) \quad (7.27)$$

where  $E_o$  is given by (7.26).

The asymptotic solution for  $\tilde{E}$  in the sheath is given by Eq. (6.37). Substituting for  $\gamma_o$  from (7.6) and using Eq. (2.19) for  $\rho_o$ ,  $\tilde{E}$  becomes

$$\begin{aligned} \tilde{E} \sim & \frac{1 - \delta_o}{1 + \delta_o \tau_o} \frac{1}{\xi} - \frac{1}{\zeta^{2/3}} \frac{1 - \delta_o}{1 + \delta_o \tau_o} \left[ \frac{\pi^2}{12} + \frac{8}{9\pi} \rho_o \epsilon_o \zeta \right] \xi \\ & + \frac{1 - \delta_o}{2\chi_o (1 + \delta_o \tau_o)^2} \frac{\tilde{E}^2(0)}{\tilde{J}(0)} \frac{1}{\xi^2} . \end{aligned} \quad (7.28)$$

The main-region and sheath solutions are expressed in terms of the common intermediate variable  $x_\eta$  through the use of (5.42) and (5.43). (7.26) and (7.27) become

$$\begin{aligned} \text{(main region): } E \sim & \frac{1 - \delta_o}{1 + \delta_o \tau_o} \frac{1}{\eta} \frac{1}{x_\eta} - \frac{1 - \delta_o}{1 + \delta_o \tau_o} \left[ \frac{\pi^2}{12} + \frac{8}{9\pi} \rho_o \epsilon_o \zeta \right] \\ & + O\left(\frac{1}{\zeta^{1/3} \eta^2}\right) . \end{aligned} \quad (7.29)$$

Using (2.50), (7.28) becomes

$$\begin{aligned} \text{(sheath): } E \sim & \frac{1 - \delta_o}{1 + \delta_o \tau_o} \frac{1}{\eta} \frac{1}{x_\eta} - \frac{1 - \delta_o}{1 + \delta_o \tau_o} \left[ \frac{\pi^2}{12} + \frac{8}{9\pi} \rho_o \epsilon_o \zeta \right] \eta x_\eta \\ & + \frac{1 - \delta_o}{2\chi_o (1 + \delta_o \tau_o)^2} \frac{\tilde{E}^2(0)}{\tilde{J}(0)} \frac{1}{\zeta^{1/3} \eta^2} \frac{1}{x_\eta^2} . \end{aligned} \quad (7.30)$$

A comparison of (7.29) and (7.30) reveals that the first two terms of the main-region and sheath solutions match identically and that the third term of the sheath solution is of the same order as the neglected contribution from  $E_1$  to the main region. The second and third terms of the sheath solution for  $E$  originate in the expression for  $\tilde{n}_e$  of Eq. (6.29). The discussion following that equation emphasizes that a comparison of the magnitudes of those two terms need not be made. A more complete representation of the main-region solution in the intermediate region requires that the neglected term be calculated. Since it must match identically with the corresponding term of the sheath solution, no new information would be acquired, and the computation is not carried out here.

Matching  $s$  and  $\tilde{s}$

The main-region solution for  $s$  is obtained from Eqs. (4.54) and (4.58). The formulas of Appendix D are used to expand it for  $y$  near 1. Only the largest terms are retained.

$$s_n = \frac{1}{\chi_o} \frac{1 - \delta_o}{1 + \delta_o \tau_o} \left\{ \frac{1}{x^2} + \frac{4}{3\pi^2} \left[ \left( \frac{8}{\pi} \frac{1}{x^3} - \frac{8}{\pi} \frac{1}{x^2} \right) + \left( -\frac{8}{\pi} \frac{1}{x^3} + \frac{\pi}{x} \right) + \frac{8}{\pi} \frac{1}{x^2} - \frac{\pi}{x} \right] \epsilon_o \zeta \rho_o \right\} + 0(1) \quad (7.31)$$

so

$$s = \frac{1}{\zeta} \frac{1}{\chi_o} \frac{1 - \delta_o}{1 + \delta_o \tau_o} \frac{1}{(1-y)^2} + 0\left(\frac{1}{\zeta}, (\epsilon_o \zeta)^2\right) \quad (7.32)$$

The asymptotic sheath solution is given by Eq. (6.40) and is rewritten below:

$$s \sim \frac{1}{\chi_0} \frac{1 - \delta_0}{1 + \delta_0} \frac{1}{\tau_0} \frac{1}{\xi^2} \quad (7.33)$$

Expressing main-region and sheath solutions in terms of the intermediate variable  $x_\eta$

$$\text{(main region):} \quad s \sim \frac{1}{\chi_0} \frac{1 - \delta_0}{1 + \delta_0} \frac{1}{\tau_0} \frac{1}{\zeta \eta^2} \frac{1}{x_\eta^2} \quad (7.34)$$

and

$$\text{(sheath):} \quad s \sim \frac{1}{\chi_0} \frac{1 - \delta_0}{1 + \delta_0} \frac{1}{\tau_0} \frac{1}{\zeta \eta^2} \frac{1}{x_\eta^2} \quad (7.35)$$

Equations (6.38), (2.47), and (2.48) are used in obtaining (7.35). The two expressions are identical, and hence all the dependent variables match in the intermediate zone between the main region and the sheath.

#### Numerical Calculation of $\gamma_1$

Equation (7.24) for  $\gamma_1$  is quite complicated and must be solved numerically by an iterative procedure.  $\epsilon_1$ ,  $\tau_1$ , and  $\delta_1$  are all functions of  $\gamma_1$  as illustrated by Eq. (2.14):

$$\epsilon_1 = \zeta^{1/3} \left[ \epsilon(\gamma_0 + \frac{\gamma_1}{\zeta^{1/3}}) - \epsilon(\gamma_0) \right] \quad (7.36)$$

etc. However,  $\epsilon$ ,  $\tau$ , and  $\delta$  are rather slowly varying functions of  $\gamma$ , and an iterative scheme is easily established in which  $\epsilon_1$ ,  $\tau_1$ , and  $\delta_1$  are evaluated using the previous estimate for  $\gamma_1$ . The method is explained sufficiently by the equations below.

First Eq. (7.24) is rewritten in slightly different form using Eq. (2.19) for  $\rho_0$ :

$$\gamma_1 = \frac{\frac{\pi E^2(0)}{2\chi_o(1 + \delta_o \tau_o)} + \frac{8}{3\pi} \epsilon_1 \zeta}{1 + \frac{4}{3\pi^2} \left(\frac{4}{\pi} - 1\right) \rho_o \epsilon_o \zeta} - \frac{\pi^2}{4(1 + \delta_o \tau_o)} \left( \frac{\delta_o \tau_1 + \delta_1 \tau_o}{\rho_o} + \frac{\tau_1}{\tau_o^2} \right) . \quad (7.37)$$

The successive approximations to  $\gamma_1$  are designated  $\gamma_1^{(0)}, \gamma_1^{(1)}, \gamma_1^{(2)}, \dots$  and the notation adopted for the corresponding values of the other parameters is

$$\epsilon_1^{(n)} = \zeta^{1/3} \left[ \epsilon(\gamma_o + \frac{\gamma_1^{(n)}}{\zeta^{1/3}}) - \epsilon(\gamma_o) \right] \quad (7.38)$$

$$\tau_1^{(n)} = \zeta^{1/3} \left[ \tau(\gamma_o + \frac{\gamma_1^{(n)}}{\zeta^{1/3}}) - \tau(\gamma_o) \right] \quad (7.39)$$

$$\delta_1^{(n)} = \zeta^{1/3} \left[ \delta(\gamma_o + \frac{\gamma_1^{(n)}}{\zeta^{1/3}}) - \delta(\gamma_o) \right] . \quad (7.40)$$

The iteration scheme is now written as

$$\gamma_1^{(n+1)} = \frac{\frac{\pi E^2(0)}{2\chi_o(1 + \delta_o \tau_o)} + \frac{8}{3\pi} \epsilon_1^{(n)} \zeta}{1 + \frac{4}{3\pi^2} \left(\frac{4}{\pi} - 1\right) \rho_o \epsilon_o \zeta} - \frac{\pi^2}{4(1 + \delta_o \tau_o)} \left( \frac{\delta_o \tau_1^{(n)} + \delta_1^{(n)} \tau_o}{\rho_o} + \frac{\tau_1^{(n)}}{\tau_o^2} \right) . \quad (7.41)$$

An initial estimate  $\gamma_1^{(0)} = 0$  is chosen to start the iteration.

In order to continue the expansion of variables and coefficients in the two asymptotic series,  $\gamma_1$  would have to be obtained as a sum of terms of order  $O(1)$  and  $O(\varepsilon_0 \zeta)$  in  $\varepsilon_0 \zeta$ . However,  $\tilde{E}(0)$  is obtained by a numerical integration and depends rather intimately on  $\varepsilon_0 \zeta$ , so such a division is not really feasible. Since the work is numerical at this stage, there is no purpose in separating terms of various orders in  $\varepsilon_0 \zeta$ . However, in a theoretical sense the solution can still be regarded as a combination of two asymptotic expansions--one for  $\zeta$  large and the other for  $\varepsilon_0 \zeta$  small.

Numerical results for  $\gamma_1$  and  $\gamma = \gamma_0 + \frac{1}{\zeta^{1/3}} \gamma_1$  are presented in Table 7 for a number of different values for  $\zeta$ .  $\gamma$  is plotted as a function of  $\zeta$  in Fig. 9.

## 8. SUMMARY

The preceding results are obtained by a sequence of rather distinct operations. In order to unify the concepts and techniques involved, a recapitulation of the objectives and the procedures is presented below.

### Objectives and Techniques

The primary purpose of the work is to obtain approximations to  $J$ ,  $n_e$ ,  $n_i$  (or  $s$ ),  $E$ , and, most importantly, to the relation between  $N_{eo}$  and  $\hat{E}_z$ . In the analytical procedures the  $N_{eo} - \hat{E}_z$  relation is replaced by the  $\zeta - \gamma$  relation; it is obtained from the  $\zeta - \gamma$  relation when the calculations are complete. The results are attained by a combination of two asymptotic expansions, one in which  $\zeta$  is a large parameter and the other in which  $\epsilon_0 \zeta$  is small. The lowest-order component of the composite expansion corresponds to the classical ambipolar situation. The relative importance of the deviations from this behavior caused by the two expansions depends on whether  $\zeta$  is "large" or "small". For large  $\zeta$  recombination is more important and the correction to ambipolar behavior comes principally from the expansion in  $\epsilon_0 \zeta$ . For small  $\zeta$ , on the other hand, space-charge effects become important, and contributions from the expansion for small  $\zeta$  dominate. The ambipolar situation is most closely approached at some intermediate  $\zeta$ . The expansion for large  $\zeta$  is the more complicated, because the assumption upon which it depends breaks down near the wall of the discharge, and a separate boundary-layer treatment must be undertaken.

Distinct solutions must be obtained in the boundary layer or sheath and in the main region, and it is not until these solutions are matched that the second term of the expansions is completely determined anywhere. The expansion in  $\epsilon_0 \zeta$  enters as the technique by which the equations are solved in the main region, and it is introduced into the sheath solution through the expansion of the coefficients in the equations and through the matching process. Expressions for the variables in the sheath can only be obtained in the asymptotic limit of large  $\xi$ . However,  $\tilde{E}(0)$  is involved in the matching, and it is calculated by solving the lowest-order sheath equations numerically.  $\gamma_1$ , and hence the entire first-order correction to the solution in the main region, is then obtained from the matching, using this estimate of  $\tilde{E}(0)$ . The algebraic equation for  $\gamma_1$  must also be solved numerically.

### Results

The solutions for  $J$ ,  $n_e$ ,  $n_i$ , and  $E$  are now known to several terms. However, the behavior of these variables is well approximated by the zero-order solution and further refinements are not really essential. On the other hand,  $\gamma$  as a function of  $\zeta$  is a constant to lowest order, and corrections are critical. The calculated  $\zeta - \gamma$  relation is presented in Fig. 9. The vertical line represents the ambipolar value of  $\gamma$ , and the two dashed curves show the deviations from the ambipolar value caused by the expansions in  $\epsilon_0 \zeta$  and  $1/\zeta^{1/3}$ . The solid curve includes both corrections and shows the final numerical results of the  $\zeta - \gamma$  relation.

The value of  $\hat{E}_z$  can be determined from that of  $\gamma$ , and  $N_{eo}$  is obtained trivially from  $\zeta$ , so the numerical values of the  $N_{eo} - \hat{E}_z$  relation are available. The values are tabulated, along with the corresponding values of  $\hat{E}_z/N_n$ , in Table 8, and the  $N_{eo} - \hat{E}_z$  curve is graphed in Fig. 10.

### Interpretation of Results

It is one of the basic objectives of this work to relate the  $N_{eo} - \hat{E}_z$  relation to the experimental voltage-current characteristic. This correspondence is discussed in the Introduction, and little more need be said except to reemphasize the caution that should be exercised in interpreting the similarities in the two curves. The subnormal regime of the discharge characteristic seems to be definitely related to the space-charge effect in the positive column, but the voltage rise in the abnormal regime is a cathode phenomena and is not likely to be related to electron-ion recombination. Figure 10 shows that recombination is of little significance until the electron density  $N_{eo}$  approaches a value of about  $10^{12} \text{ cm}^{-3}$ , and the calculations of Part III show that the effect of temperature inhomogeneities appears at a smaller value and hence obscures the interpretation of the effect of recombination. Furthermore, the discussion of the recombination coefficient in Part I reveals that its correct value is likely to be smaller than the one used in the calculations. These considerations leave the effect of recombination subject to doubt, and more definite conclusions are not offered until temperature inhomogeneities have been discussed. The interpretation of the discharge characteristic is considered again in the Summary of Part III.

Appendix A

PROOFS OF RELATIONS AMONG THE VARIABLES  $J, n_e, n_i, E$

In this appendix Eqs. (1.5) - (1.13) are used to establish certain relations of physical interest among the variables. The equations are rewritten below for reference.

$$\frac{dJ}{dy} = \gamma n_e - \varepsilon \zeta n_e n_i \quad (\text{A.1})$$

$$\frac{dn_e}{dy} = -n_e E - \delta \tau J \quad (\text{A.2})$$

$$\frac{dn_i}{dy} = \tau n_i E - \tau J \quad (\text{A.3})$$

$$\frac{dE}{dy} = \chi \zeta (n_i - n_e) = \chi \zeta s \quad (\text{A.4})$$

$$y = 0: \quad J = 0 \quad (\text{A.5})$$

$$E = 0 \quad (\text{A.6})$$

$$n_e = 1 \quad (\text{A.7})$$

$$y = 1: \quad n_e = 0 \quad (\text{A.8})$$

$$n_i = 0 \quad (\text{A.9})$$

The following relations are assumed true throughout the appendix:

$$\delta < 1 \quad (\text{A.10})$$

$$\varepsilon \zeta < \gamma \quad (\text{A.11})$$

$$n_e \geq 0 \quad \text{on} \quad 0 \leq y \leq 1 \quad (\text{A.12})$$

$$n_i \geq 0 \quad \text{on} \quad 0 \leq y \leq 1 \quad (\text{A.13})$$

Results based on the assumptions and equations above are presented in the following theorems. The lemmas contain hypothetical

results that are needed in the proofs of the theorems. The theorems generally depend on the assumption that a solution satisfying the above conditions exists.

Lemma 1

If  $s \leq 0$  at  $y = 0$ , there exists a  $y^* > 0$  in a neighborhood of  $y = 0$  such that

$$s < 0 \tag{A.14}$$

$$\frac{ds}{dy} < 0 \tag{A.15}$$

$$\frac{d^2s}{dy^2} < 0 \tag{A.16}$$

$$E < 0 \tag{A.17}$$

$$\frac{dE}{dy} < 0 \tag{A.18}$$

$$J > 0 \tag{A.19}$$

$$\frac{dJ}{dy} > 0 \tag{A.20}$$

$$n_i < 1 \tag{A.21}$$

$$\frac{dn_i}{dy} < 0 \tag{A.22}$$

$$\frac{d^2n_i}{dy^2} < 0 \tag{A.23}$$

at  $y = y^*$ .

Proof:

We assume

$$s \leq 0 \quad \text{at} \quad y = 0 \quad . \tag{A.24}$$

Since  $s = n_i - n_e$

$$n_i \leq 1 \quad \text{at} \quad y = 0 \quad . \tag{A.25}$$

From (A.1),

$$\frac{dJ}{dy} = n_e (\gamma - \epsilon \zeta n_i) \quad (A.26)$$

so (A.11) and (A.25) imply that

$$\frac{dJ}{dy} > 0 \quad \text{at} \quad y = 0 \quad . \quad (A.27)$$

From (A.4) and (A.24),

$$\frac{dE}{dy} \leq 0 \quad \text{at} \quad y = 0 \quad . \quad (A.28)$$

We now investigate the behavior of the derivatives of  $s$  at  $y = 0$  .

Subtracting (A.2) from (A.3),

$$\frac{ds}{dy} = (\tau n_i + n_e) E - \tau(1 - \delta)J \quad (A.29)$$

$$\frac{d^2s}{dy^2} = \left( \tau \frac{dn_i}{dy} + \frac{dn_e}{dy} \right) E + (\tau n_i + n_e) \frac{dE}{dy} - \tau(1 - \delta) \frac{dJ}{dy} \quad (A.30)$$

Substituting the conditions at  $y = 0$  into Eqs. (A.2), (A.3) and

(A.29), we find  $dn_e/dy = dn_i/dy = ds/dy = 0$  there. Then using (A.27)

and (A.28) in (A.30)

$$\frac{d^2s}{dy^2} < 0 \quad \text{at} \quad y = 0 \quad . \quad (A.31)$$

Also,

$$\frac{d^2n_i}{dy^2} = \tau \left[ -\frac{dn_i}{dy} E + n_i \frac{dE}{dy} - \frac{dJ}{dy} \right] \quad (A.32)$$

so

$$\frac{d^2n_i}{dy^2} < 0 \quad \text{at} \quad y = 0 \quad . \quad (A.33)$$

By continuity  $dJ/dy > 0$  ,  $d^2s/dy^2 < 0$  ,  $d^2n_i/dy^2 < 0$  in some

neighborhood of  $y = 0$ . By integrating these derivatives with respect to  $y$  from  $y = 0$  through a portion of this neighborhood, we establish the conclusions of the lemma for the variables  $J$ ,  $s$ , and  $n_1$ . (A.17) and (A.18) follow immediately using (A.4) and (A.6).

Theorem 1

$$s > 0 \quad \text{at} \quad y = 0 \quad . \quad (A.34)$$

Proof:

We prove the theorem by assuming

$$s \leq 0 \quad \text{at} \quad y = 0 \quad (A.35)$$

and obtaining a contradiction. The results of Lemma 1 can now be applied. The boundary conditions require that  $s = 0$  at  $y = 1$ . Since  $s < 0$  at  $y = y^*$  (as defined in Lemma 1),  $s$  must rise to zero. The mean value theorem of calculus then requires that the derivative  $ds/dy$  be positive somewhere on the interval between  $y = y^*$  and the  $y > y^*$  at which  $s$  first equals zero. Since by (A.15)  $ds/dy$  is also negative at  $y = y^*$ , it must pass through zero in this interval. Let the smallest  $y > y^*$  for which  $ds/dy = 0$  be denoted by  $y^{**}$ .

Then we have

$$\frac{ds}{dy} = 0 \quad \text{at} \quad y = y^{**} \quad (A.36)$$

$$\frac{ds}{dy} < 0 \quad \text{for} \quad y \in (y^*, y^{**}) \quad (A.37)$$

$$s < 0 \quad \text{for} \quad y \in (y^*, y^{**}) \quad (A.38)$$

Since  $E < 0$  at  $y = y^*$  by (A.17), it follows from (A.38) and Eq.

(A.4) that

$$E < 0 \quad \text{for} \quad y \in (y^*, y^{**}) \quad . \quad (\text{A.39})$$

From (A.2) and (A.3)

$$\frac{ds}{dy} = (\tau n_i + n_e)E - \tau(1 - \delta)J \quad (\text{A.40})$$

so (A.36) and (A.39) imply

$$J < 0 \quad \text{at} \quad y = y^{**} \quad . \quad (\text{A.41})$$

But (A.19) and (A.20) of Lemma 1 show that  $J > 0$  and  $dJ/dy > 0$  at  $y = y^*$ . Hence there must exist a  $y^{***} \in (y^*, y^{**})$  such that

$$\frac{dJ}{dy} = 0 \quad \text{at} \quad y = y^{***} \quad (\text{A.42})$$

$$\frac{dJ}{dy} > 0 \quad \text{for} \quad y \in [y^*, y^{***}) \quad (\text{A.43})$$

$$J > 0 \quad \text{for} \quad y \in [y^*, y^{***}) \quad . \quad (\text{A.44})$$

But 
$$\frac{dJ}{dy} = n_e(\gamma - \varepsilon \zeta n_i) \quad (\text{A.45})$$

and (A.42) implies

$$n_i = \frac{\gamma}{\varepsilon \zeta} \quad \text{at} \quad y = y^{***} \quad . \quad (\text{A.46})$$

From (A.43) and (A.45)

$$n_i < \frac{\gamma}{\varepsilon \zeta} \quad \text{at} \quad y = y^* \quad . \quad (\text{A.47})$$

Thus we must have

$$\frac{dn_i}{dy} > 0 \quad (\text{A.48})$$

for some  $y \in (y^*, y^{***})$ . However,

$$\frac{dn_i}{dy} = \tau[n_i E - J] \quad (A.49)$$

so (A.49), (A.39), and (A.44) show that

$$\frac{dn_i}{dy} < 0 \quad \text{for} \quad y \in (y^*, y^{***}) \quad . \quad (A.50)$$

(A.50) conflicts with (A.48). Since both follow from (A.35), this assumption must be rejected and the theorem is proved.

Lemma 2

If  $dJ/dy > 0$  on  $[0,1]$  and  $s > 0$  at  $y = 0$  but  $s = 0$  for some  $y \in (0,1)$ , then there exists a  $y^* \in (0,1)$  where

$$s < 0 \quad (A.51)$$

$$\frac{ds}{dy} < 0 \quad (A.52)$$

$$\frac{d^2s}{dy^2} < 0 \quad (A.53)$$

$$E > 0 \quad . \quad (A.54)$$

Proof:

Let  $y_0$  be the first  $y$  measured from  $y = 0$  for which  $s = 0$ . Clearly we also have  $ds/dy \leq 0$  at  $y = y_0$ . Since  $s > 0$  for  $y < y_0$ , (A.4) implies  $E > 0$  at  $y = y_0$ . Using Eq. (A.2) and the behavior of  $ds/dy$  and  $E$  at  $y_0$ , we conclude that  $dn_i/dy \leq dn_e/dy < 0$  there. The first two derivatives of  $s$  are given by Eqs. (A.29) and (A.30) in the proof of Lemma 1. Equation (A.30) now implies that  $d^2s/dy^2 < 0$  at  $y = y_0$ . By continuity there exists a  $y^* > y_0$  in a neighborhood of  $y_0$  at which  $d^2s/dy^2 < 0$  and  $E > 0$ .

The integration of  $d^2s/dy^2$  with respect to  $y$  from  $y_0$  to  $y^*$  shows that  $ds/dy < 0$  and  $s < 0$  at  $y = y^*$  and thus completes the proof.

Theorem 2

If  $dJ/dy > 0$  for  $y \in [0,1)$ , then

$$s > 0 \tag{A.55}$$

at all  $y \in [0,1)$ .

Proof:

We know from Theorem 1 that  $s > 0$  at  $y = 0$ . We proceed with the proof by assuming that  $s \leq 0$  at some  $y \in (0,1)$  and proving that such an occurrence is impossible. Lemma 2 now establishes the existence of a point  $y^* \in (0,1)$  at which  $s < 0$ ,  $ds/dy < 0$ ,  $d^2s/dy^2 < 0$ . Since conditions (A.8) and (A.9) require  $s = 0$  at  $y = 1$ , we must have  $ds/dy = 0$  for some  $y \in (y^*, 1)$ . Let the smallest such  $y$  be denoted  $y^{**}$  so that  $ds/dy < 0$  for  $y \in [y^*, y^{**})$ . The hypothesis of the theorem that  $dJ/dy > 0$  implies  $J > 0$  on  $[y^*, y^{**}]$ . We now use the formulas for  $ds/dy$  and  $d^2s/dy^2$  presented in the proof of Lemma 1. (A.29) and the fact that  $ds/dy = 0$  at  $y = y^{**}$  shows that  $E > 0$  at  $y = y^{**}$ . Since  $s < 0$  on  $[y^*, y^{**}]$ , Eq. (A.4) implies that  $E > 0$  for all  $y \in (y^*, y^{**})$ . We already know that  $ds/dy < 0$  on this interval, so (A.2) shows that  $dn_i/dy < dn_e/dy < 0$  there. Thus each term on the right-hand side of (A.30) is negative, and we conclude that  $d^3s/dy^3 < 0$  on  $(y^*, y^{**})$ . However, since  $ds/dy < 0$  at  $y = y^*$  and  $ds/dy = 0$  at  $y = y^{**}$ , the mean value theorem of calculus requires  $d^2s/dy^2 > 0$  for some  $y \in (y^*, y^{**})$ .

The contradiction shows that the hypothesis  $s \leq 0$  for some  $y \in (0,1)$  is untenable and proves the theorem.

Corollary

If  $dJ/dy > 0$  for  $y \in [0,1)$ ,

$$E > 0 \tag{A.56}$$

at all  $y \in (0,1]$ .

Proof:

The result follows trivially from Eqs. (A.4) and (A.6) and Theorem 2.

Lemma 3

Assume

$$J > 0 \quad \text{for} \quad y \in (y_1, y_2) \tag{A.57}$$

$$\frac{dn_i}{dy} > 0 \quad \text{for} \quad y \in (y_1, y_2) \tag{A.58}$$

$$s > 0 \quad \text{at} \quad y = y_1 \tag{A.59}$$

Then for all  $y \in (y_1, y_2)$

$$E > 0 \tag{A.60}$$

$$\frac{dE}{dy} > 0 \tag{A.61}$$

$$\frac{d^2E}{dy^2} > 0 \tag{A.62}$$

$$s > 0 \tag{A.63}$$

$$\frac{ds}{dy} > 0 \tag{A.64}$$

$$\frac{dn_e}{dy} < 0 \tag{A.65}$$

Proof:

Equations (A.57), (A.58), and (A.3) immediately imply

$$E > 0 \quad \text{for} \quad y \in (y_1, y_2) \quad . \quad (\text{A.66})$$

Using (A.57) and (A.66), Eq. (A.2) shows that

$$\frac{dn_e}{dy} < 0 \quad \text{for} \quad y \in (y_1, y_2) \quad . \quad (\text{A.67})$$

Since  $ds/dy = dn_i/dy - dn_e/dy$ , it follows from (A.58) and (A.67) that

$$\frac{ds}{dy} > 0 \quad \text{for} \quad y \in (y_1, y_2) \quad . \quad (\text{A.68})$$

The remaining conclusions of Lemma 3 now follow trivially from (A.59) and (A.4).

### Theorem 3

$$\frac{d^2 n_i}{dy^2} \leq 0 \quad \text{at} \quad y = 0 \quad (\text{A.69})$$

Proof:

We assume

$$\frac{d^2 n_i}{dy^2} > 0 \quad \text{at} \quad y = 0 \quad (\text{A.70})$$

and seek a contradiction. Since  $dn_i/dy = 0$  at  $y = 0$ , it becomes positive as  $y$  increases from zero. However,  $n_i(1) = 0$ , so  $n_i$  must eventually decrease. Let  $y^*$  be the smallest  $y > 0$  at which

$$\frac{dn_i}{dy} = 0 \quad \text{at} \quad y = y^* \quad . \quad (\text{A.71})$$

Then 
$$\frac{dn_i}{dy} > 0 \quad \text{for} \quad y \in (0, y^*) \quad . \quad (A.72)$$

The proof is divided into four cases depending on the behavior of  $J$  on  $[0, y^*]$  . Since

$$\frac{dJ}{dy} = n_e (\gamma - \epsilon \zeta n_i) \quad , \quad (A.73)$$

(A.72) shows that if  $dJ/dy$  ever becomes negative on the interval  $[0, y^*]$  , it remains negative for larger  $y$  on the interval. We now consider four separate cases that comprise all possible behavior of  $J$  :

I. 
$$\frac{dJ}{dy} \leq 0 \quad \text{at} \quad y = 0 \quad . \quad (A.74)$$

II. 
$$\frac{dJ}{dy} > 0 \quad \text{at} \quad y = 0 \quad (A.75)$$

$$\frac{dJ}{dy} < 0 \quad \text{at} \quad y = y^* \quad (A.76)$$

$$J < 0 \quad \text{at} \quad y = y^* \quad (A.77)$$

III. 
$$\frac{dJ}{dy} > 0 \quad \text{at} \quad y = 0 \quad (A.78)$$

$$\frac{dJ}{dy} < 0 \quad \text{at} \quad y = y^* \quad (A.79)$$

$$J \geq 0 \quad \text{at} \quad y = y^* \quad (A.80)$$

IV. 
$$\frac{dJ}{dy} \geq 0 \quad \text{at} \quad y = y^* \quad . \quad (A.81)$$

Case I.

$$\frac{dJ}{dy} \leq 0 \quad \text{at} \quad y = 0 \quad (A.82)$$

It is apparent from the comment following (A.73) that

$$J < 0 \quad \text{for} \quad y \in (0, y^*] \quad (\text{A.83})$$

$$\frac{dJ}{dy} < 0 \quad \text{for} \quad y \in (0, y^*] \quad . \quad (\text{A.84})$$

Equations (A.3), (A.71), and (A.83) now imply

$$E < 0 \quad \text{at} \quad y = y^* \quad . \quad (\text{A.85})$$

However, Theorem 1 shows that  $s > 0$  at  $y = 0$ , so from Eq. (A.4) it is seen that  $E$  and  $dE/dy$  become positive as  $y$  increases from zero. Therefore  $E$  must decrease somewhere on the interval  $(0, y^*)$ . Let  $y^{**}$  denote the smallest  $y$  for which

$$\frac{dE}{dy} = s = 0 \quad \text{at} \quad y = y^{**} \quad . \quad (\text{A.86})$$

We now have

$$E > 0 \quad \text{for} \quad y \in (0, y^{**}) \quad (\text{A.87})$$

$$s > 0 \quad \text{for} \quad y \in (0, y^{**}) \quad . \quad (\text{A.88})$$

From (A.2) and (A.3)

$$\frac{ds}{dy} = (\tau n_f + n_e)E - \tau(1 - \delta)J \quad . \quad (\text{A.89})$$

(A.83) and (A.87) now imply

$$\frac{ds}{dy} > 0 \quad \text{for} \quad y \in (0, y^{**}) \quad . \quad (\text{A.90})$$

But  $s$  must decrease to zero at  $y = y^{**}$ . Hence we arrive at a contradiction, and the theorem is proved for the hypothesis of Case I.

Case II.

$$\frac{dJ}{dy} > 0 \quad \text{at} \quad y = 0 \quad (\text{A.91})$$

$$\frac{dJ}{dy} < 0 \quad \text{at} \quad y = y^* \quad (\text{A.92})$$

$$J < 0 \quad \text{at} \quad y = y^* \quad (\text{A.93})$$

By the same reasoning used in Case I, we conclude that

$$E < 0 \quad \text{at} \quad y = y^* \quad (\text{A.94})$$

and that  $E > 0$  and  $dE/dy > 0$  for  $y > 0$  in a neighborhood of  $y = 0$ . Again let  $y^{**}$  denote the smallest  $y$  for which

$$\frac{dE}{dy} = s = 0 \quad \text{at} \quad y = y^{**} \quad (\text{A.95})$$

so that

$$E > 0 \quad \text{for} \quad y \in (0, y^{**}) \quad (\text{A.96})$$

$$s > 0 \quad \text{for} \quad y \in (0, y^{**}) \quad (\text{A.97})$$

Now let  $y^{***}$  denote the point at which  $J = 0$ . Then the comment following (A.73) shows that

$$J > 0 \quad \text{for} \quad y \in (0, y^{***}) \quad (\text{A.98})$$

$$J < 0 \quad \text{for} \quad y \in (y^{***}, y^*) \quad (\text{A.99})$$

Lemma 3 can now be applied on the interval  $(0, y^{***})$ , so from (A.60), (A.63), and (A.64) we have

$$E > 0 \quad \text{for} \quad y \in (0, y^{***}) \quad (\text{A.100})$$

$$s > 0 \quad \text{for} \quad y \in (0, y^{***}) \quad (\text{A.101})$$

$$\frac{ds}{dy} > 0 \quad \text{for} \quad y \in (0, y^{***}) \quad . \quad (\text{A.102})$$

From (A.95) and (A.101) we conclude that

$$y^{**} > y^{***} \quad . \quad (\text{A.103})$$

Hence (A.96) and (A.99) imply

$$E > 0 \quad \text{for} \quad y \in (y^{***}, y^{**}) \quad (\text{A.104})$$

$$J < 0 \quad \text{for} \quad y \in (y^{***}, y^{**}) \quad . \quad (\text{A.105})$$

Since

$$\frac{ds}{dy} = (\tau n_i + n_e) E - \tau(1 - \delta) J \quad (\text{A.106})$$

(A.104) and (A.105) require

$$\frac{ds}{dy} > 0 \quad \text{for} \quad y \in (y^{***}, y^{**}) \quad . \quad (\text{A.107})$$

However, (A.101) and (A.95) require that  $ds/dy \leq 0$  somewhere on the interval  $(y^{***}, y^{**})$ . This requirement cannot be reconciled with (A.107), and we again arrive at a contradiction.

Case III.

$$\frac{dJ}{dy} > 0 \quad \text{at} \quad y = 0 \quad (\text{A.108})$$

$$\frac{dJ}{dy} < 0 \quad \text{at} \quad y = y^* \quad (\text{A.109})$$

$$J \geq 0 \quad \text{at} \quad y = y^* \quad . \quad (\text{A.110})$$

From (A.110) and the comment following (A.73) it is apparent that

$$J > 0 \quad \text{for} \quad y \in (0, y^*) \quad . \quad (\text{A.111})$$

Now Lemma 3 can be applied on the interval  $(0, y^*)$ , so from (A.60) and (A.61) we obtain

$$E > 0 \quad \text{for} \quad y \in (0, y^*) \quad (\text{A.112})$$

$$\frac{dE}{dy} > 0 \quad \text{for} \quad y \in (0, y^*) \quad (\text{A.113})$$

We now designate the point at which  $dJ/dy = 0$  by  $y^{**}$ , so we obtain

$$\frac{dJ}{dy} < 0 \quad \text{for} \quad y \in (y^{**}, y^*) \quad (\text{A.114})$$

From (A.3)

$$\frac{d^2 n_i}{dy^2} = \tau \left[ \frac{dn_i}{dy} E + n_i \frac{dE}{dy} - \frac{dJ}{dy} \right] \quad (\text{A.115})$$

The use of (A.72), (A.112), (A.113), and (A.114) in (A.115) yields the result

$$\frac{d^2 n_i}{dy^2} > 0 \quad \text{for} \quad y \in (y^{**}, y^*) \quad (\text{A.116})$$

However, (A.71) and (A.72) require that  $dn_i/dy$  decrease to zero as  $y \rightarrow y^*$ , and hence  $d^2 n_i/dy^2 \leq 0$  for  $y < y^*$  in some neighborhood of  $y = y^*$ . (A.116) shows that Case III leads to a contradiction.

Case IV.

$$\frac{dJ}{dy} \geq 0 \quad \text{at} \quad y = y^* \quad (\text{A.117})$$

It follows from (A.117) that

$$J > 0 \quad \text{for} \quad y \in (0, y^*) \quad (\text{A.118})$$

and hence Lemma 3 applies on the interval  $(0, y^*)$ . From (A.60), (A.61),

(A.62), and (A.65),

$$E > 0 \quad \text{for} \quad y \in (0, y^*) \quad (\text{A.119})$$

$$\frac{dE}{dy} > 0 \quad \text{for} \quad y \in (0, y^*) \quad (\text{A.120})$$

$$\frac{d^2E}{dy^2} > 0 \quad \text{for} \quad y \in (0, y^*) \quad (\text{A.121})$$

$$\frac{dn_e}{dy} < 0 \quad \text{for} \quad y \in (0, y^*) \quad (\text{A.122})$$

We now consider the sign of  $d^2J/dy^2$ .

From (A.73),

$$\frac{d^2J}{dy^2} = \frac{dn_e}{dy} (\gamma - \epsilon \zeta n_i) - \epsilon \zeta n_e \frac{dn_i}{dy} \quad (\text{A.123})$$

Since  $dJ/dy > 0$  on  $(0, y^*)$ ,  $\gamma - \epsilon \zeta n_i > 0$  there. (A.72) and (A.122) now show

$$\frac{d^2J}{dy^2} < 0 \quad \text{for} \quad y \in (0, y^*) \quad (\text{A.124})$$

(A.71) and (A.72) show that  $dn_i/dy$  must decrease to zero as  $y$  approaches  $y^*$ . Since  $d^2n_i/dy^2 > 0$  at  $y = 0$ , it must change signs on the interval  $(0, y^*)$ . We let  $y^{**}$  be the smallest  $y$  for which

$$\frac{d^2n_i}{dy^2} = 0 \quad \text{at} \quad y = y^{**} \quad (\text{A.125})$$

Then

$$\frac{d^2n_i}{dy^2} > 0 \quad \text{for} \quad y \in (0, y^{**}) \quad (\text{A.126})$$

We now consider the sign of  $d^3n_i/dy^3$ . From (A.3)

$$\frac{d^3 n_i}{dy^3} = \tau \left[ \frac{d^2 n_i}{dy^2} E + 2 \frac{dn_i}{dy} \frac{dE}{dy} + n_i \frac{d^2 E}{dy^2} - \frac{d^2 J}{dy^2} \right] . \quad (\text{A.127})$$

(A.126), (A.72), (A.119), (A.120), (A.121), and (A.124) show that each term of (A.127) is positive on  $(0, y^{**})$ , and hence

$$\frac{d^3 n_i}{dy^3} > 0 \quad \text{for} \quad y \in (0, y^{**}) . \quad (\text{A.128})$$

However, from (A.125) and (A.126) it is obvious that  $d^2 n_i / dy^2$  must decrease to zero as  $y$  increases to  $y^{**}$ , and therefore (A.128) is impossible.

We have now achieved a contradiction for each case of Theorem 3. Thus the hypothesis of (A.70) is untenable and the theorem is proved.

#### Theorem 4

$n_i(0)$  is bounded by

$$1 < n_i(0) \leq \frac{1}{2\chi} (\chi - \epsilon) + \frac{1}{2\chi} \sqrt{(\chi - \epsilon)^2 + \frac{4\gamma\chi}{\zeta}} . \quad (\text{A.129})$$

If  $\chi > \epsilon$ , and  $\zeta > \frac{4\gamma\chi}{(\chi - \epsilon)^2}$ , an approximate bound is

$$1 < n_i(0) \leq 1 + \frac{\gamma}{\zeta(\chi - \epsilon)} - \frac{\epsilon}{\chi} + o\left(\frac{1}{\zeta^2}\right) . \quad (\text{A.130})$$

**Proof:**

The lower bound on  $n_i(0)$  follows immediately from (A.7) and Theorem 1. The upper bound is obtained by evaluating  $d^2 n_i / dy^2$  at  $y = 0$ . From (A.3),

$$\frac{d^2 n_i}{dy^2} = \tau \left[ -\frac{dn_i}{dy} E + n_i \frac{dE}{dy} - \frac{dJ}{dy} \right] \quad . \quad (\text{A.131})$$

$dn_i/dy$ ,  $dE/dy$ , and  $dJ/dy$  are evaluated at  $y = 0$  using (A.3), (A.4) and (A.1). Thus at  $y = 0$

$$\frac{d^2 n_i}{dy^2} = \tau [n_i(0) \chi \zeta(n_i(0) - 1) - (\gamma - \epsilon \zeta n_i(0))] \quad . \quad (\text{A.132})$$

Theorem 3 now implies

$$\tau [\chi \zeta n_i^2(0) - (\chi - \epsilon) \zeta n_i(0) - \gamma] \leq 0 \quad . \quad (\text{A.133})$$

The roots of the quadratic in  $n_i(0)$  are

$$r_1 = \frac{1}{2\chi} (\chi - \epsilon) + \frac{1}{2\chi} \sqrt{(\chi - \epsilon)^2 + \frac{4\gamma\chi}{\zeta}} \quad (\text{A.134})$$

$$r_2 = \frac{1}{2\chi} (\chi - \epsilon) - \frac{1}{2\chi} \sqrt{(\chi - \epsilon)^2 + \frac{4\gamma\chi}{\zeta}} \quad . \quad (\text{A.135})$$

Now (A.133) becomes

$$\tau \chi \zeta (n_i(0) - r_1)(n_i(0) - r_2) \leq 0 \quad . \quad (\text{A.136})$$

Clearly  $r_2 < 0$ , so (A.136) holds only if

$$n_i(0) \leq r_1 \quad (\text{A.137})$$

and (A.129) is established. If  $\chi > \epsilon$ , (A.134) can be written

$$r_1 = \frac{1}{2\chi} (\chi - \epsilon) + \frac{1}{2\chi} (\chi - \epsilon) \left( 1 + \frac{4\gamma\chi}{\zeta (\chi - \epsilon)^2} \right)^{1/2} \quad . \quad (\text{A.138})$$

If  $\zeta > 4\gamma\chi/(\chi - \varepsilon)^2$ , the square root can be expanded as a convergent binomial series, and we obtain from the first two terms

$$r_1 = \frac{\chi - \varepsilon}{\chi} + \frac{\gamma}{\zeta(\chi - \varepsilon)} + o\left(\frac{1}{\zeta^2}\right) \quad (\text{A.139})$$

$$= 1 + \frac{\gamma}{\zeta(\chi - \varepsilon)} - \frac{\varepsilon}{\chi} + o\left(\frac{1}{\zeta^2}\right) \quad (\text{A.140})$$

where the error is expressed as  $o(1/\zeta^2)$ , since we are primarily interested in large  $\zeta$ . (A.137) now shows that (A.130) is established.

Application of the requirement  $r_1 > 1$  to (A.140) implies

$$\gamma > \varepsilon\zeta \frac{\chi - \varepsilon}{\chi} .$$

(A.11) shows that this relation is satisfied.

Appendix B

ORTHOGONALITY REQUIREMENT

Consider the problem of finding the solution to the nonhomogeneous linear differential equation

$$L u = f \tag{B.1}$$

when the homogeneous equation

$$L u = 0 \tag{B.2}$$

has a solution satisfying the same boundary conditions. This problem is treated in standard texts on differential equations<sup>\*</sup>, and the results are repeated below in a somewhat more specific form for convenience.

Let  $L$  be given by

$$L u = \frac{1}{w(y)} \frac{d}{dy} \left( p(y) \frac{du}{dy} \right) + q(y) u \tag{B.3}$$

and define the scalar product

$$\langle u, v \rangle = \int_0^1 w(y) u(y) v(y) dy \tag{B.4}$$

With the initial conditions

$$\frac{du}{dy} (0) = 0 \tag{B.5}$$

$$u(1) = 0 \tag{B.6}$$

---

<sup>\*</sup> See, for instance, Friedman [8], pp. 169-171.

the differential operator is self-adjoint, since

$$\begin{aligned}
 \langle v, Lu \rangle &= \int_0^1 [v(pu')' + wvqu] dy \\
 &= \int_0^1 [-u'pv' + wuqv] dy + pvu' \Big|_0^1 \\
 &= \int_0^1 [u(pv')' + wuqv] dy + p(vu' - v'u) \Big|_0^1 \\
 &= \langle Lv, u \rangle
 \end{aligned} \tag{B.7}$$

if both  $u$  and  $v$  satisfy (B.5) and (B.6).

If  $u_h$  satisfies (B.2) with boundary conditions (B.5) and (B.6) and  $u_p$  satisfies (B.1) with the same conditions, we have

$$\langle u_h, Lu_p \rangle - \langle Lu_h, u_p \rangle = \langle u_h, f \rangle . \tag{B.8}$$

But from (B.7) we obtain the desired result

$$\langle u_h, f \rangle = 0 . \tag{B.9}$$

We have shown that if the homogeneous problem has a nontrivial solution, a solution to (B.1) with the same boundary conditions can exist only if  $f$  is orthogonal to the homogeneous solution. It can also be shown that if (B.9) is satisfied, a solution does exist\*.

---

\*See Friedman [8].

Appendix C

THE ZERO-ORDER SOLUTION IN CYLINDRICAL GEOMETRY

In cylindrical geometry the analogue to Eqs. (3.11) - (3.14) is the problem

$$\frac{1}{\rho} \frac{d}{d\rho} \left( \rho \frac{dn}{d\rho} \right) + \gamma^* n - \epsilon^* n^2 = 0 \quad (C.1)$$

$$\rho = 0 : \quad n = 1 \quad (C.2)$$

$$\frac{dn}{d\rho} = 0 \quad (C.3)$$

$$\rho = 1 : \quad n = 0 \quad (C.4)$$

Here also the recombination term is regarded as a perturbation, and  $\gamma^*$  and  $n$  are written as asymptotic series in powers of  $\epsilon^*$  :

$$n = n_0 + \epsilon^* n_1 + \epsilon^{*2} n_2 + \dots \quad (C.5)$$

$$\gamma^* = \gamma_0^* + \epsilon^* \gamma_1^* + \epsilon^{*2} \gamma_2^* + \dots \quad (C.6)$$

Substitution of these expansions for  $n$  and  $\gamma^*$  yield as the problem to lowest order,

$$\frac{1}{\rho} \frac{d}{d\rho} \left( \rho \frac{dn_0}{d\rho} \right) + \gamma_0^* n_0 = 0 \quad (C.7)$$

$$\rho = 0 : \quad n_0 = 1 \quad (C.8)$$

$$\frac{dn_0}{d\rho} = 0 \quad (C.9)$$

$$\rho = 1 : \quad n_0 = 0 \quad (C.10)$$

The solution to (C.7) satisfying the conditions at  $\rho = 0$  is the zero-order Bessel function of the first kind:

$$n_0 = J_0(\sqrt{\gamma_0^*} \rho) \quad (C.11)$$

The boundary condition at  $y = 1$  determines  $\gamma_0^*$  :

$$J_0(\sqrt{\gamma_0^*}) = 0 \quad (C.12)$$

As concluded in the discussion following Eq. (3.22), only the fundamental diffusion mode can be present, so  $\sqrt{\gamma_0^*}$  is set equal to the first zero of  $J_0$ . Then

$$\gamma_0^* \approx (2.405)^2 \quad (C.13)$$

To the next order in  $\epsilon^*$  the problem becomes

$$\frac{1}{\rho} \frac{d}{d\rho} \left( \rho \frac{dn_1}{d\rho} \right) + \gamma_0^* n_1 = n_0^2 - \gamma_1^* n_0 \quad (C.14)$$

$$\rho = 0 : \quad n_1 = 0 \quad (C.15)$$

$$\frac{dn_1}{d\rho} = 0 \quad (C.16)$$

$$\rho = 1 : \quad n_1 = 0 \quad (C.17)$$

Here the results of Appendix B can be invoked to acquire an expression for  $\gamma_1^*$  from Eq. (C.14) and the zero-order solution. The present situation is seen to be equivalent to that treated there by making the

---

\* See Handbook of Mathematical Functions [1].

identifications,

$$y \equiv \rho \quad (C.18)$$

$$w(\rho) \equiv \rho \quad (C.19)$$

$$p(\rho) \equiv \rho \quad (C.20)$$

$$q(\rho) \equiv \gamma_0^* \quad (C.21)$$

Since  $J_0(\sqrt{\gamma_0^*}\rho)$  is a solution to the homogeneous equation associated with (C.14) and satisfies the conditions (C.16) and (C.17), Appendix B implies that the existence of a solution  $n_1$  requires

$$\langle J_0(\sqrt{\gamma_0^*}\rho), n_0^2 - \gamma_1^* n_0 \rangle = 0 \quad (C.22)$$

or

$$\gamma_1^* = \frac{\langle J_0(\sqrt{\gamma_0^*}\rho), n_0^2 \rangle}{\langle J_0(\sqrt{\gamma_0^*}\rho), n_0 \rangle} \quad (C.23)$$

$$= \frac{\int_0^1 \rho J_0^3(\sqrt{\gamma_0^*}\rho) d\rho}{\int_0^1 \rho J_0^2(\sqrt{\gamma_0^*}\rho) d\rho} \quad (C.24)$$

With this value for  $\gamma_1^*$  the equation for  $n_1$  is solved by the method of variation of parameters. Assume

$$n_1(\rho) = A(\rho) J_0(\sqrt{\gamma_0^*}\rho) + B(\rho) Y_0(\sqrt{\gamma_0^*}\rho) \quad (C.25)$$

$Y_0$  is the zero-order Bessel function of the second kind, and  $J_0(\sqrt{\gamma_0^*}\rho)$  and  $Y_0(\sqrt{\gamma_0^*}\rho)$  are selected as the two linearly independent solutions of the homogeneous differential equation

$$\frac{1}{\rho} \frac{d}{d\rho} \left( \rho \frac{du}{d\rho} \right) + \gamma_0^* u = 0 \quad . \quad (C.26)$$

Differentiating (C.25)

$$\frac{dn_1}{d\rho} = \sqrt{\gamma_0^*} AJ'_0 + \sqrt{\gamma_0^*} BY'_0 + A'J_0 + B'Y_0 \quad . \quad (C.27)$$

We now impose upon A and B the condition

$$A'(\rho) J_0(\sqrt{\gamma_0^*}\rho) + B'(\rho) Y_0(\sqrt{\gamma_0^*}\rho) = 0 \quad . \quad (C.28)$$

Differentiating a second time,

$$\frac{d^2 n_1}{d\rho^2} = \gamma_0^* AJ''_0 + \gamma_0^* BY''_0 + \sqrt{\gamma_0^*} A'J'_0 + \sqrt{\gamma_0^*} B'Y'_0 \quad . \quad (C.29)$$

Now,

$$\frac{1}{\rho} \frac{d}{d\rho} \left( \rho \frac{dn_1}{d\rho} \right) + \gamma_0^* n_1 = \frac{d^2 n_1}{d\rho^2} + \frac{1}{\rho} \frac{dn_1}{d\rho} + \gamma_0^* n_1 \quad (C.30)$$

$$\begin{aligned} &= \gamma_0^* AJ''_0 + \gamma_0^* BY''_0 + \sqrt{\gamma_0^*} A'J'_0 + \sqrt{\gamma_0^*} B'Y'_0 \\ &+ \sqrt{\gamma_0^*} \frac{1}{\rho} AJ'_0 + \sqrt{\gamma_0^*} \frac{1}{\rho} BY'_0 + \gamma_0^* AJ_0 + \gamma_0^* BY_0 \quad . \quad (C.31) \end{aligned}$$

Since  $J_0(\sqrt{\gamma_0^*}\rho)$  and  $Y_0(\sqrt{\gamma_0^*}\rho)$  satisfy the equations

$$J''_0(\sqrt{\gamma_0^*}\rho) + \frac{1}{\sqrt{\gamma_0^*}\rho} J'_0(\sqrt{\gamma_0^*}\rho) + J_0(\sqrt{\gamma_0^*}\rho) = 0 \quad (C.32)$$

$$Y''_0(\sqrt{\gamma_0^*}\rho) + \frac{1}{\sqrt{\gamma_0^*}\rho} Y'_0(\sqrt{\gamma_0^*}\rho) + Y_0(\sqrt{\gamma_0^*}\rho) = 0 \quad (C.33)$$

Eq. (C.31) becomes

$$\frac{1}{\rho} \frac{d}{d\rho} \left( \rho \frac{dn_1}{d\rho} \right) + \gamma_0^* n_1 = \sqrt{\gamma_0^*} A' J_0' + \sqrt{\gamma_0^*} B' Y_0' . \quad (C.34)$$

Equation (C.28), together with the result of substituting (C.34) and (C.11) into (C.14), yields a system of equations for A' and B' :

$$A' J_0(\sqrt{\gamma_0^*} \rho) + B' Y_0(\sqrt{\gamma_0^*} \rho) = 0 \quad (C.35)$$

$$A' J_0'(\sqrt{\gamma_0^*} \rho) + B' Y_0'(\sqrt{\gamma_0^*} \rho) = \frac{1}{\sqrt{\gamma_0^*}} [J_0^2(\sqrt{\gamma_0^*} \rho) - \gamma_1^* J_0(\sqrt{\gamma_0^*} \rho)] . \quad (C.36)$$

The determinant of the coefficients is the Wronskian of  $J_0$  and  $Y_0$  and is given in the Handbook of Mathematical Functions [1], p. 360:

$$W\{J_0(\sqrt{\gamma_0^*} \rho), Y_0(\sqrt{\gamma_0^*} \rho)\} = \begin{vmatrix} J_0(\sqrt{\gamma_0^*} \rho) & Y_0(\sqrt{\gamma_0^*} \rho) \\ J_0'(\sqrt{\gamma_0^*} \rho) & Y_0'(\sqrt{\gamma_0^*} \rho) \end{vmatrix} = \frac{2}{\pi \sqrt{\gamma_0^*} \rho} . \quad (C.37)$$

The system (C.35) and (C.36) is now solved to yield

$$A' = \frac{\pi}{2} \sqrt{\gamma_0^*} \rho \begin{vmatrix} 0 & Y_0 \\ \frac{1}{\sqrt{\gamma_0^*}} [J_0^2 - \gamma_1^* J_0] & Y_0' \end{vmatrix} \quad (C.38)$$

$$= -\frac{\pi}{2} \rho Y_0(\sqrt{\gamma_0^*} \rho) [J_0^2(\sqrt{\gamma_0^*} \rho) - \gamma_1^* J_0(\sqrt{\gamma_0^*} \rho)] \quad (C.39)$$

and

$$B' = \frac{\pi}{2} \sqrt{\gamma_o^* \rho} \begin{vmatrix} J_o & 0 \\ J_o' & \frac{1}{\sqrt{\gamma_o^*}} [J_o^2 - \gamma_1^* J_o] \end{vmatrix} \quad (C.40)$$

$$= \frac{\pi}{2} \rho J_o(\sqrt{\gamma_o^* \rho}) [J_o^2(\sqrt{\gamma_o^* \rho}) - \gamma_1^* J_o(\sqrt{\gamma_o^* \rho})] \quad (C.41)$$

so

$$A(\rho) = -\frac{\pi}{2} \int_0^\rho \bar{\rho} J_o(\sqrt{\gamma_o^* \bar{\rho}}) Y_o(\sqrt{\gamma_o^* \bar{\rho}}) [J_o(\sqrt{\gamma_o^* \bar{\rho}}) - \gamma_1^*] d\bar{\rho} \quad (C.42)$$

$$B(\rho) = \frac{\pi}{2} \int_0^\rho \bar{\rho} J_o^2(\sqrt{\gamma_o^* \bar{\rho}}) [J_o(\sqrt{\gamma_o^* \bar{\rho}}) - \gamma_1^*] d\bar{\rho} \quad (C.43)$$

From (C.25) the solution for  $n_1$  becomes

$$\begin{aligned} n_1(\rho) &= -\frac{\pi}{2} \int_0^\rho \bar{\rho} J_o(\sqrt{\gamma_o^* \bar{\rho}}) Y_o(\sqrt{\gamma_o^* \bar{\rho}}) [J_o(\sqrt{\gamma_o^* \bar{\rho}}) - \gamma_1^*] d\bar{\rho} J_o(\sqrt{\gamma_o^* \rho}) \\ &+ \frac{\pi}{2} \int_0^\rho \bar{\rho} J_o^2(\sqrt{\gamma_o^* \bar{\rho}}) [J_o(\sqrt{\gamma_o^* \bar{\rho}}) - \gamma_1^*] d\bar{\rho} Y_o(\sqrt{\gamma_o^* \rho}) \quad (C.44) \end{aligned}$$

That  $n_1(\rho)$  satisfies the proper boundary conditions can be seen by using the limiting forms of the Bessel function for small arguments. For small  $z$ ,  $J_o$  and  $Y_o$  and their derivatives behave as follows:

$$J_o(z) \sim 1 - \frac{1}{4} z^2 \quad (C.45)$$

$$Y_o(z) \sim \frac{2}{\pi} \ln z \quad (C.46)$$

$$J'_0(z) = -J_1(z) \sim \frac{z}{2} \quad (C.47)$$

$$Y'_0(z) = -Y_1(z) \sim \frac{2}{\pi} \frac{1}{z} \quad (C.48)$$

Then

$$n_1(0) = \lim_{\rho \rightarrow 0} n_1(\rho) \quad (C.49)$$

$$\begin{aligned} &= -\frac{\pi}{2} \lim_{\rho \rightarrow 0} \left\{ \int_0^\rho \bar{\rho} \left( \frac{2}{\pi} \ln \sqrt{\gamma_0^* \bar{\rho}} \right) (1 - \gamma_1^*) d\bar{\rho} \right\} \\ &+ \frac{\pi}{2} \lim_{\rho \rightarrow 0} \left\{ \int_0^\rho \bar{\rho} (1 - \gamma_1^*) d\bar{\rho} \frac{2}{\pi} \ln \sqrt{\gamma_0^* \bar{\rho}} \right\} \end{aligned} \quad (C.50)$$

$$= 0 + (1 - \gamma_1^*) \lim_{\rho \rightarrow 0} \left\{ \frac{\rho^2}{2} \ln \sqrt{\gamma_0^* \rho} \right\} \quad (C.51)$$

$$= 0 \quad (C.52)$$

Similarly,

$$\frac{dn_1}{d\rho}(0) = \lim_{\rho \rightarrow 0} \frac{dn_1}{d\rho} \quad (C.53)$$

$$= -\frac{\pi}{2} \lim_{\rho \rightarrow 0} \left\{ \int_0^\rho \bar{\rho} \left( \frac{2}{\pi} \ln \sqrt{\gamma_0^* \bar{\rho}} \right) (1 - \gamma_1^*) d\bar{\rho} \left( -\frac{\gamma_0^* \bar{\rho}}{2} \right) \right\}$$

$$- \frac{\pi}{2} \lim_{\rho \rightarrow 0} \left\{ \rho \left( \frac{2}{\pi} \ln \sqrt{\gamma_0^* \rho} \right) (1 - \gamma_1^*) \right\}$$

$$+ \frac{\pi}{2} \lim_{\rho \rightarrow 0} \left\{ \int_0^\rho \bar{\rho} (1 - \gamma_1^*) d\bar{\rho} \left( \frac{2}{\pi \bar{\rho}} \right) \right\}$$

$$+ \frac{\pi}{2} \lim_{\rho \rightarrow 0} \left\{ \rho (1 - \gamma_1^*) \left( \frac{2}{\pi} \ln \sqrt{\gamma_0^* \rho} \right) \right\} \quad (C.54)$$

$$= 0 \quad (C.55)$$

The boundary condition at  $\rho = 1$  is satisfied because of the choice of  $\gamma_1^*$ .

$$n(1) = -\frac{\pi}{2} \int_0^1 \bar{\rho} J_0(\sqrt{\gamma_0^* \rho}) Y_0(\sqrt{\gamma_0^* \rho}) [J_0(\sqrt{\gamma_0^* \rho}) - \gamma_1^*] d\bar{\rho} J_0(\sqrt{\gamma_0^* \rho}) + \frac{\pi}{2} \int_0^1 \bar{\rho} J_0^2(\sqrt{\gamma_0^* \rho}) [J_0(\sqrt{\gamma_0^* \rho}) - \gamma_1^*] d\bar{\rho} Y_0(\sqrt{\gamma_0^* \rho}) \quad (C.56)$$

But  $J_0(\sqrt{\gamma_0^*}) = 0$  (C.57)

and

$$\int_0^1 \bar{\rho} J_0^2(\sqrt{\gamma_0^* \rho}) [J_0(\sqrt{\gamma_0^* \rho}) - \gamma_1^*] d\bar{\rho} = \left[ \frac{\int_0^1 \bar{\rho} J_0^3(\sqrt{\gamma_0^* \rho}) d\bar{\rho}}{\int_0^1 \bar{\rho} J_0^2(\sqrt{\gamma_0^* \rho}) d\bar{\rho}} - \gamma_1^* \right] \int_0^1 \bar{\rho} J_0^2(\sqrt{\gamma_0^* \rho}) d\bar{\rho} \quad (C.58)$$

$$= 0 \quad (C.59)$$

by Eq. (C.24). Thus the conditions (C.15) - (C.17) are satisfied, and  $n_1(\rho)$  as given by (C.44) is the desired solution.

An integral expression for  $\gamma_2^*$  can now be obtained from  $n_1$  and the equation for  $n_2$ . The contribution of  $\epsilon^{*2}$  terms to (C.1) - (C.4) yields the problem

$$\frac{1}{\rho} \frac{d}{d\rho} \left( \rho \frac{dn_2}{d\rho} \right) + \gamma_0^* n_2 = 2n_0 n_1 - \gamma_1^* n_1 - \gamma_2^* n_0 \quad (C.60)$$

$\rho = 0 :$   $n_2 = 0$  (C.61)

$$\frac{dn_2}{d\rho} = 0 \quad (C.62)$$

$\rho = 1 :$   $n_2 = 0$  (C.63)

$J_0(\sqrt{\gamma_0^* \rho})$  is again a solution of the homogeneous equation associated with (C.60) and satisfies the boundary conditions (C.62) and (C.63), so the results of Appendix B again apply. A solution  $n_2$  exists if and only if

$$\langle J_0(\sqrt{\gamma_0^* \rho}), 2n_0 n_1 - \gamma_1^* n_1 - \gamma_2^* n_0 \rangle = 0 \quad (C.64)$$

or

$$\gamma_2^* = \frac{\langle J_0(\sqrt{\gamma_0^* \rho}), 2n_0 n_1 - \gamma_1^* n_1 \rangle}{\langle J_0(\sqrt{\gamma_0^* \rho}), n_0 \rangle} . \quad (C.65)$$

Using (C.11) and (C.44) ,

$$\begin{aligned} \gamma_2^* = & \frac{1}{\int_0^1 \rho J_0^2(\sqrt{\gamma_0^* \rho}) d\rho} \int_0^1 \rho J_0(\sqrt{\gamma_0^* \rho}) [2J_0(\sqrt{\gamma_0^* \rho}) - \gamma_1^*] \left\{ -\frac{\pi}{2} \int_0^\rho \bar{\rho} J_0(\sqrt{\gamma_0^* \bar{\rho}}) \right. \\ & \times Y_0(\sqrt{\gamma_0^* \bar{\rho}}) [J_0(\sqrt{\gamma_0^* \bar{\rho}}) - \gamma_1^*] d\bar{\rho} J_0(\sqrt{\gamma_0^* \rho}) \\ & \left. + \frac{\pi}{2} \int_0^\rho \bar{\rho} J_0^2(\sqrt{\gamma_0^* \bar{\rho}}) [J_0(\sqrt{\gamma_0^* \bar{\rho}}) - \gamma_1^*] d\bar{\rho} Y_0(\sqrt{\gamma_0^* \rho}) \right\} d\rho . \quad (C.66) \end{aligned}$$

The approximations to  $\gamma^*$  and  $n$  are now available in integral form to the extent shown below:

$$\gamma^* \sim \gamma_0^* + \epsilon^* \gamma_1^* + \epsilon^{*2} \gamma_2^* \quad (C.67)$$

$$n \sim n_0 + \epsilon^* n_1 . \quad (C.68)$$

Appendix D

EXPANSIONS OF TRIGONOMETRIC FUNCTIONS

In expanding the main-region solution for  $y$  near 1, it is convenient to have available series for the various terms which occur. These series are listed below for reference.

Let

$$x = 1 - y \quad . \quad (D.1)$$

Then

$$\sin \frac{\pi}{2} y = \cos \frac{\pi}{2} x = 1 - \frac{\pi^2}{8} x^2 + 0(x^4) \quad (D.2)$$

$$\cos \frac{\pi}{2} y = \sin \frac{\pi}{2} x = \frac{\pi}{2} x - \frac{\pi^3}{48} x^3 + 0(x^5) \quad (D.3)$$

$$\begin{aligned} \cos^2 \frac{\pi}{2} y &= \left( \frac{\pi}{2} x - \frac{\pi^3}{48} x^3 + 0(x^5) \right)^2 \\ &= \frac{\pi^2}{4} x^2 + 0(x^4) \end{aligned} \quad (D.4)$$

$$\begin{aligned} y \sin \frac{\pi}{2} y &= (1 - x) \left( 1 - \frac{\pi^2}{8} x^2 + 0(x^4) \right) \\ &= 1 - x - \frac{\pi^2}{8} x^2 + \frac{\pi^2}{8} x^3 + 0(x^4) \end{aligned} \quad (D.5)$$

$$\begin{aligned} (y - \sin \frac{\pi}{2} y) \cos \frac{\pi}{2} y &= (1 - x - 1 + \frac{\pi^2}{8} x^2 + 0(x^4)) \left( \frac{\pi}{2} x - \frac{\pi^3}{48} x^3 + 0(x^5) \right) \\ &= -\frac{\pi}{2} x^2 + \frac{\pi^3}{16} x^3 + 0(x^4) \end{aligned} \quad (D.6)$$

$$\begin{aligned} \sec \frac{\pi}{2} y &= \frac{1}{\sin \frac{\pi}{2} x} = \frac{2}{\pi x} \frac{1}{1 - \frac{\pi^2}{24} x^2 + 0(x^4)} \\ &= \frac{2}{\pi} \frac{1}{x} + \frac{\pi}{12} x + 0(x^3) \end{aligned} \quad (D.7)$$

$$\begin{aligned}\tan \frac{\pi}{2} y &= \sin \frac{\pi}{2} y \sec \frac{\pi}{2} y \\ &= \left(1 - \frac{\pi^2}{8} x^2 + 0(x^4)\right) \left(\frac{2}{\pi} \frac{1}{x} + \frac{\pi}{12} x + 0(x^3)\right) \\ &= \frac{2}{\pi} \frac{1}{x} - \frac{\pi}{6} x + 0(x^3)\end{aligned}\tag{D.8}$$

$$\begin{aligned}\sec \frac{\pi}{2} y \tan \frac{\pi}{2} y &= \left(\frac{2}{\pi} \frac{1}{x} + \frac{\pi}{12} x + 0(x^3)\right) \left(\frac{2}{\pi} \frac{1}{x} - \frac{\pi}{6} x + 0(x^3)\right) \\ &= \frac{4}{\pi^2} \frac{1}{x^2} - \frac{1}{6} + 0(x^2)\end{aligned}\tag{D.9}$$

$$\begin{aligned}\sec^2 \frac{\pi}{2} y &= \left(\frac{2}{\pi} \frac{1}{x} + \frac{\pi}{12} x + 0(x^3)\right)^2 \\ &= \frac{4}{\pi^2} \frac{1}{x^2} + \frac{1}{3} + 0(x^2)\end{aligned}\tag{D.10}$$

$$\begin{aligned}y \sec^2 \frac{\pi}{2} y &= (1 - x) \left(\frac{4}{\pi^2} \frac{1}{x^2} + \frac{1}{3} + 0(x^2)\right) \\ &= \frac{4}{\pi^2} \frac{1}{x^2} - \frac{4}{\pi^2} \frac{1}{x} + \frac{1}{3} - \frac{1}{3} x + 0(x^2)\end{aligned}\tag{D.11}$$

$$\begin{aligned}\sec^2 \frac{\pi}{2} y \tan \frac{\pi}{2} y &= \left(\frac{4}{\pi^2} \frac{1}{x^2} + \frac{1}{3} + 0(x^2)\right) \left(\frac{2}{\pi} \frac{1}{x} - \frac{\pi}{6} x + 0(x^3)\right) \\ &= \frac{8}{\pi^3} \frac{1}{x^3} + 0(x)\end{aligned}\tag{D.12}$$

$$\begin{aligned}y \sec^2 \frac{\pi}{2} y \tan \frac{\pi}{2} y &= (1 - x) \left(\frac{8}{\pi^3} \frac{1}{x^3} + 0(x)\right) \\ &= \frac{8}{\pi^3} \frac{1}{x^3} - \frac{8}{\pi^3} \frac{1}{x^2} + 0(x)\end{aligned}\tag{D.13}$$

$$\begin{aligned}\sec \frac{\pi}{2} y \tan^2 \frac{\pi}{2} y &= \left( \frac{4}{\pi} \frac{1}{x} - \frac{1}{6} + o(x^2) \right) \left( \frac{2}{\pi} \frac{1}{x} - \frac{\pi}{6} x + o(x^3) \right) \\ &= \frac{8}{\pi} \frac{1}{x} - \frac{1}{\pi} \frac{1}{x} + o(x) \quad . \quad (D.14)\end{aligned}$$

Appendix E

DETERMINATION OF  $\gamma_0^*$  AND  $\gamma_1^*$  BY MATCHING

The zero-order problem for  $n_{eo}$  is solved in Section 3 using the condition  $n_{eo}(1) = 0$ . Here the same equations are solved once more, but without applying any boundary conditions. The solution contains the constants  $\gamma_0^*$  and  $\gamma_1^*$ , and these are determined by matching  $n_{eo}$  to the asymptotic expression for  $n_e$  in the sheath. The results are the same as those obtained in Section 3.

The problem is represented by Eqs. (3.11) - (3.13) and is given below:

$$\frac{d^2 n_{eo}}{dy^2} + \gamma^* n_{eo} - \epsilon^* n_{eo}^2 = 0 \quad (\text{E.1})$$

$$y = 0 : \quad n_{eo} = 1 \quad (\text{E.2})$$

$$\frac{dn_{eo}}{dy} = 0 \quad (\text{E.3})$$

$n_{eo}$  and the parameter  $\gamma^*$  are expanded as in (3.15) and (3.16):

$$n_{eo} = n_o + \epsilon^* n_1 + \dots \quad (\text{E.4})$$

$$\gamma^* = \gamma_o^* + \epsilon^* \gamma_1^* + \dots \quad (\text{E.5})$$

To lowest order in powers of  $\epsilon^*$  the problem becomes

$$\frac{d^2 n_o}{dy^2} + \gamma_o^* n_o = 0 \quad (\text{E.6})$$

$$y = 0 : \quad n_o = 1 \quad (\text{E.7})$$

$$\frac{dn_o}{dy} = 0 \quad (E.8)$$

and has the solution

$$n_o = \cos \sqrt{\gamma_o^*} y \quad (E.9)$$

where  $\gamma_o^*$  is unknown.

The equation for  $n_1$  is

$$\frac{d^2 n_1}{dy^2} + \gamma_o^* n_1 = n_o^2 - \gamma_1^* n_o \quad (E.10)$$

$$= \cos^2 \sqrt{\gamma_o^*} y - \gamma_1^* \cos \sqrt{\gamma_o^*} y \quad (E.11)$$

$$y = 0 : \quad n_1 = 0 \quad (E.12)$$

$$\frac{dn_1}{dy} = 0 \quad (E.13)$$

The solution to (E.11) - (E.13) is easily obtained as

$$n_1 = \frac{2}{3\gamma_o^*} - \frac{1}{3\gamma_o^*} \cos \sqrt{\gamma_o^*} y - \frac{1}{3\gamma_o^*} \cos^2 \sqrt{\gamma_o^*} y - \frac{\gamma_1^*}{2\sqrt{\gamma_o^*}} y \sin \sqrt{\gamma_o^*} y \quad (E.14)$$

so

$$n_{eo} = \cos \sqrt{\gamma_o^*} y + \epsilon^* \left[ \frac{2}{3\gamma_o^*} - \frac{1}{3\gamma_o^*} \cos \sqrt{\gamma_o^*} y - \frac{1}{3\gamma_o^*} \cos^2 \sqrt{\gamma_o^*} y - \frac{\gamma_1^*}{2\sqrt{\gamma_o^*}} y \sin \sqrt{\gamma_o^*} y \right] \quad (E.15)$$

Before this expression can be compared with the sheath solution, it is necessary to expand it for  $y$  near 1. The expansions are

carried out and the matching is performed only as far as is necessary to determine  $\gamma_0^*$  and  $\gamma_1^*$ . Taylor series expansions of the trigonometric functions occurring in (E.15) are listed below:

$$\cos^2 \sqrt{\gamma_0^*} y = \cos \sqrt{\gamma_0^*} + \sqrt{\gamma_0^*} (\sin \sqrt{\gamma_0^*}) (1 - y) + \dots \quad (\text{E.16})$$

$$\cos^2 \sqrt{\gamma_0^*} y = \cos^2 \sqrt{\gamma_0^*} + 2 \sqrt{\gamma_0^*} (\cos \sqrt{\gamma_0^*}) (\sin \sqrt{\gamma_0^*}) (1 - y) + \dots \quad (\text{E.17})$$

$$y \sin \sqrt{\gamma_0^*} y = \sin \sqrt{\gamma_0^*} - (\sin \sqrt{\gamma_0^*} + \sqrt{\gamma_0^*} \cos \sqrt{\gamma_0^*}) (1 - y) + \dots \quad (\text{E.18})$$

Substituting these results into (E.15) and rearranging,

$$\begin{aligned} n_{eo} = & \cos \sqrt{\gamma_0^*} + \varepsilon^* \left[ \frac{2}{3\gamma_0^*} - \frac{1}{3\gamma_0^*} \cos \sqrt{\gamma_0^*} - \frac{1}{3\gamma_0^*} \cos^2 \sqrt{\gamma_0^*} \right. \\ & \left. - \frac{\gamma_1^*}{2\sqrt{\gamma_0^*}} \sin \sqrt{\gamma_0^*} \right] + \left\{ \sqrt{\gamma_0^*} \sin \sqrt{\gamma_0^*} + \varepsilon^* \left[ \frac{-1}{3\sqrt{\gamma_0^*}} \sin \sqrt{\gamma_0^*} \right. \right. \\ & \left. \left. - \frac{2}{3\sqrt{\gamma_0^*}} \cos \sqrt{\gamma_0^*} \sin \sqrt{\gamma_0^*} + \left( \frac{\gamma_1^*}{2\sqrt{\gamma_0^*}} \sin \sqrt{\gamma_0^*} + \frac{\gamma_1^*}{2} \cos \sqrt{\gamma_0^*} \right) \right] \right\} (1 - y) \\ & + O((1 - y)^2) \quad . \quad (\text{E.19}) \end{aligned}$$

From the sheath we need only the largest contribution to the asymptotic solution in Eq. (6.29):

$$\tilde{n}_e \sim \rho_0 \tilde{J}(0) \xi \quad . \quad (\text{E.20})$$

The main-region and sheath solutions are written in terms of the intermediate variable  $x_\eta$  through the use of (5.42) and (5.43). Using

also (2.2), (E.19) becomes

$$\begin{aligned}
 \text{(main region): } n_e \sim & \cos\sqrt{\gamma_o^*} + \epsilon^* \left[ \frac{2}{3\gamma_o^*} - \frac{1}{3\gamma_o^*} \cos\sqrt{\gamma_o^*} - \frac{1}{3\gamma_o^*} \cos^3\sqrt{\gamma_o^*} \right. \\
 & - \frac{\gamma_1^*}{2\sqrt{\gamma_o^*}} \sin\sqrt{\gamma_o^*} \left. \right] + \left\{ \sqrt{\gamma_o^*} \sin\sqrt{\gamma_o^*} + \epsilon^* \left[ \frac{-1}{3\sqrt{\gamma_o^*}} \sin\sqrt{\gamma_o^*} \right. \right. \\
 & \left. \left. - \frac{2}{3\sqrt{\gamma_o^*}} \cos\sqrt{\gamma_o^*} \sin\sqrt{\gamma_o^*} + \left( -\frac{\gamma_1^*}{2\sqrt{\gamma_o^*}} + \frac{\gamma_1^*}{2} \cos\sqrt{\gamma_o^*} \right) \right] \right\} \eta \ x_\eta
 \end{aligned} \tag{E.21}$$

Using (2.47) in (E.20)

$$\text{(sheath): } n_e \sim \rho_o J_o(0) \eta \ x_\eta \tag{E.22}$$

In order that these two expressions agree, the constant term in (E.21) must equal zero:

$$\cos\sqrt{\gamma_o^*} + \epsilon^* \left[ \frac{2}{3\gamma_o^*} - \frac{1}{3\gamma_o^*} \cos\sqrt{\gamma_o^*} - \frac{1}{3\gamma_o^*} \cos^2\sqrt{\gamma_o^*} - \frac{\gamma_1^*}{2\sqrt{\gamma_o^*}} \sin\sqrt{\gamma_o^*} \right] = 0 \tag{E.23}$$

Since Eq. (E.23) must be an identity in  $\epsilon^*$ , both terms must vanish.

Then

$$\cos\sqrt{\gamma_o^*} = 0 \tag{E.24}$$

implies

$$\gamma_o^* = \frac{\pi^2}{4} \tag{E.25}$$

Using (E-25) in (E.23), the equation for the quantity in brackets becomes

$$\frac{8}{3\pi^2} - \frac{\gamma_1^*}{\pi} = 0 \quad (\text{E.26})$$

or

$$\gamma_1^* = \frac{8}{3\pi} \quad (\text{E.27})$$

It should be observed that the expressions for  $\gamma_0^*$  and  $\gamma_1^*$  in (E.25) and (E.26) are the same as those in (3.24) and (3.38). Using these results, (E.21) becomes

$$(\text{main region}): \quad n_e \sim \left\{ \frac{\pi}{2} + \epsilon^* \left[ -\frac{2}{3\pi} + \frac{8}{3\pi^2} \right] \right\} \eta \quad (\text{E.28})$$

The main-region and sheath solutions now agree provided

$$\rho_0 \tilde{J}(0) = \frac{\pi}{2} + \epsilon^* \left[ \frac{8}{3\pi^2} - \frac{2}{3\pi} \right] \quad (\text{E.29})$$

Using (3.9), Eq. (E.29) for  $\tilde{J}(0)$  becomes

$$\tilde{J}(0) = \frac{\pi}{2} \frac{1}{\rho_0} + \frac{4}{3\pi^2} \left( 2 - \frac{\pi}{2} \right) \epsilon_0 \zeta \quad (\text{E.30})$$

This result is the same as that obtained in Eq. (7.5). If (E.25) and (E.27) are used in (E.15), we obtain

$$n_{e0} = \cos \frac{\pi}{2} y + \frac{4}{3\pi^2} \left[ 2 - \cos \frac{\pi}{2} y - \cos^2 \frac{\pi}{2} y - 2y \sin \frac{\pi}{2} y \right] \epsilon^* \quad (\text{E.31})$$

This result is also the same as that obtained previously.

It is clear that the method employed here leads to results identical to those obtained in the main body of Part II.

NOMENCLATURE

The number following the descriptions gives the page on which the symbol first appears. Symbols whose use is very temporary and those which have been defined previously in Part I usually do not appear here.

Roman:

$a$	$= (2/3)(\epsilon^*/\gamma^*)$ in Section 3 (152)
$E_n$	$n^{\text{th}}$ term of the expansion for $E$ (128)
$\hat{E}_{za}$	ambipolar value of the axial electric field (111)
$\tilde{E}$	electric field in the sheath (138)
$\tilde{E}_0$	zero-order approximation to $\tilde{E}$ (180)
$F(x,k)$	elliptic integral of the first kind (156)
$F(\phi,k)$	elliptic integral of the first kind (157)
$J_0$	zero-order Bessel function of the first kind (248)
$J_n$	$n^{\text{th}}$ term of the expansion for $J$ (128)
$\tilde{J}$	electron and ion flux in the sheath (138)
$\tilde{J}_0$	zero-order approximation to $\tilde{J}$ (180)
$k$	modulus of the elliptic integral (154)
$L$	linear differential operator (245)
$n$	$= n_{e0}$ in Section 3 (143)
$n_n$	$n^{\text{th}}$ term of the series for $n$ in Section 3 (143)
$n_{en}$	$n^{\text{th}}$ term of the expansion for $n_e$ (128)
$n_o^{(1)}$	root of a cubic algebraic equation in Section 3 (153)
$n_o^{(2)}$	root of a cubic algebraic equation in Section 3 (153)
$\bar{n}$	$= n_{e1}$ in Section 4 (170)

$\bar{n}_n$	$n^{\text{th}}$ term of the series for $\bar{n}$ in Section 4 (170)
$\tilde{n}_e$	electron density in the sheath (138)
$\tilde{n}_i$	ion density in the sheath (138)
$\tilde{n}_{e0}$	zero-order approximation to $\tilde{n}_e$ (180)
$\tilde{n}_{i0}$	zero-order approximation to $\tilde{n}_i$ (180)
$q$	introduced for notational simplicity (171)
$s$	space-charge variable (123)
$s_n$	$n^{\text{th}}$ term of the expansion for $s$ (128)
$\tilde{s}$	space-charge variable in the sheath (204)
$x$	$= \sqrt{\gamma^*} y$ in Section 3 (150) $= 1 - y$ in Appendix D (256)
$x_\eta$	intermediate variable used in matching (188)
$Y_0$	zero-order Bessel function of the second kind (249)
$z$	variable used in Section 3 (154)

Greek:

$\gamma_a$	ambipolar value of $\gamma$ (145)
$\gamma_n$	$n^{\text{th}}$ term of the expansion for $\gamma$ (129)
$\gamma^*$	$= \gamma_0 \rho_0$ in Section 3 (142)
$\gamma_n^*$	$n^{\text{th}}$ term of the series for $\gamma^*$ in Section 3 (143)
$\delta_n$	$n^{\text{th}}$ term of the expansion for $\delta$ (129)
$\epsilon_n$	$n^{\text{th}}$ term of the expansion for $\epsilon$ (129)
$\epsilon^*$	$= \epsilon_0 \zeta \rho_0$ in Sections 3 and 4 (143)
$\eta(\zeta)$	provides a measure of the location of the zone between main region and sheath (188)
$\mu_n(\zeta)$	Asymptotic sequence of functions used in expansions (128)
$\xi$	independent variable in the sheath (138)

- $\rho$  independent variable in cylindrical geometry (247)
- $\rho_0$  introduced for notational simplicity (130)
- $\tau_n$   $n^{\text{th}}$  term of the expansion for  $\tau$  (129)
- $\phi_0 = \sin^{-1}(1/(k\sqrt{n_0^{(1)}}))$  (157)
- $\phi_n = \sin^{-1}(\sqrt{1-n}/(k\sqrt{n_0^{(1)}-n}))$  (157)
- $\chi_n$   $n^{\text{th}}$  term of the expansion for  $\chi$  (129)

LIST OF TABLES

1. Comparison of Approximate and Exact  $\epsilon^* - \gamma^*$  Relations
2. Comparison of Approximate and Exact Solutions for  $n_{eo}$
3. Comparison of Approximate and Exact Solutions for  $n_{eo}$
4. Comparison of Approximate and Exact Solutions for  $n_{eo}$
5. Convergence of the Iteration for  $\tilde{E}_0(0)$
6.  $\tilde{E}_0(0)$  and  $\tilde{E}(0)$  as Functions of  $\zeta$
7.  $\gamma_0$ ,  $\gamma_1$ , and  $\gamma$  as Functions of  $\zeta$
8.  $\hat{E}_z$  and  $\hat{E}_z/N_n$  as Functions of  $\zeta$

Table 1

COMPARISON OF APPROXIMATE AND EXACT  $\epsilon^* - \gamma^*$  RELATIONS

$\epsilon^*$	$\gamma^*$		$\epsilon^*/\gamma^*$	
	<u>exact</u>	<u>perturbation</u>	<u>exact</u>	<u>perturbation</u>
0.128842	2.576833	2.576833	0.05	0.05
0.269659	2.696589	2.696590	0.100	0.100
1.499793	3.749483	3.749592	0.400000	0.399988
4.385418	6.264882	6.267893	0.700000	0.699664
11.100918	12.334353	12.390164	0.900000	0.895946

Table 2

COMPARISON OF APPROXIMATE AND EXACT SOLUTIONS FOR  $n_{eo}$

$\epsilon^* = 0.269659$

$\gamma^* \text{ (exact)} = 2.696589$

$\gamma^* \text{ (perturbation)} = 2.696590$

$\epsilon^*/\gamma^* \text{ (exact)} = 0.100000$

$\epsilon^*/\gamma^* \text{ (perturbation)} = 0.100000$

<u>y</u>	<u>n (exact)</u>	<u>n (perturbation)</u>
0.	1.000000	1.000000
0.090847	0.990000	0.990001
0.128572	0.980000	0.980002
0.157586	0.970000	0.970003
0.182102	0.960000	0.960004
0.223366	0.940000	0.940006
0.258315	0.920000	0.920007
0.289250	0.900000	0.900009
0.317351	0.880000	0.880010
0.343316	0.860000	0.860011
0.367602	0.840000	0.840011
0.390524	0.820000	0.820012
0.412312	0.800000	0.800012
0.462871	0.750000	0.750012
0.509182	0.700000	0.700011
0.552349	0.650000	0.650010
0.593094	0.600000	0.600009
0.631924	0.550000	0.550007
0.669208	0.500000	0.500006
0.705229	0.450000	0.450004
0.740214	0.400000	0.400002
0.774343	0.350000	0.350001
0.807770	0.300000	0.300000
0.840625	0.250000	0.249999
0.873023	0.200000	0.199999
0.905068	0.150000	0.149999
0.936854	0.100000	0.099999
0.968469	0.050000	0.050000
1.000000	0.	0.

Table 3

COMPARISON OF APPROXIMATE AND EXACT SOLUTIONS FOR  $n_{eo}$

$$\epsilon^* = 1.499793$$

$$\gamma^* \text{ (exact)} = 3.749483$$

$$\gamma^* \text{ (perturbation)} = 3.749592$$

$$\epsilon^*/\gamma^* \text{ (exact)} = 0.400000$$

$$\epsilon^*/\gamma^* \text{ (perturbation)} = 0.399988$$

<u>y</u>	<u>n (exact)</u>	<u>n (perturbation)</u>
0.	1.000000	1.000000
0.094314	0.990000	0.990039
0.133418	0.980000	0.980075
0.163450	0.970000	0.970108
0.188792	0.960000	0.960140
0.231361	0.940000	0.940195
0.267320	0.920000	0.920242
0.299065	0.900000	0.900281
0.327827	0.880000	0.880312
0.354336	0.860000	0.860337
0.379068	0.840000	0.840355
0.402354	0.820000	0.820368
0.424435	0.800000	0.800376
0.475463	0.750000	0.750376
0.521938	0.700000	0.700355
0.565021	0.650000	0.650318
0.605478	0.600000	0.600272
0.643842	0.550000	0.550221
0.680508	0.500000	0.500170
0.715778	0.450000	0.450120
0.749893	0.400000	0.400076
0.783049	0.350000	0.350038
0.815411	0.300000	0.300008
0.847123	0.250000	0.249988
0.878309	0.200000	0.199977
0.909086	0.150000	0.149973
0.939559	0.100000	0.099978
0.969830	0.050000	0.049987
1.000000	0.	0.

Table 4

COMPARISON OF APPROXIMATE AND EXACT SOLUTIONS FOR  $n_{eo}$

$$\varepsilon^* = 4.385418$$

$$\gamma^* \text{ (exact)} = 6.264882$$

$$\gamma^* \text{ (perturbation)} = 6.267893$$

$$\varepsilon^*/\gamma^* \text{ (exact)} = 0.700000$$

$$\varepsilon^*/\gamma^* \text{ (perturbation)} = 0.699664$$

<u>y</u>	<u>n (exact)</u>	<u>n (perturbation)</u>
0.	1.000000	1.000000
0.103043	0.990000	0.990383
0.145568	0.980000	0.980735
0.178095	0.970000	0.971057
0.205433	0.960000	0.961352
0.251095	0.940000	0.941863
0.289376	0.920000	0.922280
0.322928	0.900000	0.902612
0.353115	0.880000	0.882869
0.380750	0.860000	0.863059
0.406365	0.840000	0.843191
0.430331	0.820000	0.823270
0.452918	0.800000	0.803305
0.504595	0.750000	0.753228
0.551024	0.700000	0.702982
0.593531	0.650000	0.652628
0.632988	0.600000	0.602215
0.670011	0.550000	0.551783
0.705053	0.500000	0.501360
0.738464	0.450000	0.450970
0.770521	0.400000	0.400628
0.801452	0.350000	0.350344
0.831448	0.300000	0.300125
0.860672	0.250000	0.249973
0.889273	0.200000	0.199884
0.917383	0.150000	0.149853
0.945127	0.100000	0.099871
0.972625	0.050000	0.049926
1.000000	0.	0.

Table 5

CONVERGENCE OF THE ITERATION FOR  $\tilde{E}_0(0)$

$$\zeta = 0.997823 \times 10^6$$

<u>n</u>	<u>z<sup>(n)</sup></u>	<u>g(z<sup>(n)</sup>)</u>
0	2.00000	2.00220
1	2.00220	2.00431
2	2.05348	2.05372
3	2.06013	2.06016
4	2.06114	2.06114
5	2.06116	

$$\tilde{E}_0(0) = 2.061$$

Table 6

$\tilde{E}_0(O)$  AND  $\tilde{E}(O)$  AS FUNCTIONS OF  $\zeta$

$\zeta$	$\tilde{E}_0(O)$	$\tilde{E}(O)$
$1.000 \times 10^2$	2.071	2.068
$3.162 \times 10^2$	2.071	2.068
$1.000 \times 10^3$	2.071	2.068
$3.162 \times 10^3$	2.071	2.068
$1.000 \times 10^4$	2.071	2.068
$3.162 \times 10^4$	2.070	2.068
$5.991 \times 10^4$	2.070	2.067
$1.214 \times 10^5$	2.069	2.067
$4.540 \times 10^5$	2.065	2.063
$9.978 \times 10^5$	2.061	2.059
$4.792 \times 10^6$	2.063	2.061
$1.094 \times 10^7$	2.099	2.097

Table 7

$\gamma_0$ ,  $\gamma_1$ , AND  $\gamma$  AS FUNCTIONS OF  $\zeta$

$\zeta$	$\gamma$	$\gamma_0$	$\gamma_1$	$\frac{1}{\zeta^{1/3}} \gamma_1$
$1.000 \times 10^2$	4.7458	2.4123	10.831	2.3334
$3.162 \times 10^2$	4.0021	2.4125	10.830	1.5896
$1.000 \times 10^3$	3.4959	2.4131	10.828	1.0828
$3.162 \times 10^3$	3.1524	2.4148	10.827	0.7376
$1.000 \times 10^4$	2.9228	2.4204	10.824	0.5024
$3.162 \times 10^4$	2.7799	2.4379	10.815	0.3420
$5.991 \times 10^4$	2.7366	2.4608	10.793	0.2758
$1.214 \times 10^5$	2.7278	2.5103	10.768	0.2175
$4.540 \times 10^5$	2.9112	2.7732	10.608	0.1380
$9.978 \times 10^5$	3.2923	3.1881	10.414	0.1042
$4.792 \times 10^6$	5.8654	5.8072	9.821	0.0583
$1.094 \times 10^7$	9.6857	9.6430	9.497	0.0428

Table 8

$\hat{E}_z$  AND  $\hat{E}_z/N_n$  AS FUNCTIONS OF  $\zeta$

$N_{e0}$ cm <sup>-3</sup>	$\hat{E}_z$ volt/cm	$\hat{E}_z/N_n$ volt-cm <sup>2</sup>
$1.000 \times 10^8$	23.44	$0.7289 \times 10^{-15}$
$3.162 \times 10^8$	22.73	$0.7067 \times 10^{-15}$
$1.000 \times 10^9$	22.19	$0.6901 \times 10^{-15}$
$3.162 \times 10^9$	21.80	$0.6779 \times 10^{-15}$
$1.000 \times 10^{10}$	21.53	$0.6693 \times 10^{-15}$
$3.162 \times 10^{10}$	21.35	$0.6638 \times 10^{-15}$
$5.991 \times 10^{10}$	21.29	$0.6621 \times 10^{-15}$
$1.214 \times 10^{11}$	21.28	$0.6617 \times 10^{-15}$
$4.540 \times 10^{11}$	21.51	$0.6689 \times 10^{-15}$
$9.978 \times 10^{11}$	21.97	$0.6830 \times 10^{-15}$
$4.792 \times 10^{12}$	24.40	$0.7586 \times 10^{-15}$
$1.094 \times 10^{13}$	27.02	$0.8402 \times 10^{-15}$

LIST OF FIGURES

1. Electron Production and Loss Rates as Functions of Electron Density
2. Sketch of  $N_{eo} - \hat{E}_z$  Relation
3.  $\epsilon^* - \gamma^*$  Relation
4.  $n_{eo}$  as a Function of  $y$  for Different Values of  $\epsilon^*$
5. Behavior of  $\tilde{E}_o(\xi)$  for Various  $\tilde{E}_o(0)$
6.  $\tilde{E}_o$ ,  $\tilde{n}_{eo}$ , and  $\tilde{n}_{io}$  as Functions of  $\xi$
7.  $\tilde{n}_{io}$  for Small  $\xi$
8. Behavior of  $\tilde{s}$  in Numerical Calculation of  $\tilde{E}(0)$
9.  $\zeta - \gamma$  Relation and the Relations Obtained by Separate Treatments of Recombination and Space Charge
10.  $N_{eo} - \hat{E}_z$  Relation

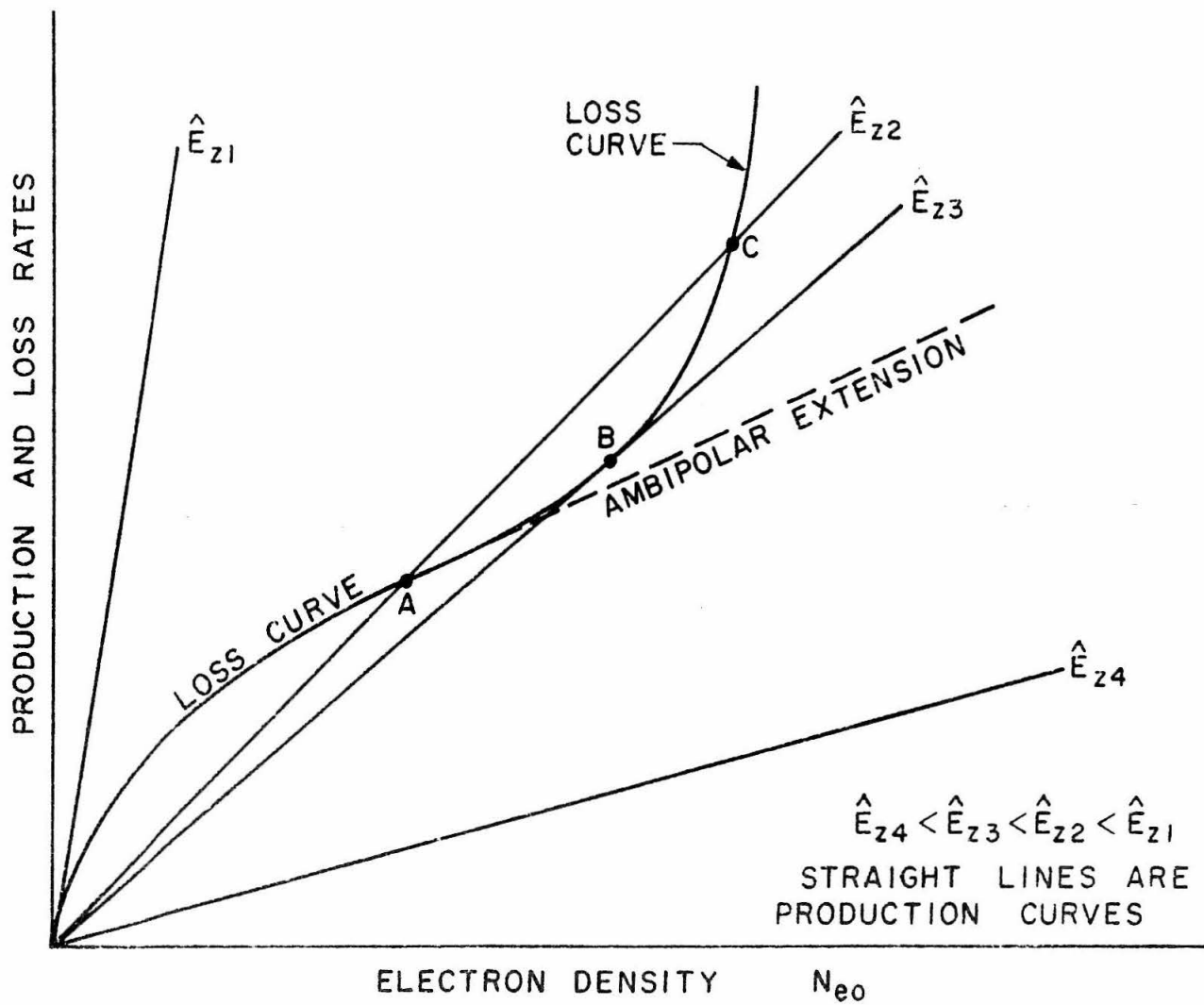


Figure 1: Electron Production and Loss Rates as Functions of Electron Density

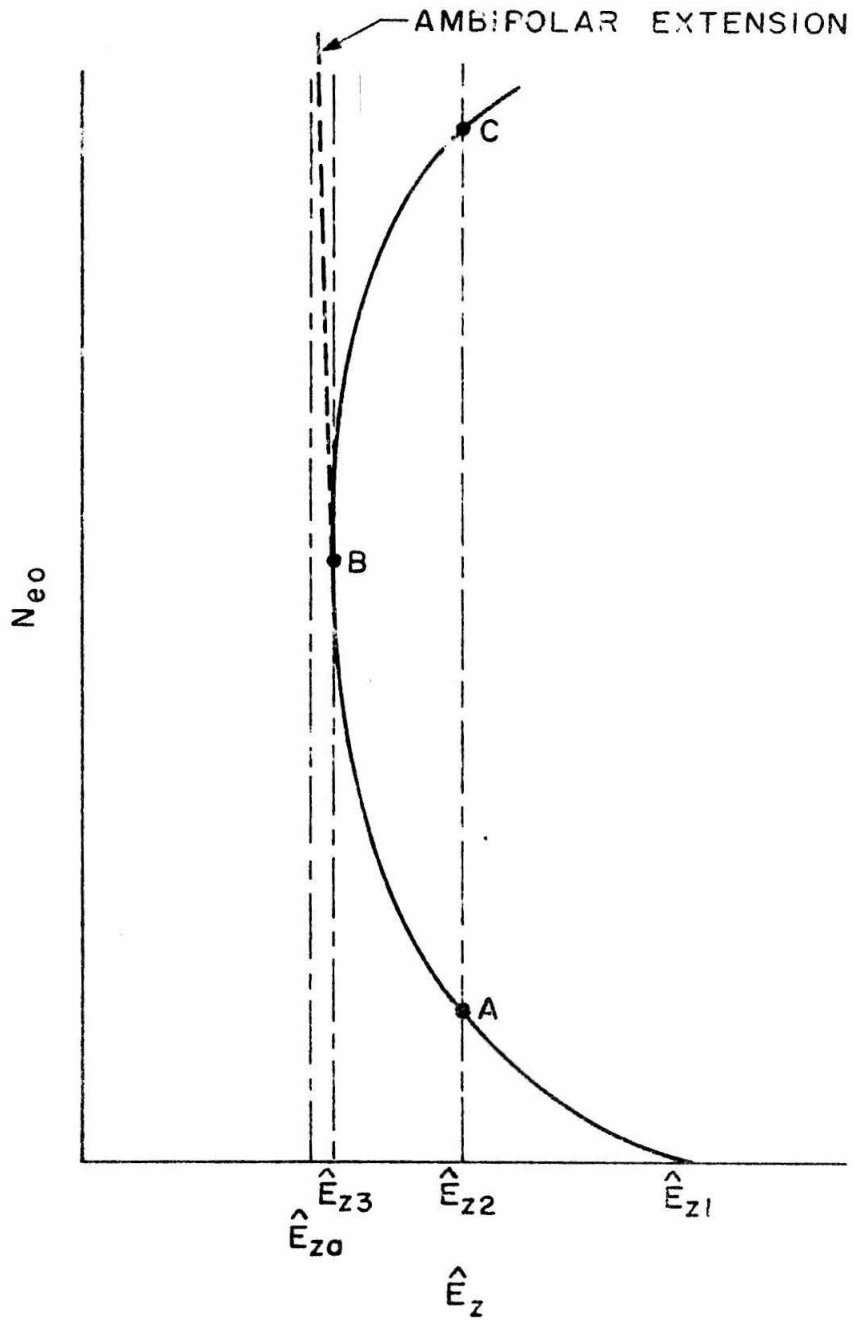


Figure 2: Sketch of  $N_{eo} - \hat{E}_z$  Relation

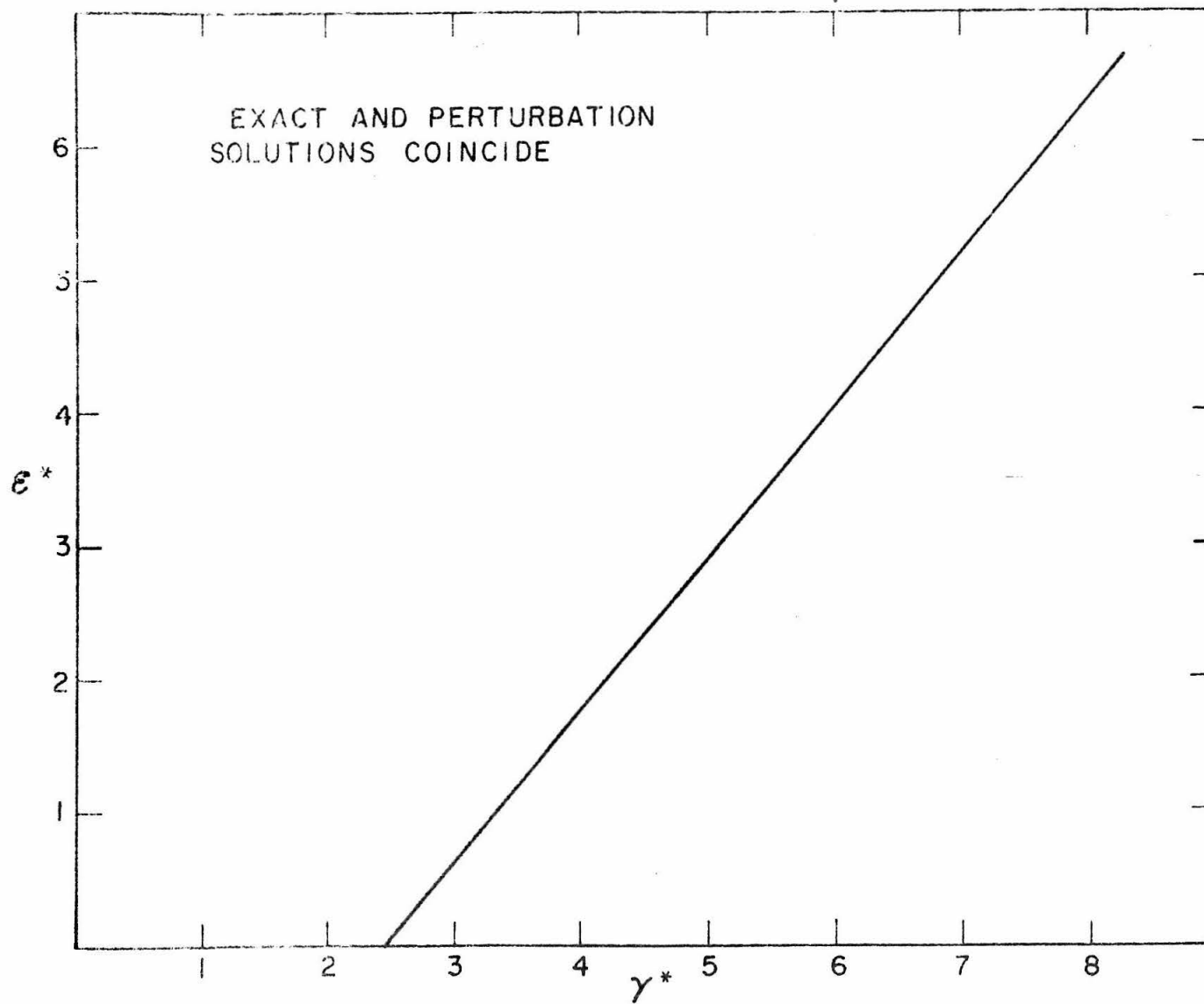


Figure 3:  $\epsilon^* - \gamma^*$  Relation

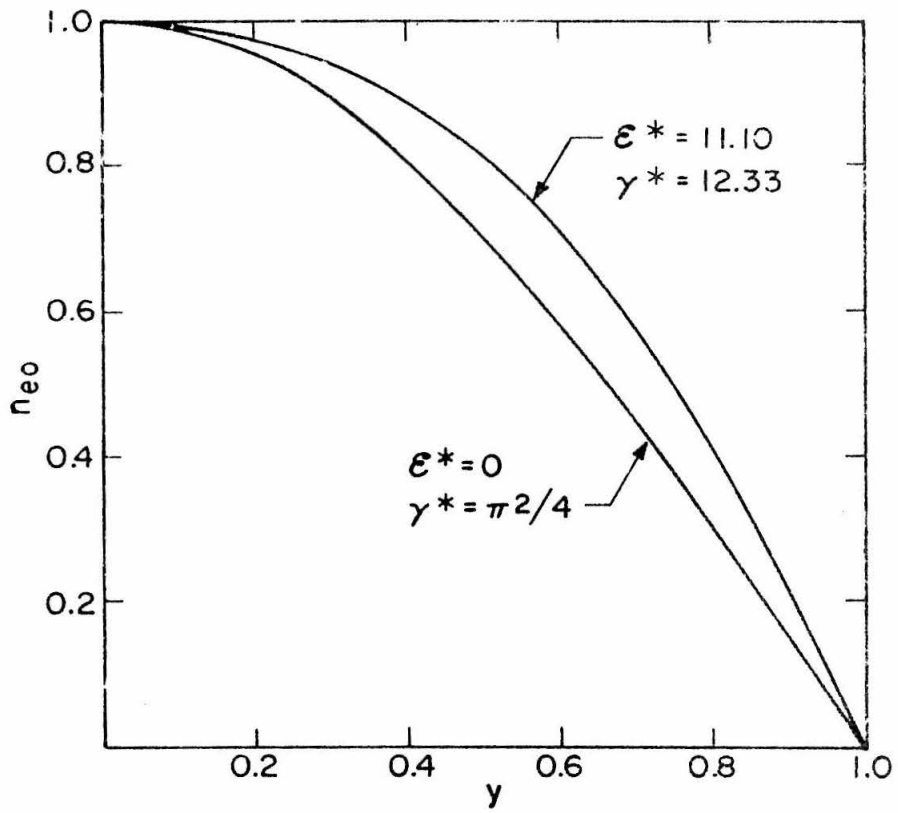


Figure 4:  $n_{eo}$  as a Function of  $y$  for Different Values of  $\epsilon^*$

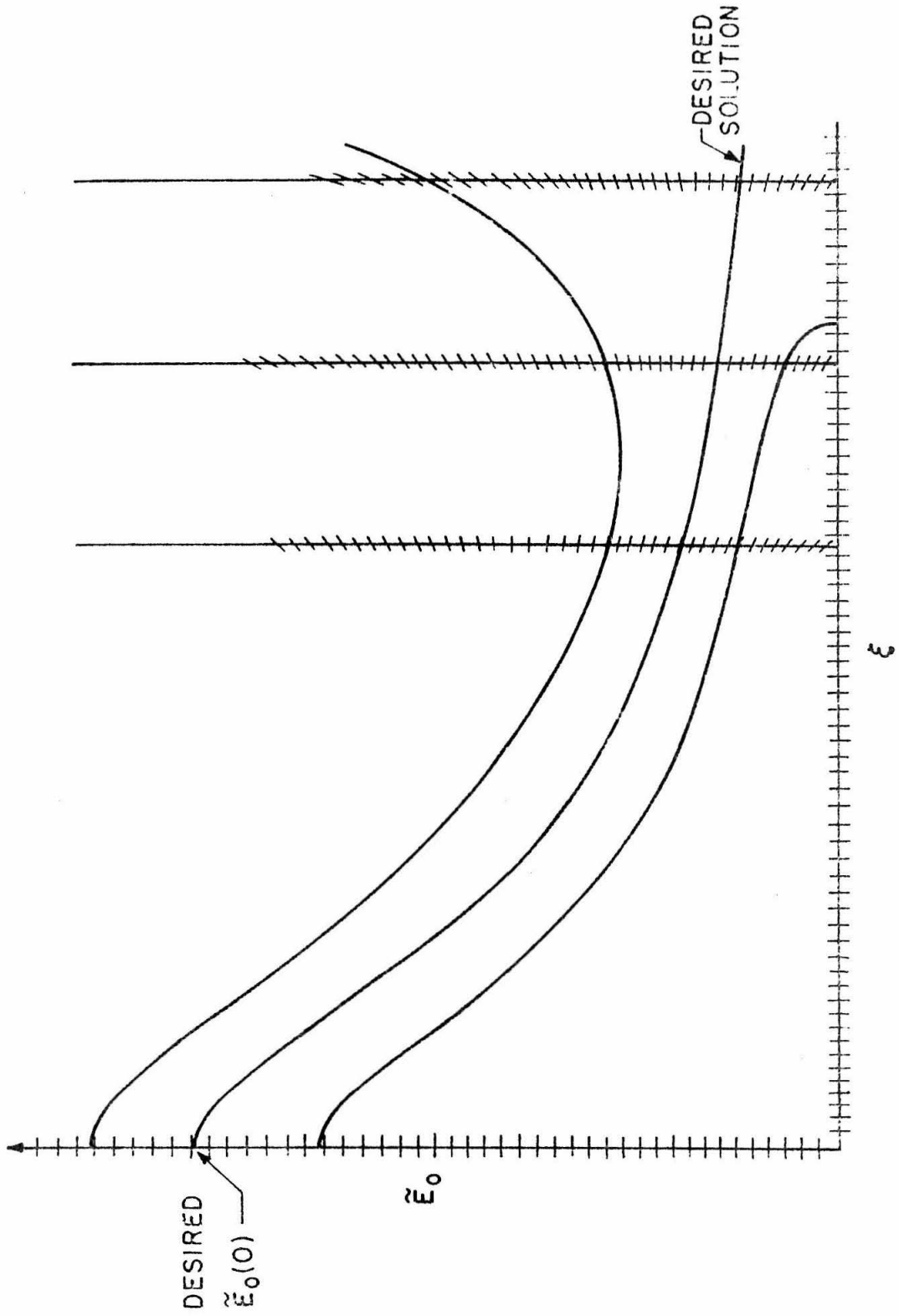


Figure 5: Behavior of  $E_0(\xi)$  for Various  $E_0(0)$

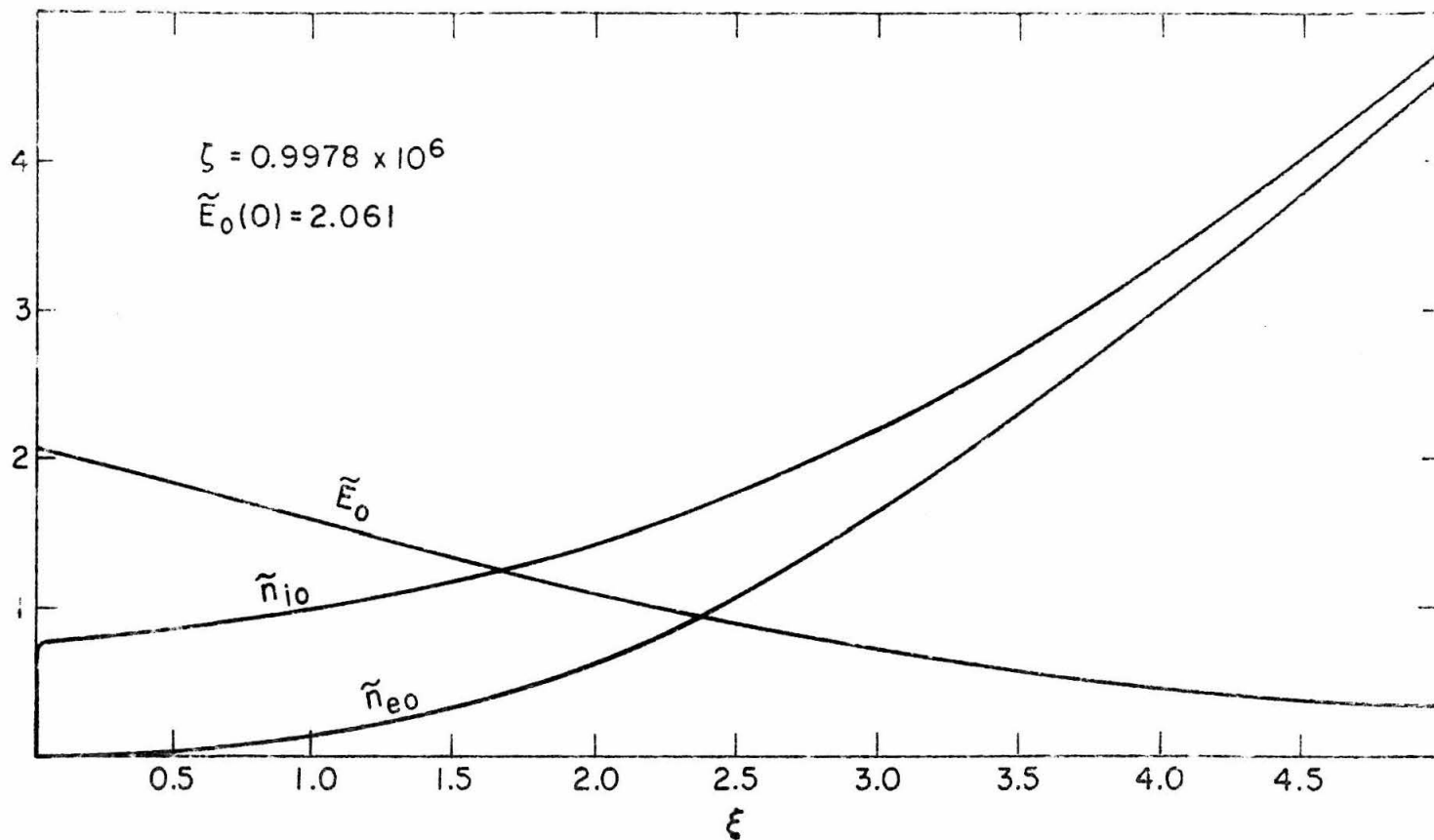


Figure 6:  $\tilde{E}_0$ ,  $\tilde{n}_{eo}$ , and  $\tilde{n}_{io}$  as Functions of  $\xi$

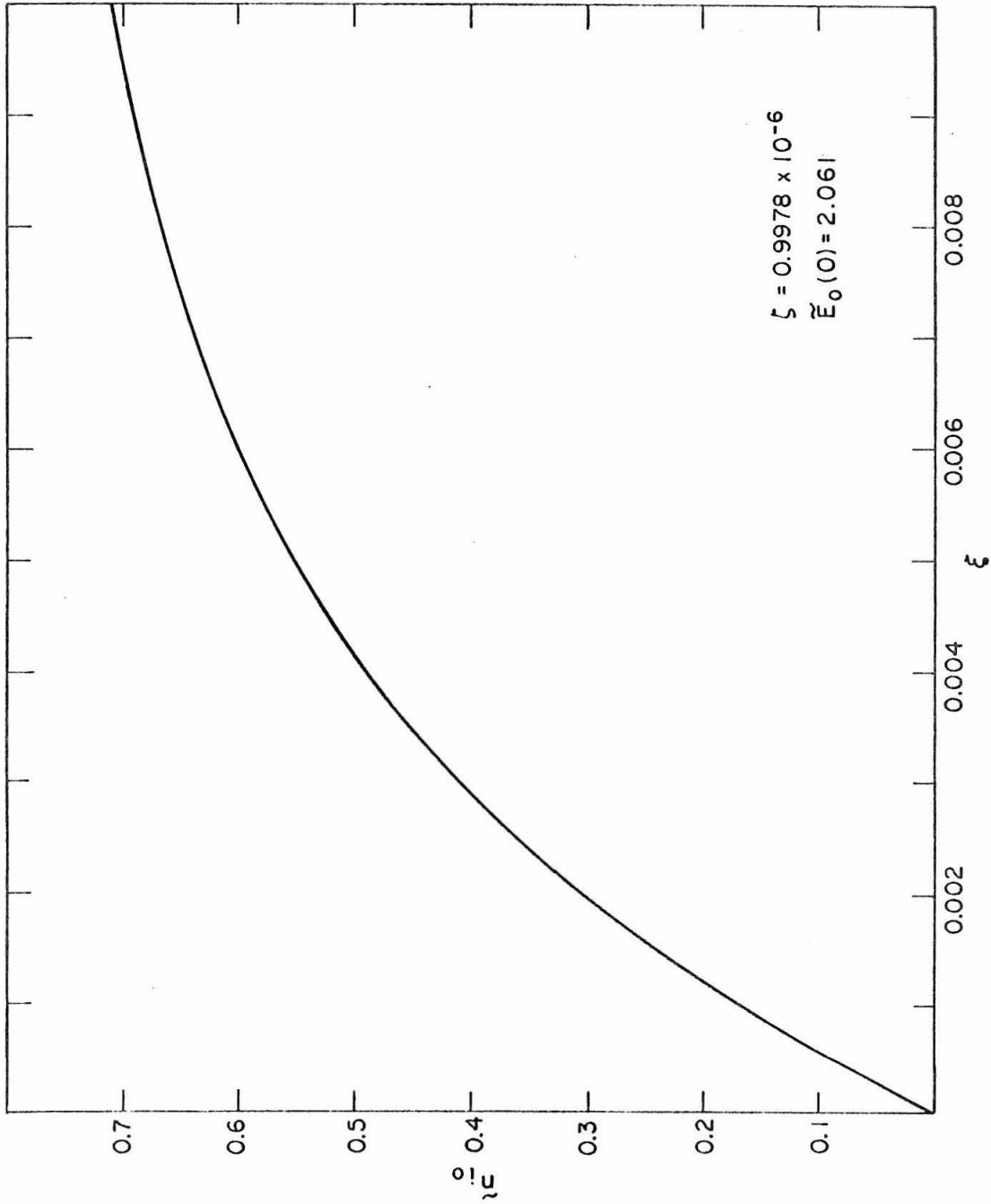


Figure 7:  $\tilde{n}_{i0}$  for Small  $\xi$

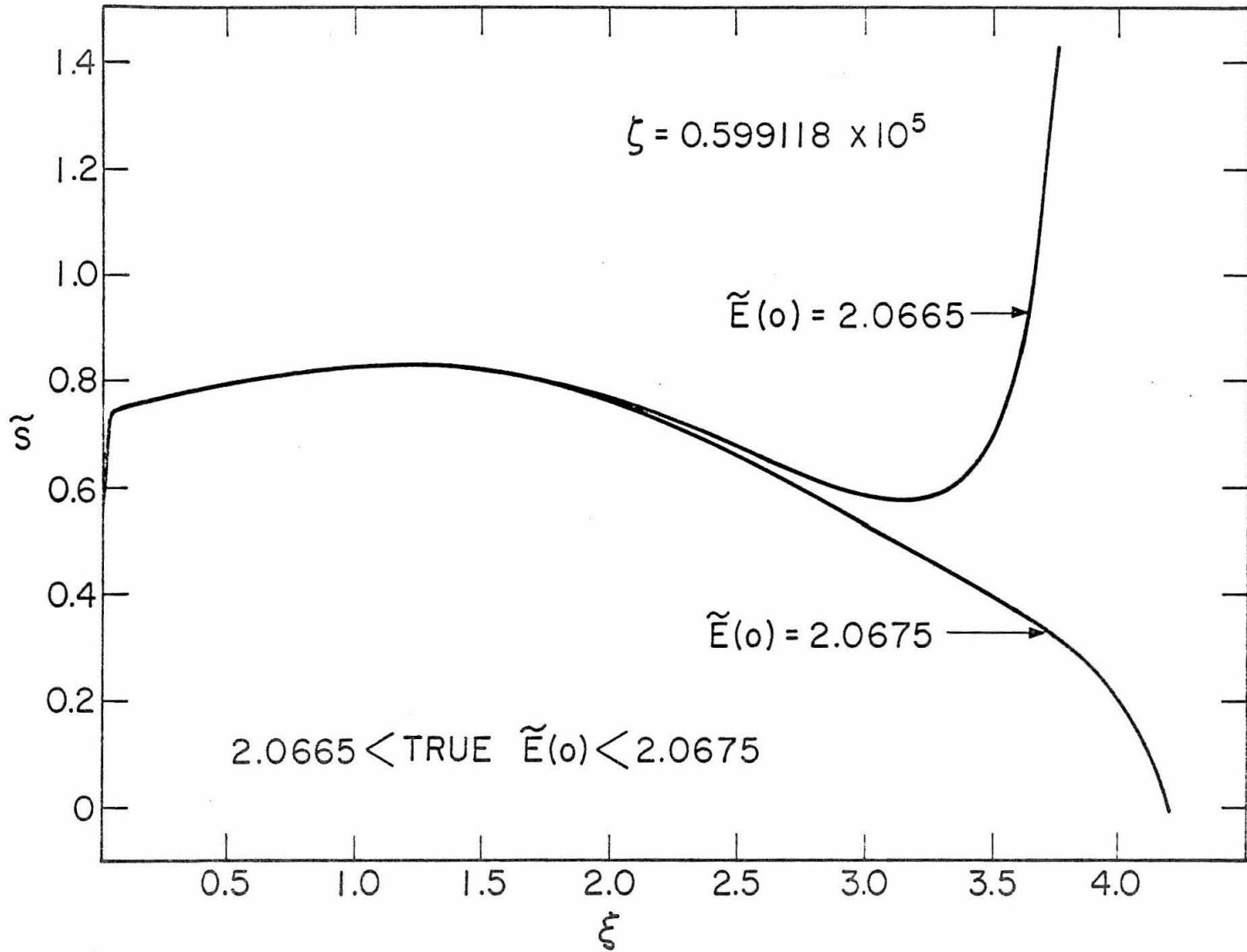


Figure 8: Behavior of  $\tilde{s}$  in Numerical Calculation of  $\tilde{E}(0)$

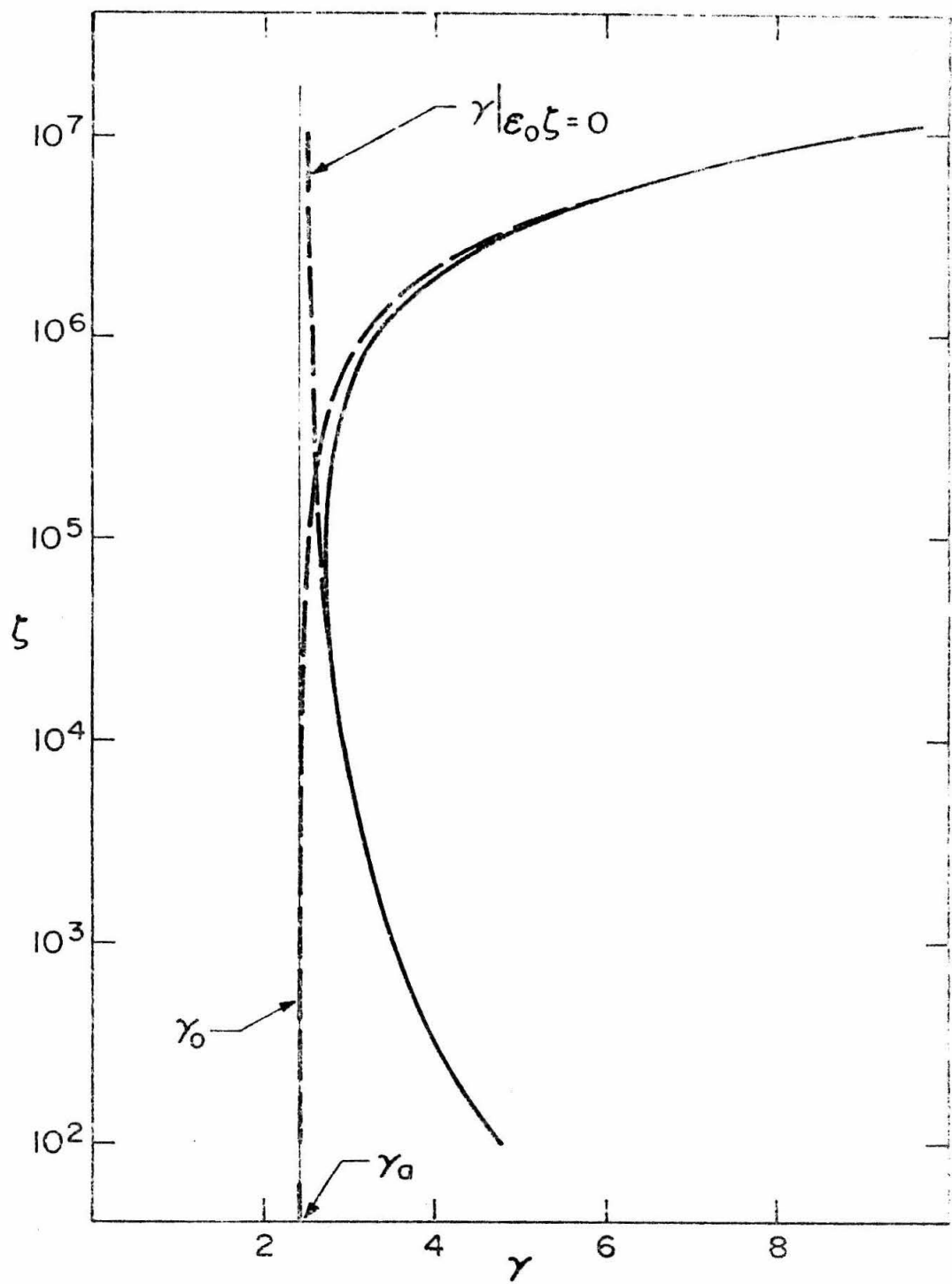


Figure 9:  $\zeta$ - $\gamma$  Relation and the Relations Obtained by Separate Treatments of Recombination and Space Charge

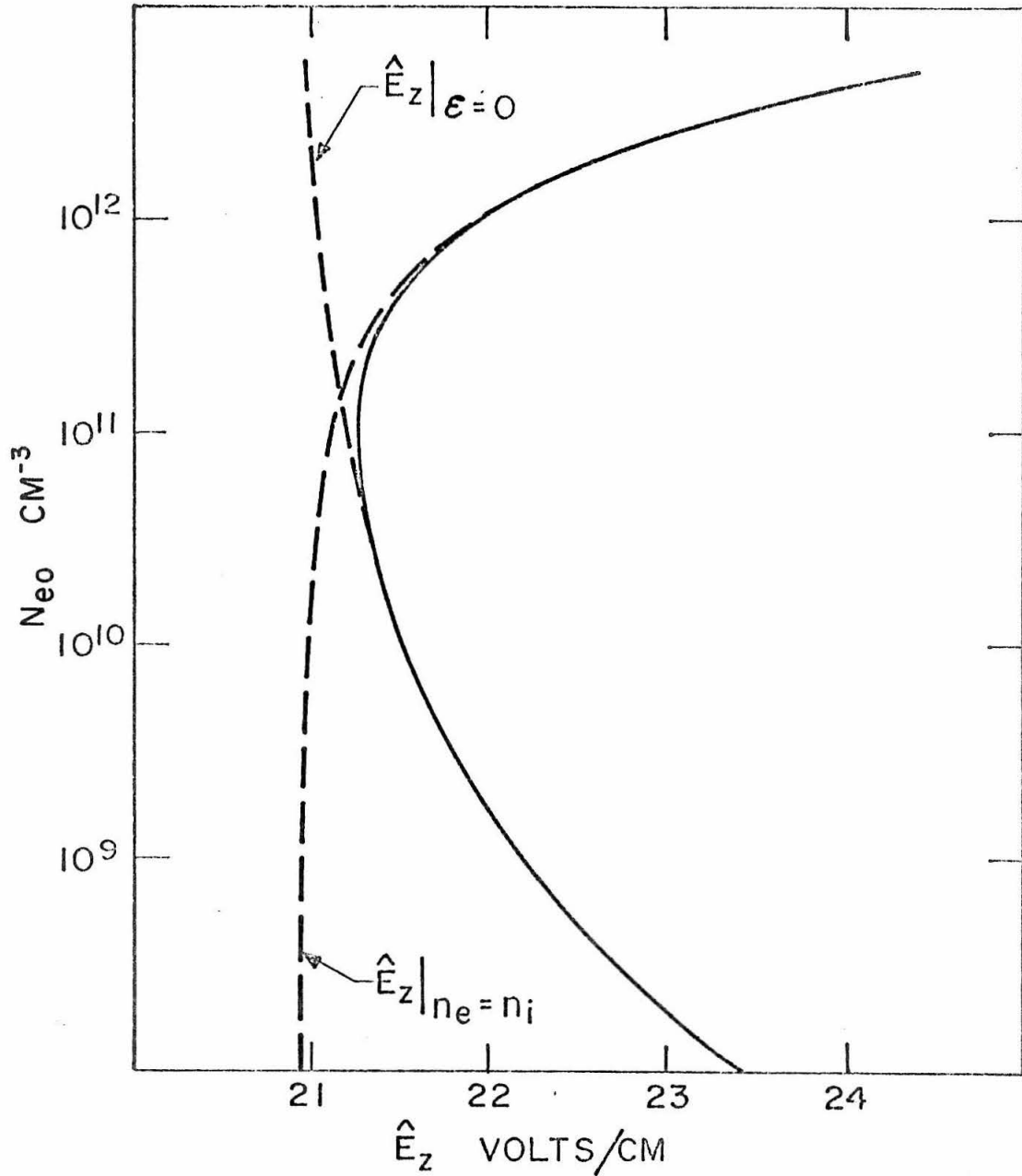


Figure 10:  $N_{eo} - \hat{E}_z$  Relation

BIBLIOGRAPHY

1. Abramowitz, Milton and Irene A. Stegun, Handbook of Mathematical Functions, National Bureau of Standards, 1964.
2. Allis, W. P. and D. J. Rose, "The Transition from Free to Ambipolar Diffusion," Physical Review 93, 84-93 (1954).
3. Cobine, James Dillon, Gaseous Conductors, Dover, 1958.
4. Cohen, Ira M., "Asymptotic Theory of Spherical Electrostatic Probes in a Slightly Ionized Collision-Dominated Gas," Physics of Fluids 6, 1492-1499 (1963).
5. Cohen, Ira M. and Martin D. Kruskal, "Asymptotic Theory of the Positive Column of a Gas Discharge," Physics of Fluids 8, 920-934 (1965).
6. Cole, Julian D., Perturbation Methods in Applied Mathematics, Blaisdell Publishing Co., 1968.
7. Davis, Harold T., Introduction to Nonlinear Differential and Integral Equations, Dover, 1962.
8. Friedman, Bernard, Principles and Techniques of Applied Mathematics Wiley & Sons, Inc., New York, 1956.
9. Isaacson, Eugene and Herbert Bishop Keller, Analysis of Numerical Methods, Wiley & Sons, Inc., 1966.
10. Seinfeld, J. H., L. Lapidus, and M. Hwang, "Numerical Integration of Stiff Ordinary Differential Equations," submitted to Industrial and Engineering Chemistry Fundamentals.
11. Von Engel, A., Ionized Gases, Oxford University Press, 1965.

PART III

EFFECT OF TEMPERATURE INHOMOGENEITIES

## INTRODUCTION

The primary purpose of the succeeding work is to isolate the effect on the  $N_{eo} - \hat{E}_z$  relation of the transverse neutral-temperature variations across the positive column. In order to facilitate the study, the equations obtained in Part I are simplified by neglecting the slight deviation of the column from charge neutrality. This approximation is the same as that made by neglecting the term involving  $dE/dy$  in Eq. (1.8) of Part II and becomes better as the electron density  $N_{eo}$  increases. Temperature variations, like recombination effects, are of significance only for large values of  $N_{eo}$ , and numerical results show that such values are sufficiently large so that corrections arising from consideration of the nonzero space charge are relatively unimportant. Although temperature variation and recombination may both be important at large electron densities, attention is focused on temperature effects by setting the recombination coefficient equal to zero in the numerical calculations. In the case of an  $H_2$  plasma this procedure is also a reasonable approximation, because the temperature variation affects the  $N_{eo} - \hat{E}_z$  relation at a considerably smaller value of  $N_{eo}$  than does recombination. Even though recombination may not substantially alter the numerical results here, it is nevertheless ignored in the numerical calculations so as to eliminate all speculation concerning the cause of the results. However, the term in the equations that represents recombination is included in the development of the problem, because it is easy to do so and because its effect on the results can be readily ascertained from the form of the solution.

The effect and, indeed, the very existence of temperature inhomogeneities have usually been ignored in investigations of the positive column. A publication by Ecker and Zöllner [2], however, studies temperature effects using basically the same equations that are used here, but the forms of the coefficients in their equations are very questionable. Furthermore, they treat the pressure of the discharge as an arbitrary parameter. The physical situation investigated here consists of a glow discharge containing a fixed amount of neutral gas. As the axial electric field (or, equivalently, the electron density) is varied, the neutral temperature profile changes. The pressure changes accordingly and hence is actually a function of the axial field or electron density. The dependence of the various quantities in the problem on the electron density is so complicated that the qualitative nature of the  $N_{eo} - \hat{E}_z$  relation cannot be determined without a detailed quantitative investigation of the experimental data. A discussion of the various qualitative aspects of the problem and the corresponding physical interpretations is postponed until the working equations are available.

The equations are solved by two different methods. The first is a regular perturbation process in which the term responsible for the nonuniformity in the temperature profile is treated as the perturbation. This term is proportional to the electron density  $N_{eo}$ , and the variables of the problem are expanded in asymptotic series in powers of  $N_{eo}$ . The first two terms of the series for  $\hat{E}_z$ ,  $p$ , and the dependent variables are calculated and used as an approximation to the solution. The truncated series are most accurate for small values of  $N_{eo}$ , but, of

course, the adjective "small" must be interpreted in a relative sense. Here a value of  $N_{eo} = 10^{10} \text{ cm}^{-3}$  is considered small.

The equations are also solved by numerical integration, and points on the  $N_{eo} - \hat{E}_z$  curve are calculated. The results show that the perturbation solution is accurate only for a rather limited range of  $N_{eo}$ . However, the perturbation procedure serves a useful purpose in providing valuable insight into the nature of the problem. In fact, the iterative process used in the numerical method closely parallels the mechanics of the perturbation technique, and the perturbation results are used as the first estimate in the iteration. The range of  $N_{eo}$  is rather restricted even in the numerical method, because the variation of the neutral temperature across the discharge causes the variables to exceed the domain of the experimental data.

### 1. WORKING EQUATIONS

The equations used to study neutral temperature inhomogeneities are obtained quite easily from those derived in Part I. The only assumption in the process is to regard  $\frac{1}{\chi \zeta} \frac{dE}{dy}$  in Eq. (5.22) as being negligible compared to  $n_i$  and  $n_e$ . The omission of this term is considered extensively in Part II. There the approximation leads to a description of the main region of the positive column given by the lowest-order term in the singular perturbation expansion. Although the temperature is assumed uniform in that development, the validity and the qualitative nature of the approximation are unaffected by temperature variations. In particular, the order of magnitude of the first-order correction found in Part II is applicable to the present situation; it shows that the corrections to the  $N_{eo} - \hat{E}_z$  relation and to the dependent variables decrease as  $N_{eo}$  increases and are of little importance at sufficiently large values of  $N_{eo}$ . However, the term containing  $dE/dy$  is necessary for an accurate description of the positive column in the sheath, a thin region near the wall in which the transverse electric field is large and electron and ion densities are small. The neglect of  $dE/dy$  here is, of course, completely unjustifiable, but the sheath is small and of no essential importance to the study of temperature effects. Furthermore, the discussion on p. 136 in Part II shows that the boundary conditions on  $n_e$  and  $n_i$  at  $y = 1$  can be applied even when the sheath is neglected; no error is introduced into the  $N_{eo} - \hat{E}_z$  relation or the dependent variables in the main region other than that caused by neglecting  $dE/dy$  there.

Equations for Dependent Variables

The neglect of  $dE/dy$  in Eq. (5.22) of Part I results in the simple algebraic equation

$$n_e = n_i \quad (1.1)$$

Denoting the common value of the electron density  $n_e$  and the ion density  $n_i$  by  $n$ , Eqs. (5.18) - (5.21) of Part I become

$$\frac{dJ}{dy} = \gamma v_I(T; \hat{E}_z, p) n - \epsilon \zeta n^2 \quad (1.2)$$

$$\begin{aligned} \frac{dn}{dy} + \frac{1}{T_e(T; \hat{E}_z, p)} \frac{\partial T_e}{\partial T} n \frac{dT}{dy} &= \frac{-1}{T_e(T; \hat{E}_z, p)} n E \\ &- \delta \tau \frac{1}{D_e(T; \hat{E}_z, p)} J \end{aligned} \quad (1.3)$$

$$\frac{dn}{dy} + \frac{1}{T} n \frac{dT}{dy} = \tau \frac{1}{T} n E - \tau \frac{1}{D_i(T; \hat{E}_z, p)} J \quad (1.4)$$

$$\frac{d^2 T}{dy^2} + \frac{1}{\lambda(T)} \frac{d\lambda}{dT} \left( \frac{dT}{dy} \right)^2 = -\beta \zeta \frac{h(T; \hat{E}_z, p)}{\lambda(T)} n \quad (1.5)$$

The appropriate boundary conditions from Eqs. (5.29) - (5.35) are

$$y = 0 : \quad n = 1 \quad (1.6)$$

$$J = 0 \quad (1.7)$$

$$\frac{dT}{dy} = 0 \quad (1.8)$$

$$y = 1 : \quad n = 0 \quad (1.9)$$

$$T = 1 \quad (1.10)$$

There is no longer a differential equation for the transverse electric field  $E$ .  $E$  can now be obtained algebraically from Eq. (1.3) or (1.4), and if these two equations are subtracted so as to eliminate  $dn/dy$ , use of the boundary conditions for the remaining dependent variables shows that  $E$  satisfies the condition  $E = 0$  at  $y = 0$ . However, the use of condition (1.9) on  $n$  in either equation shows that  $E \rightarrow \infty$  as  $y \rightarrow 1$ . This behavior is familiar from the study of Part II. When  $E$  becomes sufficiently large as  $y$  approaches unity, the approximation neglecting  $dE/dy$  breaks down, and an accurate solution for  $E$  in this region requires a special treatment of the entire problem in the sheath. In the present study, however, the solution for  $E$  is of no importance and is never actually obtained. In fact,  $E$  is eliminated from Eqs. (1.3) and (1.4) to produce a single differential equation for  $n$  and is never seen again.

The final working equations for the variables are obtained by eliminating  $E$  from the problem. Multiplying Eq. (1.3) by  $\tau T_e$  and Eq. (1.4) by  $T$  and adding the results yields

$$(T + \tau T_e) \frac{dn}{dy} + (1 + \tau \frac{\partial T_e}{\partial T}) n \frac{dT}{dy} = -\tau \left( \frac{T}{D_i} + \delta \tau \frac{T_e}{D_e} \right) J. \quad (1.11)$$

The final result is expressed more compactly by the introduction of new nomenclature. First the expression is simplified by the use of the dimensionless Einstein relations. Using Eqs. (2.56), (3.8), (3.9), (5.2) - (5.6), and (5.10) of Part I,

$$\frac{k \hat{T}_e(\hat{T}; \hat{E}_z, p)}{e} = \frac{\hat{D}_e(\hat{T}; \hat{E}_z, p)}{\hat{\mu}_e(\hat{T}; \hat{E}_z, p)} \quad (1.12)$$

$$= \frac{\hat{D}_e(\hat{T}_w; \hat{E}_{zr}, p_r) D_e(T; \hat{E}_z, p)}{\hat{\mu}_e(\hat{T}_w; \hat{E}_{zr}, p_r) \mu_e(T; \hat{E}_z, p)} \quad (1.13)$$

$$= \frac{k\hat{T}_e(\hat{T}_w; \hat{E}_{zr}, p_r)}{e} \cdot \frac{D_e(T; \hat{E}_z, p)}{\mu_e(T; \hat{E}_z, p)}, \quad (1.14)$$

so

$$\frac{D_e(T; \hat{E}_z, p)}{\mu_e(T; \hat{E}_z, p)} = T_e(T; \hat{E}_z, p) \quad (1.15)$$

Similarly, the dimensionless Einstein relation for the ions is

$$\frac{D_i(T; \hat{E}_z, p)}{\mu_i(T; \hat{E}_z, p)} = T \quad (1.16)$$

We now define the coefficients A and B by

$$A(T; \hat{E}_z, p) = \frac{1 + \tau \frac{\partial T_e}{\partial T}(T; \hat{E}_z, p)}{T + \tau T_e(T; \hat{E}_z, p)} \quad (1.17)$$

$$B(T; \hat{E}_z, p) = \tau \frac{\frac{1}{\mu_i(T; \hat{E}_z, p)} + \delta\tau \frac{1}{\mu_e(T; \hat{E}_z, p)}}{T + \tau T_e(T; \hat{E}_z, p)} \quad (1.18)$$

Using (1.15) - (1.18), Eq. (1.11) now becomes

$$\frac{dn}{dy} + A(T; \hat{E}_z, p) n \frac{dT}{dy} + B(T; \hat{E}_z, p) J = 0 \quad (1.19)$$

The final set of equations now consists of (1.2), (1.19), (1.5), and the boundary conditions (1.6) - (1.10).

### Equation for Pressure

It is mentioned in Part I and in the Introduction that the physical situation we wish to consider consists of a gas discharge containing a fixed amount of gas independent of the axial electric field or the electron density. In the slab geometry for which the equations are written, the dependent variables do not change except in the y-direction. Hence the requirement of a fixed amount of gas implies that the number of neutral molecules across the column in a unit area of the plane perpendicular to the y-direction remains constant. Denoting this number by  $2\hat{Q}$ , we obtain as the equation representing this statement,

$$2\hat{Q} = \int_{-L}^L N_n dx \quad . \quad (1.20)$$

Using the symmetry of the plasma column and the perfect gas law,

$p = N_n k\hat{T}$  (Eq. (2.78), Part I), Eq. (1.20) becomes

$$\hat{Q} = \frac{p}{k} \int_0^L \frac{dx}{\hat{T}} \quad (1.21)$$

From the definitions (5.10) and (5.16) of Part I the dimensionless form of (1.21) is

$$\hat{Q} = \frac{pL}{k\hat{T}_w} \int_0^1 \frac{dy}{T} \quad . \quad (1.22)$$

This equation serves to determine  $p$  from the temperature distribution.

### Discussion of Problem

A determination of the qualitative behavior of the  $N_{eo} - \hat{E}_z$  relation in response to temperature inhomogeneities is not available.

However, a qualitative investigation of the problem is capable of describing the general behavior of the dependent variables and leads to a better understanding of the problem. In addition, the effect of temperature on the coefficients, notably  $\nu_I$ , is analyzed to some extent and in the process the considerations necessary to the determination of  $\hat{E}_z$  become evident and reveal why a conclusion is unobtainable without detailed numerical estimates. In order to orient the discussion, the physical situation in which temperature inhomogeneities are present is contrasted to the situation that would exist if the neutral temperature were constant. The electron density  $N_{eo}$  assumes the same value in the two situations. The term containing  $\beta$  in Eq. (1.5) represents the transfer of energy from electrons to neutrals and is solely responsible for the departure from a uniform temperature distribution. Hence the mathematical representations of the nonuniform- and uniform-temperature situations are characterized by the respective inclusion or omission of this term in the equations. For clarity, recombination is ignored; a detailed qualitative description of its effect on the  $N_{eo} - \hat{E}_z$  relation is presented in the Introduction to Part II.

The general form of the temperature distribution is easily ascertained either from physical considerations or from a simple analysis of Eq. (1.5). Heat is transferred to the neutral species by interactions with electrons throughout the positive column and is lost by conduction to the walls. The neutral temperature is largest at the center of the column, where its gradient is zero, and decreases monotonically with increasing steepness to satisfy the boundary condition at the wall. The value of the temperature increases as the electron

density increases. The pressure increases as the temperature increases and is greater than in the uniform-temperature situation, where the temperature is constant at its wall value.

The effect of a temperature gradient on the electron density profile  $n$  can be determined by a study of Eq. (1.19). The term  $An \frac{dT}{dy}$  is negative and acts as a positive contribution to the density gradient  $dn/dy$ . However, certain conditions were incorporated into the equations in the nondimensionalization process. In particular,  $n$  must decrease from unity at  $y = 0$  to zero at  $y = 1$  whether a temperature gradient is present or not. In order that the average value of  $dn/dy$  remain constant, the presence of the term  $An \frac{dT}{dy}$  in the case of a nonuniform temperature must be compensated by an increase in  $B_J$  over the value it assumes in the uniform-temperature situation. Examination of Eq. (1.2) shows that  $J$  can increase only as a result of an increase in  $v_I$  or  $n$  or both. It is known that  $v_I$  varies much more with a change in parameters and variables than do the other coefficients, and that a change in  $B$  would be accompanied by a much greater change in  $v_I$ . Therefore the increase in  $B_J$  is ascribed to an increase in  $J$ , and changes in coefficients other than  $v_I$  can be ignored. Since the value of  $J$  at a particular location in the discharge is found by integrating Eq. (1.2) from  $y = 0$ , where  $J = 0$ , the greatest increase in  $J$  over its value in the uniform-temperature situation occurs near the wall.  $n$  decreases to zero as  $y \rightarrow 1$ , so the term containing  $dT/dy$  in Eq. (1.19) loses its influence near the wall, where the increase in  $J$  is most pronounced. A study of this equation for the density gradient discloses the approximate form of the

electron density across the plasma column: the density profile is flatter over the central portion of the discharge and decreases more rapidly near the wall than in the uniform-temperature case. It is now apparent that the change in the shape of the density distribution contributes to the increase in  $v_I n$  in the equation for  $J$ . Since  $N_{eo}$  is the same in both cases, the physical variables for the electron density and the flux also increase.

The spatial variation of  $v_I$  across the plasma column as the result of a nonuniform temperature can be determined by an examination of the experimental data. The dependence of  $\hat{v}_I$ , and hence of  $v_I$ , on the variables and parameters of the problem is given in Eq. (4.6) of Part I. If  $p$  and  $\hat{T}$  are eliminated in favor of  $N_n$  by the perfect gas law,  $N_n = p/(k\hat{T})$ , it is seen that  $v_I$  depends only on  $\hat{E}_z/N_n$  except for a factor  $N_n$ . However,  $v_I$  varies so rapidly with  $\hat{E}_z/N_n$  that the effect of the factor  $N_n$  can be ignored. Eq. (1.20) shows that the average value of  $N_n$  is independent of the temperature distribution, but its local value across the column varies inversely with the temperature  $T$  according to the perfect gas law. Consequently  $N_n$  is greater near the walls than in the center when the temperature is nonuniform. Since  $v_I$  is a rapidly increasing function of  $\hat{E}_z/N_n$ ,  $v_I$  is larger in the center. The ionization rate, which appears in Eq. (1.2), is obtained by multiplying the ionization coefficient  $v_I$  by the electron density  $n$ . Since  $n$  is greatest in the central portion of the column and decreases to zero at the walls, the greater values of  $v_I$  occur where the electron density is greatest and

therefore have a greater effect on the ionization rate (and hence the behavior of  $J$ ) than do the smaller values near the walls. Hence, if  $\hat{E}_z$  were to assume the same value with a uniform- as with a nonuniform- temperature distribution, the value of  $J$  in the nonuniform situation would be greater.

It is shown above that at the same value of  $N_{eo}$  the ionization rate  $v_I n$  must be greater if the temperature distribution is nonuniform than if it is uniform in order to satisfy the boundary conditions on  $n$ . It is further shown that the effect of temperature inhomogeneities on the spatial variations of  $n$  and  $v_I$  tend to increase the ionization rate.  $\hat{E}_z$  is the parameter that must vary in order to establish the ionization rate at the precise value needed to satisfy the boundary conditions. If the increase in  $v_I n$  over its value in the uniform- temperature case is too small,  $\hat{E}_z$  must increase so as to cause a further increase in  $v_I$ ; if the increase in  $v_I n$  is too large,  $\hat{E}_z$  must decrease. Since the temperature distribution and its effect on  $v_I$  and  $n$  depend on  $N_{eo}$ , the considerations above show how  $\hat{E}_z$  is determined theoretically as a function of  $N_{eo}$ . Without detailed quantitative estimates it is not possible to determine whether  $\hat{E}_z$  increases or decreases. The numerical results show  $\hat{E}_z$  to be less when the temperature distribution is nonuniform.

## 2. SOLUTION WHEN $\zeta = 0$

When  $\zeta$  is set equal to zero in Eqs. (1.2) and (1.5), the terms responsible for recombination and spatial temperature variations disappear. Superficially  $\zeta = 0$  implies that the electron density is zero, but such a physical situation is not represented by the resulting equations. In fact, the electron density was specifically restricted to values greater than zero in assuming the effects of space charge to be negligible, and the corresponding modification of the basic equations gives  $\zeta = 0$  a different interpretation. Here  $\zeta = 0$  represents a situation, possibly hypothetical, in which space charge, recombination, and temperature inhomogeneities are negligible. It is the situation characterized by the standard ambipolar diffusion equation, which is discussed in Part II on p. 111.

### Reference Values for $\hat{E}_z$ and $p$

The solution to the equations when  $\zeta = 0$  plays a special role in the ensuing development of the problem and is distinguished by special nomenclature. The values that  $J$ ,  $n$ ,  $T$ ,  $\hat{E}_z$ , and  $p$  assume when  $\zeta = 0$  are designated by  $J_0$ ,  $n_0$ ,  $T_0$ ,  $\hat{E}_{z0}$ , and  $p_0$ . The nomenclature is quite appropriate, because these quantities constitute the first terms of an eventual expansion of the variables in powers of  $\zeta$ .

The reference values  $\hat{E}_{zr}$  and  $p_r$  introduced in Section 5 of Part I in the nondimensionalization process are now defined as

$$\hat{E}_{zr} = \hat{E}_{z0} \quad (2.1)$$

$$p_r = p_0 \quad (2.2)$$

Unlike the definitions adopted in Part II,  $\hat{E}_{zr}$  and  $p_r$  are here independent of  $N_{eo}$  (or  $\zeta$ ). Consequently the constant coefficients are also independent of  $N_{eo}$ , and the definitions of Eqs. (5.23) - (5.27) of Part I become

$$\gamma = \frac{L^2 \hat{v}_I(\hat{T}_w; \hat{E}_{zo}, p_o)}{\hat{D}_i(\hat{T}_w; \hat{E}_{zo}, p_o)} \cdot \frac{\hat{T}_w}{\hat{T}_e(\hat{T}_w; \hat{E}_{zo}, p_o)} \quad (2.3)$$

$$\epsilon = \frac{L^2 \hat{\alpha} N}{\hat{D}_i(\hat{T}_w; \hat{E}_{zo}, p_o)} \cdot \frac{\hat{T}_w}{\hat{T}_e(\hat{T}_w; \hat{E}_{zo}, p_o)} \quad (2.4)$$

$$\tau = \frac{\hat{T}_e(\hat{T}_w; \hat{E}_{zo}, p_o)}{\hat{T}_w} \quad (2.5)$$

$$\delta = \frac{\hat{D}_i(\hat{T}_w; \hat{E}_{zo}, p_o)}{\hat{D}_e(\hat{T}_w; \hat{E}_{zo}, p_o)} \quad (2.6)$$

$$\beta = \frac{\hat{h}(\hat{T}_w; \hat{E}_{zo}, p_o) N L^2}{\hat{\lambda}(\hat{T}_w) \hat{T}_w} \quad (2.7)$$

Solution for  $T_o$  and  $p_o$

The equation for  $T_o$ , obtained by setting  $\zeta = 0$  in (1.5), is

$$\frac{d^2 T_o}{dy^2} + \frac{1}{\lambda(T_o)} \frac{d\lambda(T_o)}{dT_o} \left(\frac{dT_o}{dy}\right)^2 = 0 \quad (2.8)$$

and the boundary conditions, from (1.8) and (1.10) are

$$y = 0 : \quad \frac{dT_o}{dy} = 0 \quad (2.9)$$

$$y = 1 : \quad T_o = 1 \quad (2.10)$$

The solution is trivial:

$$T_o \equiv 1 \quad . \quad (2.11)$$

Equation (1.22) for  $p_o$  becomes

$$\hat{Q} = \frac{p_o L}{k \hat{T}_w} \int_0^1 \frac{dy}{T_o} = \frac{p_o L}{k \hat{T}_w} \quad (2.12)$$

so  $p_o$  can be determined from a specified value for  $\hat{Q}$ . However, it is more convenient to regard  $p_o$  as a parameter whose value is to be specified arbitrarily and rewrite Eq. (1.22) for  $p$  as

$$p \int_0^1 \frac{dy}{T} = p_o \quad (2.13)$$

The values for four parameters must be selected before numerical calculations can proceed. The values chosen for the gas temperature at the wall, the pressure  $p_o$ , and the half-width of the discharge are

$$\hat{T}_w = 300^\circ\text{K} \quad (2.14)$$

$$p_o = 1 \text{ mm Hg} \quad (2.15)$$

$$L = 1 \text{ cm.} \quad (2.16)$$

The fourth parameter  $N$  is artificially introduced into the problem for convenience. Its numerical value is selected so as to set the value of  $\beta$  near unity. The appropriate value is found to be

$$N = 10^{11} \text{ cm}^{-3} \quad (2.17)$$

As a result, the order of magnitude of the coefficient  $\beta\zeta$  in Eq. (1.5) is approximately the order of magnitude of  $\zeta$ .

Solution for  $J_0$ ,  $n_0$ , and  $\hat{E}_{z0}$

Using the definitions (2.1) and (2.2) for  $\hat{E}_{zr}$  and  $p_r$ , Eqs. (5.1) - (5.9) of Part II for the variable coefficients, when evaluated at

$$(T, \hat{E}_z, p) = (1, \hat{E}_{z0}, p_0) \quad , \quad (2.18)$$

all reduce to unity. The coefficients  $v_I$ ,  $A$ , and  $B$  appear in the equations for  $J$  and  $n$ , and special nomenclature is used for their values when  $\zeta = 0$ . From (1.17) and (1.18) we have

$$v_{I0} = v_I(1; \hat{E}_{z0}, p_0) = 1 \quad (2.19)$$

$$A_0 = A(1; \hat{E}_{z0}, p_0) = \frac{1 + \tau \frac{\partial T}{\partial T} (1; \hat{E}_{z0}, p_0)}{1 + \tau} \quad (2.20)$$

$$B_0 = B(1; \hat{E}_{z0}, p_0) = \tau \frac{1 + \delta\tau}{1 + \tau} \quad . \quad (2.21)$$

Using (2.11), Eqs. (1.2) and (1.19) for  $J$  and  $n$  at  $\zeta = 0$  become

$$\frac{dJ_0}{dy} - \gamma n_0 = 0 \quad (2.22)$$

$$\frac{dn_0}{dy} + B_0 J_0 = 0 \quad . \quad (2.23)$$

The boundary conditions obtained from (1.6), (1.7), and (1.9) are

$$y = 0 : \quad n_o = 1 \quad (2.24)$$

$$J_o = 0 \quad (2.25)$$

$$y = 1 : \quad n_o = 0 \quad (2.26)$$

Eliminating  $J_o$  between Eqs. (2.22) and (2.23), we obtain a single equation for  $n_o$  :

$$\frac{d^2 n_o}{dy^2} + \gamma B_o n_o = 0 \quad (2.27)$$

An additional boundary condition on  $n_o$  is obtained from Eqs. (2.23) and (2.25):

$$y = 0: \quad \frac{dn_o}{dy} = 0 \quad (2.28)$$

The problem for  $n_o$  is an eigenvalue problem. Physical considerations require  $n_o$  to be nonnegative and therefore restrict  $\gamma B_o$  to the lowest eigenvalue. The solution is

$$n_o = \cos \frac{\pi}{2} y \quad (2.29)$$

$$\gamma B_o = \gamma \tau \frac{1 + \delta \tau}{1 + \tau} = \frac{\pi^2}{4} \quad (2.30)$$

Observation of the expressions for  $\gamma$ ,  $\tau$ , and  $\delta$  in (2.3), (2.5) and (2.6) shows that (2.30) is an equation for  $\hat{E}_{zo}$ . It is solved numerically by a simple iterative procedure, and once the value of  $\hat{E}_{zo}$  is available, all the constant coefficients can be evaluated. The numerical values of  $\hat{E}_{zo}$  and the constant coefficients are presented in Table 1. The quantity  $\beta_o$  appearing there is  $\beta$  evaluated with

$\hat{h}(\hat{T}_w; \hat{E}_{z_0}, p_0)$  replaced by  $\hat{h}_o(\hat{T}_w; \hat{E}_{z_0}, p_0)$ , the elastic energy-transfer rate.

The expression for  $J_o$  is easily obtained from Eqs. (2.22), (2.25), and (2.29). It is given by

$$J_o = \frac{2}{\pi} \gamma \sin \frac{\pi}{2} y \quad . \quad (2.31)$$

### 3. PERTURBATION SOLUTION

An approximate approach to the problem involves an expansion of the variables in powers of  $\zeta$ . The first two terms of the expansions are readily obtained by a regular perturbation procedure. In fact, the first terms are the results presented in the previous section.  $\zeta$  occurs as a factor in the terms of Eqs. (1.2) and (1.5) that contain  $\epsilon$  or  $\beta$ , and hence these terms contribute only to higher-order results. Table 1 shows that  $\beta > \epsilon$ , and hence the accuracy of the expansions is limited by the magnitude of  $\beta\zeta$ .  $\epsilon$  represents recombination and its effect is quite small. It is retained in the equations because it is possible to do so conveniently, but it is set equal to zero in all numerical calculations so as to separate completely its effect from that of temperature inhomogeneities.

#### Expansions of Variables and Coefficients

Expansions for the variables of the problem are given by

$$J = J_0 + \zeta J_1 + \dots \quad (3.1)$$

$$n = n_0 + \zeta n_1 + \dots \quad (3.2)$$

$$T = T_0 + \zeta T_1 + \dots \quad (3.3)$$

$$p = p_0 + \zeta p_1 + \dots \quad (3.4)$$

$$\hat{E}_z = \hat{E}_{z0} + \zeta \hat{E}_{z1} + \dots \quad (3.5)$$

Since equations for terms of different orders in  $\zeta$  are obtained by substituting the expansions into the problem and equating equal powers of  $\zeta$ , the zero-order terms represent the solution when  $\zeta = 0$ .

These terms have been obtained in the previous section, and the first-order terms are obtained here to complete the calculation.

It is easier to estimate the magnitudes of relative changes in  $\hat{E}_z$  and to appraise their effects if  $\hat{E}_z$  is expressed in dimensionless form. For that purpose we define  $\psi$  by

$$\psi = \hat{E}_z / \hat{E}_{z0} \quad (3.6)$$

Using (3.5), its asymptotic expansion is

$$\psi = \psi_0 + \zeta \psi_1 + \dots \quad (3.7)$$

where  $\psi_0 = 1$  (3.8)

and  $\psi_1 = \hat{E}_{z1} / \hat{E}_{z0}$  . (3.9)

The expansions of the variables induce similar expansions of the variable coefficients. For instance,  $v_I$ , correct to an error of order  $O(\zeta^2)$ , can be written

$$v_I(T_0 + \zeta T_1; \hat{E}_{z0} + \zeta \hat{E}_{z1}, p_0 + \zeta p_1) = v_{I0} + \zeta v_{I1} + O(\zeta^2) \quad (3.10)$$

where  $v_{I0}$  and  $v_{I1}$  are coefficients in a Taylor's series expansion about  $\zeta = 0$ .  $v_{I0}$  is given by Eq. (2.19), and  $v_{I1}$  is found by differentiating  $v_I$  with respect to  $\zeta$  :

$$v_{I1} = \frac{\partial v_I}{\partial T} T_1 + \frac{\partial v_I}{\partial p} p_1 + \frac{\partial v_I}{\partial \psi} \psi_1 \quad , \quad (3.11)$$

where the derivatives are evaluated at

$$(T, \psi, p) = (1, 1, p_0) \quad . \quad (3.12)$$

Equations (3.6) and (3.9) are used to replace the differentiation with respect to  $\hat{E}_z$  by differentiation with respect to  $\psi$  .

$v_{I1}$  depends on  $y$  through the function  $T_1$  ; the other terms are constant. In the same manner  $B$  is expanded as

$$B(T_0 + \zeta T_1; \hat{E}_{z0} + \zeta \hat{E}_{z1}, p_0 + \zeta p_1) = B_0 + \zeta B_1 \quad (3.13)$$

where  $B_0$  is found in Eq. (2.21) and  $B_1$  is given as

$$B_1 = \frac{\partial B}{\partial T} T_1 + \frac{\partial B}{\partial p} p_1 + \frac{\partial B}{\partial \psi} \psi_1 \quad . \quad (3.14)$$

The derivatives are again evaluated as in (3.12), and errors of order  $0(\zeta^2)$  are neglected. Because  $T_0$  is a constant,  $dT/dy$  is order  $0(\zeta)$ , and the other variable coefficients occurring in Eqs. (1.5) and (1.19) need not be evaluated to higher order. The term containing  $d\lambda/dT$  does not contribute to the first-order equations, and to zero order

$$A = A_0 + 0(\zeta) \quad , \quad (3.15)$$

where  $A_0$  is defined in Eq. (2.20). Preceding Eq. (2.18) it is noted that  $h$  and  $\lambda$  are unity to lowest order. Hence

$$h = \lambda = 1 + 0(\zeta) \quad . \quad (3.16)$$

The derivatives in (3.11) and (3.13) are evaluated by numerical differentiation of the coefficients  $v_I$  and  $B$  . The technique used and its expected accuracy are discussed in Appendix A, and the

numerical values of  $A_o$ ,  $B_o$ , and the derivatives are tabulated in Table 2.

First-Order Problem

Equations for the first-order corrections to the variables are obtained by substituting the series expansions into the problem. Using (2.11) and neglecting terms of order  $O(\zeta^2)$ , Eqs. (1.5), (1.2), and (1.19) become

$$\zeta \frac{d^2 T_1}{dy^2} = -\beta \zeta n_o \quad (3.17)$$

$$\frac{dJ_o}{dy} + \zeta \frac{dJ_1}{dy} = \gamma [v_{I0} n_o + \zeta (v_{I0} n_1 + v_{I1} n_o)] - \epsilon \zeta n_o^2 \quad (3.18)$$

$$\frac{dn_o}{dy} + \zeta \frac{dn_1}{dy} + \zeta A_o n_o \frac{dT_1}{dy} + B_o J_o + \zeta (B_o J_1 + B_1 J_o) = 0 \quad (3.19)$$

Using (2.19) and Eqs. (2.22) and (2.23) for the zero-order problem, we obtain

$$\frac{d^2 T_1}{dy^2} = -\beta n_o \quad (3.20)$$

$$\frac{dJ_1}{dy} - \gamma n_1 = \gamma v_{I1} n_o - \epsilon n_o^2 \quad (3.21)$$

$$\frac{dn_1}{dy} + B_o J_1 = -B_1 J_o - A_o n_o \frac{dT_1}{dy} \quad (3.22)$$

The boundary conditions, obtained by substituting the expansions for the variables into Eqs. (1.6) - (1.10), are

$$y = 0 : \quad n_1 = 0 \quad (3.23)$$

$$J_1 = 0 \quad (3.24)$$

$$\frac{dT_1}{dy} = 0 \quad (3.25)$$

$$y = 1 : \quad n_1 = 0 \quad (3.26)$$

$$T_1 = 0 \quad (3.27)$$

An equation for the first-order correction to the pressure is obtained from (2.13) using (2.11):

$$0 = p \int_0^1 \frac{dy}{T} - p_0 \quad (3.28)$$

$$= (p_0 + \zeta p_1) \int_0^1 \frac{dy}{1 + \zeta T_1} - p_0 \quad (3.29)$$

$$= (p_0 + \zeta p_1) \int_0^1 (1 - \zeta T_1) dy - p_0 + O(\zeta^2) \quad (3.30)$$

$$= p_0 + \zeta (p_1 - p_0) \int_0^1 T_1 dy - p_0 \quad (3.31)$$

so

$$p_1 = p_0 \int_0^1 T_1 dy \quad (3.32)$$

### Solution for $T_1$ and $p_1$

The solution for  $T_1$  and  $p_1$  is obtained very easily. Using the form of  $n_0$  given by (2.29), Eq. (3.20) for  $T_1$  becomes

$$\frac{d^2 T_1}{dy^2} = -\beta \cos \frac{\pi}{2} y \quad (3.33)$$

The solution, subject to the boundary conditions (3.25) and (3.27), is

$$T_1 = \frac{4}{\pi^2} \beta \cos \frac{\pi}{2} y \quad . \quad (3.34)$$

Equation (3.32) for  $p_1$  now yields

$$p_1 = \frac{4}{\pi^2} \beta p_o \int_0^1 \cos \frac{\pi}{2} y \, dy \quad (3.35)$$

$$= \frac{8}{\pi^3} \beta p_o \quad . \quad (3.36)$$

Solution for  $\hat{E}_{z1}$  and  $n_1$

An equation for  $n_1$  is acquired by eliminating  $J_1$  between (3.21) and (3.22). Using (2.30), which shows that  $\gamma B_o = \pi^2/4$ , and arranging the terms in the desired manner, we obtain

$$\begin{aligned} \frac{d^2 n_1}{dy^2} + \frac{\pi^2}{4} n_1 &= - \frac{d}{dy} (B_1 J_o) - A_o \frac{d}{dy} (n_o \frac{dT_1}{dy}) \\ &- \frac{\pi^2}{4} \nu_{11} n_o + \epsilon B_o n_o^2 \end{aligned} \quad (3.37)$$

An additional boundary condition on  $n_1$  is found by using the boundary conditions on  $J_o$ ,  $J_1$ , and  $T_1$  at  $y = 0$  in Eq. (3.22):

$$y = 0 : \quad \frac{dn_1}{dy} = 0 \quad (3.38)$$

The homogeneous equation associated with (3.37) has a solution,  $\cos \frac{\pi}{2} y$ , which satisfies the boundary conditions (3.38) and (3.26). Appendix B of Part II can now be applied with the functions  $w(y)$ ,  $p(y)$ , and  $q(y)$  given by  $w \equiv 1$ ,  $p \equiv 1$ ,  $q \equiv \pi^2/4$ . The theorem in

the Appendix states that the right-hand side of (3.37) must be orthogonal to  $\cos \frac{\pi}{2} y$  if a solution for  $n_1$  is to exist. Writing this statement as an equation, we have

$$\int_0^1 \cos \frac{\pi}{2} y \left[ \frac{d}{dy} (B_1 J_0) + A_0 \frac{d}{dy} (n_0 \frac{dT_1}{dy}) + \frac{\pi^2}{4} v_{11} n_0 - \epsilon B_0 n_0^2 \right] dy = 0 . \quad (3.39)$$

All the quantities in the integrand are known except  $\psi_1$ , which appears through the expressions for  $v_{11}$  and  $B_1$ , and hence (3.39) serves as the equation for  $\hat{E}_{z1}$ . The operations necessary to obtain an explicit expression for  $\psi_1$  or  $\hat{E}_{z1}$  are tedious and boring, but since the result is very important, the details are given in Appendix B. Using (3.9),  $\hat{E}_z$  can be written from Eq. (B.21) of Appendix B as

$$\begin{aligned} \hat{E}_{z1} = & -\left(\frac{4}{3\pi} \beta \frac{\partial v_I}{\partial T} + \frac{1}{\pi} \beta \frac{\partial v_I}{\partial p} p_0 + \frac{8}{3\pi^3} \gamma \beta \frac{\partial B}{\partial T} + \frac{4}{\pi^3} \gamma \beta \frac{\partial B}{\partial p} p_0 \right. \\ & \left. - \frac{2}{3\pi} \beta A_0 - \frac{4}{3\pi} \epsilon B_0\right) \hat{E}_{z0} / \left( \frac{\pi^2}{8} \frac{\partial v_I}{\partial \psi} + \frac{1}{2} \gamma \frac{\partial B}{\partial \psi} \right) . \quad (3.40) \end{aligned}$$

Several observations can be made about this expression. First, it should be noticed that if the term containing  $\epsilon$  were omitted,  $\hat{E}_{z1}$  would be proportional to  $\beta$ . This result is expected, because if  $\epsilon$  were removed from the problem, the only term that is treated as a perturbation in the original equations contains  $\beta$  and  $\zeta$  as factors. Since there is some ambiguity involved in the definition of  $\beta$  (see Part I, pp. 30-34), it is reassuring to find that only the magnitude, and not the sign, of  $\hat{E}_{z1}$  depends on  $\beta$ . The effect of  $\epsilon$  on  $\hat{E}_z$  can now be determined quantitatively from the expression

for  $\hat{E}_{z1}$ . An examination of Tables 1 and 2 shows that it is very small. Table 2 also shows that  $\hat{E}_{z1}$  is composed of differences of rather large terms and reveals quantitatively the difficulty in predicting the sign of  $\hat{E}_{z1}$ .

The terms on the right-hand side of Eq. (3.37) are written as functions of  $y$  in Appendix B. Using (B.11), (B.14), (B.15), and (B.16), the equation for  $n_1$  becomes

$$\begin{aligned} \frac{d^2 n_1}{dy^2} + \frac{\pi^2}{4} n_1 = & \frac{4}{\pi^2} \gamma \beta \frac{\partial B}{\partial T} - \beta A_o - [\gamma (\frac{\partial B}{\partial p} p_1 + \frac{\partial B}{\partial \psi} \psi_1) \\ & + \frac{\pi^2}{4} (\frac{\partial v_I}{\partial p} p_1 + \frac{\partial v_I}{\partial \psi} \psi_1)] \cos \frac{\pi}{2} y + (-\frac{8}{\pi^2} \gamma \beta \frac{\partial B}{\partial T} \\ & + 2\beta A_o - \beta \frac{\partial v_I}{\partial T} + \epsilon B_o) \cos^2 \frac{\pi}{2} y \quad . \end{aligned} \quad (3.41)$$

The solution satisfying boundary conditions (3.23) and (3.38) is obtained by standard techniques. After eliminating  $\psi_1$  with Eq. (B.21) of Appendix B,  $n_1$  can be written as

$$\begin{aligned} n_1 = & \frac{4}{3\pi^2} (\beta \frac{\partial v_I}{\partial T} - \frac{4}{\pi^2} \gamma \beta \frac{\partial B}{\partial T} + \beta A_o - \epsilon B_o) \cos \frac{\pi}{2} y \\ & + \frac{4}{3\pi^2} (\beta \frac{\partial v_I}{\partial T} + \frac{8}{\pi^2} \gamma \beta \frac{\partial B}{\partial T} - 2\beta A_o - \epsilon B_o) \cos^2 \frac{\pi}{2} y \\ & - \frac{4}{3\pi^2} (2\beta \frac{\partial v_I}{\partial T} + \frac{4}{\pi^2} \gamma \beta \frac{\partial B}{\partial T} - \beta A_o - 2\epsilon B_o) (1 - y \sin \frac{\pi}{2} y). \end{aligned} \quad (3.42)$$

It is apparent that by virtue of the solution for  $\psi_1$ ,  $n_1$  satisfies the boundary condition (3.26) at  $y = 1$ . Equation (3.42) shows that  $n_1$ ,

like  $\psi_1$ , would be proportional to  $\beta$  if  $\epsilon$  were not present.  $n_0$  and  $n_1$  are presented as functions of  $y$  in Fig. 1. The values of  $n_1$  on the graph are obtained after setting  $\epsilon = 0$ . The form of  $n_1$  verifies the qualitative conclusions reached in Section 1 concerning the shape of  $n$ : the electron density  $n_0 + \zeta n_1$  remains flatter over the central portion of the discharge and drops more rapidly near the wall than does  $n_0$ , the density profile in the absence of temperature gradients.

Since the other first-order variables are known,  $J_1$  can be obtained in a routine manner from either equation (3.21) or (3.22). However,  $J_1$  is not needed and the calculation is not performed here.

### Numerical Results

$\epsilon$  is set equal to zero in all numerical calculations. Evaluating Eq. (B.21) of Appendix B for  $\psi_1$ , we find that to first order  $\psi$  is given by

$$\psi = 1 - 0.08811\beta\zeta \quad . \quad (3.43)$$

Inserting the value of  $\beta$ , we find

$$\psi = 1 - 0.3926\zeta \quad . \quad (3.44)$$

If the value of  $\beta_0$  is used in place of  $\beta$  in Eq. (3.43), we obtain

$$\psi \Big|_{\beta=\beta_0} = 1 - 0.03609\zeta \quad . \quad (3.45)$$

The discussion on pp. 30 - 34 of Part I shows that  $\hat{h}$ , and hence  $\beta$ , is not a clearly defined quantity. The value selected for  $\hat{h}$  (and  $\beta$ ) is actually an upper bound, although it is expected to be a good

estimate. Use of the value of  $\beta_0$  for  $\beta$  is not a good estimate, but it does represent a lower bound. After converting  $\psi$  to  $\hat{E}_z$  and  $\zeta$  to  $N_{eo}$ , Eqs. (3.44) and (3.45) are plotted in Fig. 2. It is obvious from equation (3.43) that the result of a lower value of  $\beta$  is to delay the onset of significant temperature-inhomogeneity effects to a larger value of  $\zeta$ . Replacing  $\psi$  and  $\zeta$  in (3.44) by the corresponding dimensioned quantities, we obtain

$$\hat{E}_z = (20.84411 \text{ volt/cm})(1 - 0.3926 \times 10^{-11} \text{ cm}^3 N_{eo}) \quad (3.46)$$

Graphs of Eqs. (3.46) and (3.44) are presented in Figs. 3 and 4.

The temperature at the center of the discharge provides a measure of the increase in temperature above its wall value, and it is of interest to observe this quantity as a function of electron density. From Eqs. (2.11), (3.3), and (3.34) we obtain to first order

$$T(y) = 1 + \frac{4}{\pi} \beta \zeta \cos \frac{\pi}{2} y, \quad (3.47)$$

so

$$T(0) = 1 + \frac{4}{\pi} \beta \zeta. \quad (3.48)$$

A plot of  $\zeta$  versus  $T(0)$  is presented in Fig. 5. By eliminating  $\zeta$  between Eqs. (3.43) and (3.48), it is possible to relate  $T(0)$  and  $\psi$ . The relationship is independent of  $\beta$  and is plotted in Fig. 6.

The pressure, correct to first order, is obtained from Eqs. (3.4) and (3.36):

$$p = p_0 \left(1 + \frac{8}{3} \beta \zeta\right). \quad (3.49)$$

A plot of  $\zeta$  versus  $p$  is presented in Fig. 7.

#### 4. NUMERICAL SOLUTION

In this section the differential equations for  $J$ ,  $n$ , and  $T$  (with  $\varepsilon$  set equal to zero) are integrated numerically. Before solving,  $\zeta$  is assigned a value, so the solution corresponds to a particular  $N_{eo}$ .  $\hat{E}_z$  is determined in the process of solving the equations, so by repeating the procedure for various values of  $\zeta$  enough points are obtained to plot the  $N_{eo} - \hat{E}_z$  relation. Since recombination is ignored, the deviation of  $\hat{E}_z$  from  $\hat{E}_{z0}$  is attributable solely to the effect of temperature inhomogeneities.

##### Outline of Procedure

The method used to solve the equations dissects the problem into two two-point boundary value problems.  $J$ ,  $n$ , and  $\hat{E}_z$  are determined simultaneously in one of the problems, and  $T$  is obtained from the other. The two problems are solved repeatedly in an iterative process which leads to the final solution for a specific  $\zeta$ .

The procedure is explained by the following outline, which is in turn followed by a detailed description of the individual steps:

- Step 1: Choose  $\zeta$ .
- Step 2: Obtain  $T(y)$  for this value of  $\zeta$  from perturbation results.
- Step 3: Calculate  $p$  from the function  $T(y)$ .
- Step 4: Solve for  $J$ ,  $n$ , and  $\hat{E}_z$  using the values of  $T(y)$  and  $p$ . Integrate from  $y = 0$  using the boundary conditions there, and vary  $\hat{E}_z$  until the condition at  $y = 1$  is satisfied.

Step 5: Solve for  $T$  using the values of  $p$ ,  $\hat{E}_z$ , and  $n(y)$ . Integrate from  $y = 0$  using the boundary condition there, and vary  $T(0)$  until the condition at  $y = 1$  is satisfied.

Step 6: Return to Step 3 (iterate).

Step 1

The value of  $\zeta$  is not changed in the process of solving the equations.  $\hat{E}_z$ ,  $p$ , and the dependent variables all correspond only to the value selected.

Step 2

The first approximation to the temperature distribution  $T(y)$  is obtained from Eq. (3.47) and is denoted  $T^{(0)}(y)$  :

$$T^{(0)}(y) = 1 + \frac{4}{\pi^2} \beta \zeta \cos \frac{\pi}{2} y \quad . \quad (4.1)$$

It is the quantity used to start the iterative process, and its accuracy as an approximation to the exact solution  $T(y)$  is primarily responsible for the number of iterative cycles necessary to achieve a satisfactory solution.

Step 3

The determination of the pressure from the temperature distribution is the first step of the iterative cycle. The superscript  $n$  denotes the number of the iteration, and  $p^{(n)}$  is obtained from Eq. (2.13):

$$p^{(n)} = p_0 \int_0^1 \frac{dy}{T^{(n-1)}} \quad (4.2)$$

where  $n = 1, 2, \dots$ . The integral is evaluated numerically using Simpson's rule with a stepsize of 0.02. This value of the stepsize yields very accurate results and poses no significant limitation on the convergence criteria for the iteration schemes.

Step 4

The differential equations for  $J$  and  $n$  are solved simultaneously using the most recent estimates for  $p$  and  $T(y)$ . From Eqs. (1.2) and (1.19) we have

$$\frac{dJ^{(n)}}{dy} = \gamma \nu_I (T^{(n-1)}; \hat{E}_z^{(n)}, p^{(n)}) n^{(n)} \quad (4.3)$$

$$\begin{aligned} \frac{dn^{(n)}}{dy} = & -A(T^{(n-1)}; \hat{E}_z^{(n)}, p^{(n)}) n^{(n)} \frac{dT^{(n-1)}}{dy} \\ & - B(T^{(n-1)}; \hat{E}_z^{(n)}, p^{(n)}) J^{(n)} \end{aligned} \quad (4.4)$$

The boundary conditions correspond to (1.6), (1.7), and (1.9):

$$y = 0: \quad n^{(n)} = 1 \quad (4.5)$$

$$J^{(n)} = 0 \quad (4.6)$$

$$y = 1: \quad n^{(n)} = 0 \quad (4.7)$$

where  $n = 1, 2, \dots$ . The integration is performed by the classical fourth-order Runge-Kutta method<sup>\*</sup>, and a stepsize of 0.02 is sufficient to insure the desired accuracy. The integration is begun at  $y = 0$

---

<sup>\*</sup>See, for instance, Henrici [3], pp. 67-68, 122.

using the boundary conditions (4.5) and (4.6), and the parameter  $\hat{E}_z^{(n)}$  is changed and the integration repeated until the condition (4.7) is satisfied.

The sequence of estimates of  $\hat{E}_z^{(n)}$  is determined by the method of false position\*. We let  $z$  represent the value of  $\hat{E}_z^{(n)}$ ,

$$z = \hat{E}_z^{(n)} \quad (4.8)$$

and denote the successive estimates by the sequence  $z^{(k)}$ ,  $k=0,1,2,\dots$ . A function  $f(z)$  is defined as the value of  $n^{(n)}(1)$  obtained by solving the problem (4.3) - (4.6) with  $z$  substituted as the value of  $\hat{E}_z^{(n)}$ :

$$f(z) \equiv n^{(n)}(1) \Big|_{\hat{E}_z^{(n)} = z} \quad (4.9)$$

The correct value of  $\hat{E}_z^{(n)}$  for which the condition (4.7) is satisfied is then given by the solution to the algebraic equation

$$f(z) = 0 \quad (4.10)$$

The sequence  $z^{(k)}$ , which converges to the root  $z$ , is defined by

$$z^{(k+1)} = z^{(k)} - \frac{f(z^{(k)})}{m^{(k)}} \quad (4.11)$$

for  $k = 1,2,\dots$ , where

---

\* See Isaacson and Keller [4], pp. 99-102.

$$m^{(k)} = \begin{cases} \frac{f(z^{(k)}) - f(z^{(k-1)})}{z^{(k)} - z^{(k-1)}} , & \text{if } |z^{(k)} - z^{(k-1)}| \geq \epsilon \\ \frac{f(z^{(i)}) - f(z^{(i-1)})}{z^{(i)} - z^{(i-1)}} , & i < k, \text{ if } |z^{(k)} - z^{(k-1)}| < \epsilon \end{cases} \quad (4.12)$$

The conditional definition of  $m^{(k)}$  is necessitated by the round-off error in single-precision computer calculations. When the difference between the successive estimates  $z^{(k)}$  and  $z^{(k-1)}$  becomes small, round-off error can seriously alter the value of  $m^{(k)}$ .  $i$  represents a value of  $k$  for which  $|z^{(k)} - z^{(k-1)}| \geq \epsilon$ . The value  $\epsilon = 0.1$  is used in the calculations. The first term  $z^{(0)}$  of the sequence is selected either from the perturbation results or as  $\hat{E}_z^{(n-1)}$ , depending on the value of  $n$ . Using (3.5), we define

$$z^{(0)} = \begin{cases} \hat{E}_{z_0} + \zeta \hat{E}_{z_1} , & \text{if } n = 1 \\ \hat{E}_z^{(n-1)} , & \text{if } n > 1 \end{cases} \quad (4.13)$$

The value of  $z^{(1)}$  must also be specified before the recursion formula (4.11) can be applied. Its value is selected arbitrarily in the vicinity of  $z^{(0)}$ . The sequence is terminated when the fractional difference between successive terms becomes less than  $10^{-5}$ , and the value of the last term is assigned to  $\hat{E}_z^{(n)}$ . The convergence is rapid, and usually Eqs. (4.3) and (4.4) have to be integrated only three or four times before an acceptable value of  $\hat{E}_z^{(n)}$  is determined. Typical results are presented in Table 4.

Step 5

The differential equation for the temperature is solved using the most recent estimates for  $p$ ,  $\hat{E}_z$ , and  $n$ . From (1.5), (1.8), and (1.10) we obtain the problem for  $T^{(n)}$ :

$$\frac{d^2 T^{(n)}}{dy^2} + \frac{1}{\lambda(T^{(n)})} \frac{d\lambda}{dT} (T^{(n)}) \left( \frac{dT^{(n)}}{dy} \right)^2 = -\beta \zeta \frac{h(T^{(n)}; \hat{E}_z^{(n)}, p^{(n)})}{\lambda(T^{(n)})} n^{(n)} \quad (4.14)$$

$$y = 0 : \quad \frac{dT^{(n)}}{dy} = 0 \quad (4.15)$$

$$y = 1 : \quad T^{(n)} = 1 \quad (4.16)$$

where  $n = 1, 2, \dots$ . The integration is again performed by the classical Runge-Kutta method using a stepsize of 0.02.

The problem for  $T^{(n)}$  is a two-point boundary value problem similar to the one just discussed for  $J^{(n)}$  and  $n^{(n)}$ , and the solution is obtained by a similar procedure. The integration is again begun at  $y = 0$ , but here the value of  $T^{(n)}(0)$  is varied and the integration repeated until the boundary condition at  $y = 1$  is satisfied. The correlation between the iterative processes of the two problems can be emphasized by a redefinition of  $z$  and  $f(z)$  in the present context. First the problem for  $T^{(n)}$  is converted to an initial value problem in which the boundary condition (4.16) is replaced by

$$y = 0 : \quad T^{(n)} = z \quad (4.17)$$

$f(z)$  is defined as the solution to this problem evaluated at  $y = 1$  minus the value it should assume:

$$f(z) = T^{(n)}(1) \Big|_{T^{(n)}(0) = z}^{-1} . \quad (4.18)$$

The value of  $z$  for which the boundary condition (4.16) is satisfied is now the solution to Eq. (4.10). The sequence  $z^{(k)}$ ,  $k=0,1,2,\dots$ , consists of successive approximations to this root of  $f(z)$ . It is generated by Eqs. (4.11) and (4.12), and the problem (4.14), (4.15), and (4.17) must be solved at each step in order to determine  $f(z^{(k)})$ .  $\epsilon$  is here given the value 0.005, and the initial term of the sequence is defined by

$$z^{(0)} = T^{(n-1)}(1) . \quad (4.19)$$

$z^{(1)}$  must also be specified, and its value is selected arbitrarily in the vicinity of  $z^{(0)}$ . The sequence is again terminated when the fractional difference between successive terms becomes less than  $10^{-5}$ . The rate of convergence is similar to that of the sequence approximating  $\hat{E}_z^{(n)}$ , and typical results are presented in Table 5. Since the temperature distribution corresponding to the last term of the sequence is never found, the value of the preceding term is assigned to  $T^{(n)}(0)$ .

#### Step 6

This step consists of a return to Step 3 to begin another cycle of the iterative procedure. The value of the superscript  $n$  is increased by one, and in Step 3 a new pressure is calculated from the new temperature distribution. The iteration is continued until the fractional difference between  $\hat{E}_z^{(n)}$  and  $\hat{E}_z^{(n-1)}$  becomes less than

$10^{-4}$  in magnitude. The number of iterations needed to satisfy this convergence criterion depends principally upon the accuracy of the initial approximation to the temperature distribution. For instance, when  $\zeta = 0.1$ , the perturbation solution is reasonably accurate, and the iteration is stopped after the variables corresponding to  $n = 4$  are calculated; when  $\zeta = 0.4$ , an acceptable solution is not obtained until  $n = 8$ . Typical values of the sequences for  $\hat{E}_z^{(n)}$ ,  $p^{(n)}$ , and  $T^{(n)}(0)$  are presented in Table 6.

### Results

By executing the procedure described above for a number of different  $\zeta$ 's, enough information is obtained to show the behavior of  $\hat{E}_z$ ,  $p$ ,  $J$ ,  $n$ , and  $T$  as functions of  $\zeta$ . The effect of temperature inhomogeneities on the shape of  $n$  is shown in Fig. 8, where  $n_0$ ,  $n$ ,  $J$ , and  $T$  are plotted as functions of  $y$  for a specific value of  $\zeta$ . Graphs of  $\hat{E}_z$  (or  $\psi$ ),  $p$ , and  $T(0)$  versus  $\zeta$  (or  $N_{e0}$ ) are plotted along with the perturbation values in Figs. 3, 4, 5, 7, and Fig. 6 shows  $T(0)$  versus  $\psi$ . A comparison of the numerical and the perturbation results shows that the latter are not very accurate except for small values of  $\zeta$ . Tabulated values of  $\psi$ ,  $p$ , and  $T(0)$  for various  $\zeta$  are presented in Table 7.

Unfortunately, the numerical procedure cannot be applied at large values of  $\zeta$ , because the variation of  $T$  with  $y$  causes the domain of the data to be exceeded. Eq. (4.29) of Part I shows that the data for the coefficients of the equations can be evaluated only for a limited range of  $\hat{E}_z/N_n = \hat{E}_z k\hat{T}/p$ . Since  $T$  varies more extensively between the wall and the center of the discharge as  $\zeta$  increases, the quantity

$\hat{E}_z/N_n$  exceeds its limits during the integration over  $y$  if  $\zeta$  is too large. The solution to the problem when  $\zeta = 0.4$  involves a slight extrapolation of the least-squares fit for the data and hence 0.4 serves as an upper bound on  $\zeta$ . This value of  $\zeta$  corresponds to an electron density of  $N_{eo} = 4 \times 10^{10} \text{ cm}^{-3}$ . Since the solution to the problem depends qualitatively on the coefficients, the form of the  $N_{eo} - \hat{E}_z$  relation beyond this value cannot be predicted.

## 5. SUMMARY

Results of the calculations investigating effects of temperature inhomogeneities, recombination, and space charge can be interpreted by comparison with the experimental behavior of discharge columns. Calculations combining the effects of all three factors are not available, but qualitative conclusions can be reached from the studies of Parts II and III.

### Combined Effects

Deviations from ambipolar conditions as a result of space charge are most pronounced at small values of the electron density. Calculations combining its effect with that of recombination are performed in Part II, and a discussion of its omission in temperature calculations begins on p.292. Since recombination and temperature inhomogeneities are only significant at large values of the electron density, the lower portion of the  $N_{eo} - \hat{E}_z$  curve is essentially the same as that shown in Fig. 10 of Part II. Calculations involving effects of both space charge and temperature inhomogeneities would be so tedious and involved as to be unprofitable.

Recombination and temperature inhomogeneities both become important at large values of the electron density, and the contribution of each to the equations is discussed on p. 307 . The perturbation results of Eq. (3.40) show the effect of each on the  $N_{eo} - \hat{E}_z$  relation. These results, the characteristic curves of Parts II and III, and the relative magnitudes of  $\beta$  and  $\epsilon$  show that temperature inhomogeneities become important at a considerably lower value of  $N_{eo}$  than does

recombination. Calculations cannot be performed at values of  $N_{eo}$  where both are important, because the large spatial variations of the temperature exceed the range where experimental data are available. The individual effects of recombination and temperature inhomogeneities on the  $N_{eo} - \hat{E}_z$  relation are shown in Fig. 10 of Part II and Fig. 2 of Part III, but the combined effect is left to conjecture. It is possible that as the electron density increases, recombination might eventually become more important than temperature effects. In that case the  $N_{eo} - \hat{E}_z$  curve would bend left and then back right with increasing  $N_{eo}$ . However, such qualitative behavior cannot be reliably predicted without more data.

#### Interpretation of Results

In Part II the effect of space charge on the  $N_{eo} - \hat{E}_z$  relation at low  $N_{eo}$  is shown to correspond to the shape of the discharge characteristic in the subnormal-glow regime. The portion of the discharge characteristic in which temperature inhomogeneities and recombination are likely to be significant is that corresponding to the abnormal glow or arc (see Fig. 2, Part I).

In Part II recombination is submitted as a possible factor in shaping the discharge characteristic in the abnormal-glow regime. However, the possibility that recombination is important here is actually quite small; the calculations above show that temperature inhomogeneities become important at lower values of the electron density (or current), and their effect on the discharge characteristic must be accounted for first. Furthermore, it is known that the

voltage drop in the vicinity of the cathode increases with current in the abnormal regime, and, in fact, this increase is considered the defining property of the abnormal glow<sup>\*</sup>. The voltage coordinate of the discharge characteristic (Fig. 2, Part I) represents the total voltage drop along the discharge. It is quite possible that the rise of the characteristic in the abnormal regime is caused only by voltage changes in the cathode region and that the rise is totally unrelated to the behavior of the electric field in the positive column. In particular, the electric field in the positive column may actually decrease with increasing current in the manner predicted by calculations concerning temperature inhomogeneities.

The discharge characteristic shows that the total voltage drop decreases markedly in the transition from the abnormal glow to the arc regime. It is known that the large decrease is primarily a cathode phenomenon and that, in general, the voltage continues to decrease with increasing current in the arc regime although it does so less rapidly<sup>\*\*</sup>. Furthermore, the electric field in the positive column decreases as the current (or, equivalently, the electron density) increases<sup>\*\*\*</sup>, so the positive column contributes to and may play a significant role in determining the discharge characteristic in the arc regime. Figures 2 and 3 show that the calculated  $N_{eo} - \hat{E}_z$

---

\* See Cobine [1], pp. 214-215, 226-228; Von Engel [5], pp. 225-234.

\*\* See Cobine [1], pp. 290-298, 311-312; Von Engel [5], pp. 259-263.

\*\*\* See Cobine [1], pp. 298-299, 316-317, 327-329.

relations agree qualitatively with this behavior, and hence the effect of temperature inhomogeneities as calculated here may contribute substantially to the form of the discharge characteristic in the arc regime.

It would be of interest to continue the calculations to larger values of the electron density, but the extent of the data limits our efforts. However, Ecker and Zöller [2], using their approximate coefficients, are able to do so, and they also find a negative voltage-current characteristic caused by temperature inhomogeneities. Their concluding remark that the calculated behavior corresponds to the subnormal-glow regime should be reconsidered, however.

At very high values of the electron density, recombination may be important. The discussion of the recombination coefficient in Part I shows that its actual value for hydrogen is probably considerably less than the value used in the calculations of Part II, and hence its effect on the  $N_{eo} - \hat{E}_z$  relation would occur at larger values of  $N_{eo}$ . Although other gases possess larger coefficients, the effect of recombination is not likely to be felt except far into the arc regime. At very large currents, the voltage drop begins to increase again<sup>\*</sup>, and the effects of recombination may help explain the behavior of the discharge characteristic here. With the appropriate choice of electrodes and operating conditions, the discharge may remain a glow at unusually high currents<sup>\*\*</sup>. In such unusual circumstances it is conceivable that

---

\* See Cobine [1], p. 299.

\*\* See Cobine [1], pp. 251, 315.

the effect of recombination on the discharge characteristic may appear before transition to an arc.

It is perhaps useful to reiterate our final conclusions concerning the relation of the calculated positive-column characteristic to the discharge characteristic. The effect of space charge on the  $N_{eo} - \hat{E}_z$  relation can account for the subnormal discharge, and the region of the  $N_{eo} - \hat{E}_z$  curve where  $\hat{E}_z$  changes only slightly with  $N_{eo}$  corresponds to the normal glow. The effect of temperature inhomogeneities helps explain the decreasing characteristic of the arc, and the effect of recombination is not expected to appear except at very high electron densities; it is not expected to be of significance in the abnormal-glow regime.

Appendix A

NUMERICAL DIFFERENTIATION OF COEFFICIENTS

The derivatives of  $v_I$  and  $B$  with respect to  $T$ ,  $\psi$ , and  $p$  are obtained numerically by the method described here. The method is well illustrated by a formula for the derivative of a function of a single variable.

Differentiation Formula

The procedure by which the formula is obtained consists of expanding a function  $f(x)$  in various Taylor's series about  $x$  and combining them in such a way that certain higher-order derivatives cancel. We begin by writing the expansions

$$f(x+h) = f(x) + hf'(x) + \frac{h^2}{2} f''(x) + \frac{h^3}{6} f'''(x) + \frac{h^4}{24} f^{(iv)}(x) + 0(h^5) \quad (A.1)$$

$$f(x-h) = f(x) - hf'(x) + \frac{h^2}{2} f''(x) - \frac{h^3}{6} f'''(x) + \frac{h^4}{24} f^{(iv)}(x) + 0(h^5) \quad (A.2)$$

$$f(x+2h) = f(x) + 2hf'(x) + 2h^2 f''(x) + \frac{4}{3} h^3 f'''(x) + \frac{2}{3} h^4 f^{(iv)}(x) + 0(h^5) \quad (A.3)$$

$$f(x-2h) = f(x) - 2hf'(x) + 2h^2 f''(x) - \frac{4}{3} h^3 f'''(x) + \frac{2}{3} h^4 f^{(iv)}(x) + 0(h^5) \quad (A.4)$$

Subtracting (A.2) from (A.1), we obtain

$$f(x+h) - f(x-h) = 2hf'(x) + \frac{h^3}{3} f'''(x) + 0(h^5) \quad (A.5)$$

which can be rearranged to yield

$$f'(x) = \frac{f(x+h) - f(x-h)}{2h} + O(h^2) \quad . \quad (A.6)$$

In a similar manner all four expansions are combined to produce the formula,

$$f'(x) = \frac{2}{3h}[f(x+h) - f(x-h) - \frac{1}{8}f(x+2h) + \frac{1}{8}f(x-2h)] + O(h^4) \quad . \quad (A.7)$$

### Error Analysis

The derivatives of the coefficients  $v_I$  and  $B$  are evaluated by applying formulas (A.6) and (A.7) for various values of  $h$ . The calculations of the coefficients from the least-squares fits for the experimental data is done in single-precision accuracy on the computer, so it is necessary to select  $h$  so as to avoid either a large truncation error or a large round-off error. An example of the accuracy of the results is shown in Table 3, where various calculations of  $\frac{\partial B}{\partial p} p_0$  are listed. By observing such results, it was decided to evaluate the derivatives by Eq. (A.7) using

$$h = 0.02 \quad . \quad (A.8)$$

The answers obtained are expected to be accurate to approximately four significant digits.

Appendix B

CALCULATION OF  $\psi$

$\psi_1$  is obtained in a straightforward manner by performing the integrations in Eq. (3.39), which is rewritten below:

$$\int_0^1 \cos \frac{\pi}{2} y \left[ \frac{d}{dy} (B_1 J_0) + A_0 \frac{d}{dy} \left( n_0 \frac{dT_1}{dy} \right) + \frac{\pi^2}{4} v_{11} n_0 - \epsilon B_0 n_0^2 \right] dy = 0 \quad (B.1)$$

Various derivatives of  $n_0$ ,  $J_0$ , and  $T_1$  are needed and are obtained from Eqs. (2.29), (2.31), and (3.34):

$$n_0 = \cos \frac{\pi}{2} y \quad (B.2)$$

$$\frac{dn_0}{dy} = -\frac{\pi}{2} \sin \frac{\pi}{2} y \quad (B.3)$$

$$J_0 = \frac{2}{\pi} \gamma \sin \frac{\pi}{2} y \quad (B.4)$$

$$\frac{dJ_0}{dy} = \gamma \cos \frac{\pi}{2} y \quad (B.5)$$

$$T_1 = \frac{4}{\pi^2} \beta \cos \frac{\pi}{2} y \quad (B.6)$$

$$\frac{dT_1}{dy} = -\frac{2}{\pi} \beta \sin \frac{\pi}{2} y \quad (B.7)$$

$$\frac{d^2 T_1}{dy^2} = -\beta \cos \frac{\pi}{2} y \quad (B.8)$$

The terms in the integrand are now evaluated using Eqs. (3.11) and (3.14) and the relations above:

$$\frac{d}{dy}(B_1 J_o) = \frac{\partial B}{\partial T} \frac{dT_1}{dy} J_o + \left( \frac{\partial B}{\partial T} T_1 + \frac{\partial B}{\partial p} p_1 + \frac{\partial B}{\partial \psi} \psi_1 \right) \frac{dJ_o}{dy} \quad (B.9)$$

$$= -\frac{4}{\pi^2} \gamma \beta \frac{\partial B}{\partial T} \sin^2 \frac{\pi}{2} y + \frac{4}{\pi^2} \gamma \beta \frac{\partial B}{\partial T} \cos^2 \frac{\pi}{2} y + \gamma \left( \frac{\partial B}{\partial p} p_1 + \frac{\partial B}{\partial \psi} \psi_1 \right) \cos \frac{\pi}{2} y \quad (B.10)$$

$$= -\frac{4}{\pi^2} \gamma \beta \frac{\partial B}{\partial T} + \frac{8}{\pi^2} \gamma \beta \frac{\partial B}{\partial T} \cos^2 \frac{\pi}{2} y + \gamma \left( \frac{\partial B}{\partial p} p_1 + \frac{\partial B}{\partial \psi} \psi_1 \right) \cos \frac{\pi}{2} y \quad (B.11)$$

$$A_o \frac{d}{dy} \left( n_o \frac{dT_1}{dy} \right) = A_o \frac{dn_o}{dy} \frac{dT_1}{dy} + A_o n_o \frac{d^2 T_1}{dy^2} \quad (B.12)$$

$$= \beta A_o \sin^2 \frac{\pi}{2} y - \beta A_o \cos^2 \frac{\pi}{2} y \quad (B.13)$$

$$= \beta A_o - 2\beta A_o \cos^2 \frac{\pi}{2} y \quad (B.14)$$

$$\frac{\pi^2}{4} v_{I1} n_o = \beta \frac{\partial v_I}{\partial T} \cos^2 \frac{\pi}{2} y + \frac{\pi^2}{4} \left( \frac{\partial v_I}{\partial p} p_1 + \frac{\partial v_I}{\partial \psi} \psi_1 \right) \cos \frac{\pi}{2} y \quad (B.15)$$

$$\epsilon B_o n_o^2 = \epsilon B_o \cos^2 \frac{\pi}{2} y \quad (B.16)$$

The integrations can be performed most economically if a few definite integrals are evaluated first. They are

$$\int_0^1 \cos \frac{\pi}{2} y dy = \frac{2}{\pi} \quad (B.17)$$

$$\int_0^1 \cos^2 \frac{\pi}{2} y \, dy = \int_0^1 \left( \frac{1}{2} + \frac{1}{2} \cos \pi y \right) dy = \frac{1}{2} \quad (\text{B.18})$$

$$\begin{aligned} \int_0^1 \cos^3 \frac{\pi}{2} y \, dy &= \int_0^1 \cos \frac{\pi}{2} y \, dy - \int_0^1 \cos \frac{\pi}{2} y \sin^2 \frac{\pi}{2} y \, dy \\ &= \frac{2}{\pi} - \frac{2}{3\pi} = \frac{4}{3\pi} \quad . \end{aligned} \quad (\text{B.19})$$

Using (B.11), (B.14), (B.15), and (B.16), Eq. (B.1) becomes

$$\begin{aligned} & - \frac{8}{\pi^3} \gamma \beta \frac{\partial B}{\partial T} + \frac{32}{3\pi^3} \gamma \beta \frac{\partial B}{\partial T} + \frac{\gamma}{2} \left( \frac{\partial B}{\partial p} p_1 + \frac{\partial B}{\partial \psi} \psi_1 \right) \\ & + \frac{2}{\pi} \beta A_o - \frac{8}{3\pi} \beta A_o + \frac{4}{3\pi} \beta \frac{\partial v_I}{\partial T} + \frac{\pi^2}{8} \left( -\frac{\partial v_I}{\partial p} p_1 + \frac{\partial v_I}{\partial \psi} \psi_1 \right) - \frac{4}{3\pi} \epsilon B_o = 0 \quad (\text{B.20}) \end{aligned}$$

Solving for  $\psi_1$  and eliminating  $p_1$  with Eq. (3.36), we obtain

$$\begin{aligned} \psi_1 &= - \left( \frac{4}{3\pi} \beta \frac{\partial v_I}{\partial T} + \frac{1}{\pi} \beta \frac{\partial v_I}{\partial p} p_o + \frac{8}{3\pi^3} \gamma \beta \frac{\partial B}{\partial T} + \frac{4}{\pi^3} \gamma \beta \frac{\partial B}{\partial p} p_o \right. \\ & \left. - \frac{2}{3\pi} \beta A_o - \frac{4}{3\pi} \epsilon B_o \right) / \left( \frac{\pi^2}{8} \frac{\partial v_I}{\partial \psi} + \frac{\gamma}{2} \frac{\partial B}{\partial \psi} \right) \quad . \end{aligned} \quad (\text{B.21})$$

NOMENCLATURE

The number following the descriptions gives the page on which the symbol first appears. Symbols whose use is very temporary and those which have been defined previously in Part I usually do not appear here.

Roman

A	variable coefficient in the equations (295)
$A_0$	A at $\zeta = 0$ (304)
B	variable coefficient in the equations (295)
$B_0$	B at $\zeta = 0$ (304)
$B_1$	second term in the expansion of B (309)
$\hat{E}_{z0}$	$\hat{E}_z$ at $\zeta = 0$ (301)
$\hat{E}_{zn}$	$n^{\text{th}}$ term of the expansion for $\hat{E}_z$ (307)
$\hat{E}_z^{(n)}$	$n^{\text{th}}$ approximation of $\hat{E}_z$ (319)
$J_0$	J at $\zeta = 0$ (301)
$J_n$	$n^{\text{th}}$ term of the expansion for J (307)
$J^{(n)}$	$n^{\text{th}}$ approximation of J (319)
n	electron and ion density (293)
$n_0$	n at $\zeta = 0$ (301)
$n_n$	$n^{\text{th}}$ term of the expansion for n (307)
$n^{(n)}$	$n^{\text{th}}$ approximation of n (319)
$p_0$	p at $\zeta = 0$ (301)
$p_n$	$n^{\text{th}}$ term of the expansion for p (307)
$p^{(n)}$	$n^{\text{th}}$ approximation of p (318)

$Q$	quantity of gas in discharge (296)
$T_o$	$T$ at $\zeta = 0$ (301)
$T_n$	$n^{\text{th}}$ term of the expansion for $T$ (307)
$T^{(o)}$	initial approximation of $T$ (318)
$T^{(n)}$	$n^{\text{th}}$ approximation of $T$ (318)

Greek

$\beta_o$	$\beta$ with $\hat{h}$ replaced by $\hat{h}_o$ (305)
$v_{I0}$	$v_I$ at $\zeta = 0$ (304)
$v_{I1}$	second term in the expansion of $v_I$ (308)
$\psi$	dimensionless axial electric field (308)
$\psi_o$	$\psi$ at $\zeta = 0$ (308)
$\psi_n$	$n^{\text{th}}$ term of the expansion for $\psi$ (308)

LIST OF TABLES

1. Values of  $\hat{E}_{z_0}$  and Constant Coefficients
2. Values of  $A_0$ ,  $B_0$ , and Derivatives of  $v_I$  and  $B$
3. Calculated Values of  $\frac{\partial B}{\partial p} p_0$
4. Examples of the Convergence of  $z^{(k)}$  to  $\hat{E}_z^{(n)}$
5. Examples of the Convergence of  $z^{(k)}$  to  $T^{(n)}(0)$
6. Example of the Sequences  $\hat{E}_z^{(n)}$ ,  $p^{(n)}$ ,  $T^{(n)}(0)$
7.  $\psi$ ,  $p$ , and  $T(0)$  as Functions of  $\zeta$

Table 1

VALUES OF  $\hat{E}_{z0}$  AND CONSTANT COEFFICIENTS

$$\hat{E}_{z0} = 20.84411 \text{ volts/cm}$$

$$\gamma = 2.412279$$

$$\epsilon = 0.09612836$$

$$\tau = 1.164970 \times 10^2$$

$$\delta = 2.715121 \times 10^{-4}$$

$$\beta = 4.455542$$

$$\beta_0 = 0.4095883$$

Table 2

VALUES OF  $A_o$ ,  $B_o$ , AND DERIVATIVES OF  $v_I$  AND  $B$

Derivatives of  $v_I$  and  $B$  are evaluated at

$$(T, \psi, p) = (1, 1, p_o)$$

$$A_o = 0.860228$$

$$B_o = 1.02285$$

$$\frac{\partial v_I}{\partial T} = 6.42579$$

$$\frac{\partial v_I}{\partial p} p_o = -6.42542$$

$$\frac{\partial v_I}{\partial \psi} = 7.42569$$

$$\frac{\partial B}{\partial T} = -2.00052$$

$$\frac{\partial B}{\partial p} p_o = 1.99178$$

$$\frac{\partial B}{\partial \psi} = -0.968976$$

Table 3

CALCULATED VALUES OF  $\frac{\partial B}{\partial p} p_o$

The numbers are the values of  $\frac{\partial B}{\partial p} p_o$  calculated by the numerical differentiation formulas (A.6) and (A.7) of Appendix A. The headings  $O(h^2)$  and  $O(h^4)$  represent the truncation errors of the formulas used in the respective columns.

<u>h</u>	<u><math>O(h^2)</math></u>	<u><math>O(h^4)</math></u>
0.100	1.99651	1.99213
0.050	1.99307	1.99193
0.020	1.99200	1.99178
0.010	1.99189	1.99186
0.005	1.99204	1.99208
0.002	1.99080	1.99064
0.001	1.98984	1.98952

Table 4

EXAMPLES OF THE CONVERGENCE OF  $z^{(k)}$  TO  $\hat{E}_z^{(n)}$

$\zeta = 0.3$

<u>n = 1</u> :	<u>k</u>	<u><math>z^{(k)}</math></u>
	0	18.38934
	2	18.84865
	3	18.84923
	4	18.84923

$\hat{E}_z^{(1)} = 18.84923$

$n^{(1)}(1) = 0.7 \times 10^{-5}$

<u>n = 2</u> :	<u>k</u>	<u><math>z^{(k)}</math></u>
	0	18.84923
	2	19.27286
	3	19.27399
	4	19.27400

$\hat{E}_z^{(2)} = 19.27400$

$n^{(2)}(1) = 0.7 \times 10^{-5}$

<u>n = 7</u> :	<u>k</u>	<u><math>z^{(k)}</math></u>
	0	19.19473
	2	19.19376
	3	19.19374

$\hat{E}_z^{(7)} = 19.19374$

$n^{(7)}(1) = -0.5 \times 10^{-5}$

Table 5

EXAMPLES OF THE CONVERGENCE OF  $z^{(k)}$  TO  $\hat{T}^{(n)}(0)$

$\zeta = 0.3$

<u>n = 1</u> :	<u>k</u>	<u>z<sup>(k)</sup></u>
	0	1.541728
	2	1.423100
	3	1.423812
	4	1.423805

$$T^{(1)}(0) = 1.423812$$

$$T^{(1)}(1) = 1.00001$$

<u>n = 2</u> :	<u>k</u>	<u>z<sup>(k)</sup></u>
	0	1.423812
	2	1.457333
	3	1.457508
	4	1.457516

$$T^{(2)}(0) = 1.457508$$

$$T^{(2)}(1) = 0.99999$$

<u>n = 7</u> :	<u>k</u>	<u>z<sup>(k)</sup></u>
	0	1.449483
	2	1.449376
	3	1.449377

$$T^{(7)}(0) = 1.449376$$

$$T^{(7)}(1) = 1.00000$$

Table 6

EXAMPLE OF THE SEQUENCES  $\hat{E}_z^{(n)}$ ,  $p^{(n)}$ ,  $T^{(n)}(0)$

$\zeta = 0.3$

<u>n</u>	<u><math>\hat{E}_z^{(n)}</math></u>	<u><math>p^{(n)}</math></u>	<u><math>T^{(n)}(0)</math></u>
0	-	-	1.541728
1	18.84923	1.322584	1.423812
2	19.27400	1.264105	1.457508
3	19.16916	1.283759	1.446916
4	19.20161	1.277559	1.450170
5	19.19156	1.279457	1.449165
6	19.19473	1.278877	1.449483
7	19.19374	1.279060	1.449376
8	-	1.278996	-

$$\hat{E}_z = 19.194$$

$$p = 1.2790$$

$$T(0) = 1.4494$$

Table 7

$\psi$ ,  $p$ , AND  $T(0)$  AS FUNCTIONS OF  $\zeta$

<u><math>\zeta</math></u>	<u><math>\psi</math></u>	<u><math>p</math></u>	<u><math>T(0)</math></u>
0	1	1	1
0.05	0.98191	1.0549	1.0867
0.10	0.96636	1.1054	1.1674
0.15	0.95284	1.1525	1.2432
0.20	0.94094	1.1969	1.3151
0.25	0.93033	1.2389	1.3836
0.30	0.92084	1.2790	1.4494
0.35	0.91220	1.3174	1.5127
0.40*	0.90438	1.3544	1.5739

---

\* Values corresponding to this  $\gamma$  involve a slight extrapolation of data.

LIST OF FIGURES

1.  $n_o$  and  $n_o$  as Functions of  $y$
2. Perturbation Results for the  $N_{eo} - \hat{E}_z$  Relation for  $\beta$  and  $\beta_o$
3.  $N_{eo}$  versus  $\hat{E}_z$
4.  $\zeta$  versus  $\psi$
5.  $\zeta$  versus  $T(0)$
6.  $T(0)$  versus  $\psi$
7.  $\zeta$  versus  $p/p_o$
8.  $n_o$ ,  $n$ ,  $J$ , and  $T$  as Functions of  $y$

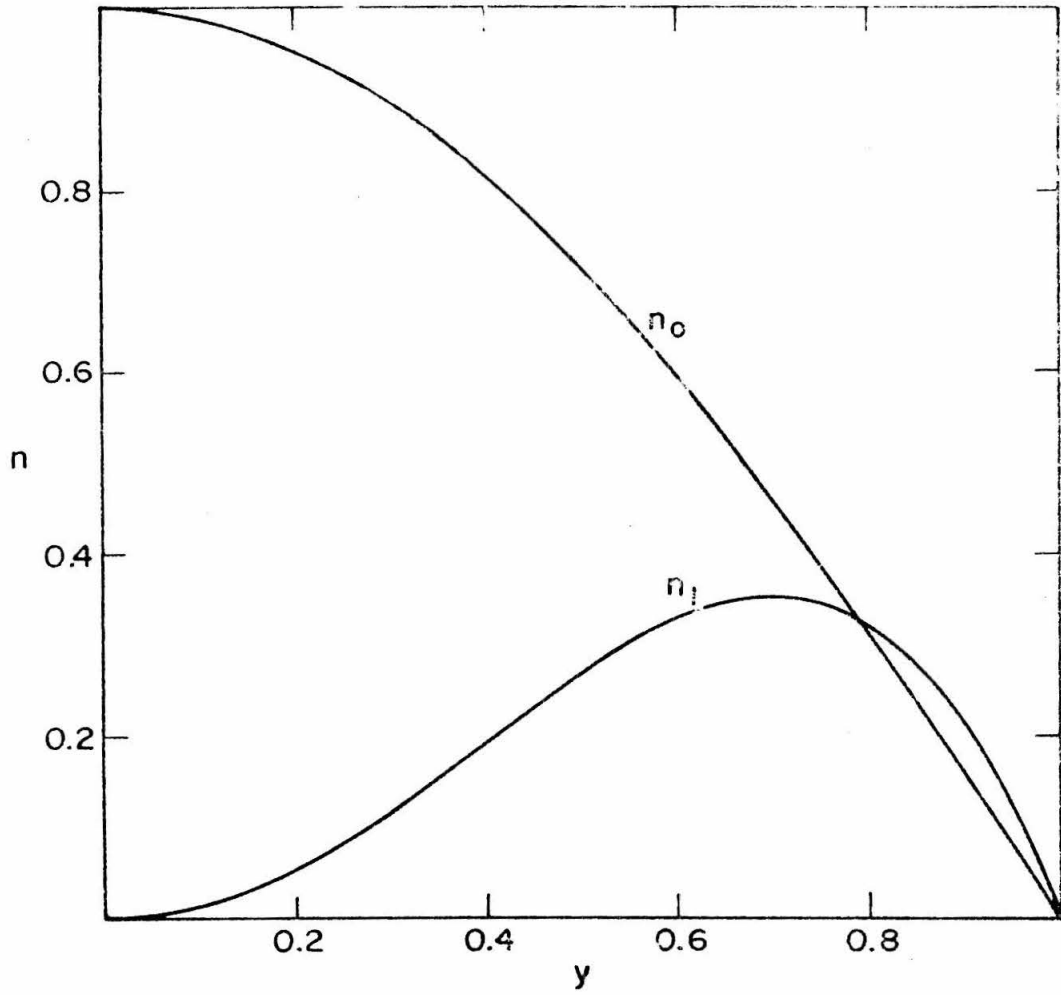


Figure 1:  $n_0$  and  $n_1$  as Functions of  $y$

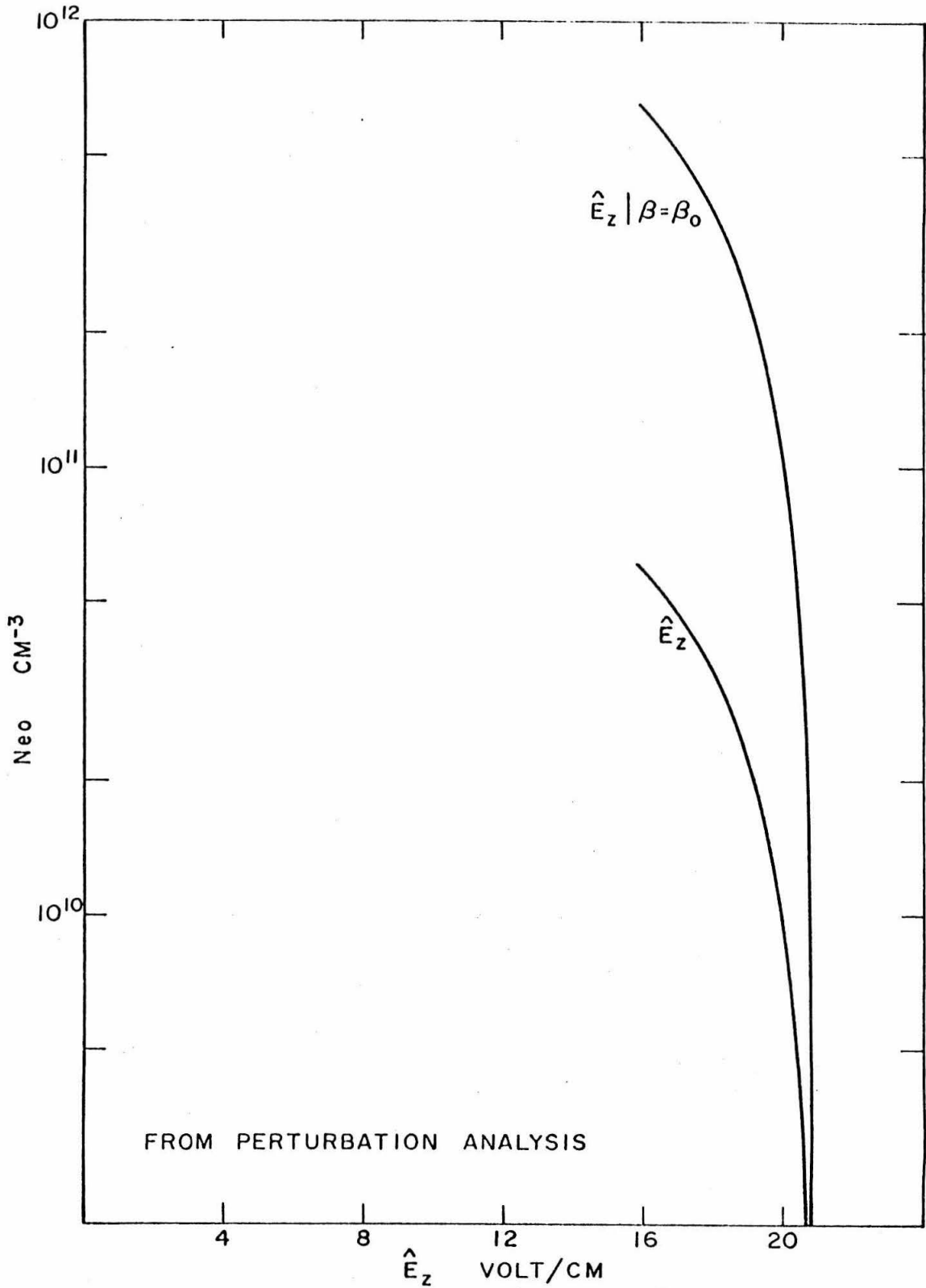


Figure 2: Perturbation Results for the  $N_{eo} - \hat{E}_z$  Relation for  $\beta$  and  $\beta_0$

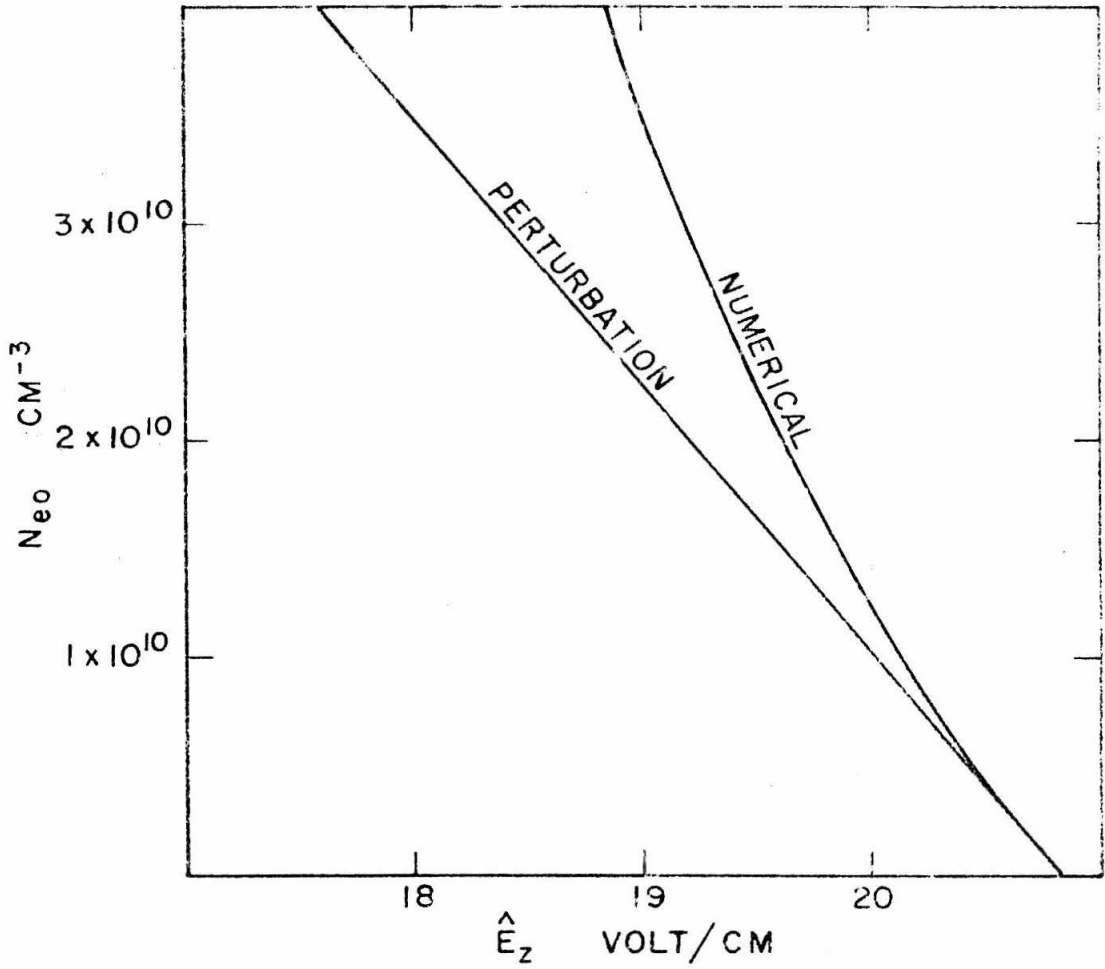


Figure 3:  $N_{eo}$  versus  $\hat{E}_z$

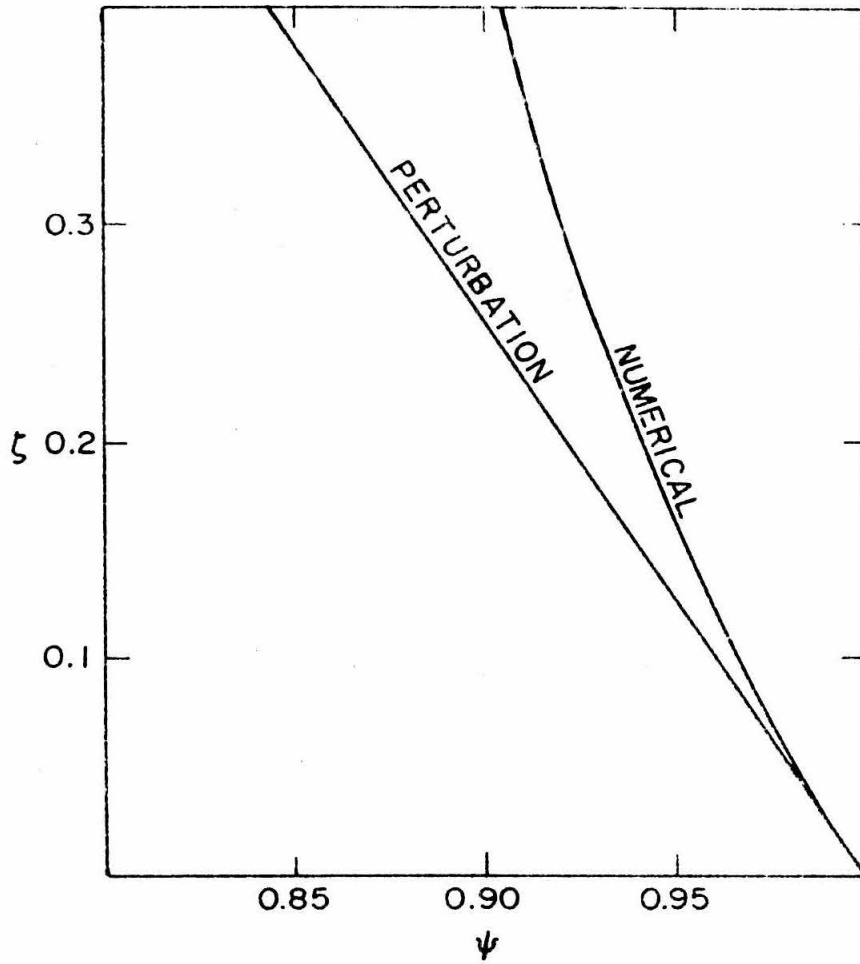


Figure 4:  $\zeta$  versus  $\psi$

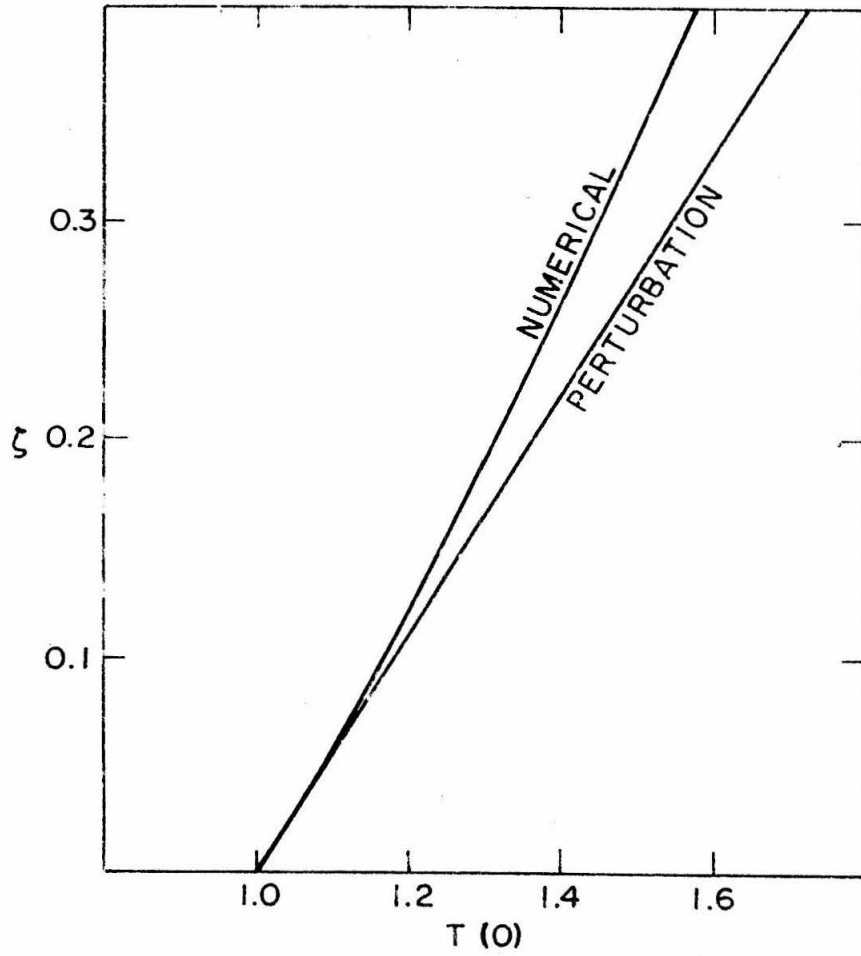


Figure 5:  $\zeta$  versus  $T(0)$

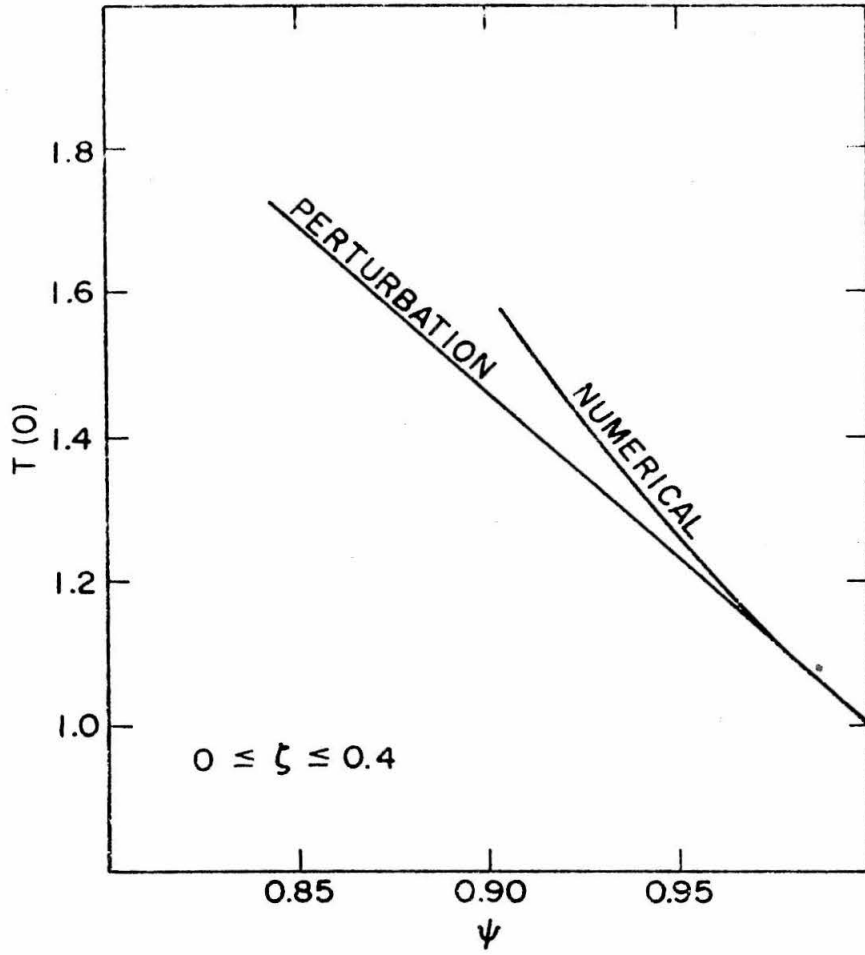


Figure 6:  $T(0)$  versus  $\psi$

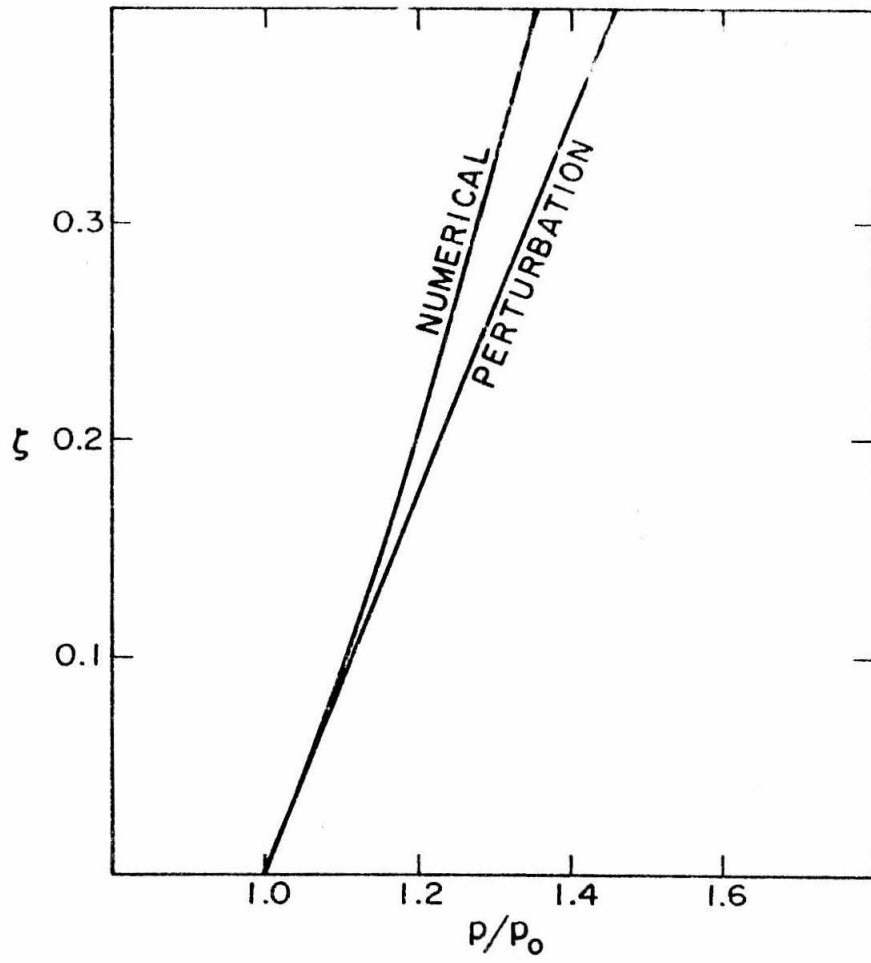


Figure 7:  $\zeta$  versus  $p/p_0$

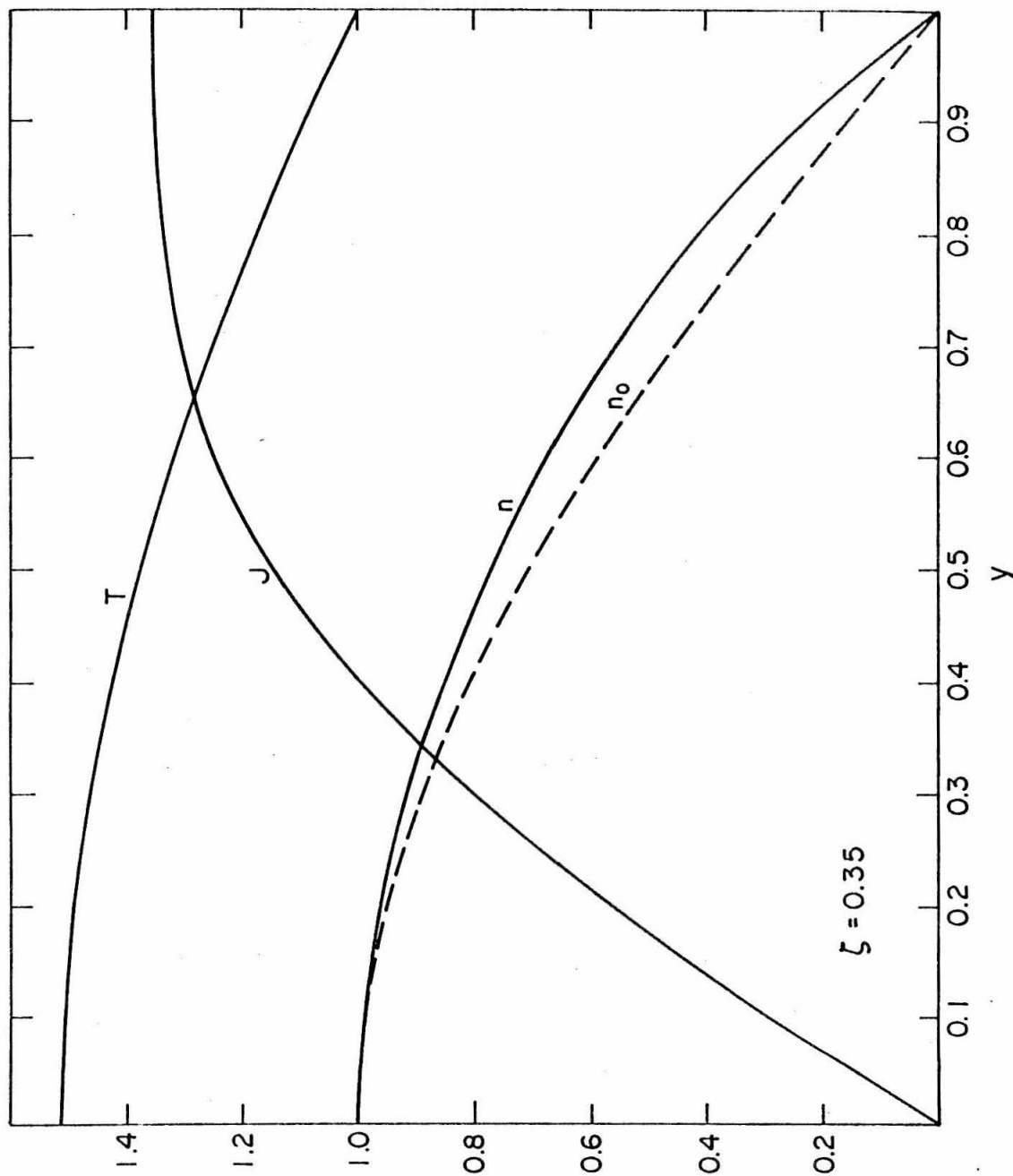


Figure 8:  $n_0$ ,  $n$ ,  $J$ , and  $T$  as Functions of  $y$

BIBLIOGRAPHY

1. Cobine, James Dillon, Gaseous Conductors, Dover, 1958.
2. Ecker, G. and O. Zoller, "Thermally Inhomogeneous Plasma Column," Physics of Fluids 7, 1996-2000 (1964).
3. Henrici, Peter, Discrete Variable Methods in Ordinary Differential Equations, Wiley & Sons, Inc., 1962.
4. Isaacson, Eugene and Herbert Bishop Keller, Analysis of Numerical Methods, Wiley & Sons, Inc., 1966.
5. Von Engel, A., Ionized Gases, Oxford University Press, 1965.

PROPOSITIONS

1. Relaxation of the Electron Distribution Function to the Maxwellian State
2. Jump Discontinuities in Concentration Profiles for Fixed-Column Adsorption
3. The Equations of Surface Flow in a Rotating Frame of Reference

Proposition 1

RELAXATION OF THE ELECTRON DISTRIBUTION FUNCTION TO  
THE MAXWELLIAN STATE

In a plasma typical of the positive column of a glow discharge, the applied electric field maintains the mean electron energy at a level much higher than that of the neutral molecules. If the field is suddenly removed, the mean electron energy or electron temperature decreases until it equals the temperature of the neutrals at equilibrium, where both electrons and neutrals have Maxwellian velocity distributions at the same temperature. In the following work the response of the electron distribution function to the abrupt removal of the electric field is studied analytically in an attempt to determine the "relaxation time"--the time needed for the distribution function to evolve significantly toward its asymptotic Maxwellian form. An estimate of the relaxation time is obtained by an approximate method based on energy-transfer considerations, and this value is checked by a numerical integration that yields the transient behavior of the entire distribution function.

The analysis is based on the Boltzmann equation for the electron distribution function. The plasma is assumed to be spatially uniform, and inelastic collisions are neglected. Consequently there is no mechanism for production or loss of electrons, and the electron density remains constant. The analytical work proceeds by expanding the distribution function in spherical harmonics and substituting the expansion into the Boltzmann equation. Equations are obtained for the first two

terms of the expansion, and it is these equations that are solved numerically to determine the relaxation time.

This study of the relaxation time is prompted by the necessity of choosing the proper approach when solving the Boltzmann equation for the electron distribution function in a plasma with an alternating electric field. If the frequency of the field is very high (microwave frequency, for instance) so that the field completes a cycle in a time much less than the relaxation time, the equation can be simplified greatly by averaging it with respect to time over one cycle<sup>\*</sup>. On the other hand, if the frequency is low (power-line frequency), the distribution function at a given time can be found by solving the equation treating the electric field as a constant parameter and using in the solution the value of the field at the time in question. Such simplifying procedures are not available when the frequency is near the reciprocal of the relaxation time, and it is important to know the relaxation time in order to determine when the approximations can be made. Of course, knowledge of the relaxation time is also important in other applications involving interruption or alteration of the electric field.

#### The Boltzmann Equation

Omitting the terms involving spatial gradients and inelastic collisions, the Boltzmann equation for the electron distribution function can be written as

---

\*This approach is demonstrated by Holstein [9].

$$\frac{\partial f}{\partial t} - \frac{e}{m} \underline{E} \cdot \frac{\partial f}{\partial \underline{v}} = \left(\frac{\partial f}{\partial t}\right)_{e.c.} \quad (1)$$

where

$f(\underline{v}, t)$  is the distribution function normalized so that  $f \, d\underline{v}$  represents the probability of an electron lying in the element of velocity space  $d\underline{v}$  ;

$\underline{E}$  is the (constant) electric field ;

$e$  is the magnitude of the electronic charge ;

$m$  is the electron mass ;

$(\partial f / \partial t)_{e.c.}$  is the rate of increase in  $f$  caused by elastic electron-neutral collisions

Although the term containing the electric field is not present when the equation is solved during the relaxation process, it is included in the derivation of the final equations in order to show the appropriateness of the choice of initial conditions and to demonstrate the motivation for expanding  $f$  in spherical harmonics. The collision integral can be written in terms of electron and neutral distribution functions and the elastic-scattering cross section as\*

$$\left(\frac{\partial f}{\partial t}\right)_{e.c.} = N_n \iint [F(\underline{V}, t) f(\underline{v}, t) - F(\underline{v}, t) f(\underline{V}, t)] g \, q(g, \chi) \, d\Omega \, d\underline{V} \quad (2)$$

where

$N_n$  is the number density of neutral molecules ;

---

\* See, for instance, Holt and Haskell [10], p. 122.

$F(\underline{V},t)$  is the distribution function for the neutral molecules normalized so that its integral over all values of the velocity  $\underline{V}$  is unity ;

$\underline{\tilde{v}}, \underline{\tilde{V}}$  are the post-collision velocities of an electron and a neutral molecule with pre-collision velocities  $\underline{v}$  and  $\underline{V}$  ;

$g$  is the magnitude of the relative velocity,  $\underline{v} - \underline{V}$  ;

$q(g,\chi)$  is the differential elastic-scattering cross section;

$\chi$  is the angle of deflection in relative coordinates;

$d\Omega$  is an element of solid angle\* .

Because the random electron velocity is much greater than the drift velocity, the electron distribution function is almost isotropic and can be represented accurately by the first few terms of a spherical-harmonic expansion in velocity space. If the polar axis is taken in the direction of the electric field, there is azimuthal symmetry, and the expansion in spherical harmonics reduces to an expansion in Legendre polynomials. Consequently  $f$  can be written as

$$f(\underline{v},t) = f(v,\theta,t) = \sum_{n=0}^{\infty} f_n(v,t) P_n(\cos \theta) \quad (3)$$

where  $P_n(z)$  is the  $n^{\text{th}}$  Legendre polynomial and  $\theta$  is the polar angle.

---

\* These quantities are discussed in detail in Appendices A and B of Part I.

The substitution of the spherical-harmonic expansion for  $f$  into the Boltzmann equation is treated by various writers<sup>\*</sup>, but the derivation of the equations for the  $f_n$  is also included here for completeness. Equations for the  $f_n$  are obtained by expressing each term of the Boltzmann equation as a series expansion in spherical harmonics. Since the spherical harmonics are linearly independent and the Boltzmann equation must hold as an identity in  $\theta$ , terms proportional to the same spherical harmonic are associated to form an equation.

#### Expansion of the Left-Hand Side

If the expansion (3) is substituted into the left-hand side of Eq. (1), various properties of the Legendre polynomials can be exploited to express the entire side as a series expansion. The gradient is written in spherical coordinates in velocity space with the polar axis taken in the direction of the electric field, and this direction is expressed by the unit vector  $\underline{k}$  in Fig. 1. Using the unit vectors  $\underline{e}_v$ ,  $\underline{e}_\theta$  and  $\underline{e}_\phi$  shown there, the gradient in spherical coordinates becomes

$$\underline{\frac{\partial f}{\partial v}} = \underline{e}_v \frac{\partial f}{\partial v} + \underline{e}_\theta \frac{1}{v} \frac{\partial f}{\partial \theta} + \underline{e}_\phi \frac{1}{v \sin \theta} \frac{\partial f}{\partial \phi} \quad . \quad (4)$$

It is apparent from Fig. 1 that  $\underline{k}$  can also be expressed in terms of these coordinates as

$$\underline{k} = \underline{e}_v \cos \theta - \underline{e}_\theta \sin \theta \quad . \quad (5)$$

---

\* See, for instance, Allis [1].

From Eqs. (4) and (5) we obtain the inner product

$$\underline{k} \cdot \frac{\partial f}{\partial \underline{v}} = \cos \theta \frac{\partial f}{\partial v} - \frac{\sin \theta}{v} \frac{\partial f}{\partial \theta} \quad (6)$$

Substituting the expansion (3) into (6)

$$\underline{k} \cdot \frac{\partial f}{\partial \underline{v}} = \sum_{n=0}^{\infty} \left[ \frac{\partial f_n}{\partial v} \cos \theta P_n(\cos \theta) + \frac{f_n}{v} \sin^2 \theta P'_n(\cos \theta) \right] \quad (7)$$

This expression can be simplified using the following identities\* :

$$\cos \theta P_n(\cos \theta) = \frac{n+1}{2n+1} P_{n+1}(\cos \theta) + \frac{n}{2n+1} P_{n-1}(\cos \theta) \quad (8)$$

$$\sin^2 \theta P'_n(\cos \theta) = \frac{n(n+1)}{2n+1} [P_{n-1}(\cos \theta) - P_{n+1}(\cos \theta)] \quad (9)$$

for  $n \geq 0$  , provided it is understood that

$$P_{-1}(\cos \theta) = 0 \quad (10)$$

Substituting these formulas into (7) ,

$$\begin{aligned} \underline{k} \cdot \frac{\partial f}{\partial \underline{v}} &= \sum_{n=0}^{\infty} \left\{ \frac{\partial f_n}{\partial v} \left[ \frac{n+1}{2n+1} P_{n+1}(\cos \theta) + \frac{n}{2n+1} P_{n-1}(\cos \theta) \right] \right. \\ &\quad \left. + \frac{f_n}{v} \left[ \frac{n(n+1)}{2n+1} P_{n-1}(\cos \theta) - \frac{n(n+1)}{2n+1} P_{n+1}(\cos \theta) \right] \right\} \quad (11) \end{aligned}$$

$$\begin{aligned} &= \sum_{n=0}^{\infty} \left[ \frac{n}{2n-1} \frac{\partial f_{n-1}}{\partial v} - \frac{n(n-1)}{2n-1} \frac{f_{n-1}}{v} + \frac{n+1}{2n+3} \frac{\partial f_{n+1}}{\partial v} \right. \\ &\quad \left. + \frac{(n+1)(n+2)}{2n+3} \frac{f_{n+1}}{v} \right] P_n(\cos \theta) \quad (12) \end{aligned}$$

---

\* See Sansone [13], pp. 178-179.

Now we can write

$$\frac{\partial f}{\partial t} - \frac{e}{m} \underline{E} \cdot \frac{\partial f}{\partial \underline{v}} = \sum_{n=0}^{\infty} H_n(\underline{v}, t) P_n(\cos \theta) \quad , \quad (13)$$

where

$$H_n(\underline{v}, t) = \frac{\partial f_n}{\partial t} - \frac{eE}{m} \left[ \frac{n}{2n-1} \frac{\partial f_{n-1}}{\partial v} - \frac{n(n-1)}{2n-1} \frac{f_{n-1}}{v} + \frac{n+1}{2n+3} \frac{\partial f_{n+1}}{\partial v} + \frac{(n+1)(n+2)}{2n+3} \frac{f_{n+1}}{v} \right] . \quad (14)$$

### Expansion of the Collision Integral

After various manipulations the collision integral can also be expressed as an expansion in Legendre polynomials. Substituting (3) into (2) and writing the integration over  $\Omega$  in more detail,

$$\left( \frac{\partial f}{\partial t} \right)_{e.c.} = N_n \sum_{n=0}^{\infty} \iiint [F(\underline{\tilde{v}}, t) f_n(\underline{\tilde{v}}, t) P_n(\cos \tilde{\theta}) - F(\underline{v}, t) f_n(\underline{v}, t) P_n(\cos \theta)] \times g q(g, \chi) \sin \chi \, d\chi \, d\epsilon \, d\underline{v} . \quad (15)$$

$\tilde{\theta}$  is the angle between  $\underline{\tilde{v}}$  and  $\underline{k}$  and can be expressed in terms of  $\theta$  and the angle between  $\underline{\tilde{v}}$  and  $\underline{v}$ .  $\chi$  is the angle between  $\underline{\tilde{v}} - \underline{\tilde{v}}$  and  $\underline{v} - \underline{v}$  and differs from the angle between  $\underline{\tilde{v}}$  and  $\underline{v}$  by a term of order  $O(m/M)^*$ , where  $M$  is the mass of a neutral molecule. Neglecting this term,  $\underline{\tilde{v}}$  can be expressed in a spherical coordinate system with  $\underline{v}$  as polar axis and  $\chi$  as polar angle. If  $\epsilon$  is measured from  $\underline{e}_\theta$  (see Fig. 2),

---

\* See, for instance, Delcroix [4], p. 94.

$$\underline{\tilde{v}} = \underline{e}_{\tilde{v}} \tilde{v} \cos \chi + \underline{e}_{\theta} \tilde{v} \sin \chi \cos \varepsilon + \underline{e}_{\phi} \tilde{v} \sin \chi \sin \varepsilon . \quad (16)$$

$\cos \tilde{\theta}$  can now be obtained from (5) and (16) as

$$\cos \tilde{\theta} = \underline{k} \cdot \frac{\underline{\tilde{v}}}{\tilde{v}} \quad (17)$$

$$= \cos \theta \cos \chi - \sin \theta \sin \chi \cos \varepsilon . \quad (18)$$

The addition theorem of spherical harmonics\* can be used to write  $P_n(\cos \tilde{\theta})$  in a more convenient form:

$$P_n(\cos \tilde{\theta}) = P_n(\cos \theta \cos \chi - \sin \theta \sin \chi \cos \varepsilon) \quad (19)$$

$$= P_n(\cos \theta) P_n(\cos \chi)$$

$$+ 2 \sum_{m=1}^n (-1)^m \frac{(n-m)!}{(n+m)!} P_n^m(\cos \theta) P_n^m(\cos \chi) \cos m\varepsilon , \quad (20)$$

for  $n \geq 1$  . If this expression is substituted into Eq. (15) and integrated over  $\varepsilon$  , all terms involved in the summation over  $m$  disappear. Hence

$$\left(\frac{\partial f}{\partial t}\right)_{e.c.} = \sum_{n=0}^{\infty} S_n(v,t) P_n(\cos \theta) \quad (21)$$

where

$$S_n(v,t) = N_n \iint [F(\underline{\tilde{v}},t) f_n(\underline{\tilde{v}},t) P_n(\cos \chi) - F(\underline{v},t) f_n(\underline{v},t)] g q(g,\chi) d\Omega d\underline{v} . \quad (22)$$

---

\* See Sansone [13], p. 268.

In order to obtain equations for  $f_0$  and  $f_1$ , it is necessary to express  $S_0$  and  $S_1$  in more convenient forms. Before the integrals can be simplified, it is necessary to specify the neutral distribution function. The neutral velocity distribution is approximately Maxwellian at the gas temperature  $T$ , so we write

$$F(\underline{V}, t) = \left(\frac{M}{2\pi kT}\right)^{3/2} \exp\left[-\frac{MV^2}{2kT}\right] \quad (23)$$

The transformations to the desired expressions involve some rather cumbersome algebra and are not presented here. The final forms of  $S_0$  and  $S_1$  are given by

$$S_0 = N_n \iint [F(\underline{\tilde{V}}, t) f_0(\underline{\tilde{v}}, t) - F(\underline{V}, t) f_0(\underline{v}, t)] g q(g, \chi) d\Omega d\underline{V} \quad (24)$$

$$= \frac{m}{M} \frac{1}{v^2} \frac{\partial}{\partial v} [v^3 v_m(v) f_0] + \frac{kT}{M} \frac{1}{v^2} \frac{\partial}{\partial v} [v^2 v_m(v) \frac{\partial f_0}{\partial v}] \quad (25)$$

$$S_1 = N_n \iint [F(\underline{\tilde{V}}, t) f_1(\underline{\tilde{v}}, t) \cos \chi - F(\underline{V}, t) f_1(\underline{v}, t)] g q(g, \chi) d\Omega d\underline{V} \quad (26)$$

$$= -v_m(v) f_1 \quad (27)$$

where

$$v_m(v) = N_n v \int (1 - \cos \chi) q(v, \chi) d\Omega \quad (28)$$

$$= N_n v Q_m(v) \quad (29)$$

and

$$Q_m(v) = \int (1 - \cos \chi) q(v, \chi) d\Omega \quad (30)$$

The collision frequency  $v_m$  and the momentum-transfer cross section  $Q_m$  are discussed in Appendix B of Part I.

Derivations of the above are presented with varying degrees of clarity in several of the references listed. Perhaps the most systematic method, the one showing most clearly the approximations involved, is that of Desloge and Matthysse [5], although they begin with a somewhat different but equivalent form of the Boltzmann equation and proceed through some very tedious manipulations. Besides the assumption that  $F$  is Maxwellian, the derivation sometimes ignores the difference between the relative velocity and the electron velocity. Because of the large difference between the magnitudes of the electron and the molecular velocities, the relative velocity can be expressed as the electron velocity plus terms involving the ratio of electron mass to molecular mass. In the expressions for  $S_0$  and  $S_1$ , terms involving higher relative orders in the mass ratio are neglected.

Equations for  $f_0$  and  $f_1$

Equations for the  $f_n$  are obtained by equating the  $H_n$  and the  $S_n$ . In the following development the electron mean free path  $\lambda$  is assumed constant, so  $v_m$ , which appears in the expressions for  $S_0$  and  $S_1$  is replaced according to the equation

$$\lambda = v/v_m \quad . \quad (31)$$

From Eqs. (14) and (25) we now obtain

$$\begin{aligned} \frac{\partial f_0}{\partial t} = & \frac{eE}{3m} \frac{1}{v^2} \frac{\partial}{\partial v} (v^2 f_1) + \frac{m}{M} \frac{1}{\lambda} \frac{1}{v^2} \frac{\partial}{\partial v} (v^4 f_0) \\ & + \frac{kT}{M\lambda} \frac{1}{v^2} \frac{\partial}{\partial v} (v^3 \frac{\partial f_0}{\partial v}) \quad . \end{aligned} \quad (32)$$

From Eq. (14) it is seen that  $f_2$  appears in the expression for  $H_1$  so a closed system of equations for  $f_0$  and  $f_1$  is not obtained by equating  $H_1$  and  $S_1$ . Consequently it is necessary to truncate the system of equations by neglecting  $f_2$ . Ginsburg and Gurevich [8] discuss the validity of this procedure in detail and conclude that  $f_2$  is indeed negligible except for very small and very large velocities. Equating  $H_1$  and  $S_1$  from Eqs. (14) and (27) then yields

$$\frac{\partial f_1}{\partial t} = \frac{eE}{m} \frac{\partial f_0}{\partial v} - \frac{1}{\lambda} v f_1 \quad . \quad (33)$$

#### Formulation of the Problem

In studying the relaxation of the electron distribution function, the equations for  $f_0$  and  $f_1$  are solved with  $E$  set equal to zero. However, initial conditions on  $f_0$  and  $f_1$  must be prescribed, and these initial conditions are taken to be an approximation to the steady-state solution of the equations in the presence of an electric field. It is easily verified that the steady-state solution to Eqs. (32) and (33) for  $f_0$  is the Druyvesteyn distribution

$$g_0(v) = C \exp[-3m^3 v^4 / (4Me^2 E^2 \lambda^2)] \quad (34)$$

provided the term involving  $kT/M$  in (32) is neglected. It can be shown\* that the term in (32) which contains  $m/M$  represents the change in  $f_0$  that would result from electron-neutral collisions if the neutrals were stationary before collision. The term that contains  $kT/M$

---

\* See Chapman and Cowling [2], pp. 346-352.

represents the change in  $f_0$  caused by energy given to electrons in collisions because of the thermal energy of the neutrals. The relative importance of the two terms can be determined by a study of the equation and is roughly the ratio of mean electron energy to mean neutral energy. Actually the complete steady-state solution can be obtained analytically<sup>\*</sup>, and it reduces to the Druyvesteyn distribution if

$$\frac{M}{3v^2} \left(\frac{eE\lambda}{m}\right)^2 \gg kT \quad . \quad (35)$$

Thus the term involving  $kT/M$  can be neglected when a strong electric field is present but must be retained in studying the relaxation of the electron temperature to that of the neutrals.

The steady-state solution of Eqs. (32) and (33) for  $E = 0$  is readily seen to be the Maxwellian distribution

$$f_0(v) = C' \exp[-mv^2/(2kT)] \quad (36)$$

$$f_1(v) = 0 \quad . \quad (37)$$

$f_0$  and  $f_1$  must approach these functions asymptotically in the relaxation process.

#### Statement of Problem

The equations to be solved following the abrupt removal of the electric field can now be written along with the appropriate initial and boundary conditions.

---

<sup>\*</sup> See Wu [14].

$$\frac{\partial f_o}{\partial t} = \frac{m}{M} \frac{1}{\lambda} \frac{1}{v^2} \frac{\partial}{\partial v} (v^4 f_o) + \frac{kT}{M\lambda} \frac{1}{v^2} \frac{\partial}{\partial v} (v^3 \frac{\partial f_o}{\partial v}) \quad (38)$$

$$\frac{\partial f_1}{\partial t} = -\frac{1}{\lambda} v f_1 \quad (39)$$

t = 0 :

$$f_o(v,0) = g_o(v) = \frac{1}{\pi\Gamma(\frac{3}{4})} \left( \frac{3m^3}{4Me^2 E^2 \lambda^2} \right)^{3/4} \exp\left[-\frac{3m^3 v^4}{4Me^2 E^2 \lambda^2}\right] \quad (40)$$

$$f_1(v,0) = g_1(v) = \frac{-4}{\pi\Gamma(\frac{3}{4})} \frac{eE\lambda}{m} \left( \frac{3m^3}{4Me^2 E^2 \lambda^2} \right)^{7/4} v^2 \exp\left[-\frac{3m^3 v^4}{4Me^2 E^2 \lambda^2}\right] \quad (41)$$

$$v = 0 : \quad \frac{\partial f_o}{\partial v}(0,t) = 0 \quad (42)$$

$$f_1(0,t) = 0 \quad (43)$$

As  $v \rightarrow \infty$  :

$$f_o, f_1 \rightarrow 0, \text{ exponentially.} \quad (44)$$

The coefficient in Eq. (40) is chosen so that  $g_o(v)$  is normalized:

$$\int g_o(v) \underline{dv} = 1 \quad (45)$$

$$\text{where} \quad \underline{dv} = v^2 \sin \theta \, dv \, d\theta \, d\phi \quad (46)$$

in spherical coordinates. That (45) is true is readily established using the following integration formula from Dwight [6] :

$$\int_0^{\infty} x^n \exp[-(rx)^m] dx = \Gamma\left(\frac{n+1}{m}\right) / (mr^{n+1}) \quad (47)$$

$g_1(v)$  is selected as the time-independent solution of Eq. (33) corresponding to the Druyvesteyn distribution:

$$g_1(v) = \frac{eE\lambda}{m} \frac{1}{v} \frac{dg_0}{dv} \quad (48)$$

The desired asymptotic form of  $f_0$  is normalized to unity as written below

$$f_0 \sim \left(\frac{m}{2\pi kT}\right)^{3/2} \exp[-mv^2/(2kT)] \quad (49)$$

That  $f_0$  remains normalized for all  $t$  can be seen from Eq. (38); if the equation is integrated over all velocities,

$$\int \frac{\partial f_0}{\partial t} dv = 4\pi \frac{m}{M} \frac{1}{\lambda} \int_0^{\infty} \frac{\partial}{\partial v} (v^4 f_0) dv + 4\pi \frac{kT}{M\lambda} \int_0^{\infty} \frac{\partial}{\partial v} (v^3 \frac{\partial f_0}{\partial v}) dv \quad (50)$$

$$= 4\pi \frac{m}{M} \frac{1}{\lambda} \left[ v^4 f_0 \right]_0^{\infty} + 4\pi \frac{kT}{M\lambda} \left[ v^3 \frac{\partial f_0}{\partial v} \right]_0^{\infty} \quad (51)$$

$$= 0 \quad (52)$$

after condition (44) is applied. If  $\partial f_0 / \partial t$  is continuous and if  $\int_0^{\infty} v^2 \frac{\partial f_0}{\partial t} dv$  converges uniformly in  $t$ , the differentiation and integration can be interchanged to yield

$$\frac{\partial}{\partial t} \int f_0 dv = 0 \quad (53)$$

From the initial conditions it follows that

$$\int f_0 \, d\underline{v} = 1 \quad (54)$$

for all  $t$  .

The boundary conditions at  $v = 0$  are chosen by requiring the distribution function  $f(\underline{v}, t)$  to behave well at the origin in velocity space.  $f(\underline{v}, t)$  is approximated by

$$f(\underline{v}, t) = f_0(v, t) + f_1(v, t) \cos \theta \quad (55)$$

and the condition on  $f_1$  is obtained by requiring that  $f$  be independent of  $\theta$  at  $v = 0$  . The condition that  $\partial f_0 / \partial v = 0$  at  $v = 0$  is applied in order that the distribution function be smooth at the origin. If the condition were not satisfied, the velocity gradient of the distribution function  $f$  would be discontinuous at  $\underline{v} = 0$  .

The requirement that  $f_0$  and  $f_1$  exhibit exponential decay with increasing  $v$  is somewhat arbitrary and is not used explicitly. However, both the initial and the asymptotic distribution functions possess such behavior, and it is essential to Eq. (54) that  $v^4 f_0 \rightarrow 0$  as  $v \rightarrow \infty$  (see Eq. (51)).

#### Solution for $f_1$

Equation (39) for  $f_1$  subject to the conditions (41) and (43) can be solved immediately and yields

$$f_1(v, t) = g_1(v) \exp[-vt/\lambda] \quad (56)$$

$$= g_1(v) \exp[-v_m(v)t] \quad (57)$$

The latter formula shows that the reciprocal of the collision frequency provides a measure of the "relaxation time" for  $f_1$ . Since the electric current is obtained from  $f_1$  by calculating the average electron velocity, which depends on  $f_1$  but not on  $f_0$ , it is apparent that the current is effectively zero within a few collisions of the removal of the field.

#### Estimate of Relaxation Time

The equation for  $f_0$  is a second-order parabolic equation, and its solution shows the evolution of  $f_0$  with time and thus yields the relaxation time, the time required for the isotropic term of the distribution function to undergo an appreciable portion of the change from Druyvesteyn to Maxwellian. Before proceeding with a numerical solution, it is convenient to obtain an estimate of the relaxation time. Such an estimate can be obtained from Eq. (B.34) in Appendix B of Part I, which gives the rate per unit volume at which energy is transferred from electrons to neutrals through elastic collisions. In rewriting the formula in the present nomenclature,  $f$  must be replaced by  $N_e f$ , where  $N_e$  is the electron density, and  $v_m$  is eliminated by Eq. (31). Then we obtain

$$R = -2 \frac{m}{M} \frac{N_e}{\lambda} \int f(\underline{v}) \left( \frac{1}{2} m v^2 - \left\langle \frac{1}{2} M V^2 \right\rangle \right) \underline{v} \, d\underline{v} \quad . \quad (58)$$

If we let  $v_0$  represent the electron root-mean-square velocity at equilibrium, we must have

$$\frac{1}{2} m v_0^2 = \left\langle \frac{1}{2} M V^2 \right\rangle \quad . \quad (59)$$

Furthermore, the average functions of velocity resulting from the

integration over  $\underline{v}$  do not differ significantly from the same functions of the average speed or the root-mean-square velocity. Consequently, we discard the distinction between the various average speeds and write the functions in terms of some average speed  $u$ . Now Eq. (58) can be written as

$$\frac{d}{dt} (N_e \frac{1}{2} \mu u^2) = - 2 \frac{m}{M} \frac{N_e}{\lambda} u (\frac{1}{2} \mu u^2 - \frac{1}{2} m v_o^2) \quad (60)$$

or

$$\frac{du}{dt} = - \frac{m}{M} \frac{1}{\lambda} (u^2 - v_o^2) \quad (61)$$

This equation can be integrated easily as follows:

$$[ \frac{1}{u - v_o} - \frac{1}{u + v_o} ] du = - 2 \frac{m}{M} \frac{v_o}{\lambda} dt \quad (62)$$

Integrating from 0 to  $t$

$$\frac{u - v_o}{u + v_o} = \frac{u_o - v_o}{u_o + v_o} \exp[-2 \frac{m}{M} \frac{v_o}{\lambda} t] \quad (63)$$

where  $u = u_o$  at  $t = 0$ . Solving for  $u$

$$u = v_o \frac{1 + \frac{u_o - v_o}{u_o + v_o} \exp[-2 \frac{m}{M} \frac{v_o}{\lambda} t]}{1 - \frac{u_o - v_o}{u_o + v_o} \exp[-2 \frac{m}{M} \frac{v_o}{\lambda} t]} \quad (64)$$

The fractional change in  $u - v_o$  is given by

$$\frac{u - v_o}{u_o - v_o} = \frac{2v_o}{u_o + v_o} \frac{\exp[-2 \frac{m}{M} \frac{v_o}{\lambda} t]}{1 - \frac{u_o - v_o}{u_o + v_o} \exp[-2 \frac{m}{M} \frac{v_o}{\lambda} t]} . \quad (65)$$

From this equation it is apparent that the proper choice for the relaxation time  $t_r$  is

$$t_r = \frac{1}{2} \frac{M}{m} \frac{\lambda}{v_o} . \quad (66)$$

For a Maxwellian distribution  $v_o$  is given by Eqs. (A.29) and (A.31) of Appendix A, and  $t_r$  becomes

$$t_r = \frac{1}{2} \frac{M}{m} \sqrt{\frac{m}{3kT}} \lambda . \quad (67)$$

### Dimensionless Equations

The relaxation time defined above provides a convenient unit in which to measure the time. In order to make the velocity dimensionless also, it is necessary to select a unit velocity. The measure adopted is the root-mean-square velocity of the Maxwellian distribution. The new independent variables are denoted by

$$\tau = t/t_r = t / \left( \frac{1}{2} \frac{M}{m} \sqrt{\frac{m}{3kT}} \lambda \right) \quad (68)$$

$$\xi = v / \sqrt{\frac{3kT}{m}} . \quad (69)$$

A dimensionless distribution function is defined so that the velocity distribution remains normalized to unity:

$$\int f_0 \, d\underline{v} = (3kT/m)^{3/2} \int f_0 \, d\underline{\xi} = \int F \, d\underline{\xi} \quad (70)$$

where  $F(\xi, \tau) = (3kT/m)^{3/2} f_0(v, t) \quad . \quad (71)$

In the new variables the Maxwellian distribution function is

$$F \sim \left(\frac{3}{2\pi}\right)^{3/2} \exp\left[-\frac{3}{2} \xi^2\right] \quad (72)$$

and the Druyvesteyn is

$$G(\xi) = \frac{1}{\pi\Gamma\left(\frac{3}{4}\right)} \left(\frac{27}{4} \frac{m}{M}\right)^{3/4} \left(\frac{kT}{eE\lambda}\right)^{3/2} \exp\left[-\frac{27}{4} \frac{m}{M} \frac{k^2 T^2}{e^2 E^2 \lambda^2} \xi^4\right] \quad . \quad (73)$$

After changing to the new variables, Eq. (38) becomes

$$\frac{\partial F}{\partial \tau} = \frac{1}{6} \frac{1}{\xi^2} \frac{\partial}{\partial \xi} \left(\xi^3 \frac{\partial F}{\partial \xi}\right) + \frac{1}{2} \frac{1}{\xi^2} \frac{\partial}{\partial \xi} \left(\xi^4 F\right) \quad . \quad (74)$$

This equation can be rewritten after completing the differentiation, and the formulation of the problem in dimensionless variables becomes

$$\frac{\partial F}{\partial \tau} = \frac{1}{6} \xi \frac{\partial^2 F}{\partial \xi^2} + \frac{1}{2} (\xi^2 + 1) \frac{\partial F}{\partial \xi} + 2\xi F \quad (75)$$

for  $0 \leq \xi < \infty, \quad 0 < \tau < \infty$

$$F(\xi, 0) = G(\xi) = \frac{1}{\pi\Gamma\left(\frac{3}{4}\right)} \left(\frac{27}{4} \frac{m}{M}\right)^{3/4} \left(\frac{kT}{eE\lambda}\right)^{3/2} \exp\left[-\frac{27}{4} \frac{m}{M} \frac{k^2 T^2}{e^2 E^2 \lambda^2} \xi^4\right] \quad (76)$$

$$= 3.588 \times 10^{-4} \exp\left[-1.538 \times 10^{-4} \xi^4\right] \quad . \quad (77)$$

$$\frac{\partial F}{\partial \xi}(0, \tau) = 0 \quad (78)$$

As  $\xi \rightarrow \infty$

$$F(\xi, \tau) \rightarrow 0, \text{ exponentially.} \quad (79)$$

From Eq. (72) the asymptotic behavior is

$$F \sim 0.330 \exp\left[-\frac{3}{2} \xi^2\right] . \quad (80)$$

The numerical values for the coefficients in (77) are obtained from Eqs. (A.41) and (A.42). Before proceeding with a numerical integration of (75), it is important to obtain some idea of the magnitude of the variables and parameters involved. Numerical values of quantities associated with the initial and asymptotic distributions and with the dimensionless variables are calculated in Appendix A.

### Numerical Solution

The problem defined above is solved numerically for  $F(\xi, \tau)$  by a finite-difference method that is described in Appendix B. The integration is performed to  $\tau = 1$ , and the form of the distribution function at various times is shown in Fig. 3. The form of the distribution function at  $\tau = 1$  shows that the relaxation time defined by Eq. (67) and selected as a result of approximate considerations is a good choice.

Figure 3 also shows that a maximum exists in the curves for  $F(\xi, \tau)$  which is present in neither the initial nor the asymptotic distributions. However, this occurrence can be explained on a physical basis: since the collision frequency of the fast electrons is much

higher than that of the slow ones, they lose energy much more rapidly, and the concentration of electrons of intermediate velocity is greatly increased.

Appendix A

PRELIMINARY CALCULATIONS

The function  $f_0(v,t)$  (or  $F(\xi,\tau)$ ) is determined numerically, so it is necessary to select values for the electric field and the mean free path. Also, in order to obtain an order of magnitude estimate for the behavior of  $f_0(v,t)$ , certain quantities associated with the initial and asymptotic distributions, such as root-mean-square velocities, are calculated.

In order to perform physically meaningful calculations, the equations are applied to the positive column of a glow discharge in neon at a pressure of 2 mm Hg and a gas temperature of 300°K. Data presented in Cobine\* indicate that with a discharge chamber of appropriate geometry an electric field of 0.4 volts/cm may be sufficient to sustain the discharge at the assigned pressure, and that value is used throughout the following calculations.

Using Eqs. (29) and (31), the mean free path can be expressed as

$$\lambda = 1/(N_n Q_m) \quad . \quad (A.1)$$

The number density of neon atoms  $N_n$  is calculated from the ideal gas law:

$$N_n = p/(kT) \quad (A.2)$$

$$= 6.438 \times 10^{16} \text{ atoms/cm}^3 \quad . \quad (A.3)$$

---

\* See Cobine [3], p. 235.

Cross section data for  $Q_m$  as a function of electron energy are available in Massey and Burhop [11], p. 15. Since a constant  $\lambda$  is assumed in the equations, a particular value must be selected as an approximation. For a given velocity distribution the mean energy could be determined as a function of  $\lambda$ . By evaluating  $Q_m$  (and hence  $\lambda$ ) at the mean energy, an iterative procedure can be easily developed that determines both  $\lambda$  and the mean energy. However, the velocity distribution and the mean energy change with time, so  $Q_m$  is evaluated at an energy that lies between the values of the mean energy for the Druyvesteyn and the Maxwellian distributions. The value adopted is

$$Q_m = 2.5\pi a_o^2 \tag{A.4}$$

$$= 2.20 \times 10^{-16} \text{ cm}^2 \tag{A.5}$$

where

$$a_o = 0.5292 \times 10^{-8} \text{ cm} \tag{A.6}$$

is the radius of the first Bohr orbit. Then  $\lambda$  becomes

$$\lambda = 0.0706 \text{ cm} . \tag{A.7}$$

The mass  $M$  of a neon atom is also needed and is obtained by dividing the atomic weight of neon by Avogadro's number:

$$\begin{aligned} M &= (20.183)/(6.0228 \times 10^{23}) \\ &= 3.351 \times 10^{-23} \text{ gm} . \end{aligned} \tag{A.8}$$

Various quantities of interest in comparing the Druyvesteyn and the Maxwellian distributions are calculated below.

Druyvesteyn:

$$\langle v \rangle = \int v g_o(v) dv \quad (\text{A.9})$$

$$= \frac{4}{\Gamma(\frac{3}{4})} \left( \frac{3m^3}{4Me^2 E^2 \lambda^2} \right)^{3/4} \int_0^\infty v^3 \exp\left[-\frac{3m^3 v^4}{4Me^2 E^2 \lambda^2}\right] dv \quad (\text{A.10})$$

$$= \frac{1}{\Gamma(\frac{3}{4})} \left( \frac{4Me^2 E^2 \lambda^2}{3m^3} \right)^{1/4} \quad (\text{A.11})$$

$$= 8.557 \times 10^7 \text{ cm/sec} \quad (\text{A.12})$$

$$\langle v^2 \rangle = \int v^2 g_o(v) dv \quad (\text{A.13})$$

$$= \frac{2}{\sqrt{3}} \frac{\Gamma(\frac{5}{4})}{\Gamma(\frac{3}{4})} \sqrt{\frac{M}{m}} \frac{eE\lambda}{m} \quad (\text{A.14})$$

$$= \Gamma(\frac{3}{4}) \Gamma(\frac{5}{4}) \langle v \rangle^2 \quad (\text{A.15})$$

$$= 8.134 \times 10^{15} \text{ cm}^2/\text{sec}^2 \quad (\text{A.16})$$

The root-mean-square velocity of an electron is

$$\sqrt{\langle v^2 \rangle} = 9.018 \times 10^7 \text{ cm/sec} \quad (\text{A.17})$$

and the mean energy is

$$\langle \frac{1}{2} mv^2 \rangle = 3.704 \times 10^{-12} \text{ ergs} \quad (\text{A.18})$$

$$= 2.312 \text{ eV} \quad (\text{A.19})$$

The variance of  $v$  is

$$\text{var}(v) = \langle v^2 \rangle - \langle v \rangle^2 \quad (\text{A.20})$$

$$= 8.12 \times 10^{14} \text{ cm}^2/\text{sec}^2 \quad (\text{A.21})$$

and so a standard deviation is

$$\sqrt{\text{var}(v)} = 0.342 \langle v \rangle \quad (\text{A.22})$$

$$= 2.85 \times 10^7 \text{ cm/sec} . \quad (\text{A.23})$$

Maxwellian:

$$\langle v \rangle = \left(\frac{m}{2\pi kT}\right)^{3/2} \int v \exp\left[-\frac{mv^2}{2kT}\right] dv \quad (\text{A.24})$$

$$= 4\pi \left(\frac{m}{2\pi kT}\right)^{3/2} \int_0^{\infty} v^3 \exp\left[-\frac{mv^2}{2kT}\right] dv \quad (\text{A.25})$$

$$= \left(\frac{8kT}{\pi m}\right)^{1/2} \quad (\text{A.26})$$

$$= 1.076 \times 10^7 \text{ cm/sec} \quad (\text{A.27})$$

$$\langle v^2 \rangle = 4\pi \left(\frac{m}{2\pi kT}\right)^{3/2} \int_0^{\infty} v^4 \exp\left[-\frac{mv^2}{2kT}\right] dv \quad (\text{A.28})$$

$$= 3kT/m \quad (\text{A.29})$$

$$= 1.364 \times 10^{14} \text{ cm}^2/\text{sec}^2 \quad (\text{A.30})$$

$$\sqrt{\langle v^2 \rangle} = 1.168 \times 10^7 \text{ cm/sec} \quad (\text{A.31})$$

The mean energy of an electron is

$$\left\langle \frac{1}{2} m v^2 \right\rangle = \frac{3}{2} kT \quad (\text{A.32})$$

$$= 6.21 \times 10^{-14} \text{ ergs} \quad (\text{A.33})$$

$$= 0.0388 \text{ eV} . \quad (\text{A.34})$$

The previous calculations provide a rough comparison of the two distribution functions. The ratio of root-mean-square velocities is

$$\frac{\sqrt{\langle v^2 \rangle} \text{ (Druyvesteyn)}}{\sqrt{\langle v^2 \rangle} \text{ (Maxwellian)}} = 7.73 \quad (\text{A.35})$$

The ratio of mean electron energies is

$$\frac{\langle \frac{1}{2} mv^2 \rangle \text{ (Druyvesteyn)}}{\langle \frac{1}{2} mv^2 \rangle \text{ (Maxwellian)}} = 59.7 \quad . \quad (\text{A.36})$$

This quantity shows that the thermal energy of the atoms is virtually negligible compared with the energy supplied to the electrons by the electric field. Such relative values are necessary if the Druyvesteyn distribution is to provide an accurate description of the electron behavior. Since the root-mean-square velocity of the Druyvesteyn distribution is considerably greater than that of the Maxwellian, it is obvious that the coefficient of the Druyvesteyn distribution function must be much smaller. Their values are listed below:

$$\frac{1}{\pi \Gamma(\frac{3}{4})} \left( \frac{3m^3}{4Me^2 E^2 \lambda^2} \right)^{3/4} = 2.252 \times 10^{-25} \text{ sec}^3/\text{cm}^3 \quad (\text{A.37})$$

$$\left( \frac{m}{2\pi kT} \right)^{3/2} = 2.071 \times 10^{-22} \text{ sec}^3/\text{cm}^3 \quad (\text{A.38})$$

Their ratio is

$$\frac{1}{\pi \Gamma(\frac{3}{4})} \left( \frac{3m^3}{4Me^2 E^2 \lambda^2} \right)^{3/4} / \left( \frac{m}{2\pi kT} \right)^{3/2} = 1.09 \times 10^{-3} \quad . \quad (\text{A.39})$$

The calculations above also provide a means of evaluating the effect of inelastic collisions, which are neglected in the equations. The lowest excited state of the neon atom possesses an energy 16.61 eV above the ground state, and the ionization potential is 21.56 eV.\* Since the mean energy of the Druyvesteyn distribution is 2.312 eV, we conclude that inelastic collisions have little effect on the form of the distribution function.

Several quantities occurring in the dimensionless equations must also be calculated. The relaxation time of Eq. (67) has the value

$$t_r = 1.112 \times 10^{-4} \text{ sec.} \quad (\text{A.40})$$

The characteristic quantity used in creating the dimensionless velocity is just the Maxwellian root-mean-square velocity of Eq. (A.31). The coefficient and the exponent of the dimensionless Druyvesteyn distribution are listed below:

$$\frac{1}{\pi \Gamma(\frac{3}{4})} \left(\frac{27}{4} \frac{m}{M}\right)^{3/4} \left(\frac{kT}{eE\lambda}\right)^{3/2} = 3.588 \times 10^{-4} \quad (\text{A.41})$$

$$\frac{27}{4} \frac{m}{M} \frac{k^2 T^2}{e^2 E^2 \lambda^2} = 1.538 \times 10^{-4} \quad (\text{A.42})$$

It is of interest to evaluate  $(u - v_o)/(u_o - v_o)$  of Eq. (65) when  $t = t_r$ . Then

$$\frac{u - v_o}{u_o - v_o} = \frac{2v_o}{u_o + v_o} \left(\exp(1) - \frac{u_o - v_o}{u_o + v_o}\right)^{-1} \quad (\text{A.43})$$

---

\*See Moore [12].

Using Eq. (A.35) for  $u_o/v_o$  ,

$$\frac{u - v_o}{u_o - v_o} = 0.118 \quad (\text{A.44})$$

at  $t = t_r$  .

Appendix B

THE FINITE-DIFFERENCE CALCULATION\*

Equation (75) is solved numerically by an implicit finite-difference method. The solution proceeds stepwise in the  $\tau$  direction with values of  $F$  being calculated at all net points in the  $\xi$  direction at each step.

If  $h$  and  $k$  represent the increments and  $s$  and  $n$  the net points in the  $\xi$  and  $\tau$  directions respectively, the finite-difference equation corresponding to (75) can be written

$$\frac{F_{s,n+1} - F_{s,n}}{k} = \frac{sh}{6} \left[ \frac{F_{s+1,n+1} - 2F_{s,n+1} + F_{s-1,n+1}}{h^2} \right] + \frac{1}{2} [(sh)^2 + 1] \left[ \frac{F_{s+1,n+1} - F_{s-1,n+1}}{2h} \right] + 2sh F_{s,n} \quad (B.1)$$

where the  $\xi$  derivatives have been replaced by their central differences. This equation is to be solved for quantities on the  $n+1$  time level in terms of those below. Stability considerations require that both the first and second  $\xi$ -derivatives be written on the  $n+1$  level. A rearrangement of (B.1) changes it to the usual form for a system of linear equations:

$$\left[ \frac{\lambda}{4} h(s^2 h^2 + 1) - \frac{\lambda}{6} sh \right] F_{s-1,n+1} + \left[ 1 + \frac{\lambda}{3} sh \right] F_{s,n+1} - \left[ \frac{\lambda}{4} h(s^2 h^2 + 1) + \frac{\lambda}{6} sh \right] F_{s+1,n+1} = (1 + 2\lambda h^2 sh) F_{s,n} \quad (B.2)$$

---

\* See, for instance, Forsythe and Wasow [7] for a discussion of the techniques.

where

$$\lambda = k/h^2 . \tag{B.3}$$

Equation (B.2) written for all  $s$  is a tridiagonal system of linear equations and is solved by Gaussian elimination.

In order to solve (B.2) it is necessary to use finite-difference formulations of the boundary conditions at the ends of the  $\xi$  interval. Equation (78) implies

$$F_{0,n+1} = F_{1,n+1} . \tag{B.4}$$

The solution of the finite-difference equation in the  $\xi$ -direction is terminated at  $\xi = 12$ , and the boundary condition there has a considerable effect on the stability of the problem. The logarithm of the last  $F$  is obtained by a Lagrangian interpolation formula involving values of the three previous  $F$ 's in the  $\xi$ -direction. Following a partial reduction of the system (B.2) by Gaussian elimination, the  $F$ 's in the interpolation formula can be expressed in terms of the final  $F$ . The solution of this equation for the final  $F$  is found by a Newton-Raphson iteration, and once this value is obtained, (B.2) can be solved completely for the  $n+1$  time level.

The solution of the finite-difference equation is obtained in the region

$$0 \leq \xi \leq 12 \tag{B.5}$$

$$0 \leq \tau \leq 1 . \tag{B.6}$$

The increments in the net spacing are

$$h = 0.25 \tag{B.7}$$

$$k = 0.01 . \tag{B.8}$$

NOMENCLATURE

Derivatives:

$\partial f / \partial \underline{v}$	velocity gradient of $f$
$(\partial f / \partial t)_{e.c.}$	time rate of change of $f$ from elastic collisions
$d\underline{v}$	volume element in velocity space
$d\underline{\xi}$	volume element in $\xi$ -space
$d\Omega$	element of solid angle

Roman:

$a_0$	radius of the first Bohr orbit
$e$	magnitude of the electronic charge
$\underline{e}_v$	unit vector in the $v$ -direction
$\underline{e}_\theta$	unit vector in the $\theta$ -direction
$\underline{e}_\phi$	unit vector in the $\phi$ -direction
$E$	magnitude of the electric field
$\underline{E}$	the electric field
$f$	electron distribution function
$f_n(v, t)$	coefficient of $P_n(\cos \theta)$ in the expansion of $f$
$F(\underline{V}, t)$	distribution function for neutral molecules
$F(\xi, \tau)$	dimensionless electron distribution function
$F_{s, n}$	finite-difference approximation to $F(\xi, \tau)$
$g$	magnitude of the relative velocity
$g_0(v)$	isotropic term of Druyvesteyn distribution
$g_1(v)$	anisotropic term of Druyvesteyn distribution
$G(\xi)$	dimensionless isotropic Druyvesteyn distribution

$H_n(v,t)$	coefficient of $P_n(\cos \theta)$ in the expansion of the left-hand side of the Boltzmann equation
$\underline{i}$	unit vector
$\underline{j}$	unit vector
$k$	Boltzmann constant
$\underline{k}$	unit vector in the direction of the electric field
$m$	mass of an electron
$M$	mass of a neutral molecule
$N_n$	number density of neutral molecules
$P_n(z)$	Legendre polynomial
$P_n^m(z)$	associated Legendre function
$q$	differential elastic-scattering cross section
$Q_m$	momentum-transfer cross section
$S_n(v,t)$	coefficient of $P_n(\cos \theta)$ in the expansion of the collision integral
$t$	time
$t_r$	relaxation time
$T$	temperature of neutral molecules
$u$	some average electron speed
$u_0$	initial value of $u$
$v$	magnitude of $\underline{v}$
$\underline{v}$	electron velocity
$\tilde{\underline{v}}$	electron velocity after collision
$v_0$	electron root-mean-square velocity in Maxwellian state
$\underline{V}$	molecular velocity

$\tilde{v}$

molecular velocity after collision

Greek:

$\Gamma$

gamma function

$\epsilon$

azimuthal angle about  $\underline{e}_v$

$\theta$

polar angle measured from  $\underline{k}$

$\tilde{\theta}$

$\theta$  after collision

$\lambda$

electron mean free path

$\nu_m$

collision frequency for momentum transfer

$\xi$

dimensionless velocity

$\tau$

dimensionless time

$\phi$

azimuthal angle about  $\underline{k}$

$\chi$

angle of deflection in relative coordinates and  
polar angle measured from  $\underline{e}_v$

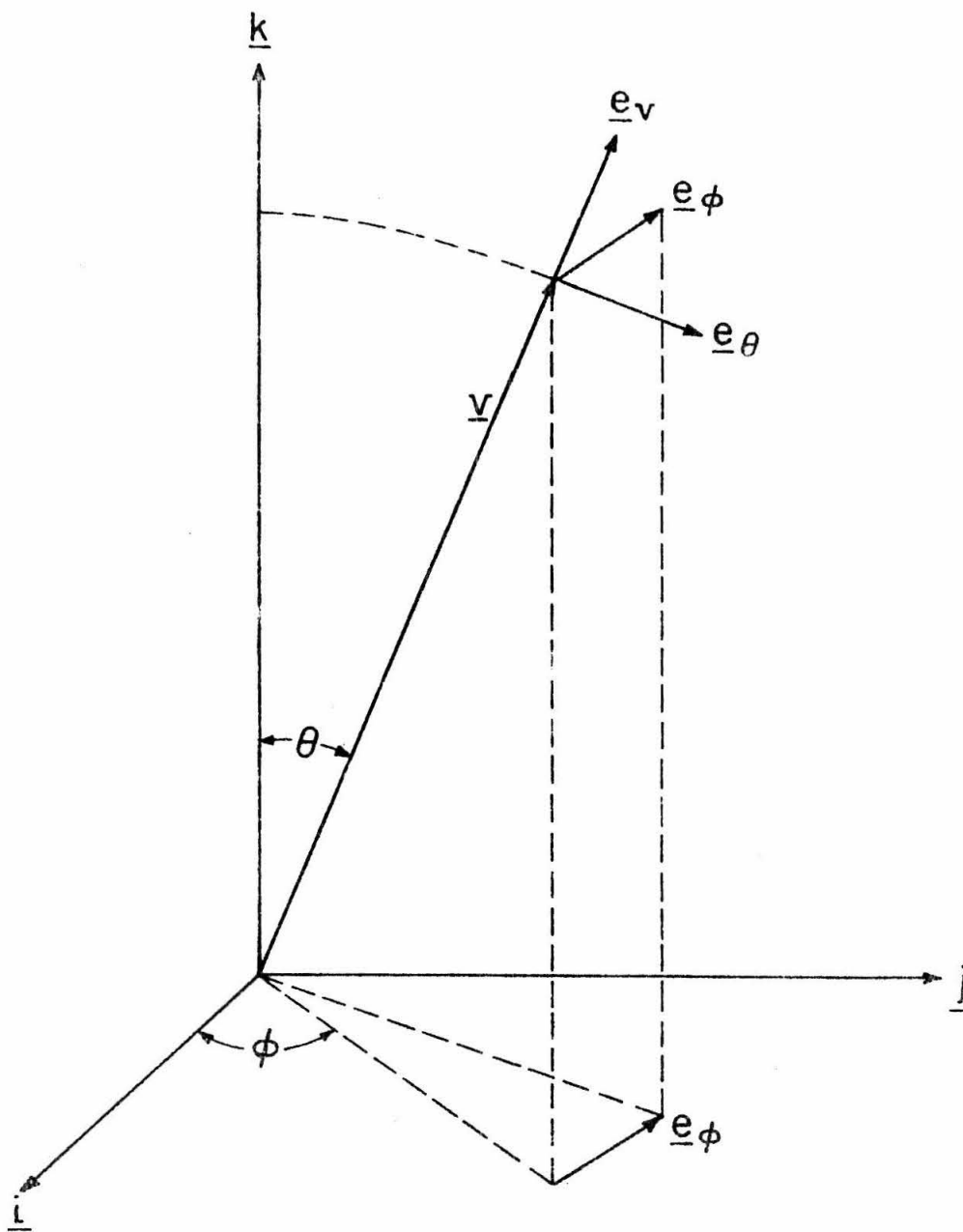


Figure 1: Spherical Coordinates and Base Vectors

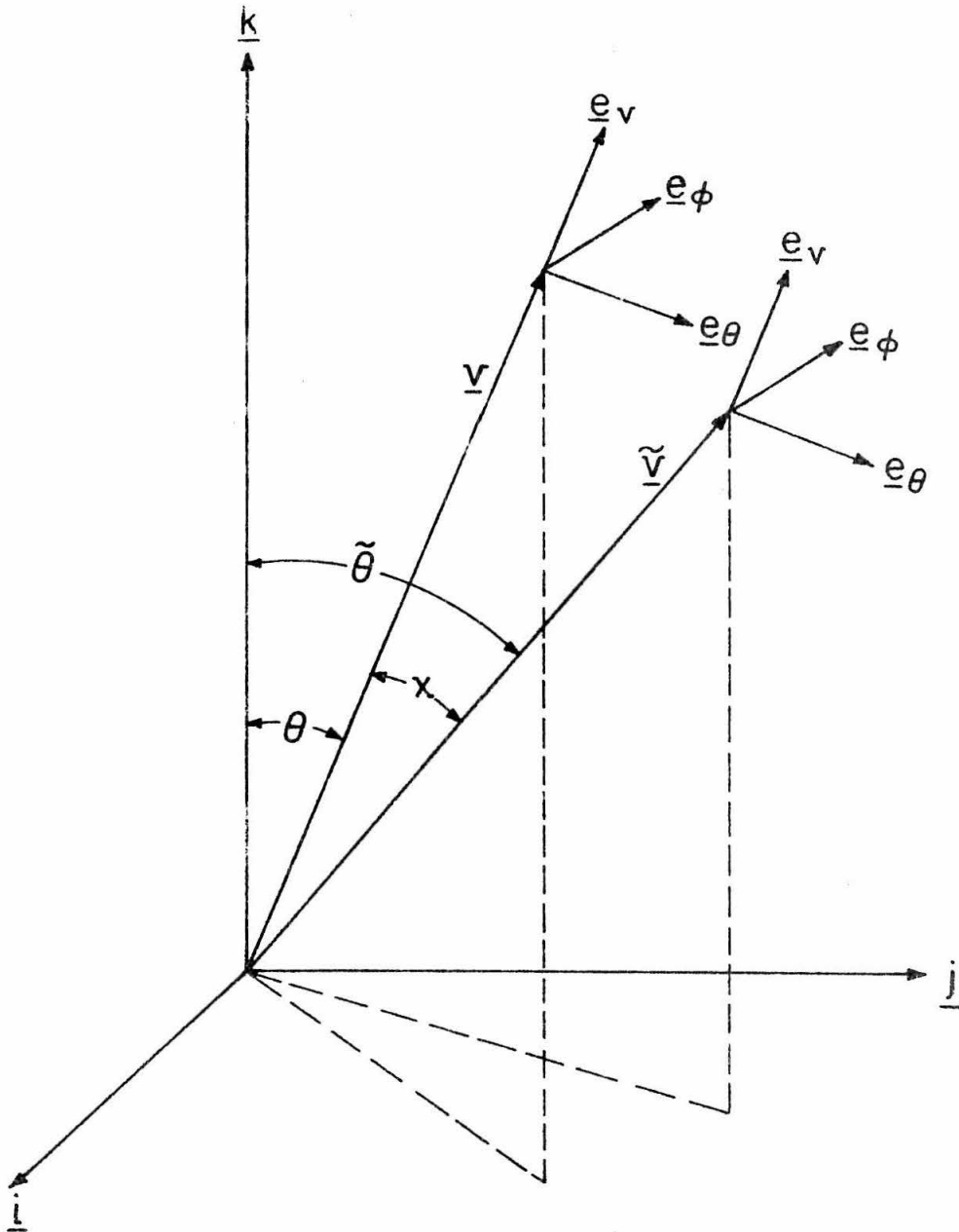


Figure 2: Relation of  $\tilde{\underline{v}}$  to  $\underline{v}$

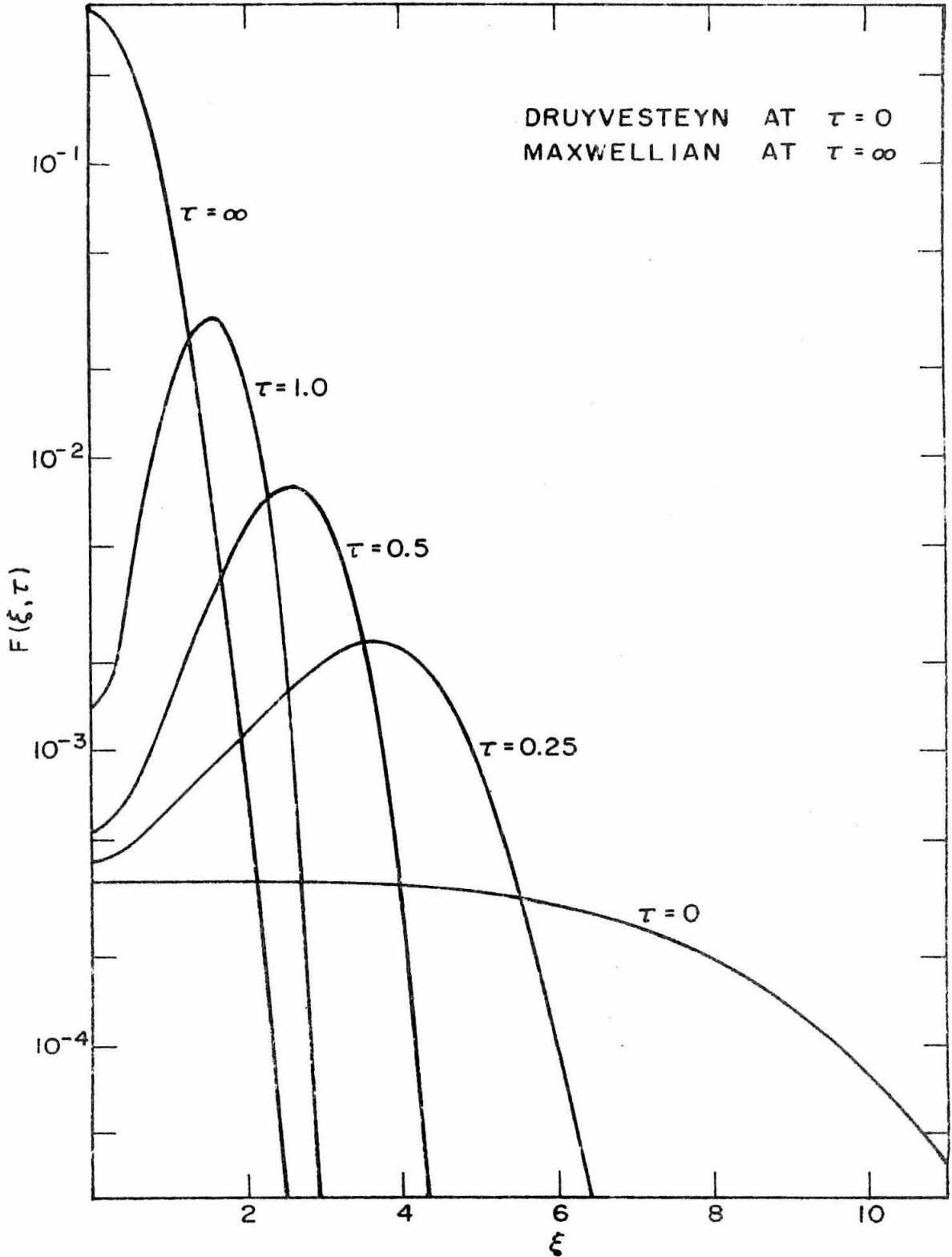


Figure 3: Numerical Results

BIBLIOGRAPHY

1. Allis, W. P., "Motions of Ions and Electrons," Handbuch der Physik 21, 383-429 (1956).
2. Chapman, Sydney and T. G. Cowling, The Mathematical Theory of Non-Uniform Gases, Cambridge University Press, 1952.
3. Cobine, James Dillon, Gaseous Conductors, Dover, 1958.
4. Delcroix, J. L., Plasma Physics, Wiley & Sons, Ltd., 1965.
5. Desloge, E. A. and S. W. Matthysee, "Collision Term in the Boltzmann Transport Equation," American Journal of Physics 28, 1-11 (1960).
6. Dwight, Herbert Bristol, Tables of Integrals and Other Mathematical Data, The Macmillan Company, 1961.
7. Forsythe, G. E. and W. R. Wasow, Finite-Difference Methods for Partial Differential Equations, John Wiley & Sons, Inc., 1960.
8. Ginzburg, V. L. and A. V. Gurevich, "Nonlinear Phenomena in a Plasma Located in an Alternating Electromagnetic Field," Soviet Physics Uspekhi 3, 115-146 (1960).
9. Holstein, T., "Energy Distribution of Electrons in High Frequency Gas Discharges," Physical Review 70, 367-384 (1946).
10. Holt, E. H. and R. E. Haskell, Foundations of Plasma Dynamics, The Macmillan Company, 1965.
11. Massey, H. S. W. and E. H. S. Burhop, Electronic and Ionic Impact Phenomena, Oxford University Press, 1952.

12. Moore, Charlotte E., "Atomic Energy Levels," Circular of the National Bureau of Standards 467, U. S. Government Printing Office, 1949.
13. Sansone, G., Orthogonal Functions, Interscience Publishers, 1959.
14. Wu, Ching-Sheng, "On the Distribution Function and Mean Energy of Electrons in the Presence of Magnetic and Electric Fields," Tech. Report No. 32-14, Jet Propulsion Laboratory, California Institute of Technology, July 1, 1960.

Proposition 2

JUMP DISCONTINUITIES IN CONCENTRATION PROFILES  
FOR FIXED-COLUMN ADSORPTION

Exchange processes such as chromatography and ion exchange, which involve adsorption in fixed columns, can be described by a first-order nonlinear partial differential equation if equilibrium is assumed. A continuous solution is easily obtained, but it becomes multiple-valued with increasing time. It can be made practicable by introducing a jump discontinuity. The literature describes a means of determining the size and location of the discontinuity that is usable only for special initial conditions. In this presentation equations are developed whose solutions provide an analytical determination of the size and location for arbitrary initial conditions.

Material Balance

The basic equation that is used in the following development is obtained by a material balance. The physical situation is sketched in Fig. 1 and consists of fluid flowing through a column containing a fixed bed of solid matter as in the case of chromatography or ion exchange. The fluid is assumed to flow with a constant velocity  $V$  that is uniform throughout the column. A solute is transferred between the liquid phase and the solid phase and its concentrations in the two phases are to be found as functions of distance  $x$  along the column and time  $t$ . The following definitions are adopted:

$\rho$  concentration of solute in liquid, based on a unit volume of liquid;

- q concentration of solute on solid, based on a unit volume of solid;
- $\alpha$  fraction of volume in column that is occupied by liquid.

Using the above terms, an equation is obtained by equating the rate of increase of solute within the region bounded by  $x_1$  and  $x_2$  in Fig. 1 to the convective flux through the boundaries:

$$\frac{\partial}{\partial t} \left[ \int_{x_1}^{x_2} \alpha \rho(x,t) dx + \int_{x_1}^{x_2} (1-\alpha) q(x,t) dx \right] = \alpha V \rho(x_1,t) - \alpha V \rho(x_2,t). \quad (1)$$

Diffusion is neglected. If  $\rho$  and  $q$  are continuously differentiable, a differential equation can be obtained:

$$\frac{\partial \rho}{\partial t} + v \frac{\partial \rho}{\partial x} + \frac{1-\alpha}{\alpha} \frac{\partial q}{\partial t} = 0. \quad (2)$$

One of the dependent variables can be eliminated from this equation if equilibrium between the amount of solute in solution and that adsorbed on the solid is assumed at each point. Then a given value of  $\rho$  determines  $q$ :

$$q = f(\rho). \quad (3)$$

Now Eq. (2) becomes

$$\frac{\partial \rho}{\partial t} + c(\rho) \frac{\partial \rho}{\partial x} = 0 \quad (4)$$

where

$$c(\rho) = \frac{v}{1 + \frac{1-\alpha}{\alpha} f'(\rho)}. \quad (5)$$

The Continuous Solution

Equation (4) becomes

$$\frac{d\rho}{dt} = 0 \quad (6)$$

if the differentiation is performed along the characteristics defined by

$$\frac{dx}{dt} = c(\rho) \quad (7)$$

With initial conditions given by

$$\rho(x,0) = \rho_0(x) \quad (8)$$

and  $c_0$  defined by

$$c_0(x) = c(\rho_0(x)) \quad (9)$$

the solutions of (6) and (7) are

$$x = c_0(\xi)t + \xi \quad (10)$$

$$\rho = \rho_0(\xi) \quad (11)$$

$\xi$  corresponds to the point at which the characteristic intersects the abscissa. The situation is illustrated in Fig. 2.

Equations (10) and (11) are capable of an instructive physical interpretation. If  $\rho$  is plotted against  $x$ , each point of the curve can be regarded as moving parallel to the  $x$ -axis with a velocity  $c(\rho)$  that depends upon its ordinate. The situation is depicted by Fig. 3. These considerations show how multiple-valued solutions can arise with the passage of time. Two possibilities are schematically presented in Fig. 4.

Such a development is, of course, physically unreasonable and corresponds to a discrepancy between the mathematical model and the actual physical situation. It has been found that a suitable approximation to the physics and to solutions of more accurate equations is obtained if a discontinuity is introduced in the multiple-valued region. An illustration is provided by the dashed lines in Fig. 4. The problem remaining is to determine the size and the location of the discontinuity as functions of time.

Introduction of the Discontinuity

One relation between the quantities involved can be obtained from Eq. (1), which represents conservation of material. If it is assumed that  $\rho(x,t)$  has a jump discontinuity at a point  $s(t)$  between  $x_1$  and  $x_2$ , the integrals can be written

$$\int_{x_1}^{x_2} \rho(x,t) dx = \int_{x_1}^{s(t)} \rho(x,t) dx + \int_{s(t)}^{x_2} \rho(x,t) dx \quad (12)$$

and the derivative of the integral becomes

$$\frac{\partial}{\partial t} \int_{x_1}^{x_2} \rho(x,t) dx = \frac{ds}{dt} (\rho(s_-,t) - \rho(s_+,t)) + \int_{x_1}^{x_2} \frac{\partial \rho}{\partial t} dx \quad (13)$$

If  $x_1$  and  $x_2$  are permitted to approach  $s$ , (1) becomes

$$-\alpha \frac{ds}{dt} [\rho]_{x=s} - (1-\alpha) \frac{ds}{dt} [f(\rho)]_{x=s} = -\alpha v [\rho]_{x=s} \quad (14)$$

where  $[\rho]_{x=s} = \rho(s_+,t) - \rho(s_-,t)$  . (15)

After a rearrangement we obtain

$$\frac{ds}{dt} = \frac{V[\rho]_{x=s}}{[\rho]_{x=s} + \frac{1-\alpha}{\alpha} [f(\rho)]_{x=s}} \quad (16)$$

The above equation must hold when a discontinuity exists. The need for a discontinuity first appears when Eq. (10) cannot be solved for  $\xi$  as a function of  $x$  and  $t$ . The analytical requirement for this situation is that the derivative of the expression in (10) with respect to  $\xi$  be zero, i.e.,

$$c'_0(\xi)t + 1 = 0 \quad (17)$$

A calculation of the partial derivatives of  $\rho(x,t)$  from (10) and (11), regarding  $\xi$  as an implicit function of  $x$  and  $t$ , shows that they are infinite when (17) is satisfied. If  $c'_0(\xi)$  is positive, no discontinuity is necessary. If  $c'_0(\xi)$  is negative, a discontinuity is first necessary at

$$t_m = \min_{\xi} (-1/c'_0(\xi)) \quad (18)$$

or

$$c''_0(\xi_m) = 0 \quad (19)$$

This is the time at which characteristics first intersect. The analytical determination of the need for a discontinuity can be compared with the description in Fig. 4 by considering the sign of

$$c'_0(\xi) = \frac{dc}{d\rho} \rho'_0(\xi) \quad (20)$$

From (5)

$$\frac{dc}{d\rho} = - \frac{V \frac{1-\alpha}{\alpha} f''(\rho)}{\left[1 + \frac{1-\alpha}{\alpha} f'(\rho)\right]^2} \quad (21)$$

Location of the Discontinuity

The values of  $\rho$  on the two sides of the discontinuity are determined by the intersection of the characteristics on the two sides with  $s(t)$  as shown in Fig. 5. A particular point along  $s(t)$  can be described by the following equations:

$$s = \xi_1 + c_o(\xi_1)t \quad (22)$$

$$s = \xi_2 + c_o(\xi_2)t \quad (23)$$

$$\frac{ds}{dt} = \frac{V[\rho_o(\xi_2) - \rho_o(\xi_1)]}{[\rho_o(\xi_2) - \rho_o(\xi_1)] + \frac{1-\alpha}{\alpha}[f(\rho_o(\xi_2)) - f(\rho_o(\xi_1))]} \quad (24)$$

The last equation is (16) rewritten in different nomenclature. These three equations involve the four quantities  $\xi_1$ ,  $\xi_2$ ,  $s$ , and  $t$ , and serve to determine  $\xi_1$ ,  $\xi_2$ , and  $s$  as functions of  $t$ . In the process of solving, it is easier to eliminate  $t$  and  $s$  and obtain a relation between  $\xi_1$  and  $\xi_2$ . From (22) and (23)

$$t = - \frac{\xi_2 - \xi_1}{c_o(\xi_2) - c_o(\xi_1)} \quad (25)$$

$$dt = - \frac{[c_o(\xi_2) - c_o(\xi_1)](d\xi_2 - d\xi_1) - (\xi_2 - \xi_1)[c'_o(\xi_2)d\xi_2 - c'_o(\xi_1)d\xi_1]}{[c_o(\xi_2) - c_o(\xi_1)]^2} \quad (26)$$

Also from (22) and (23)

$$ds = c_o(\xi_1)dt + (1 + c'_o(\xi_1)t) d\xi_1 \quad (27)$$

$$ds = c_o(\xi_2)dt + (1 + c'_o(\xi_2)t) d\xi_2 \quad (28)$$

Taking the average of these to maintain symmetry between  $\xi_1$  and  $\xi_2$

$$ds = \frac{1}{2}[c_o(\xi_2) + c_o(\xi_1)]dt + \frac{1}{2}[d\xi_1 + d\xi_2] + \frac{1}{2}t[c'_o(\xi_2)d\xi_2 + c'_o(\xi_1)d\xi_1]. \quad (29)$$

Substituting from (25) and (26) and rearranging,

$$\begin{aligned} ds &= \frac{1}{2} \frac{\xi_2 - \xi_1}{[c_o(\xi_2) - c_o(\xi_1)]^2} \{ [c_o(\xi_2) + c_o(\xi_1)][c'_o(\xi_2)d\xi_2 - c'_o(\xi_1)d\xi_1] \\ &\quad - [c_o(\xi_2) - c_o(\xi_1)][c'_o(\xi_2)d\xi_2 + c'_o(\xi_1)d\xi_1] \} \\ &+ \frac{1}{2} \frac{1}{c_o(\xi_2) - c_o(\xi_1)} \{ - [c_o(\xi_2) + c_o(\xi_1)](d\xi_2 - d\xi_1) \\ &\quad + [c_o(\xi_2) - c_o(\xi_1)](d\xi_1 + d\xi_2) \} \quad (30) \\ &= \frac{(\xi_2 - \xi_1)[c_o(\xi_1)c'_o(\xi_2)d\xi_2 - c_o(\xi_2)c'_o(\xi_1)d\xi_1]}{[c_o(\xi_2) - c_o(\xi_1)]^2} \\ &\quad + \frac{c_o(\xi_2)d\xi_1 - c_o(\xi_1)d\xi_2}{c_o(\xi_2) - c_o(\xi_1)} \quad (31) \end{aligned}$$

$$\begin{aligned}
 &= \frac{1}{[c_o(\xi_2) - c_o(\xi_1)]^2} \{ c_o(\xi_1) [(\xi_2 - \xi_1)c'_o(\xi_2) - (c_o(\xi_2) - c_o(\xi_1))] d\xi_2 \\
 &\quad - c_o(\xi_2) [(\xi_2 - \xi_1)c'_o(\xi_1) - (c_o(\xi_2) - c_o(\xi_1))] d\xi_1 \} \quad . \quad (32)
 \end{aligned}$$

From (24) and (26)

$$\begin{aligned}
 ds &= \frac{1}{[c_o(\xi_2) - c_o(\xi_1)]^2} \frac{V}{1 + \frac{1-\alpha}{\alpha} \frac{f(\rho_o(\xi_2)) - f(\rho_o(\xi_1))}{\rho_o(\xi_2) - \rho_o(\xi_1)}} \\
 &\quad \times \left\{ [(\xi_2 - \xi_1)c'_o(\xi_2) - (c_o(\xi_2) - c_o(\xi_1))] d\xi_2 \right. \\
 &\quad \left. - [(\xi_2 - \xi_1)c'_o(\xi_1) - (c_o(\xi_2) - c_o(\xi_1))] d\xi_1 \right\} \quad . \quad (33)
 \end{aligned}$$

If the expressions for  $ds$  in (32) and (33) are equated, a differential equation relating  $\xi_1$  and  $\xi_2$  is obtained:

$$\begin{aligned}
 &\left[ \frac{V}{1 + \frac{1-\alpha}{\alpha} \frac{f(\rho_o(\xi_2)) - f(\rho_o(\xi_1))}{\rho_o(\xi_2) - \rho_o(\xi_1)}} - c_o(\xi_1) \right] \{ (\xi_2 - \xi_1)c'_o(\xi_2) \\
 &\quad - [c_o(\xi_2) - c_o(\xi_1)] \} d\xi_2 = \left[ \frac{V}{1 + \frac{1-\alpha}{\alpha} \frac{f(\rho_o(\xi_2)) - f(\rho_o(\xi_1))}{\rho_o(\xi_2) - \rho_o(\xi_1)}} - c_o(\xi_2) \right] \\
 &\quad \times \{ (\xi_2 - \xi_1)c'_o(\xi_1) - [c_o(\xi_2) - c_o(\xi_1)] \} d\xi_1 \quad . \quad (34)
 \end{aligned}$$

The constant of integration is determined by the requirement that

$$\xi_1 = \xi_2 = \xi_m \quad (35)$$

at the beginning of the  $\xi_1$  versus  $\xi_2$  curve.  $\xi_m$  is the value of  $\xi$  that minimizes the expression  $(-1/c'_0(\xi))$  in (18). It must also satisfy (19). The results of the integration are used to evaluate  $t$  from (25) and  $s$  from (22) or (23).

#### Literature Treatment of the Discontinuity

The literature on the subject treats the utilization of discontinuities, but the method given for placing the discontinuity is useful only in special cases. DeVault [2] obtains an equation involving the discontinuity by relating the area under the  $\rho$ -versus- $x$  curve that contains the discontinuity to the area under the multiple-valued solution. Although the multiple-valued solution is physically unsuitable, it nevertheless represents conservation of solute and it is essential that the discontinuous solution do the same. In writing an integral relation for the conservation of solute, it is necessary to account for the solute adsorbed on the solid. The material balance, based on unit cross-sectional area and using the notation described in Fig. 6, can be written as

$$\int_{\rho_2}^{\rho_1} (s-x_b) [\alpha + (1-\alpha)f'(\rho)] d\rho = \int_{\rho_2}^{\rho_1} (x_f - x_b) [\alpha + (1-\alpha)f'(\rho)] d\rho \quad (36)$$

or

$$\alpha s(\rho_1 - \rho_2) + (1-\alpha) s(f(\rho_1) - f(\rho_2)) = \int_{\rho_2}^{\rho_1} x_f [\alpha + (1-\alpha) f'(\rho)] d\rho . \quad (37)$$

From (10)

$$x_f = c_o(\xi)t + \xi \quad (38)$$

and the expression for  $s$  becomes

$$s = \frac{\int_{\rho_2}^{\rho_1} [c_o(\xi)t + \xi] [\alpha + (1-\alpha) f'(\rho)] d\rho}{\alpha(\rho_1 - \rho_2) + (1-\alpha)(f(\rho_1) - f(\rho_2))} . \quad (39)$$

Substituting for  $\alpha + (1-\alpha) f'(\rho)$  from (5)

$$s = \frac{vt(\rho_1 - \rho_2) + v \int_{\rho_2}^{\rho_1} \frac{\xi}{c(\rho)} d\rho}{(\rho_1 - \rho_2) + \frac{1-\alpha}{\alpha} (f(\rho_1) - f(\rho_2))} . \quad (40)$$

The reason for the limited usefulness of this expression is that  $\rho_1$  and  $\rho_2$  are unknown. The special case considered in the literature has the initial condition

$$\rho_o(\xi) = \begin{cases} \rho_c , & \xi < 0 \\ 0 , & \xi > 0 \end{cases} . \quad (41)$$

In that case the integral in (40) vanishes, because  $\xi = 0$  for  $\rho$  between 0 and  $\rho_c$ . Then  $s$  is given by

$$s = \frac{vt \rho_c}{\rho_c + \frac{1-\alpha}{\alpha} f(\rho_c)} . \quad (42)$$

An examination of Eq. (24) shows that it reduces to the same expression in this case; Eqs. (22) and (23) are not needed to determine the location of the discontinuity.

#### The Equilibrium Assumption

In the preceding development equilibrium is assumed throughout the column, and  $q$  is written as an unspecified function of  $\rho$ . Experimental studies indicate that the assumption of equilibrium is frequently justified and provide adsorption rate expressions that are generally valid. The rate expressions for nonequilibrium situations are discussed by Gilliland and Baddour [3], Thomas [7], and Goldstein [5]. Their usual form is

$$\text{rate of adsorption} = k_f \rho(Q-q) - k_b q(C - \rho) \quad (43)$$

or

$$\text{rate of adsorption} = k_f \rho(Q-q) - k_b q \quad (44)$$

where  $Q$  and  $C$  are constants. At equilibrium the rate is zero, and it is possible to solve (43) and (44) for  $q$  as a function of  $\rho$ . The experimental validity of the equilibrium assumption and of the expressions for  $q$  is discussed by DeVault [2], Walter [8], and Goldstein [6].

An example of the typical behavior of a concentration profile can be obtained by solving (44) for  $q$  at equilibrium:

$$q = f(\rho) = k_f Q \rho / (k_b + k_f \rho) \quad (45)$$

$$f'(\rho) = k_f k_b Q / (k_b + k_f \rho)^2 \quad (46)$$

From (5)

$$c(\rho) = \frac{v}{1 + \frac{1-\alpha}{\alpha} \frac{k_f k_b Q}{(k_b + k_f \rho)^2}} \quad (47)$$

Since  $f''(\rho) < 0$ , Eq. (21) and Fig. 4 show that the discontinuity occurs at the front of the concentration profile.

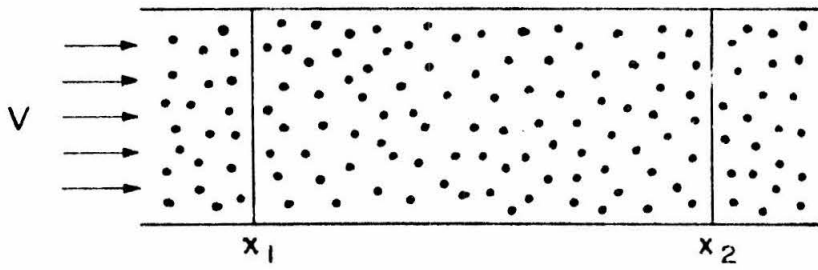


Figure 1: Flow through Fixed Column

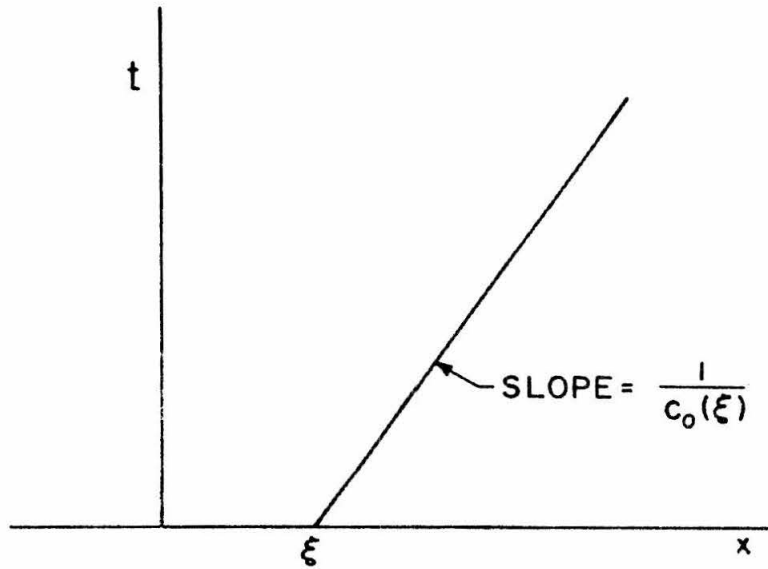


Figure 2: Characteristic

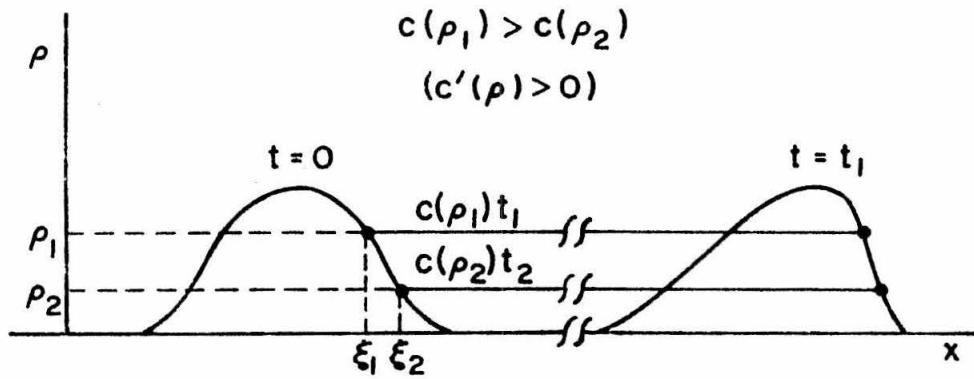


Figure 3:  $\rho$  as a Function of  $x$  for Different Times

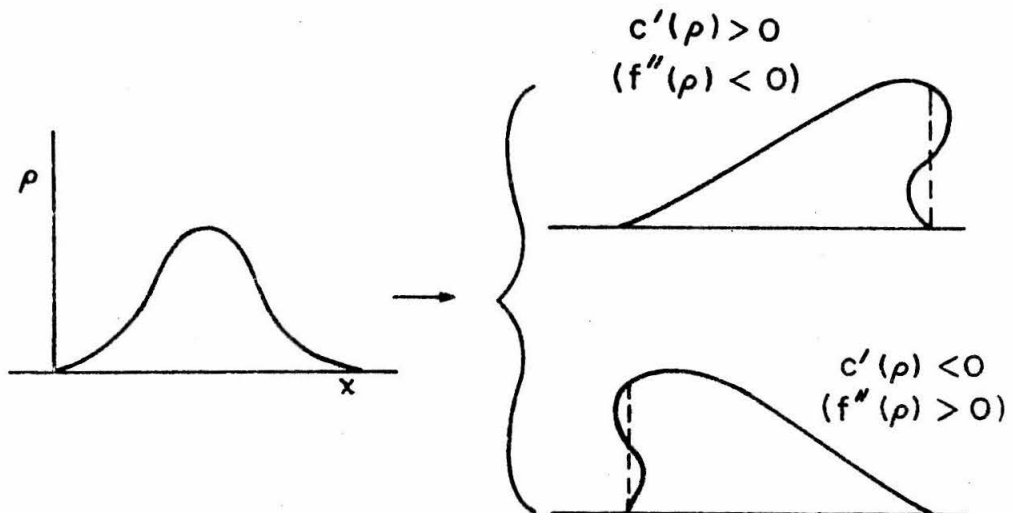


Figure 4: Possible Behavior of  $\rho(x)$  with Time

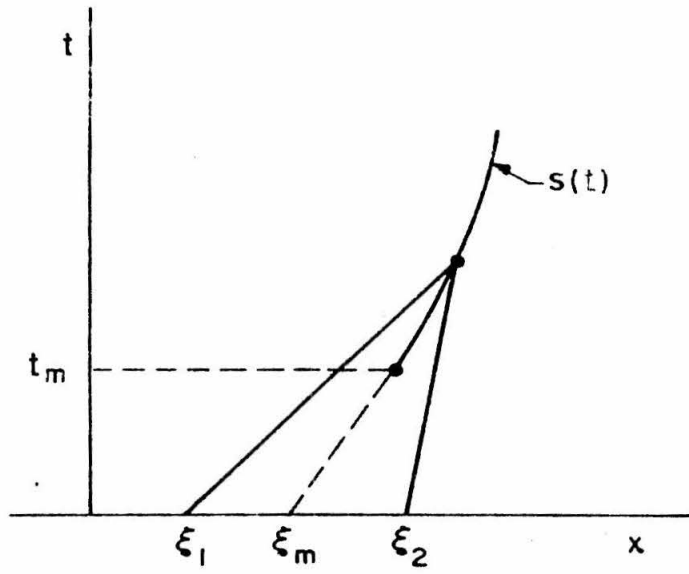


Figure 5: Location of Discontinuity

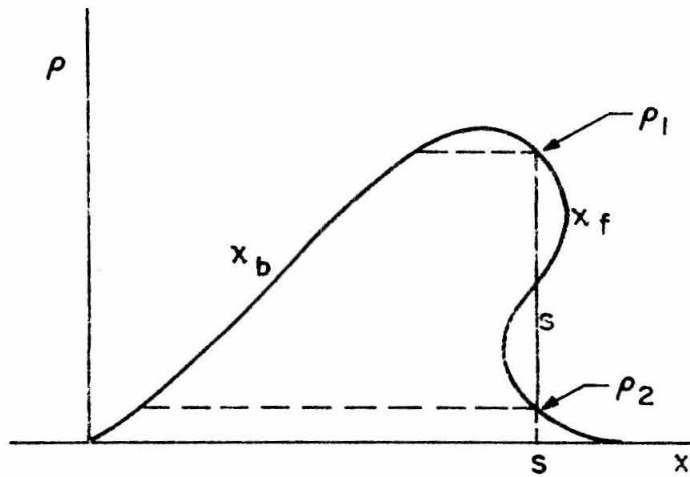


Figure 6: Multiple-Valued and Discontinuous Solutions

BIBLIOGRAPHY

1. Coates, J. I. and E. Glueckauf, "Theory of Chromatography. Part III - Experimental Separation of Two Solutes and Comparison with Theory," Journal of the Chemical Society pp. 1308-1314 (1947).
2. DeVault, Don, "The Theory of Chromatography," Journal of the American Chemical Society 65, 532-540 (1943).
3. Gilliland, E. R. and R. F. Baddour, "The Rate of Ion Exchange," Industrial and Engineering Chemistry 45, 330-337 (1953).
4. Glueckauf, E., "Theory of Chromatography. Part II - Chromatograms of a Single Solute," Journal of the Chemical Society, pp. 1302-1308 (1947).
5. Goldstein, S., "On the Mathematics of Exchange Processes in Fixed Columns. Part I - Mathematical Solutions and Asymptotic Expansions," Proceedings of the Royal Society 219, 152-171 (1953).
6. Goldstein, S., "On the Mathematics of Exchange Processes in Fixed Columns. Part II - The Equilibrium Theory as the Limit of the Kinetic Theory," Proceedings of the Royal Society 219, 171-185 (1953).
7. Thomas, Henry C., "Heterogeneous Ion Exchange in a Flowing System," Journal of the American Chemical Society 66, 1664-1666 (1944).
8. Walter, John E., "Multiple Adsorption from Solutions," Journal of Chemical Physics 13, 229-234 (1945).
9. Weiss, Joseph, "On the Theory of Chromatography," Journal of the Chemical Society, 297-303 (1943).
10. Whitham, G. B., Course notes from AMa 152a, California Institute of Technology, Fall 1965.

Proposition 3

THE EQUATIONS OF SURFACE FLOW  
IN A ROTATING FRAME OF REFERENCE

A system of equations analogous to the continuity and Navier-Stokes equations of fluid mechanics is presented by Scriven [4] and Aris [1] as a description of fluid flow in a surface or interface. Their development begins in a manner similar to that of ordinary fluid mechanics. Two coordinate systems are set up in the surface. One, although the surface is moving in space, is called "fixed", and the other, the material coordinate system, moves with the fluid particles. The fixed system is so defined that a point remains in a fixed location in the surface if its motion is entirely normal to the surface. However, this definition is conceptually undesirable in many cases. For instance, if a segment of a plane were to translate parallel to itself, the fixed coordinate system would remain behind. If a circular cylinder were to rotate about its axis, a fixed fluid particle would remain stationary. In these cases it would be desirable to have a "fixed" particle participate in the overall motion and to define fluid motion in the surface as motion relative to such fixed particles. With such considerations in mind we introduce in the three-dimensional space a frame of reference that is translating and rotating with respect to the inertial frame. Although it is actually irrelevant to the development that follows, we assume for concreteness that the origin of the moving frame is at the center of mass of the fluid and that the angular velocity of rotation is equal to the mass-average angular velocity of the

fluid about the center of mass. The fixed surface coordinate system is defined as above except that it is "fixed" with respect to the rotating frame of reference. In calculating the momentum equation for the surface, Newton's second law must be applied in the inertial frame of reference. When these equations are finally expressed in terms of surface quantities, fictitious forces appear as a result of the motion of the rotating frame of reference.

Because of the time dependence of the surface, some of the equations involved in the development are somewhat more complex than those ordinarily encountered in differential geometry and tensor calculus. For the sake of continuity, brief derivations of some of these are included in the various appendices. Also, quantities are not always defined when they are introduced, and it may be necessary to refer to the Nomenclature section on occasion.

#### Surface Coordinates and the Velocity

The position vector in the inertial frame of reference is denoted by  $\underline{r}$  and is related to  $\underline{R}$ , the position vector in the rotating center-of-mass frame, by the equation

$$\underline{r} = \underline{r}_{CM} + \underline{R} \quad (1)$$

where  $\underline{r}_{CM}$  is the location of the center of mass. The surface can be represented parametrically by

$$\underline{R} = \underline{R}(u^\alpha, t) \quad (2)$$

where the  $u^\alpha$  ( $\alpha = 1, 2$ ) serve as coordinates on the surface. Base

vectors tangential to the surface can be defined by differentiating  $\underline{R}$  :

$$\underline{a}_{-\alpha} = \frac{\partial \underline{R}}{\partial u^{\alpha}} \quad (3)$$

The  $u^{\alpha}$  are used to represent the coordinate system fixed in the surface. The convected system has coordinates  $u^{*\alpha}$ , and when there is danger of confusion, quantities whose independent variables are to be regarded as the  $u^{*\alpha}$  are also marked by an asterisk. Then we also have

$$\underline{R} = \underline{R}(u^{*\alpha}, t) \quad (4)$$

and

$$\underline{a}_{-\alpha}^* = \frac{\partial \underline{R}}{\partial u^{*\alpha}} \quad (5)$$

In order to represent general three-dimensional vectors at points of the surface, a third base vector is needed. The unit normal, defined by

$$\underline{n} = \frac{\underline{a}_1 \times \underline{a}_2}{|\underline{a}_1 \times \underline{a}_2|} \quad (6)$$

serves this purpose.

The time derivatives of  $\underline{R}(u^{\alpha}, t)$  and  $\underline{R}(u^{*\alpha}, t)$  give velocities associated with the surface relative to the rotating frame of reference. Since a point in the fixed coordinate system moves only in the normal direction, we have by definition

$$\frac{\partial \underline{CM}^R}{\partial t} = \underline{n} v^{(n)} \quad (7)$$

where  $v^{(n)}$  is the normal velocity of the surface. Nomenclature should be consulted for definitions of the various time derivatives. It

follows from the definition of the convected coordinate system that the velocity of a fluid particle in the surface is

$$\underline{v} = \frac{d_{CM} R}{dt} \quad (8)$$

$$= \frac{d_{CM} u^\alpha}{dt} \frac{\partial R}{\partial u^\alpha} + \frac{\partial_{CM} R}{\partial t} \quad (9)$$

$$= \underline{a}_\alpha v^\alpha + \underline{nv}^{(n)} \quad (10)$$

$$= \underline{v}_{II} + \underline{nv}^{(n)} \quad (11)$$

where

$$\underline{v}_{II} = \underline{a}_\alpha v^\alpha \quad (12)$$

is the velocity component tangential to the surface. The procedure followed in the above sequence of equations relates the two time derivatives by the operator equation

$$\frac{d_{CM}}{dt} = \frac{\partial_{CM}}{\partial t} + v^\alpha \frac{\partial}{\partial u^\alpha} \quad (13)$$

In all equations a repeated index ( $\alpha$  in this case) implies a summation over both its values.

The velocity in the inertial frame of reference is related to that above through the motion of the center-of-mass system. If  $\underline{w}$  is adopted as the symbol for velocity in the inertial frame:

$$\underline{w} = \frac{d\underline{r}}{dt} \quad (14)$$

application of Eq. (D.4) of Appendix D yields

$$\underline{w} = \underline{v} + \underline{\omega} \times \underline{R} + \underline{w}_{CM} \quad (15)$$

where  $\underline{\omega}$  is the angular velocity of the rotating system and

$$\underline{w}_{CM} = \frac{d\underline{r}_{CM}}{dt} \quad (16)$$

is the velocity of the center of mass.

### The Continuity Equation

The surface analogue of the continuity equation is obtained by equating the rate of change of mass in an arbitrary convected surface to that added from the surrounding bulk phase. If  $\gamma$  is the surface density in mass per unit area and  $Q$  the amount of mass added from the bulk phase per unit area per unit time, we have

$$\frac{d_{CM}}{dt} \int_{S^*} \gamma dS^* = \int_{S^*} Q dS^* \quad (17)$$

With the aid of equations developed in Appendix C, the differentiation and integration can be interchanged. Using Eq. (C.14), (17) becomes

$$\int_{S^*} \left[ \frac{d_{CM}\gamma}{dt} + (-2Hv^{(n)} + v^{\alpha, \alpha})\gamma \right] dS^* = \int_{S^*} Q dS^* \quad (18)$$

Since the surface is arbitrary, the integral sign can be removed:

$$\frac{d_{CM}\gamma}{dt} + v^{\alpha, \alpha} \gamma - 2H v^{(n)} \gamma = Q \quad (19)$$

The rate of change can be expressed in the fixed surface system with the use of Eq. (13):

$$\frac{\partial_{CM}\gamma}{\partial t} + v^{\alpha} \frac{\partial \gamma}{\partial u^{\alpha}} + v^{\alpha, \alpha} \gamma - 2H v^{(n)} \gamma = Q \quad (20)$$

or

$$\frac{\partial CM^\gamma}{\partial t} + (\gamma v^\alpha)_{,\alpha} - 2H v^{(n)} \gamma = Q \quad . \quad (21)$$

The Momentum Equation

A differential equation expressing conservation of momentum in terms of surface quantities is more difficult to obtain, because the rate of change of momentum must be expressed in the inertial frame of reference in order to equate it to the force acting on the surface. The force is divided into two terms. One, denoted  $\underline{F}$ , has units of force per unit area and represents forces caused by interaction with the bulk phase and also body forces such as gravity. It includes momentum convected in from outside. The other term involves forces associated with the surface itself, such as surface tension and rate of strain. It can be expressed in terms of a surface stress tensor. The tensor is symmetric and its inner product with the unit normal to a curve in the surface yields the force per unit length of curve. With these considerations Newton's second law can be applied to the fluid in a convected portion of the surface to produce the equation

$$\frac{d}{dt} \int_{S^*} \gamma \underline{w} \, dS^* = \int_{S^*} \underline{F} \, dS^* + \oint_{C^*} \underline{T}_{II} \cdot \underline{m} \, ds \quad . \quad (22)$$

Here  $C^*$  is the curve bounding  $S^*$ , and  $s$  is arc length along the curve.  $\underline{m}$  is the outward unit normal to  $C^*$  and is tangent to the surface. The stress tensor  $\underline{T}_{II}$  can be written

$$\underline{T}_{II} = a_{\alpha} a_{\beta} T_{II}^{\alpha\beta} \quad . \quad (23)$$

In order to obtain a differential equation, it is necessary to express all the terms in Eq. (22) as integrals over  $S^*$ . The term on the left-hand side is the most involved and is considered first. The time derivative can be expressed in the rotating frame of reference through the use of Eq. (D.1) with the integral as  $\underline{z}$ . If  $\underline{w}$  is written as in Eq. (15), we obtain

$$\begin{aligned} \frac{d}{dt} \int_{S^*} \gamma \underline{w} dS^* &= \frac{d_{CM}}{dt} \int_{S^*} \gamma (\underline{v} + \underline{\omega} \times \underline{R} + \underline{w}_{CM}) dS^* \\ &+ \underline{\omega} \times \int_{S^*} \gamma (\underline{v} + \underline{\omega} \times \underline{R} + \underline{w}_{CM}) dS^* . \end{aligned} \quad (24)$$

The first term on the right can be transformed using Eq. (C.14):

$$\begin{aligned} \frac{d_{CM}}{dt} \int_{S^*} \gamma (\underline{v} + \underline{\omega} \times \underline{R} + \underline{w}_{CM}) dS^* &= \int_{S^*} \frac{d_{CM} \gamma}{dt} (\underline{v} + \underline{\omega} \times \underline{R} + \underline{w}_{CM}) dS^* \\ &+ \int_{S^*} \gamma \left( \frac{d_{CM} \underline{v}}{dt} + \frac{d_{CM} \underline{\omega}}{dt} \times \underline{R} + \underline{\omega} \times \underline{v} + \frac{d_{CM} \underline{w}_{CM}}{dt} \right) dS^* \\ &+ \int_{S^*} \gamma (\underline{v} + \underline{\omega} \times \underline{R} + \underline{w}_{CM}) (-2H v^{(n)} + v^{\alpha, \alpha}) dS^* . \end{aligned} \quad (25)$$

Equation (D.1) shows that

$$\frac{d_{CM} \underline{\omega}}{dt} = \frac{d \underline{\omega}}{dt} \quad (26)$$

and

$$\frac{d_{CM} \underline{w}_{CM}}{dt} = \frac{d \underline{w}_{CM}}{dt} - \underline{\omega} \times \underline{w}_{CM} . \quad (27)$$

Using these results and the expression for  $d_{CM}\gamma/dt$  given in Eq. (19), (25) becomes

$$\begin{aligned} \frac{d_{CM}}{dt} \int_{S^*} \gamma(\underline{v} + \underline{\omega} \times \underline{R} + \underline{w}_{CM}) dS^* &= \int_{S^*} (2H v^{(n)} \gamma - v^{\alpha}_{,\alpha} \gamma + Q) (\underline{v} + \underline{\omega} \times \underline{R} + \underline{w}_{CM}) dS^* \\ &+ \int_{S^*} \gamma \left( \frac{d_{CM} \underline{v}}{dt} + \frac{d\underline{\omega}}{dt} \times \underline{R} + \underline{\omega} \times \underline{v} + \frac{d\underline{w}_{CM}}{dt} - \underline{\omega} \times \underline{w}_{CM} \right) dS^* \\ &+ \int_{S^*} \gamma (\underline{v} + \underline{\omega} \times \underline{R} + \underline{w}_{CM}) \left( -2H v^{(n)} + v^{\alpha}_{,\alpha} \right) dS^* \end{aligned} \quad (28)$$

$$\begin{aligned} &= \int_{S^*} (\underline{v} + \underline{\omega} \times \underline{R} + \underline{w}_{CM}) Q dS^* \\ &+ \int_{S^*} \gamma \left( \frac{d_{CM} \underline{v}}{dt} + \frac{d\underline{\omega}}{dt} \times \underline{R} + \underline{\omega} \times \underline{v} + \frac{d\underline{w}_{CM}}{dt} - \underline{\omega} \times \underline{w}_{CM} \right) dS^* \end{aligned} \quad (29)$$

The  $\underline{\omega}$  in the last term of (24) can be taken inside the integral. If the expression in (29) is then substituted into (24), we obtain

$$\begin{aligned} \frac{d}{dt} \int_{S^*} \gamma \underline{w} dS^* &= \int_{S^*} \left[ \gamma \frac{d_{CM} \underline{v}}{dt} + Q \underline{v} + \gamma \underline{\omega} \times (\underline{\omega} \times \underline{R}) + 2\gamma \underline{\omega} \times \underline{v} \right. \\ &\left. + \gamma \frac{d\underline{\omega}}{dt} \times \underline{R} + \gamma \frac{d\underline{w}_{CM}}{dt} + (\underline{\omega} \times \underline{R} + \underline{w}_{CM}) Q \right] dS^* \end{aligned} \quad (30)$$

The line integral in Eq. (22) can be transformed into a surface integral through the surface analogue of Green's theorem in the plane

$$\oint_{C^*} \underline{T}_{II} \cdot \underline{m} ds = \int_{S^*} \nabla_{II} \cdot \underline{T}_{II} dS^* \quad (31)$$

where

$$\nabla_{II} = \underline{a}^\alpha \frac{\partial}{\partial u^\alpha} \quad . \quad (32)$$

A proof can be found in Aris [1].

Substituting (30) and (31) into (22)

$$\begin{aligned} \int_{S^*} \left[ \gamma \frac{d_{CM} \underline{v}}{dt} + Q \underline{v} + \gamma \underline{\omega} \times (\underline{\omega} \times \underline{R}) + 2\gamma \underline{\omega} \times \underline{v} \right. \\ \left. + \gamma \frac{d\underline{\omega}}{dt} \times \underline{R} + \gamma \frac{d\underline{w}_{CM}}{dt} + (\underline{\omega} \times \underline{R} + \underline{w}_{CM}) Q \right] dS^* \\ = \int_{S^*} [\underline{F} + \nabla_{II} \cdot \underline{T}_{II}] dS^* \quad . \quad (33) \end{aligned}$$

Since  $S^*$  is arbitrary, the integrands must be equal, and the surface momentum equation is obtained:

$$\begin{aligned} \gamma \frac{d_{CM} \underline{v}}{dt} + Q \underline{v} + \gamma \underline{\omega} \times (\underline{\omega} \times \underline{R}) + 2\gamma \underline{\omega} \times \underline{v} + \gamma \frac{d\underline{\omega}}{dt} \times \underline{R} \\ + \gamma \frac{d\underline{w}_{CM}}{dt} + (\underline{\omega} \times \underline{R} + \underline{w}_{CM}) Q = \underline{F} + \nabla_{II} \cdot \underline{T}_{II} \quad . \quad (34) \end{aligned}$$

Equation (D.5) shows that in the inertial frame of reference (34) becomes

$$\gamma \frac{d\underline{w}}{dt} + Q \underline{w} = \underline{F} + \nabla_{II} \cdot \underline{T}_{II} \quad . \quad (35)$$

#### The Momentum Equation in Surface Coordinates

In order to apply Eq. (34), it must be written in terms of its components. It is convenient first to write the acceleration terms caused by the rotation and translation of the surface as a fictitious

force. If we set

$$\underline{f} = -\gamma \underline{\omega} \times (\underline{\omega} \times \underline{R}) - 2\gamma \underline{\omega} \times \underline{v} - \gamma \frac{d\underline{\omega}}{dt} \times \underline{R} - \gamma \frac{d\underline{w}_{CM}}{dt} - (\underline{\omega} \times \underline{R} + \underline{w}_{CM})Q, \quad (36)$$

Eq. (34) becomes

$$\gamma \frac{d_{CM} \underline{v}}{dt} + Q \underline{v} = \underline{f} + \underline{F} + \nabla_{II} \cdot \underline{T}_{II}. \quad (37)$$

The time derivative in (37) can be expressed in surface coordinates through the use of Eq. (B.18)

$$\begin{aligned} \frac{d_{CM} \underline{v}}{dt} = & \underline{a}_{\alpha} \left( \frac{\partial_{CM} v^{\alpha}}{\partial t} + v^{\beta} v^{\alpha}_{,\beta} - 2b_{\beta}^{\alpha} v^{\beta} v^{(n)}_{,\beta} - a^{\alpha\beta} v^{(n)}_{,\beta} \right) \\ & + \underline{n} \left( \frac{\partial_{CM} v^{(n)}}{\partial t} + 2v^{\alpha} v^{(n)}_{,\alpha} + b_{\alpha\beta} v^{\alpha} v^{\beta} \right). \end{aligned} \quad (38)$$

$\nabla_{II} \cdot \underline{T}_{II}$  can also be expanded

$$\nabla_{II} \cdot \underline{T}_{II} = \underline{a}^{\alpha} \frac{\partial}{\partial u^{\alpha}} \cdot (a_{\beta} a_{\gamma} T_{II}^{\beta\gamma}). \quad (39)$$

Using Eq. (A.8)

$$\begin{aligned} \nabla_{II} \cdot \underline{T}_{II} = & a_{\gamma} \frac{\partial T_{II}^{\alpha\gamma}}{\partial u^{\alpha}} + \underline{a}^{\alpha} \cdot [ \{ \alpha \beta \}_{\delta} a_{\delta} + b_{\alpha\beta} \underline{n} ] a_{\gamma} T_{II}^{\beta\gamma} \\ & + [ \{ \alpha \gamma \}_{\delta} a_{\delta} + \underline{n} b_{\alpha\gamma} ] T_{II}^{\alpha\gamma} \end{aligned} \quad (40)$$

$$= \underline{a}_{\alpha} \left[ \frac{\partial T_{II}^{\alpha\beta}}{\partial u^{\beta}} + \{ \gamma \beta \} T_{II}^{\beta\alpha} + \{ \gamma \beta \} T_{II}^{\beta\gamma} \right] + \underline{n} b_{\alpha\beta} T_{II}^{\alpha\beta} \quad (41)$$

$$= \underline{a}_{\alpha} T_{II}^{\alpha\beta}_{,\beta} + \underline{n} b_{\alpha\beta} T_{II}^{\alpha\beta}. \quad (42)$$

Scriven [4] and Aris [1] decompose  $T_{II}^{\alpha\beta}$  into the form

$$T_{II}^{\alpha\beta} = \sigma a^{\alpha\beta} + \tau_{II}^{\alpha\beta} \quad (43)$$

where  $\sigma$  is the surface tension and  $\tau_{II}^{\alpha\beta}$  is the surface analogue of the viscous stress tensor and depends on velocity gradients. The differentiation then results in a large number of rather complex terms. This process is not repeated here.

With the aid of (38) and (42) the tangential component of Eq. (37) can be written

$$\begin{aligned} \frac{a}{\alpha} \gamma \left( \frac{\partial_{CM} v^\alpha}{\partial t} + v^\beta v^\alpha_{,\beta} - 2b_\beta^\alpha v^\beta v^{(n)} - a^{\alpha\beta} v_{,\beta}^{(n)} v^{(n)} \right) + \frac{a}{\alpha} Q v^\alpha \\ = \frac{a}{\alpha} f^\alpha + \frac{a}{\alpha} F^\alpha + \frac{a}{\alpha} T_{II}^{\alpha\beta}_{,\beta} \end{aligned} \quad (44)$$

In the usual tensor notation with base vectors suppressed

$$\begin{aligned} \gamma \left( \frac{\partial_{CM} v^\alpha}{\partial t} + v^\beta v^\alpha_{,\beta} - 2b_\beta^\alpha v^\beta v^{(n)} - a^{\alpha\beta} v_{,\beta}^{(n)} v^{(n)} \right) + Q v^\alpha \\ = f^\alpha + F^\alpha + T_{II}^{\alpha\beta}_{,\beta} \end{aligned} \quad (45)$$

The normal component of (37) is

$$\begin{aligned} \gamma \left( \frac{\partial_{CM} v^{(n)}}{\partial t} - 2v^\alpha v_{,\alpha}^{(n)} + b_{\alpha\beta} v^\alpha v^\beta \right) + Q v^{(n)} \\ = f^{(n)} + F^{(n)} + b_{\alpha\beta} T_{II}^{\alpha\beta} \end{aligned} \quad (46)$$

### Conclusion

The notation used in the equations written above for  $\gamma$  and  $\underline{v}$  appears overwhelming, and the equations seem utterly intractable. Indeed, solutions cannot be obtained until such quantities as  $Q$ ,  $\underline{f}$ ,

$\underline{F}$  and  $\underline{T}_{II}$  are either specified or related to  $\gamma$  and  $\underline{v}$ . However, the purpose of introducing the translating and rotating frame of reference is to simplify the equations. Although the equations in their general form appear quite formidable, the description of the fluid behavior in special cases can be simplified considerably by viewing it from the proper frame of reference. The introduction of the translating and rotating frame of reference into the equations permits this flexibility and increases the number of situations to which the surface equations can be applied economically.

As mentioned previously, the fact that the moving frame of reference is associated with the center of mass and with the mass-average angular velocity is irrelevant to the derivation above. Any translating and rotating frame of reference can be employed, and a specific one is mentioned only because its general behavior in relation to the surface motion exemplifies the reason for introducing a moving frame. In a particular application  $\underline{w}_{CM}$  and  $\underline{\omega}$  would usually be selected or given a priori, but their values would generally be close to those for the center of mass and the mass-average angular velocity.

Appendix A

FORMULAS FROM DIFFERENTIAL GEOMETRY

The formulas listed below can be obtained from Sokolnikoff [5] or Kreyszig [2] or some other text on differential geometry. They are needed for the development of the other appendices. The time dependence of the quantities is irrelevant here, and the same results are valid in both the fixed and convected surface coordinate systems.

The covariant metric tensor is

$$a_{\alpha\beta} = \underline{a}_{\alpha} \cdot \underline{a}_{\beta} \quad (\text{A.1})$$

and it measures distance in the surface through the first fundamental form:

$$(ds)^2 = a_{\alpha\beta} du^{\alpha} du^{\beta} \quad (\text{A.2})$$

The set of base vectors reciprocal to  $\underline{a}_{\alpha}$  (and  $\underline{n}$  in three dimensions) is denoted by  $\underline{a}^{\alpha}$  (and  $\underline{n}$  in three dimensions). The contravariant metric tensor is

$$a^{\alpha\beta} = \underline{a}^{\alpha} \cdot \underline{a}^{\beta} \quad (\text{A.3})$$

and the matrix  $(a^{\alpha\beta})$  is the inverse of  $(a_{\alpha\beta})$

$$a^{\alpha\gamma} a_{\gamma\beta} = a_{\beta\gamma} a^{\gamma\alpha} = \delta_{\beta}^{\alpha} \quad (\text{A.4})$$

The  $a_{\alpha\beta}$  and  $a^{\alpha\beta}$  can raise and lower indices as in the following examples:

$$a^{\alpha\beta} b_{\beta\gamma} = b_{\gamma}^{\alpha} = a_{\gamma\beta} b^{\alpha\beta} \quad (\text{A.5})$$

$$\underline{a}_{\alpha} a^{\alpha\beta} = \underline{a}^{\beta} \quad (\text{A.6})$$

$$\underline{a}^{\alpha} a_{\alpha\beta} = \underline{a}_{\beta} \quad . \quad (\text{A.7})$$

The surface derivative of the base vectors are denoted

$$\frac{\partial \underline{a}_{\alpha}}{\partial u^{\beta}} = \{ \begin{smallmatrix} \gamma \\ \alpha \beta \end{smallmatrix} \} \underline{a}_{\gamma} + b_{\alpha\beta} \underline{n} \quad (\text{A.8})$$

where  $\{ \begin{smallmatrix} \gamma \\ \alpha \beta \end{smallmatrix} \} = \{ \begin{smallmatrix} \gamma \\ \beta \alpha \end{smallmatrix} \} = \underline{a}^{\gamma} \cdot \frac{\partial \underline{a}_{\alpha}}{\partial u^{\beta}}$  (A.9)

and  $b_{\alpha\beta} = b_{\beta\alpha} = \underline{n} \cdot \frac{\partial \underline{a}_{\alpha}}{\partial u^{\beta}}$  (A.10)

The quantity  $\{ \begin{smallmatrix} \gamma \\ \alpha \beta \end{smallmatrix} \}$  is a Christoffel symbol of the second kind, and  $b_{\alpha\beta} du^{\alpha} du^{\beta}$  is called the second fundamental form of a surface. From these definitions the following equations are readily obtained:

$$\frac{\partial \underline{a}^{\alpha}}{\partial u^{\beta}} = -\{ \begin{smallmatrix} \alpha \\ \gamma \beta \end{smallmatrix} \} \underline{a}^{\gamma} + b_{\beta}^{\alpha} \underline{n} \quad (\text{A.11})$$

$$\frac{\partial \underline{n}}{\partial u^{\beta}} = -\underline{a}_{\alpha} b_{\beta}^{\alpha} \quad . \quad (\text{A.12})$$

The mean curvature of a surface is

$$H = \frac{1}{2} a^{\alpha\beta} b_{\alpha\beta} \quad (\text{A.13})$$

$$= \frac{1}{2} \left( \frac{1}{R_1} + \frac{1}{R_2} \right) \quad (\text{A.14})$$

where  $R_1$  and  $R_2$  are the principal radii of curvature.

Appendix B

TIME DIFFERENTIATION FORMULAS

Formulas for the time derivatives of surface base vectors and the unit normal are derived below. These formulas are needed to calculate the derivatives of vectors expressed in component form.

$$\frac{\partial \underline{CM}^a}{\partial t} = \frac{\partial}{\partial u^\alpha} \left( \frac{\partial \underline{CM}^R}{\partial t} \right) \quad (B.1)$$

$$= \frac{\partial}{\partial u^\alpha} (\underline{n} \cdot v^{(n)}) \quad (B.2)$$

after using Eq. (7). From (A.12) we obtain

$$\frac{\partial \underline{CM}^a}{\partial t} = - \underline{a}_\beta b_\alpha^\beta v^{(n)} + \underline{n} \frac{\partial v^{(n)}}{\partial u^\alpha} \quad (B.3)$$

$$= - \underline{a}_\beta b_\alpha^\beta v^{(n)} + \underline{n} v^{(n)}_{,\alpha} \quad (B.4)$$

An expression for  $\partial \underline{CM}^n / \partial t$  is obtained by differentiating

$$\underline{n} \cdot \underline{a}_\alpha :$$

$$\frac{\partial \underline{CM}^n}{\partial t} \cdot \underline{a}_\alpha = - \underline{n} \cdot \frac{\partial \underline{CM}^a}{\partial t} \quad (B.5)$$

$$= - v^{(n)}_{,\alpha} \quad (B.6)$$

from (B.4). Since  $\partial \underline{CM}^n / \partial t$  must be orthogonal to  $\underline{n}$  and hence tangent to the surface,

$$\frac{\partial \underline{CM}^n}{\partial t} = - \underline{a}^\alpha v^{(n)}_{,\alpha} \quad (B.7)$$

$$= - \nabla_{II} v^{(n)} \quad (B.8)$$

The formulas above can be used to obtain the derivative of any vector

$$\underline{z} = \underline{a}_\alpha z^\alpha + \underline{n} z^{(n)} \quad (\text{B.9})$$

$$\begin{aligned} \frac{\partial \underline{CM}^z}{\partial t} &= \underline{a}_\alpha \frac{\partial \underline{CM}^z}{\partial t} - \underline{a}_\beta b_\alpha^\beta v^{(n)} z^\alpha + \underline{n} v^{(n)}_{,\alpha} z^\alpha + \underline{n} \frac{\partial \underline{CM}^z}{\partial t} \\ &\quad - \underline{a}^\alpha v^{(n)}_{,\alpha} z^{(n)} \end{aligned} \quad (\text{B.10})$$

$$\begin{aligned} &= \underline{a}_\alpha \left( \frac{\partial \underline{CM}^z}{\partial t} - b_\beta^\alpha v^{(n)} z^\beta - a^{\alpha\beta} v^{(n)}_{,\beta} z^{(n)} \right) \\ &\quad + \underline{n} \left( \frac{\partial \underline{CM}^z}{\partial t} + v^{(n)}_{,\alpha} z^\alpha \right) . \end{aligned} \quad (\text{B.11})$$

The formula for  $\frac{d \underline{CM}^z}{dt}$  can be obtained from that above by application of (13):

$$\frac{d \underline{CM}^z}{dt} = \frac{\partial \underline{CM}^z}{\partial t} + v^\alpha \frac{\partial \underline{z}}{\partial u^\alpha} \quad (\text{B.12})$$

$$= \frac{\partial \underline{CM}^z}{\partial t} + v^\alpha \frac{\partial}{\partial u^\alpha} (\underline{a}_\beta z^\beta + \underline{n} z^{(n)}) . \quad (\text{B.13})$$

Using (A.8) and (A.12)

$$\begin{aligned} \frac{d \underline{CM}^z}{dt} &= \frac{\partial \underline{CM}^z}{\partial t} + v^\alpha \left[ \underline{a}_\beta \frac{\partial z^\beta}{\partial u^\alpha} + \{ \beta \alpha \}^\gamma \underline{a}_\gamma + b_{\beta\alpha} \underline{n} \right] z^\beta \\ &\quad + \underline{n} \left[ \frac{\partial z^{(n)}}{\partial u^\alpha} - \underline{a}_\beta b_\alpha^\beta z^{(n)} \right] \end{aligned} \quad (\text{B.14})$$

$$= \frac{\partial \text{CM}^z}{\partial t} + \underline{a}_{\alpha} (v^{\beta} [\frac{\partial z^{\alpha}}{\partial u^{\beta}} + \{\beta \gamma^{\alpha}\} z^{\gamma}] - b_{\beta}^{\alpha} v^{\beta} z^{(n)}) + \underline{n} (\frac{\partial z^{(n)}}{\partial u^{\alpha}} v^{\alpha} + b_{\alpha\beta} v^{\alpha} z^{\beta}) \quad (\text{B.15})$$

$$= \frac{\partial \text{CM}^z}{\partial t} + \underline{a}_{\alpha} (v^{\beta} z^{\alpha}_{,\beta} - b_{\beta}^{\alpha} v^{\beta} z^{(n)}) + \underline{n} (v^{\alpha} z^{(n)}_{,\alpha} + b_{\alpha\beta} v^{\alpha} z^{\beta}) \quad (\text{B.16})$$

where  $z^{\alpha}_{,\beta} = \frac{\partial z^{\alpha}}{\partial u^{\beta}} + \{\beta \gamma^{\alpha}\} z^{\gamma}$  . (B.17)

Substituting from (B.11),

$$\frac{d \text{CM}^z}{dt} = \underline{a}_{\alpha} (\frac{\partial \text{CM}^z}{\partial t} + v^{\beta} z^{\alpha}_{,\beta} - b_{\beta}^{\alpha} v^{(n)} z^{\beta} - b_{\beta}^{\alpha} v^{\beta} z^{(n)} - a^{\alpha\beta} v^{(n)}_{,\beta} z^{(n)}) + \underline{n} (\frac{\partial \text{CM}^z}{\partial t} + v^{(n)}_{,\alpha} z^{\alpha} + v^{\alpha} z^{(n)}_{,\alpha} + b_{\alpha\beta} v^{\alpha} z^{\beta}) \quad (\text{B.18})$$

In the convected system

$$\frac{d \text{CM}^{a*}}{dt} = \frac{\partial}{\partial u^{*\alpha}} \frac{d \text{CM}^R}{dt} \quad (\text{B.19})$$

$$= \frac{\partial}{\partial u^{*\alpha}} (\underline{a}^{*\beta} v^{*\beta} + \underline{n}^* v^{(n)*}) \quad (\text{B.20})$$

$$= \underline{a}^{*\beta} \frac{\partial v^{*\beta}}{\partial u^{*\alpha}} + (\{\beta \gamma^{\alpha}\}^* \underline{a}^{*\gamma} + b^{*\beta}_{\beta\alpha} \underline{n}) v^{*\beta} + \underline{n} \frac{\partial v^{(n)*}}{\partial u^{*\alpha}} - \underline{a}^{*\beta} b^{*\beta}_{\alpha} v^{(n)*} \quad (\text{B.21})$$

$$= \underline{a}^{*\beta} (\frac{\partial v^{*\beta}}{\partial u^{*\alpha}} + \{\alpha \gamma^{\beta}\} v^{*\gamma} - b^{*\beta}_{\alpha} v^{(n)*}) + \underline{n} (\frac{\partial v^{(n)*}}{\partial u^{*\alpha}} + b^{*\beta}_{\alpha\beta} v^{*\beta}) \quad (\text{B.22})$$

$$\begin{aligned}
 &= \underline{a}^*_{\beta} (v^{*\beta}_{,\alpha} - b^{*\beta}_{\alpha} v^{(n)*}) \\
 &+ \underline{n} (v^{(n)*}_{,\alpha} + b^{*\beta}_{\alpha\beta} v^{*\beta}) \quad .
 \end{aligned} \tag{B.23}$$

From (B.23) the derivative of the metric tensor can be obtained

$$\frac{d}{dt} \text{CM}^{a*}_{\alpha\beta} = \frac{d}{dt} \text{CM}^{a*}_{\alpha} \cdot \frac{a^*}{\beta} + \frac{a^*}{\alpha} \cdot \frac{d}{dt} \text{CM}^{a*}_{\beta} \tag{B.24}$$

$$\begin{aligned}
 &= a^*_{\beta\gamma} (v^{*\gamma}_{,\alpha} - b^{*\gamma}_{\alpha} v^{(n)*}) \\
 &+ a^*_{\alpha\gamma} (v^{*\gamma}_{,\beta} - b^{*\gamma}_{\beta} v^{(n)*}) \tag{B.25}
 \end{aligned}$$

$$= v^*_{\beta,\alpha} + v^*_{\alpha,\beta} - 2b^*_{\alpha\beta} v^{(n)*} \quad . \tag{B.26}$$

Appendix C

TIME DIFFERENTIATION OF AN INTEGRAL

The object here is to derive a means of interchanging differentiation and integration in an expression of the form

$$\frac{d_{CM}}{dt} \int_{S^*} G^* dS^*$$

where  $G^*$  is an arbitrary function of  $u^{*\alpha}$ ,  $t$ , and the area  $S^*$  is moving with the fluid on the surface.

An element of surface area is given in terms of the convected coordinates by

$$dS^* = |\underline{a}_1^* \times \underline{a}_2^*| du^{*1} du^{*2} \quad . \quad (C.1)$$

A simple calculation shows that

$$(\underline{a}_1^* \times \underline{a}_2^*) \cdot (\underline{a}_1^* \times \underline{a}_2^*) = a_{22}^* a_{11}^* - a_{12}^* a_{21}^* \quad (C.2)$$

$$= \det(a_{\alpha\beta}^*) \quad (C.3)$$

$$= a^* \quad . \quad (C.4)$$

Therefore

$$dS^* = \sqrt{a^*} du^{*1} du^{*2} \quad . \quad (C.5)$$

Then we have

$$\frac{d_{CM}}{dt} \int_{S^*} G^* dS^* = \frac{d_{CM}}{dt} \int_{S^*} G^* \sqrt{a^*} du^{*1} du^{*2} \quad (C.6)$$

$$= \int_{S^*} \left( \frac{d_{CM} G^*}{dt} \sqrt{a^*} + G^* \frac{1}{2\sqrt{a^*}} \frac{d_{CM} a^*}{dt} \right) du^{*1} du^{*2} \quad (C.7)$$

$$= \int_{S^*} \left( \frac{d_{CM} G^*}{dt} + \frac{1}{2} G^* \frac{d_{CM}}{dt} (\ln a^*) \right) dS^* \quad . \quad (C.8)$$

$\frac{d_{CM} a^*}{dt}$  can be obtained with the aid of (B.26):

$$\begin{aligned} \frac{d_{CM} a^*}{dt} &= a_{22}^* \frac{d_{CM} a_{11}^*}{dt} + a_{11}^* \frac{d_{CM} a_{22}^*}{dt} - a_{21}^* \frac{d_{CM} a_{12}^*}{dt} - a_{12}^* \frac{d_{CM} a_{21}^*}{dt} \quad (C.9) \\ &= -2v^{(n)*} (a_{22}^* b_{11}^* + a_{11}^* b_{22}^* - a_{21}^* b_{12}^* - a_{12}^* b_{21}^*) \\ &\quad + 2a_{22}^* v_{1,1}^* + 2a_{11}^* v_{2,2}^* \\ &\quad - a_{21}^* (v_{1,2}^* + v_{2,1}^*) - a_{12}^* (v_{2,1}^* + v_{1,2}^*) \quad . \quad (C.10) \end{aligned}$$

Since the matrix  $(a^{*\alpha\beta})$  is the inverse to  $(a_{\alpha\beta}^*)$ ,

$$\begin{aligned} \frac{d_{CM} a^*}{dt} &= -2v^{(n)*} a^* (a^{*11} b_{11}^* + a^{*22} b_{22}^* + a^{*12} b_{12}^* + a^{*21} b_{21}^*) \\ &\quad + 2a^* (a^{*11} v_{1,1}^* + a^{*22} v_{2,2}^* + a^{*12} v_{1,2}^* + a^{*21} v_{2,1}^*) \quad (C.11) \end{aligned}$$

$$= -2v^{(n)*} a^* a^{*\alpha\beta} b_{\alpha\beta}^* + 2a^* a^{*\alpha\beta} v_{\alpha,\beta}^* \quad (C.12)$$

and

$$\frac{d_{CM} \ln a^*}{dt} = -4 H v^{(n)} + 2v_{\alpha,\alpha}^* \quad (C.13)$$

where (A.13) has been applied.

If (C.13) is substituted into (C.8), the final equation is obtained:

$$\frac{d_{CM}}{dt} \int_{S^*} G^* dS^* = \int_{S^*} \left[ \frac{d_{CM} G^*}{dt} + G^* (-2H v^{(n)} + v_{\alpha,\alpha}^*) \right] dS^* \quad . \quad (C.14)$$

Appendix D

RELATION BETWEEN DERIVATIVES

IN THE ROTATING AND THE INERTIAL FRAMES OF REFERENCE

The equations listed here can be found in Symon [6]. If the center-of-mass frame of reference is rotating with an angular velocity  $\underline{\omega}$  relative to the inertial frame, the time derivatives of any vector  $\underline{z}$  are related by

$$\frac{d\underline{z}}{dt} = \frac{d_{\text{CM}}\underline{z}}{dt} + \underline{\omega} \times \underline{z} \quad . \quad (\text{D.1})$$

If the differentiation is performed a second time,

$$\frac{d^2\underline{z}}{dt^2} = \frac{d_{\text{CM}}^2\underline{z}}{dt^2} + \underline{\omega} \times (\underline{\omega} \times \underline{z}) + 2\underline{\omega} \times \frac{d_{\text{CM}}\underline{z}}{dt} + \frac{d\underline{\omega}}{dt} \times \underline{z} \quad . \quad (\text{D.2})$$

If we set

$$\underline{z} = \underline{r} - \underline{r}_{\text{CM}} = \underline{R} \quad (\text{D.3})$$

we obtain

$$\underline{w} = \underline{v} + \underline{\omega} \times \underline{R} + \underline{w}_{\text{CM}} \quad (\text{D.4})$$

and

$$\frac{d\underline{w}}{dt} = \frac{d_{\text{CM}}\underline{v}}{dt} + \underline{\omega} \times (\underline{\omega} \times \underline{R}) + 2\underline{\omega} \times \underline{v} + \frac{d\underline{\omega}}{dt} \times \underline{R} + \frac{d\underline{w}_{\text{CM}}}{dt} \quad . \quad (\text{D.5})$$

NOMENCLATURE

Symbols

$\frac{d}{dt}$  convected time derivative in the inertial frame of reference

$\frac{\partial}{\partial t}_{CM}$  =  $\left(\frac{\partial}{\partial t}\right)_{u^\alpha}$ , time derivative relative to the fixed surface coordinates

$\frac{d}{dt}_{CM}$  =  $\left(\frac{\partial}{\partial t}\right)_{u^{*\alpha}}$ , convected time derivative in the surface

\*

the asterisk designates quantities associated with the convected surface coordinates

,

the comma represents covariant differentiation, e.g.,  $T_{II}^{\alpha\beta},_{\gamma}$  is the  $u^\gamma$  covariant derivative of the tensor  $T_{II}^{\alpha\beta}$ .

$\nabla_{II}^\alpha$  =  $\underline{a}^\alpha \frac{\partial}{\partial u^\alpha}$ , the surface gradient operator

$\left\{ \begin{matrix} \alpha \\ \beta \gamma \end{matrix} \right\}$  Christoffel symbol of the second kind

Roman

$\underline{a}_\alpha$  surface base vector in the fixed coordinate system

$\underline{a}^\alpha$  reciprocal base vector in the fixed coordinate system

$a_{\alpha\beta}$  covariant metric tensor in the fixed surface coordinate system

$a^{\alpha\beta}$  contravariant metric tensor in the fixed surface coordinate system

$\underline{a}^*_\alpha$  surface base vector in the convected coordinate system

$a^*$  =  $\det(a^*_{\alpha\beta})$

$b_{\alpha\beta}$  tensor associated with the second fundamental form of a surface ( $b_{\alpha\beta} du^\alpha du^\beta$ )

$C^*$  surface curve bounding  $S^*$

$\underline{f}$	fictitious force arising from the rotation of the center-of-mass frame of reference
$\underline{F}$	force per unit area of surface as a result of interaction with the bulk phase
$G^*$	any quantity (scalar, vector, or tensor) with variables $u^{*\alpha}, t$
$H$	mean curvature of the surface
$\underline{m}$	unit normal to $C^*$ and tangent to the surface
$\underline{n}$	unit normal to surface
$Q$	mass per unit area per unit time added to the surface from the bulk phase
$\underline{r}$	position vector in the inertial frame of reference
$\underline{r}_{CM}$	position vector to the center of mass
$\underline{R}$	position vector in the rotating frame of reference
$s$	arc length in the surface
$S^*$	an area in the surface which is convected with the fluid
$t$	time
$\underline{T}_{II}$	surface stress dyadic
$T_{II}^{\alpha\beta}$	surface stress tensor
$u^\alpha$	coordinate in the fixed surface system
$u^{*\alpha}$	coordinate in the convected surface system
$\underline{v}$	fluid velocity in the rotating frame of reference
$\underline{v}_{II}$	component of $\underline{v}$ tangent to the surface
$v^\alpha$	component of $\underline{v}$ in the fixed surface coordinate system
$v^{(n)}$	component of $\underline{v}$ normal to the surface

$\underline{w}$  fluid velocity in the inertial frame of reference

$\underline{w}_{CM}$  velocity of the center of mass

$\underline{z}$  arbitrary vector

Greek

$\gamma$  surface density in mass per unit area

$\delta_{\beta}^{\alpha}$  Kronecker delta

$\sigma$  surface tension

$\tau_{II}^{\alpha\beta}$  surface viscous stress tensor

$\underline{\omega}$  angular velocity of the rotating frame of reference

BIBLIOGRAPHY

1. Aris, Rutherford, Vectors, Tensors, and the Basic Equations of Fluid Mechanics, Prentice-Hall, Inc., 1962.
2. Kreyszig, Erwin, Differential Geometry, University of Toronto Press, 1959.
3. Scriven, L. E., Course notes from ChEn 225 (Fall, 1964) and ChEn 226 (Winter, 1965), University of Minnesota.
4. Scriven, L. E., "Dynamics of a Fluid Interface," Chemical Engineering Science 12, 98-108 (1960).
5. Sokolnikoff, I. S., Tensor Analysis. Theory and Applications to Geometry and Mechanics of Continua, John Wiley & Sons, Inc., 1964.
6. Symon, Keith R., Mechanics, Addison-Wesley, 1960.